Annex 43

Fuel Driven Sorption Heat Pumps

Final Report

Submitted by
Fraunhofer-Institute for Solar Energy Systems ISE
Heidenhofstr. 2
79110 Freiburg, Germany

Contributors list (alphabetical order):
Axel Albers, Marcello Aprile, Corey Blackman, Robert Critoph, Johan Emhofer, Andrea Frazzica, Gerrit Füldner, Michael Garrabrant, Kyle Gluesenkamp, Stefan Henninger, Ivan Malenkovic, Patricia Melograno, Steven Metcalf, Mario Motta, Björn Niedburg, Valeria Palomba, Ángeles Rivero-Pacho, Peter Schossig, Lindsay Sugden, Luigi Tischer, Tommaso Toppi, Andreas Velte, Ursula Wittstadt, Zhiyao Yang

Website:
https://heatpumpingtechnologies.org/annex43/

September 2020

Report no. HPT-AN43-1

Published by

Heat Pump Centre
c/o RISE – Research Institutes of Sweden
Box 857, SE-501 15, Borås
Sweden
Phone: +46 10 16 55 12
Fax: +46 33 13 19 79

Production

Heat Pump Centre, Borås, Sweden

ISBN 978-91-89167-50-6
Report No. HPT-AN43-1

Preface
This project was carried out within the Technology Collaboration Programme on Heat Pumping Technologies (HPT TCP) which is an Implementing agreement within the International Energy Agency, IEA.

The IEA
The IEA was established in 1974 within the framework of the Organization for Economic Cooperation and Development (OECD) to implement an International Energy Programme. A basic aim of the IEA is to foster cooperation among the IEA participating countries to increase energy security through energy conservation, development of alternative energy sources, new energy technology and research and development (R&D). This is achieved, in part, through a programme of energy technology and R&D collaboration, currently within the framework of over 40 Implementing Agreements.

The Technology Collaboration Programme on Heat Pumping Technologies (HPT TCP)
The Technology Collaboration Programme on Heat Pumping Technologies (HPT TCP) forms the legal basis for the Heat Pumping Technologies Programme. Signatories of the TCP are either governments or organizations designated by their respective governments to conduct programmes in the field of energy conservation.

Under the TCP collaborative tasks or “Annexes” in the field of heat pumps are undertaken. These tasks are conducted on a cost-sharing and/or task-sharing basis by the participating countries. An Annex is in general coordinated by one country which acts as the Operating Agent (manager). Annexes have specific topics and work plans and operate for a specified period, usually several years. The objectives vary from information exchange to the development and implementation of technology. This report presents the results of one Annex. The Programme is governed by an Executive Committee, which monitors existing projects and identifies new areas where collaborative effort may be beneficial.

The Heat Pump Centre
A central role within the HPT TCP is played by the Heat Pump Centre (HPC). Consistent with the overall objective of the HPT TCP the HPC seeks to advance and disseminate knowledge about heat pumps and promote their use wherever appropriate. Activities of the HPC include the production of a quarterly newsletter and the webpage, the organization of workshops, an inquiry service and a promotion programme. The HPC also publishes selected results from other Annexes, and this publication is one result of this activity.

For further information about the Technology Collaboration Programme on Heat Pumping Technologies (HPT TCP) and for inquiries on heat pump issues in general contact the Heat Pump Centre at the following address:

Heat Pump Centre
c/o RISE - Research Institutes of Sweden
Box 857, SE-501 15, BORÅS, Sweden
Phone: +46 10 16 55 12

Annex 43: Fuel Driven Sorption Heat Pumps – Final Report

Submitted by

Fraunhofer-Institute for Solar Energy Systems ISE
Heidenhofstr. 2
79110 Freiburg, Germany

Contributors list (alphabetical order):

Axel Albers, Marcello Aprile, Corey Blackman, Robert Critoph, Johan Emhofer, Andrea Frazzica, Gerrit Füldner, Michael Garrabrant, Kyle Gluesenkamp, Stefan Henninger, Ivan Malenkovic, Patricia Melograno, Steven Metcalf, Mario Motta, Björn Niedburg, Valeria Palomba, Ángeles Rivero-Pacho, Peter Schossig, Lindsay Sugden, Luigi Tischer, Tommaso Toppi, Andreas Velte, Ursula Wittstadt, Zhiyao Yang

Table of Content

List of figures

List of tables

List of abbreviations

AdHP	Adsorption Heat Pump
AdHX	Adsorption Heat Exchanger
AEF	Auxiliary Energy Factor
AEH	Auxiliary Electric Heater
BSRIA	Building Services Research and Information Association
CCC	Commitee on Climate Change
Cfa/ Cfb	Climate Classifications
CHP	Combined Heat and Power
CNR-ITAE	Consiglio Nazionale delle Ricerche - Istituto di Tecnologie Avanzate per Energia
COP	Coefficient of Performance
CSPM	Composite Salt inside Porous Matrix
DHW	Domestic Hot Water
DoE	Department of Energy
DVGW	Deutscher Verein des Gas- und Wasserfaches e.V. - Technisch-wissenschaftlicher Verein (German Technical and Scientific Association for Gas and Water
EC	Evaporator/Condenser
EHP	Electric Heat Pump
EHPA	European Heat Pump Association
EIA	U.S. Energy Information Administration
ErP	Energy related Products
FDHP	Fuel Driven Heat Pump
GAHP	Gas Absorption Heat Pump
GCV	Gross calorific value
GEHP	Gas Engine Heat Pump
GHP	Gas Heat Pump
GTI	Gas Technologies Institute
GUE	Gas Utilisation Efficiency (GUE_h for heating mode, GUE_c for cooling mode)
GWP	Global Warming Potential
HEX	Heat Exchanger
HP	Heat Pump

HS	Hydraulic Separator
HSPF	Heating Seasonal Performance Factor
HTF	Heat Transfer Fluid
IEA	International Energy Agency
MFH	Multi-Family House
MOF	Metal-organic framework
ODP	Ozone Depletion Potential
PEF	Primary Energy Factor
PER	The Primary Energy Ratio indicator
PST	Partial-Support-Transformation
QNc	Rated cooling capacity
RECS	Residential Energy Consumption Survey
RRT	Round Robin Test
SAEF	Seasonal Auxiliary Energy Factor
SFH	Single Family House
SFUE	Seasonal Fuel Utilization Efficiency
SGUE	Seasonal Gas Utilisation Efficiency (SGUEh in heating mode, SGUEc in cooling mode)
SGUENCV	SGUE based on the Net Calorific Value
SMTI	Stone Mountain Technology Inc.
SPER	Seasonal primary energy efficiency (SPERh for heating mode, SPERc for cooling mode)
TDHP	Thermally Driven Heat Pump

Summary and Outlook

Fuel Driven Sorption Heat Pumps (FDHP) are known for many years as an interesting option in many cases for efficient heating of buildings and domestic hot water preparation as well as industrial heat supply, using fuel (gas or oil) to run a heat pumping process based on ab- or adsorption processes. Though market available for a long time, they still represent a niche market compared to mechanical driven vapour compression heat pumps and even more compared to gas condensing boilers.

This IEA-HPT Annex 43 “Fuel Driven Sorption Heat Pumps” started as a follow-up of Annex 34 “Thermally driven heat pumps for heating and cooling”, now with a narrow focus on fuel driven sorption heat pumps for heating applications to widen their market penetration.

The technology of sorption heat pumps suffers from various obstacles. There are still technical barriers like complexity, power density and in some cases long-term reliability, but mainly cost reasons as well as lack of knowledge and trust of customers, installers and decision makers. Until now, fuel driven sorption heat pumps need to compete especially with gas condensing boilers.

Therefore this Annex aimed to overcome some of these barriers, bringing researchers and industry together to develop new, more efficient and cost effective appliances and generate trust and awareness by the means of workshops, conference participations and publications as well as more available best case examples. Several workshops and two conferences dedicated to sorption heat pumps with large industry participation are among the highlights of this highly interactive working group.

Also missing knowledge about the possibilities of this type of heat pumps and the pros and cons compared to different heating technologies as well as missing standards and performance evaluation tools have been addressed within this framework. The open source software tool SorpSim was enhanced by members of this Annex and much more knowledge and data have been generated and added to a database of sorption materials.

A round robin test of different performance evaluation standards has been carried out on a market available gas driven adsorption heat pump among four labs and pre-normative work was fed into the normative bodies. Especially the European standard EN12309 has been within the focus of this pre-normative work

Three simulation studies have been carried out to model the role of FDHP in different markets and to determine best types and system configurations for different applications. This information was used to derive a potential road map for a market increase for this technology. FDHP are a competitive option e.g. for multi-family homes with higher heating supply temperatures. They can become very attractive as well for other cases when wall-hung solutions are developed.

But not all expectations could be met. Some companies stopped their engagement in this field during the lifetime of this Annex and therefore fieldtesting could not be done in the planned extent.

Nevertheless there is still a lot more work to do to give this technology a robust place in the family of heat pumps.

There are still several companies developing new types of fuel driven sorption heat pumps and most members of this Annex will continue their work within the framework of the EHPA Working Group Thermally Driven Heat Pumps.

1. Introduction to Fuel Driven Sorption Heat Pumps

1.1 The Scope of the Annex

The scope of the work under HPT TCP Annex 43 was the usage of fuel driven sorption heat pumps in domestic and small commercial or industrial buildings or applications. The main goal was to widen the use of fuel driven sorption heat pumps by accelerating technical development and market readiness of the technology, as well as to identify market barriers and supporting measures. Moreover, a field test as well as proposing performance evaluation figures and optimal system layouts were among the planned means of this Annex.

The objectives were grouped into the following task structure shown in Fig. 1-1 and adopted by the partners:

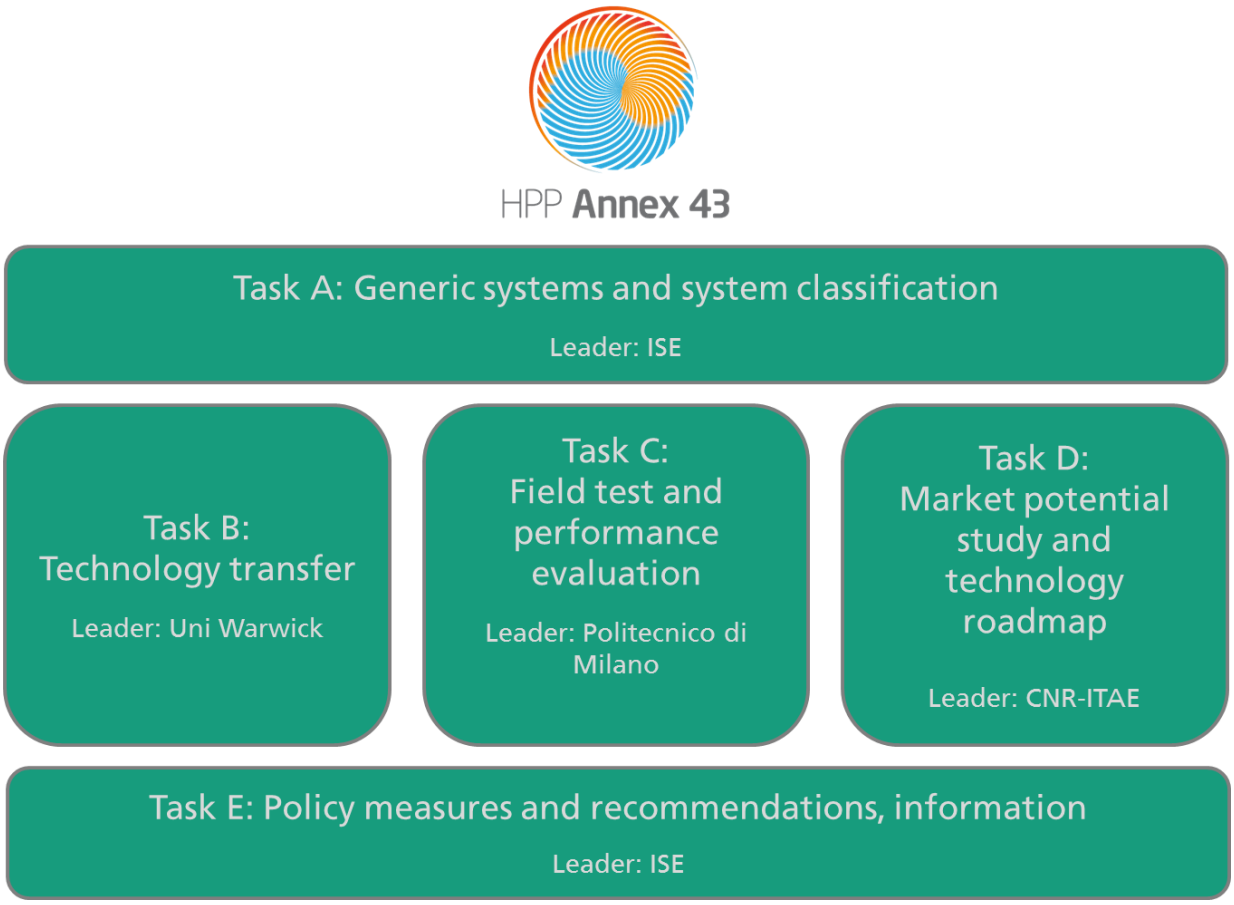

Fig. 1-1: Structure of Annex 43

1.1.1 Task A: Generic systems and system classification (Fraunhofer ISE)

It was necessary for the purposes of comparing sorption systems to categorize and classify them by heat source, type of heat distribution (Low temperature radiators, underfloor heating etc) and by the fuel used. In addition, the safety and other regulations applying to different types in different countries needed to be compared. This information has been compiled, together with status and market prospects in a series of Country Reports.

1.1.2 Task B: Technology transfer (University of Warwick)

Warwick facilitated the knowledge transfer between partners and also developers / manufacturers prepared to share their experience. The purpose was to inform Task D below as well as disseminating via national meetings and reports. Results are presented in chapter 2 of this report.

1.1.3 Task C: Field test and performance evaluation (Politecnico di Milano)

Measurement/monitoring procedures and standardisation (e.g. how to cope with different fuel quality, system boundaries, aux. energy etc.) was an important issue to be addressed. The work from the IEA Annex 34 (Thermally Driven Heat Pumps for Heating and Cooling, 2009-2012) and Task 44 (Solar and Heat Pump Systems 2010-2013), has been continued and standards extended to seasonal performance factors at the system level. Procedures have been established in cooperation with IEA SHC Task 48 (Quality Assurance & Support Measures for Solar Cooling Systems). This activity was planned to be backed up with laboratory testing and field trials. Due to lack of field test ready systems, field trials have not been done in the previously expected amount. Results can be found in chapter 3.

1.1.4 Task D: Market potential study and technology roadmap (CNR-ITAE)

Simulation studies were performed to evaluate different technologies in different climate zones, different building types and building standards. The results of the studies were combined with the market data and actual building stock to derive a technology roadmap, which is presented in chapter 4.

1.1.5 Task E: Policy measures and recommendations, information

Another task of the Annex 43 was the dissemination of the knowledge, e.g. in workshops for planners, installers and decision makers as well as the development of recommendations for policies like building codes and funding schemes. Several national and international workshops have been organized and are reported in the annual reports.

1.2 State of the Art

Heat pumps for heating and domestic hot water preparation can be realized in several ways. Most commonly, an electrically driven vapour compression cycle is used. Apart from this, there are other ways of pumping heat from an environmental low temperature heat source to heating supply temperature: a vapour compression cycle can also be driven by a gas engine (Gas Engine Heat Pump, GEHP). Furtheron, ad- and absorption cycles can be used. Annex 43 focused on ad- and absorption heat pumps which are run by a fuel boiler (gas or oil).

1.2.1 Background

Basically, a heat-driven heat pump/chiller works at three levels of temperature: the machine is driven by a heat source at high temperature T_h, heat is rejected at medium temperature T_m and extracted at low temperature T_c. The heat rejected at medium temperature is the useful effect provided in heat pumping operation. The cold produced at low temperature is the useful effect provided in chilling mode.

Basic thermodynamics limits performance in the same way as for mechanically driven systems (Fig. 1-2) with COP being a function of the three temperature levels; the upper limit for T_h = 200°C, T_m = 45°C and T_c = -5°C would be 2.8 but half the Carnot limit would be typical. Additional discussions of performance limits is provided in [1] and [2].

$$COP_{\mathrm{HP}} = \frac{Q_m}{Q_h} \leq \frac{\frac{1}{T_c} - \frac{1}{T_h}}{\frac{1}{T_c} - \frac{1}{T_m}}$$

REVERSIBLE for equality

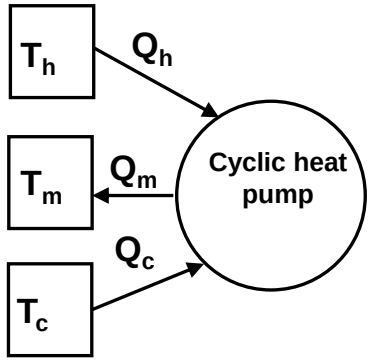

Fig. 1-2: Ideal thermodynamic limitations

The most important representatives of heat-driven cooling systems are absorption and adsorption closed-cycles. Other options are also available and are discussed in the former IEA HPT Annex 34 report [3].

Sorption technologies range from small units of 10 kW (or even less) to huge units of a few MW, and may be driven by a large variety of heat sources, including waste or solar heat and direct combustion of fuel. Another advantage is the utilization of a “thermal compressor” instead of a mechanical compressor, ensuring silent operation, which is particularly attractive for application in buildings like residential houses, museums, theatres, etc. An additional advantage of thermally driven heat pumps compared to compression heat pumps is much lower need of ambient heat which can make a big difference in terms of noise especially when air is used as heat source.

An overview of thermally driven technologies, including open sorption, closed sorption and thermo-mechanical cycles, and their application to micro CHP, is provided in [4], [5] and [6]. Further details of matching thermally-driven equipment to engine waste heat sources are discussed in [7]. Solar cooling options are reviewed in [8].

1.2.2 Liquid absorption and solid adsorption closed-cycles

Both technologies are based on a working pair of a refrigerant and a sorption medium. In absorption devices the refrigerant is absorbed, i.e. dissolved, in the liquid sorption medium changing its concentration. The most common working pairs are Lithium Bromide/Water (Fig. 1-3) and Ammonia/Water [9]. In case of adsorption chillers, the refrigerant is adsorbed in the pores of the solid adsorption medium. The most common working pairs are Zeolite/water, Silica Gel/water, Activated carbon/ammonia, and Activated carbon/methanol [10] and [11]. The technologies are thermodynamically similar and have an analogous basic configuration, which consists of four main components: a reactor termed a generator, where the sorbent (liquid or solid) is heated at high temperature; the condenser, where the desorbed refrigerant vapour is condensed into liquid; the evaporator, where the cooling effect is produced; a reactor called ab-/adsorber that receives refrigerant vapour from the evaporator. In the case of liquid absorption machines, a pump is used to continuously circulate the rich solution from the absorber to the generator and the weak solution back to the absorber. The two reactors of a solid adsorption machine operate in counter-phase to ensure continuous useful cooling effect and are alternatively heated for desorption and cooled for adsorption. Unlike an absorption machine, a circulation pump is not required. A more detailed description of the absorption and adsorption cycle is given in the former IEA HPT Annex 34 report [3].

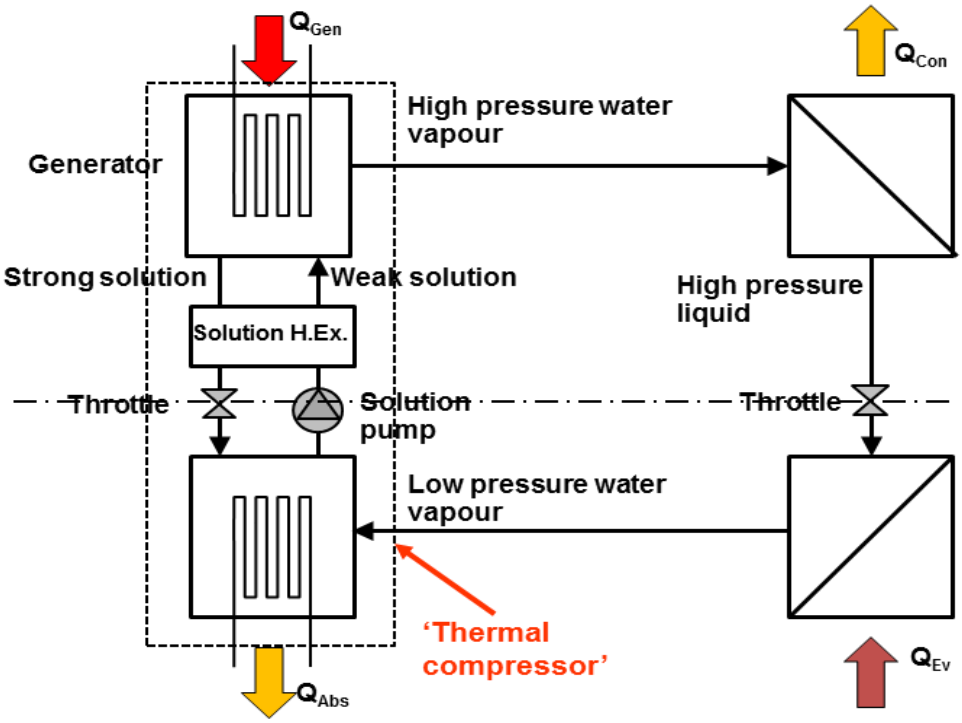

Fig. 1-3: Simple water - LiBr absorption cycle schematic

The evaporator and condenser have the same function as in mechanical vapour compression cycles and, in the case of high pressure refrigerants such as ammonia can be standard components. Where the refrigerant is water or methanol, specially designed evaporators and condensers are needed because of the very low density of the refrigerant, particularly in evaporation. Routing the refrigerant through

conventional tubes would result in pressure drops resulting in much reduced performance. It is common to house a pool boiling or falling film evaporator or generator in the same vessel as the ab-/adsorber to avoid this. Liquid absorbers are commonly of the falling film type.

Adsorption generators are very different in that the adsorbent stays within the vessel and must be alternately heated and cooled. Loose packed adsorbents have very low thermal conductivity (c. 0.1 W/mK) and so heat transfer is a major challenge. Attempting to improve heat transfer with, for example, large numbers of fins can be counterproductive, because of the thermal mass of the fins and vessel. When the whole assembly is heated and cooled through one cycle, a certain fixed amount of heat is pumped from a low to a high level. The heat that enters the adsorbent is useful but the heat that simply raises the temperature of the vessel and fins is wasted. Some of this heat can be recovered but minimising the thermal mass of the container and any inert material that is cycled in temperature is essential. Previous solutions have included lightweight plate fin-tubes, micro channels, micro-tube in shell, finned tubes, etc.

In order to increase the performance of the machines, some more sophisticated configurations have been developed, such as double and triple effect liquid absorption machines and multi-bed (Fig. 1-4) or thermal wave solid adsorption machine (Fig. 1-5). Also combinations of single and double effect chillers are possible. See [12] as an example. Such advanced configurations are thermodynamically more efficient but may be driven by a heating source at higher temperature and usually require complex hydronic arrangements and elaborate control strategies.

Table 1-1 summarises the technologies, the pairs used and compares the main properties and performance of the most used thermally driven products.

More details on Ab- and Adsorption Heat Pumps can be found in Final Report IEA HPT Annex 34 [3].

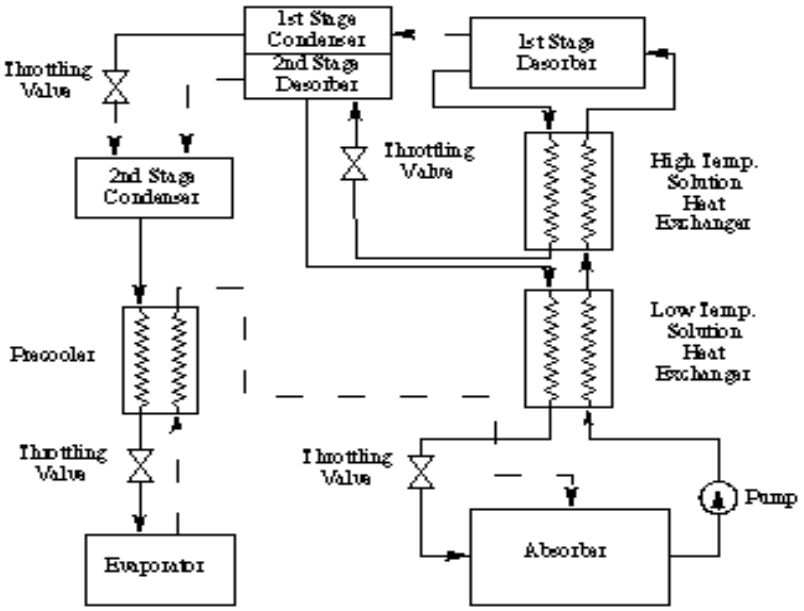

Fig. 1-4: Double effect absorption machine

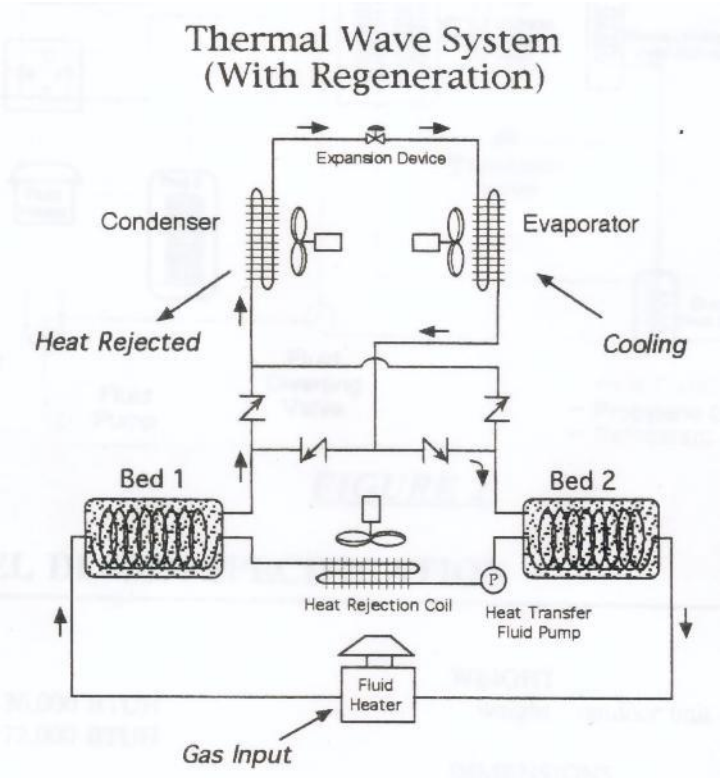

Fig. 1-5: Thermal wave adsorption heat pump patented by Shelton. - Wave Air Corporation, 1993. Solid-Sorption Gas Heat Pump: Technology and market description, internal report, August 1993.

Table 1-1: Available thermally driven sorption heat pumps

Process	Adsorption		Absorption		
Refrigerant/sorbent	water silica gel	water zeolite	water/LiBr Single-effect	water/LiBr double-effect	ammonia water
Temperature Heat source [°C]	60-90	75-150	75-110	135-200	100-180
Capacity [kW]	7.5-500	7-15	15-12000	200-6000	18-700
COP heat pumping	1.4-1.6	1.15-1.5	1.4-1.6	1.8-2.2	1.4-1.6
COP cooling	0.5-0.7	0.4-0.6	0.6-0.7	0.9-1.3	0.5-0.7

1.2.3 Alternative TDHP Technologies

Alternative TDHP technologies to ab- and adsorption cycles are available and were partly discussed within the IEA HPT Annex 43 framework. Such cycles are e.g.:

- TDHPs based on the double Rankine cycle (presented by École Polytechnique de Lausanne);
- Boostheat principle (GRDF, Boostheat)

BoostHeat (France) have been developing a 'thermal compressor' (not a sorption device) for nearly five years [13, 14]. It uses carbon dioxide as a working fluid with heat input at high temperature (600 °C) from a gas flame. Predicted performance (also proven in prototype measurements) is good at a GUE of 1.75 (gross, -10/55 °C) in a 20 kW unit. A 20 kW machine was launched in 2018 for sale in France, Germany, Belgium and Switzerland at a cost of €14,300 for the unit and an estimated installed cost of €21,000. The size is 1850x600x880 mm indoor unit and 1020x1130x500 mm outdoor unit [14].

Another option of a TDHP is the ORC-ORC cycle. ORC stands for organic Rankine cycle. In power plants a clockwise operated ORC process can be used to convert heat to mechanical (and with the usage of a generator into electrical) energy. A counterclockwise ORC can be used as heat pump powered by mechanical energy. In an ORC-ORC process the mechanical energy of the clockwise ORC is used to power the compressor of the counterclockwise ORC. Therefore such a device is a thermally driven heat pump. More information about this technology and first results of a new prototype can be found in [15–17].

Thermally driven heat pumps/air conditioners using environmental friendly refrigerants represent an energy efficient technology. Their use, in comparison with traditional electrically driven vapour compression systems, can create a benefit in terms of reduction of electricity peak load, mitigation of Global Warming Potential and of primary energy saving, especially when waste heat or solar energy are used as the driving energy (for cooling). Gas-driven heat pumps for heating represent a follow-up technology to make more efficient use of gas for heating and domestic hot water (DHW) preparation than conventional condensing or non-condensing gas boilers.

1.3 Market overview

The heat pump has been globally identified as a technology which can reduce greenhouse gas emissions locally, regionally and globally. Global heat pump market is projected to grow rapidly over the next few years, owing partly to the growing urbanization in the developing countries across the globe and the need to improve the air quality and reduce the greenhouse gas emissions simultaneously. According to a market research company, the global heat pump market was valued at USD 53.14 billion in 2019 and predicted to reach USD 98.39 billion by 2025 [18]. Due to technical improvements, the production cost and the market price should continue to decrease.
Global heat pump market share was driven until now mainly by the Asia Pacific region (China, India, the Philippines, Indonesia, and Malaysia). Subsidies to replace coal boilers with air-to-water heat pumps through the "Coal to Electricity" program in northern China helped raise sales to 1.3 million units in 2017 [19]. Also, the European heat pump market has grown by double-digit figures successively for the fourth year in a row. More than one million heat pumps were sold in Europe in 2018, or 12% more than in 2017.

That brings the total number of installed heat pumps to 11.8 million, or on average of one for every ten buildings, according to the European Heat Pump Association (EHPA). There is no consolidated data for the gas heat pump market.

1.3.1 Global demand for heating

Most of the energy consumption in the households worldwide can be attributed to space heating. Together with domestic hot water (DHW) production, it makes up to 60 % of the whole energy consumption in residential buildings and just about 50 % in the commercial ones [20]. Fig. 1-6 shows the world regions with heating and cooling demand, or both.

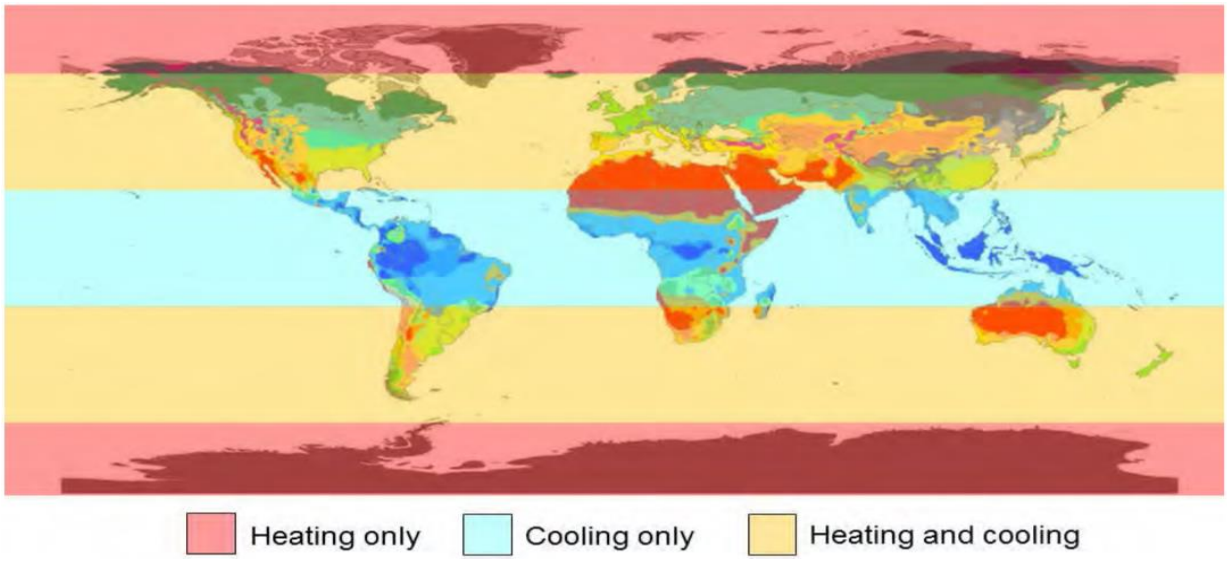

Fig. 1-6: Classification of the global heating and cooling regions. World map of Köppen-Geiger climate classification (university of Malbourne, 2010) as basis and category groups according to [21]

For example, the space and domestic hot water heating were the top two energy consuming applications in the U.S. homes in 2015, according to EIA[1]'s latest Residential Energy Consumption Survey (RECS). Similar share for heating can be also found in Europe.

According to the IEA Organization, the energy use for space and water heating worldwide has been decreasing steadily at a rate of 3 % annually since 2010 [19]. This trend should continue due to improvements in the energy efficiency in the main space heating markets. Fig. 1-7 shows the percentage of heat consumption for residential applications in different European countries:

[1] EIA: U.S. Energy Information Administration

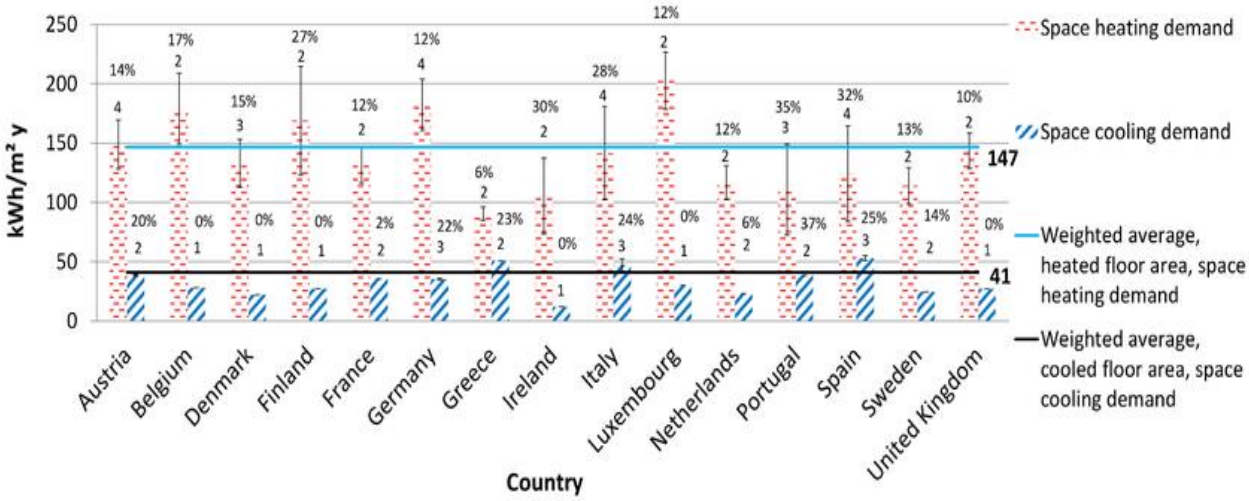

Fig. 1-7 Space heating and cooling demand per country, residential sector, kWh/m² y [22]

Until now, the energy consumption for heating was mainly based on fossil fuels and contributes with electricity generation for 25 % the global energy-related CO_2 emissions [23]. Fig. 1-8 shows that less than 35 % of the global heat demand in 2017 was covered by non-fossil fuel equipment. However, a growth in the sales of other heat equipment is expected, especially that of the heat pump units.

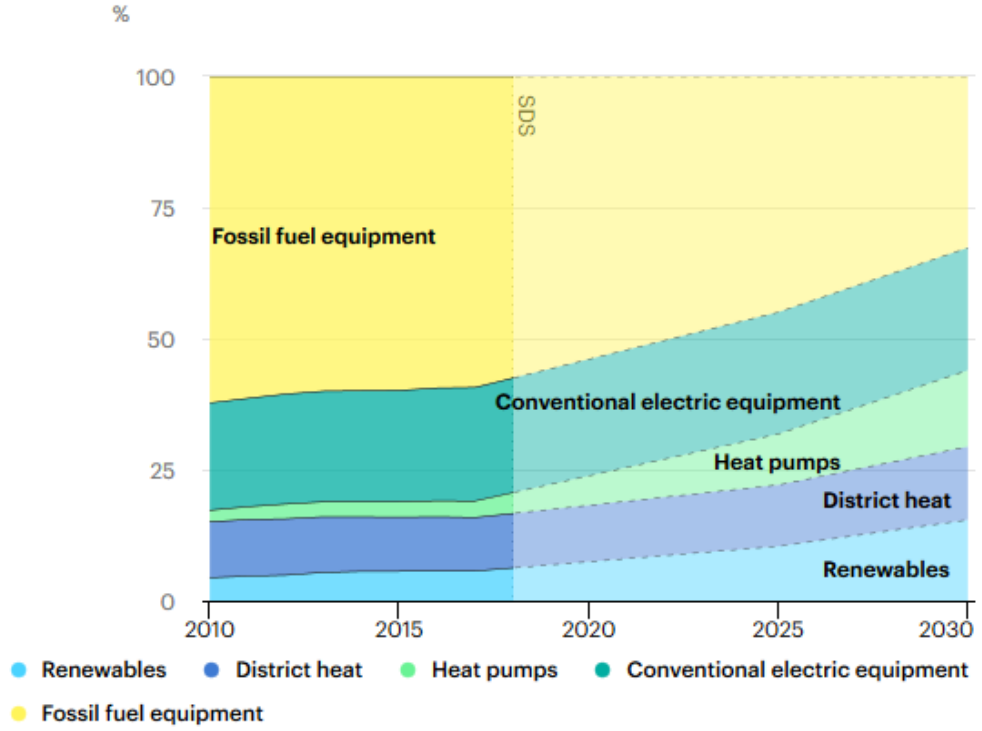

Fig. 1-8 Heating technology sales in the Sustainable Development Scenario, 2010-2030. Source: [19]

1.3.2 Global energy demand for heating – possible development trends

As stated above, the heating system plays an important role regarding the possible reduction of CO_2 emissions, especially in the existing building stock. Although fossil fuel based technologies currently dominate the market, a diversification of technologies, system hybridization and broader usage of energy storage as wellas an increasing share of renewable energy sources are expected. Moreover, new technologies should be introduced and find its place in the heating market until 2030. According to technology roadmap report for energy efficient builidings [24], the overall system optimization including heat production, transfer, storage and distribution should yield an additional efficiency increase, which will be accompanied with increasing investment costs in the residential sector. As shown in Fig. 1-9, the heat pump market is expected to grow further in the next years, which will obviously cause the rise of the accumulative investment expences in the residential sector, especially the introduction of the CHP[2] technology will be costly at the first implementation phase until 2030, but it is expected that the costs will fall in the subsequent period.

It is expected that the heating demand will continue to decrease due to investments in the building envelopes, but the price will be higher cooling demand due to climate changes and internal heat sources.

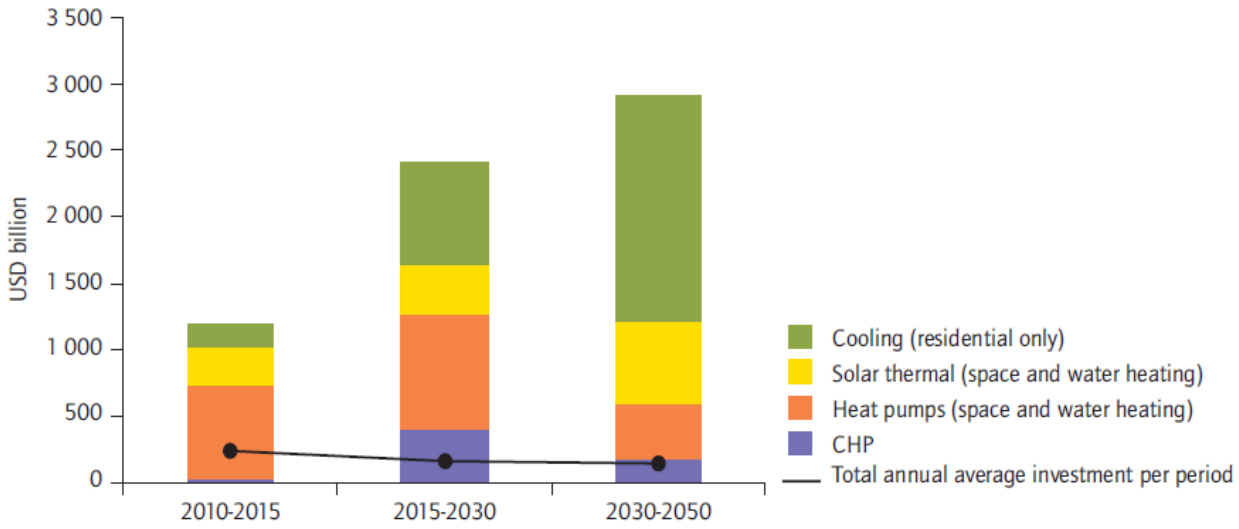

Fig. 1-9 Development of the market for heating and cooling technologies in the residential sector. Source: [24]

1.3.3 Germany – taking climate change into account

Since the global warming is unequivocal, many countries have set plans and goals to combat it. Germany is one of the countries, which is at the front line when it comes to plans and measures to reduce the greenhouse gas emissions. These measures are widely accepted by the general public with rising awareness of eco friendly behavior. With the climate action plan 2050, which was presented in November 2016, the German federal government confirmed and further specified its ambitious national

[2] CHP: Combined heat pump

climate protection goals. It's sticking also to its existing national goal of reducing its greenhouse gas emissions by at least 40 % by 2020 in comparison to 1990. Latest calculations showed that the goal was missed by around 5 %.

A study to identify the optimal technology mixtures both on the energy production and demand sides in terms of overall annual costs until 2050 was carried out at the Fraunhofer Institute for Solar Energy Systems and reported in [25]. The simulations were based on a comprehensive model of the overall German energy sector which takes into account the geographical, political, social, economic and technological characteristics of the location and forecasts their development in the upcoming decades. Having the minimum cumulative cost of the transition from the current energy system to an energy system with a substantial reduction of CO_2 emissions as the target function, the simulations yielded the optimal technology mix for a number of different target values.

A large number of simulations with different targets and boundary conditions were carried out in order to evaluate possible scenarios for future development. Almost all scenarios see a domination of heat pumps as heating systems in buildings by 2050. For example, one prominent scenario has a target of 85 % CO_2 emission reduction compared to 1990 values. This scenario seems to be slightly optimistic since the proclaimed policy of the German government sees an emission reduction of 80 % for the same time period.

According to this scenario, most of the electricity will be produced by solar and wind power plants by 2050. Fluctuating electricity production will require considerable storage capacities to ensure a reliable energy supply. In that context, production of combustibles by power-to-gas processes and usage of current gas grid and its storage potentials will play a very important role in the future. This means that, even in an electricity-dominated energy system, the need for efficient gas fired energy conversion appliances using existing gas infrastructure will most probably exist.

The scenario sees a domination of heat pumps as heating systems in buildings by 2035 and a complete takeover by late 2040s and foresees a considerable share of fuel driven heat pumps with a number of installed units measured in several hundred thousands to millions as the year 2050 approaches. Although this estimation seems to be rather enthusiastic considering just a couple of thousands of currently installed units and not more than a handful of products available on the market, it shows the potential of the technology if the presumed cost and efficiency targets are met and a decarbonisation of energy system is pushed at projected pace. Needless to say, this estimation is highly dependable on a number of factors, including further technology development and acceptance, future energy system configuration, development of energy prices, incentive policy and development of competing technologies, among many others.

The policy in Germany is currently discussing other measures to limit the CO_2 emissions such as the CO_2 pricing as a further instrument for the reduction of greenhouse gases. It sets an effective upper limit ("cap") on the total CO_2 emissions that may be emitted by energy-intensive plants in the power generation and manufacturing industries.

1.3.4 Heat pump market

1.3.4.1 Conventional heat pumps in Europe – current situation

Europe is estimated to be one of the largest contributing regions to the global heat pumps market in the years ahead. The European heat pump market growth in the last years is considerably influenced by the France's rapid market growth. Spain and Italy are at the second and third place in European heat pump market and together with France, they are making more than the half of the European heat pump sales every year [26]. From Fig. 1-10 a few trends in several EU countries can be observed. Air-to-air heat pump sales are advancing very quickly in the last years, followed by the air-to-water heat pump sales, which are also rising. The sales of air-to-water heat pumps rose sharply in the last three years and this trend is expected to continue in the following years. The sales of the ground source heat pumps (GSHPs) declined from 2011 until 2015 but then remained stable until present. Currently, it is not expected that this trend for GSHP will change in the next years [26].

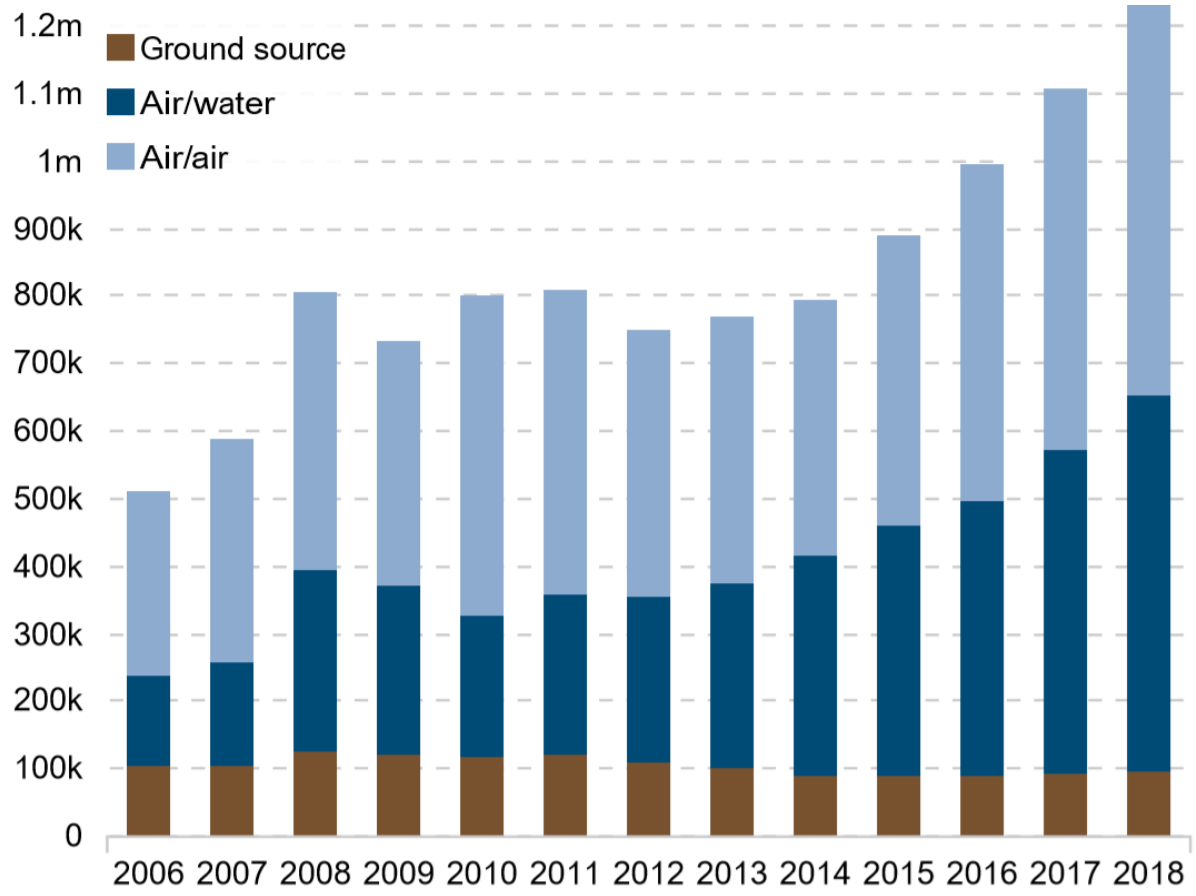

Fig. 1-10 Heat pump Sales development in Europe by technology, 2006-2018. Source: [27]

However, in order to achieve the European climate goals, the implementation of the heat pump technology should be pushed forward and needs a more determining governmental plans to obtain the desired results. In this context, the EHPA has estimated the potential sizes of heat pumps for several European heating markets and and compared it to the actual market sizes, Fig. 1-11. It can be seen that

in most of the countries, only a small share of the total estimated market potential is being used.

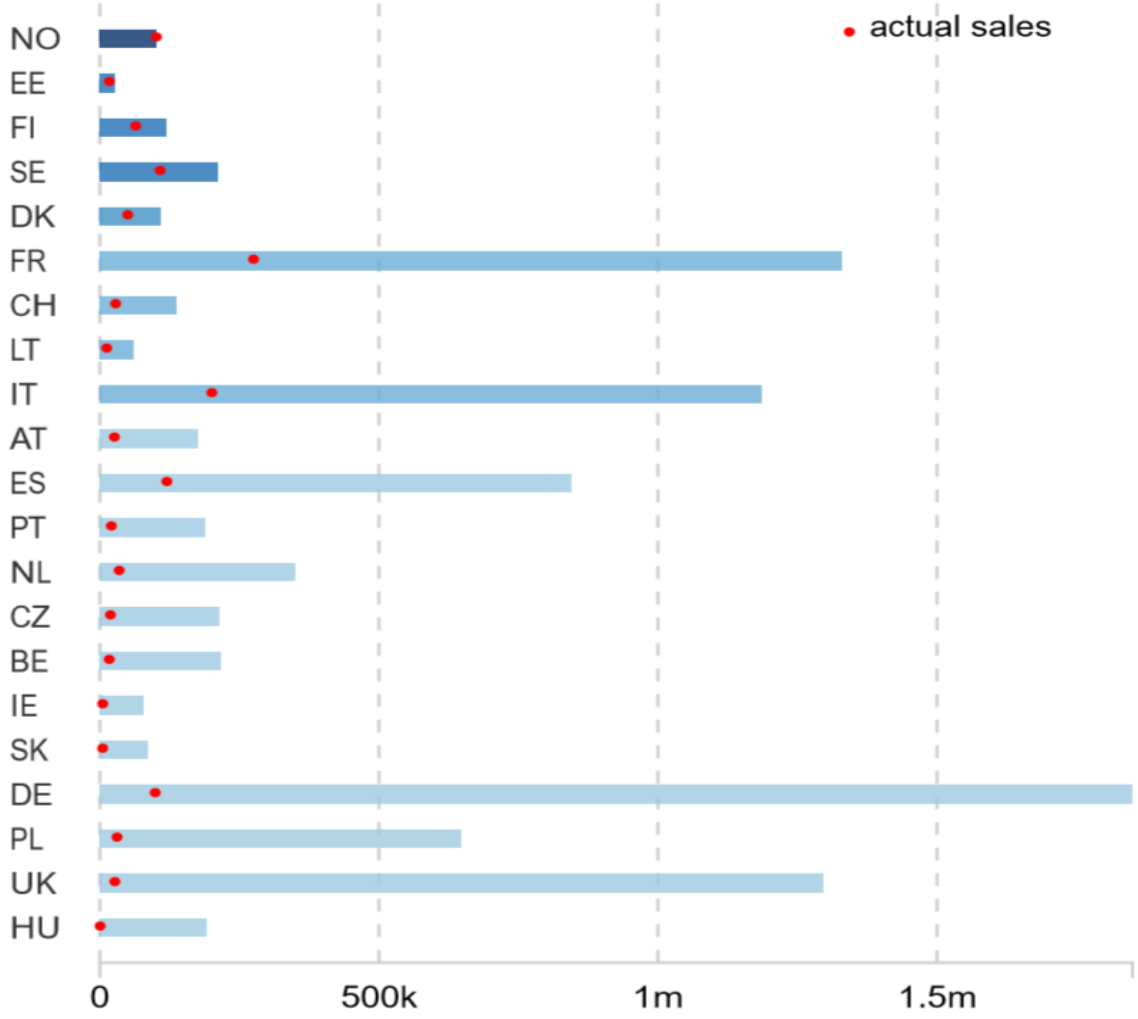

Fig. 1-11 Market potential vs. actual sales of heat pump units. Source: [27]

1.3.4.2 Conventional heat pumps in other regions – current situation

In the last decade, the heat pump market has witnessed a growth which was largely supported by different regulations in some countries with considerable heating and/or cooling demands. For example, the past decade has been a successful period for China's heat pump market. Alone in 2016, around 160,000 new air-to-water heat pumps were installed in Beijing only in the framework of a China wide "Coal to Electricity" program as a part of a wider effort to increase the usage of renewable energies and to improve the air quality. According to some sources, the local government managed to reach 76.8 % of the goal to exchange coal boilers with air source heat pumps [28] [29].

UK heat pump market for heat pumps is likely to double by 2025 following the announcement by the government that gas heating will be banned in all new homes built after 2025 [30]. Accordingly, there

will be a significant growth in UK's heat pump market in the next few years. According to one study by the CCC's[3], some 4.6 million heat pumps should be installed by 2030 [31] in the UK in order to achieve a emission reduction which would contribute to the global climate goals. That means, that 265,000 units would have to be installed every year. However, the current average annual sales over the last two years were just around 22,000 units per year according to BSRIA[4] [32]. Further, a substantial growth in heat market would correspond to a massive demand for electricity and would be a challenge for the UK's power grid.

Chine has currently the world's largest heat pump market [28]. As can be seen from the Fig. 1-12, China has also the world's largest market share of heat pumps in the residential heating market. It is followed by the USA, where the heat pump market is recovering and expanding, due to the new regulation in 2018, which required a higher efficiency (HSPF[5]) for heating systems in the USA. With these new standards it is expected to reach savings related to energy consumption of USD 12.2 billion after 30 years. Currently, there are 11.8 million units installed in the USA [33]. Inspite of the complicated regulation for geothermal heat pumps, their share was still growing steadily until 2016 to make about 11 % of the whole heat pump share in the USA. This increase war a result the 30 % federal tax credit, which lasted only until the end of 2016 and therefore, a decrease of the geothermal heat pumps shipments is expected after that [34].

Rapid increase in the number of installed units in Europe has been observed in the Netherlands (+62.8 %) and the Republic of Ireland (+47.0 %) [35]. However, these markets are relatively small and the absolute number of units sold does not significantly contribute to the overall European sales.

[3] CCC: the Committee on Climate Change

[4] the Building Services Research and Information Association

[5] Heating Season Performance Factor: the higher the HSPF, the more efficient the heating performance of the heat pump.

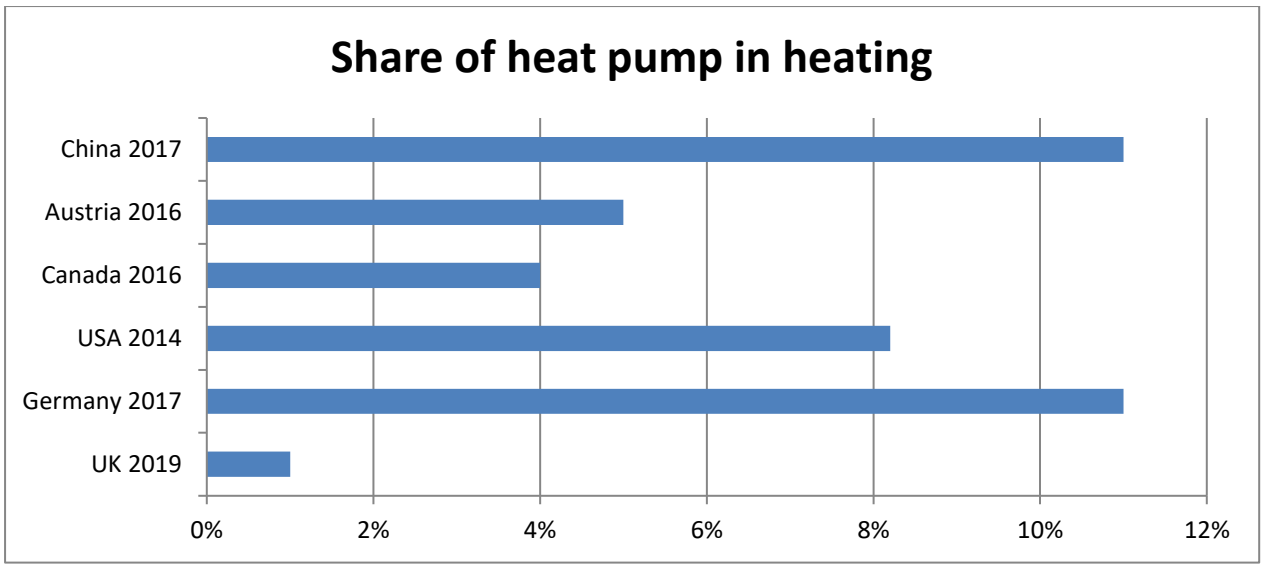

Fig. 1-12 Share of heat pump technology for heating purpose in different countries (Personal collection, Sources:[for UK [35], for China [28], for Austria [36], for Canada [34], for the USA [37], for Germany [38])

1.3.4.3 Fuel driven heat pump market – current situation and perspectives

There are no consolidated data for the fuel driven heat pump market. Some estimation go from several hundreds of units installed annually. Since its market entry in the mid-2000s and until 2010, only one manufacturer (Robur S.p.A.) of gas driven heat pumps was active on the European market. With heating capacities of around 40 kW the appliances were used mainly in small commercial installations. From 2010 onwards, a number of products aiming at single family house market – both new and retrofit – were introduced by major heating equipment manufacturers. All available products were built using sorption technologies. However, almost all these products have been removed from the market in the last 2-3 years leaving Robur to be the sole provider of this technology once again.

Two main concepts were being pursued by the manufacturers: bivalent appliances with an adsorption heat pump using water as refrigerant supported by a modulating condensing boiler. These units need a heat source above 0 °C to avoid freezing – a ground heat source or solar collectors are needed. The adsorption heat pumps were sized to cover only one part of the nominal load up to ca. 4-5 kW. The concept did not prove to be interesting for the market and these appliances were withdrawn by the manufacturers. Absorption appliances are monovalent machines and run with ammonia-water working pair. Due to a lower freezing point of ammonia, they can operate with ambient air as heat source at temperatures well below 0 °C. These units can modulate their output capacities in the range of ca. 30 to 100 % of nominal thermal power.

									
Manufacturer	Viessmann		Vaillant		Robur			Bosch Thermotechnik	BoostHeat
Model	Vitosorp 200-F D2RA 001|002	Vitosorp 200-F D2RA 003|004	zeoTHERM VAS 106/4	zeoTHERM VAS 156/4	GAHP - GS | WS [5]	GAHP - A [6]	K18	Junkers Supraeco 9000i-G Buderus Logatherm GWPS(L)192-18 i	BOOSTHEAT.20
Nom. Capacity [kW] [1]	11.00	16.70	10.20	15.00	42.61 | 43.90	41.00	17.6	18.00 [3]	20 kW
Technology	adsorption		adsorption		absorption			absorption	mechanical compression
Working pair	water/zeolite		water/zeolite		ammonia/water			ammonia/water	carbon dioxide
Heat source	geothermal | solar		solar		borehole | ground water	air	air	borehole | air	air | borehole | ground water
Aux. heat source	condensing gas boiler		condensing gas boiler		-	-	-	-	condensing gas boiler
Annual GUE [%] [1]	1.38 | 1.39	1.31 | 1.35	1.31	1.22	1.58 | 1.53	1.36	-	>1,25	1.95 | 1.65 [7]
Nominal GUE [%]							1.69 [2]	1.70 [4]	2.29 [8]
Market entry	2013	2013	2010	2012	2004	2004	2016	2016 (planned)	2019
Not available since	2017	2017	2016	2016	-	-	-	2018 (abandoned)	-

[1] According to VDI4650-2 for supply and return temperatures 35-28°C, except values for Robur K18 and Bosch Thermotechnik. Source: www.bafa.de
[2] According to EN12309-2 for air inlet temperature 7 °C and water supply temperature 35 °C. Source: www.robur.it
[3] According to the manufacturer for brine inlet temperature at heat source 0 °C and supply temperature of 65 °C. Source: www.junkers.com
[4] Test conditions not known. Source: www.junkers.com
[5] Products with same specifications available from Bosch Thermotechnik (Logatherm GWPS/GWPW 41), and OERTLI-ROHLEDER (GAWP 40 SW)
[6] Products with same specifications available from Bosch Thermotechnik (Logatherm GWPL 41), OERTLI-ROHLEDER (GAWP 35 LW) and Remeha (GAS HP 35 A)
[7] According to VDI4650-2 for supply and return temperatures 35-28°C
[8] According to VDI4650-2 for supply and return temperatures 55-45°C

Fig. 1-13 Overview of available (marked green) and withdrawn (marked red) GHPs in the European market with their main characteristics

In 2019, a start-up company BOOSTHEAT SA brought up their heat pump to the market after eight years of development. Unlike all other gas driven appliances for heating, it is not based on sorption technology but uses an own-developed mechanical compression system.

It is expected that the main market, due to its size, availability of gas mains and technology characteristics will be boiler replacement, especially in countries which are traditionally dominated by this fuel. Fig. 1-13 gives an overview of currently available and withdrawn products with their main characteristics.

Even though there are only a few products on the market for residential heating and sanitary hot water application and a slow market development, a considerable amount of R&D activity is reported from many countries. The current EU legislative, including the Ecodesign and the Energy Labelling Regulations include the technology, which is a very important market drive. Further, gas heat pumps are explicitly eligible to obtain the Heat Pump Keymark, the main voluntary quality scheme in Europe – also a very important signal for the end consumers, as well as governmental subsidies, which are available for fuel driven heat pumps in most of the principal European markets. There are testing and performance standards available – both on the CEN and national levels. The CEN standards are currently in the process of harmonisation with the Energy Labelling directive.

The main driver for these R&D activities in Europe is to find an efficient solution for retrofit for heating in countries with well-developed gas grid. In the USA, the legislation on the minimum efficiency of sanitary water heaters created a need for more efficient gas-fired appliances. Although the technology is seen in

many studies as an important one in a future transitional energy system, especially in the residential sector, the success of it depends on a number of boundary conditions. Success of current development projects as well as further developments in the fields of material science, legislation, gas grid decarbonisation, governmental policies and incentives as well as advances of competing technologies (e.g. fuel cells) – just to mention a few – will have an influence on the market development in the upcoming years.

2. Apparatus Technology, Material and Component Development and Technology Transfer

2.1 Adsorption components

2.1.1 Overview on adsorber developments

University of Warwick Carbon/Ammonia Adsorber Development

Since ammonia is a high-pressure refrigerant, mass transfer is less of a critical issue in carbon/ammonia adsorption heat pumps. The main challenge is to reduce the conduction path length in the low conductivity active carbon material whilst minimising the thermal mass of the heat exchanger. Previous designs at the University of Warwick used a shell and micro-tube heat exchanger as shown in Fig. 2-1 below. The 1.2 mm diameter tubes were on a 3 mm pitch, which gave a mean conduction path length of only 0.5 mm.

Fig. 2-1: Shell and micro-tube sorption generator core

High specific heating powers of circa 2 kW kg^{-1} adsorbent were achieved with a low thermal mass of around 1 kg of stainless steel tube per kg of carbon. The drawback of this design was the number of tubes required (around 3,000 for a 10 kW heat pump). Although the cost of the tubes was low, each

generator required thousands of nickel brazed joints in the end plates – an expensive process with a high probability of failure given the large number of joints.

This led to the development of a shell and finned tube heat exchanger design in order to reduce the number of tubes required and reduce the production cost. This design achieves the same specific heating power and thermal mass ratio as the micro-tube design but with a two orders of magnitude reduction in the number of tubes required (s. Fig. 2-2). The design has been proven in small-scale large temperature jump tests and is now ready for incorporation in a laboratory proof of concept system.

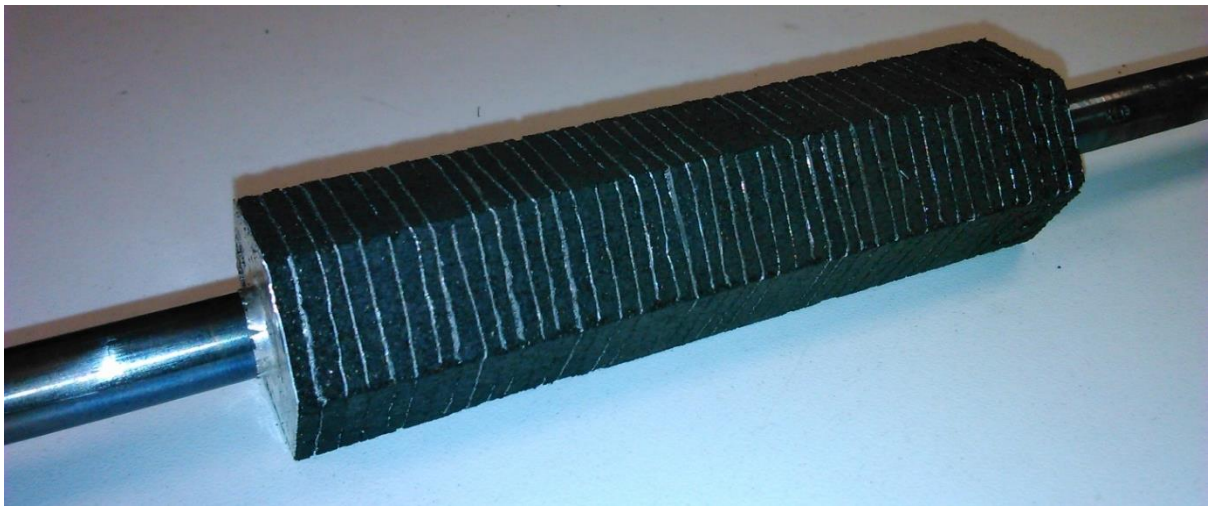

Fig. 2-2: Shell and finned tube heat exchanger

The target is to produce a 10 kW heat pump with a seasonal GUE of around 1.2 for a UK climate with 2 generators of approximately 6 litres each. Fig. 2-3 below shows the predicted performance for 55°C delivery temperature and 10°C ambient.

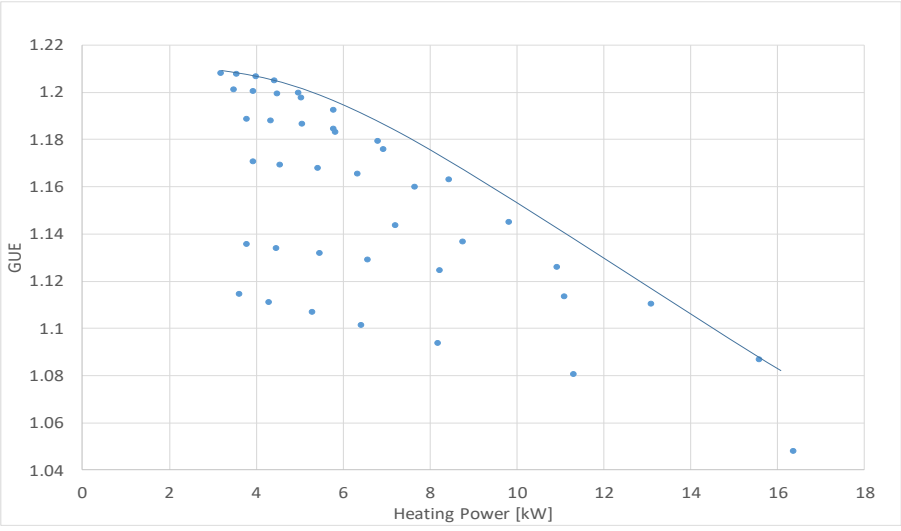

Fig. 2-3 Warwick heat pump model performance prediction

Fraunhofer ISE / Fahrenheit GmbH Alumnium Fiber Adsorber Development

Fibrous structures as shown in Fig. 2-4 have a good thermal conductivity and a high surface area relative to their volume, more than 7000 m^2/m^3 [39]. The partial-support-transformation (PST) technique as presented by Bauer et al. [40] makes it possible to crystallize the zeo-type adsorbent SAPO-34 directly on an aluminum surface.

Fig. 2-4: Fibrous structure with SAPO-34 directly crystallized on the fibers, the dimensions of the fibrous structure are 20x20x5 mm

These two technologies were combined in the research projects WISA-THOKA and ADOSO in order to manufacture adsorption heat exchangers based on fibrous structures [41–45]. Aluminum fibres with a diameter of approximately 100-200 µm are sintered together, brazed onto the aluminum flat tubes and finally coated with adsorbent crystals [42]. The experimental results for directly crystallized fibrous structures showed the potential of this approach to increase the power density [42].

In the course of the project ADOSO [44] a complete adsorption module including two fiber heat exchangers for adsorber and a combined evaporator / condenser was built by Fahrenheit GmbH [43]. The adsorption heat exchanger is shown in Fig. 2-5. The fibres have a mean diameter of approximately 130 µm. The mean thickness of the SAPO-34 crystallite layer is approximately 50 µm. The amount of adsorbent (dry mass) is 3.3 kg.

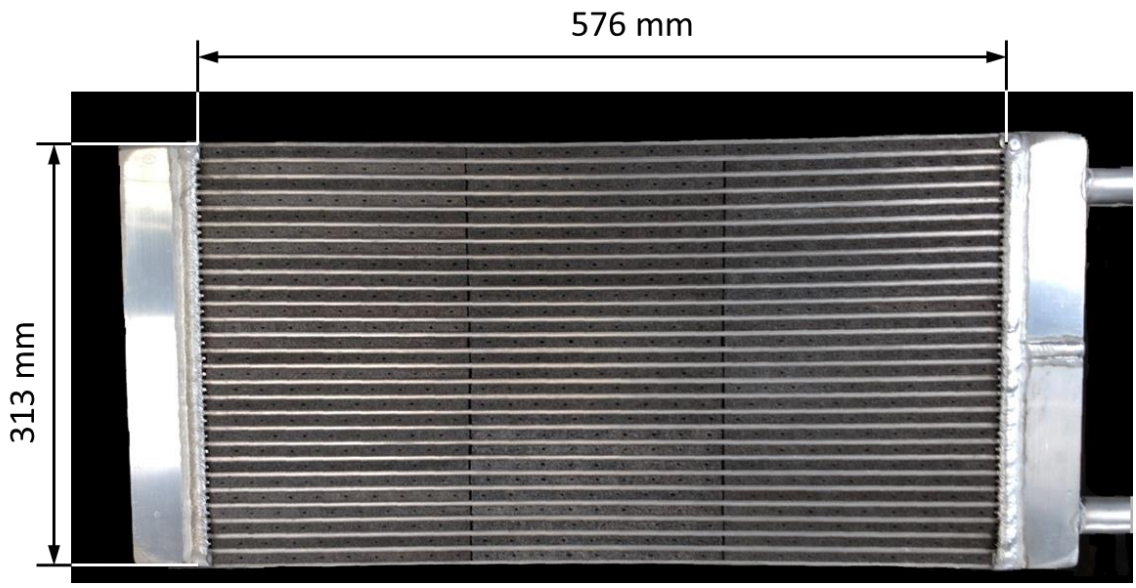

Fig. 2-5: Fiber heat exchanger developed and tested by Fraunhofer ISE and Fahrenheit GmbH, the heat exchanger with headers has a length of 700 mm, the width is 45 mm. The volume with headers is approximately 10 liters.

In Table 2-1 the temperature boundary conditions and the results for efficiency and power are listed. The values for the efficiency and the power are plotted in Fig. 2-6. Of course, the efficiency depends strongly on the temperature levels of evaporation and adsorption / condensation. At an elevated adsorption / condensation temperature of 45 °C the SAPO-34 cannot be desorbed anymore, resulting in a low value for the efficiency. The efficiency is below 1 because of the heating and cooling of the thermal mass of the combined evaporator / condenser.

Table 2-1: Experimentally obtained efficiency and averaged power for the adsorption module with fiber heat exchangers

No of experiment	Temperature triple	Half cycle time in s	COP_{heat}	P_{heat} in kW
1	85 / 27 / 19 °C	200	1.33	10.9
2	90 / 32 / 12 °C	200	1.20	9.3
3	90 / 45 /12 °C	200	0.72	3.0
4	85 / 27 / 19 °C	300	1.37	8.5
5	90 / 25 / 21 °C	300	1.39	9.0
6	90 / 35 / 15 °C	300	1.25	6.9

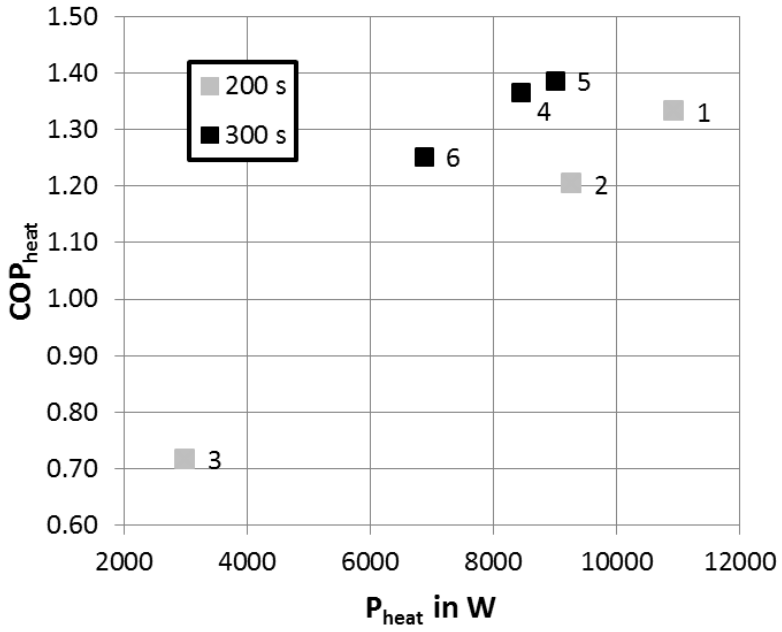

Fig. 2-6: Heating efficiency and power for different measurements of the adsorption module with fiber heat exchangers, the numbers 1-6 refer to Table 2-1, the colours of the symbols indicate the half cycle time.

The mean power of all measurements (excluding No. 3) is approximately 8900 W, resulting in a power density of 890 W/dm³ relative to the volume of the adsorption heat exchanger (10 dm³) and 260 W/dm³ relative to the volume of the module (34.3 dm³).

The measurements of the module indicate that the thermal mass of the housing plays a role for the efficiency. One phenomenon is the heat loss, since heat is transferred from adsorber and the combined evaporator / condenser to the housing and from the housing to the ambient. Another effect is the condensation of water vapour on the cold parts of the housing, this lowers the efficiency in case of heating application. In case of the cooling application, the evaporation of the condensed water on the housing surface will also lower the efficiency.

2.1.2 Evaporator developments

Water is obviously considered as one of the best alternative choices to standard refrigerants, for its zero Global Warming Potential (GWP) and zero Ozone Depletion Potential (ODP) and its abundance, and is one of the most employed in adsorption systems. Nevertheless, under the operating conditions typical of a heat pump, water evaporation occurs at low pressures, i.e. under sub-atmospheric pressures.

In these conditions, water is close to its triple point (0.611 kPa, 0.01 °C) and it was experimentally demonstrated that the factors that mostly influence its phase change significantly differ from those observed in water evaporation at higher pressures. Among the other factors, the pressure increase due to the height of the liquid is of the same order of magnitude of saturation pressure, thus cannot be neglected. Accordingly, dedicated experimental and numerical analyses are needed to understand the complex phenomena occurring under these conditions.

At the CNR ITAE, a new testing rig was designed and realized to investigate small, but relevant, evaporator scale (with evaporation capacity up to 20 kW). The testing rig is flexible enough to let investigating evaporators working under different operating conditions (e.g. pool boiling, thin-film, falling film).

A schematic layout is shown in Fig. 2-7. The testing rig mainly consists of two vacuum chambers, the condenser (1 in Fig. 2-7) and the evaporator (2 in Fig. 2-7), connected by means of two electrically-actuated pneumatic vacuum valves. In addition, a tube with a manual valve connecting condenser to the evaporator, allows the control of the water level inside the evaporator. The condenser is thermostated by means of a big aluminium fin-and-tube heat exchanger (4), whereas the temperature level of the pool of the evaporator, when operate as stagnant pool, is controlled by means of a spiral finned coil copper heat exchanger (5). A vacuum circuit is used to keep the pressure at the desired level. The chamber of the evaporator is equipped with two quartz viewports, for visual inspection.

The side view of the evaporator testing chamber is represented in Fig. 2-8.

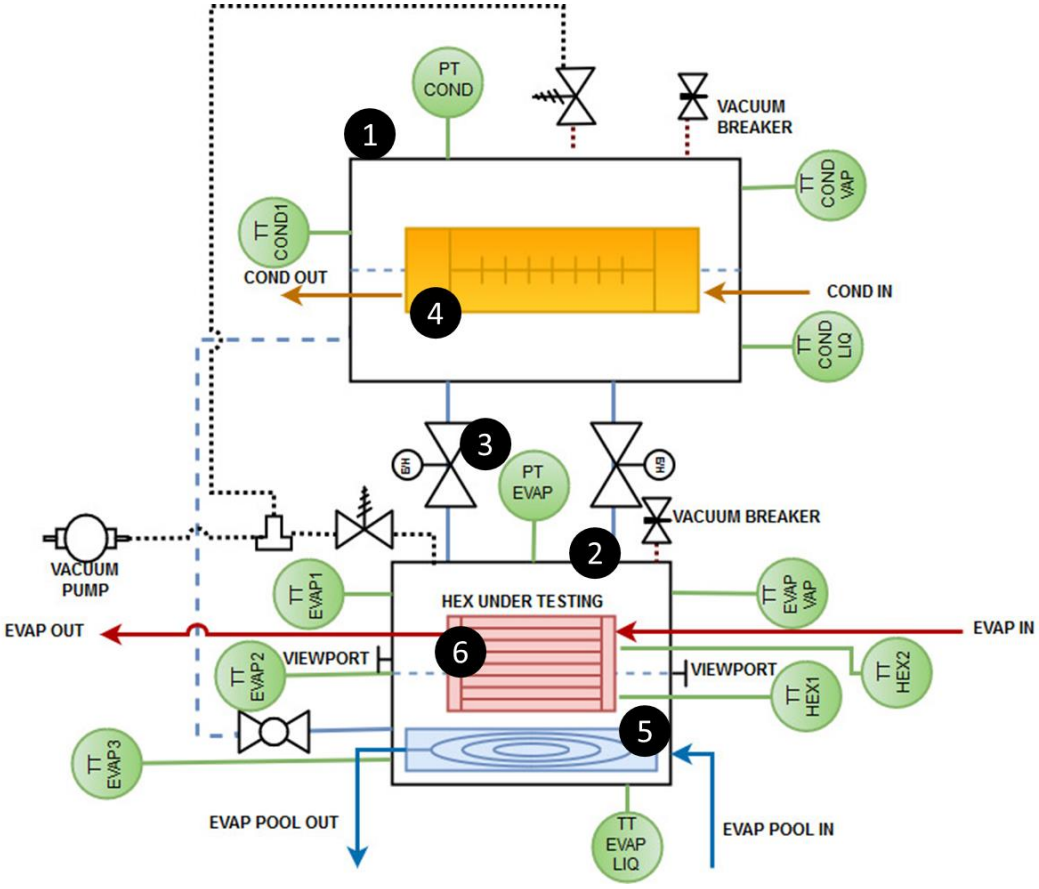

Fig. 2-7: Schematic of the testing rig for the characterization of evaporators under sub-atmospheric conditions at CNR ITAE.

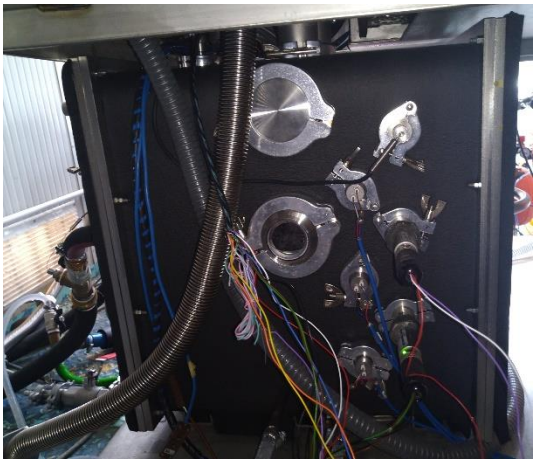

Fig. 2-8: Side view of the evaporator vacuum chamber where the HEX is tested.

Preliminary tests were conducted on a pool boiling evaporator using a finned flat-tube aluminium HEX, characterized by the following dimension: 200mm x 272mm with 20 fluid passages of 45mm depth and 2.5 fin pitch. These tests were performed in horizontal position. The main aim is to investigate almost state-of-the-art HEXs, easily available on the market and at a reasonable price, to understand whether these solutions are applicable or not in order to limit the cost of this component.

The first investigated effect is the difference between the evaporator temperature and the pool temperature, defined as ΔT_{pool}. Fig. 2-9 shows how the ΔT_{pool} varies as a function of the HTF flow rate and the ΔT between the evaporator and condenser. The inlet temperature at the evaporator was always fixed at 40 °C. It can be noticed that under these conditions the ΔT_{pool} decreases with increasing the HTF flow rate, while the condenser-evaporator temperature difference has a minor role.

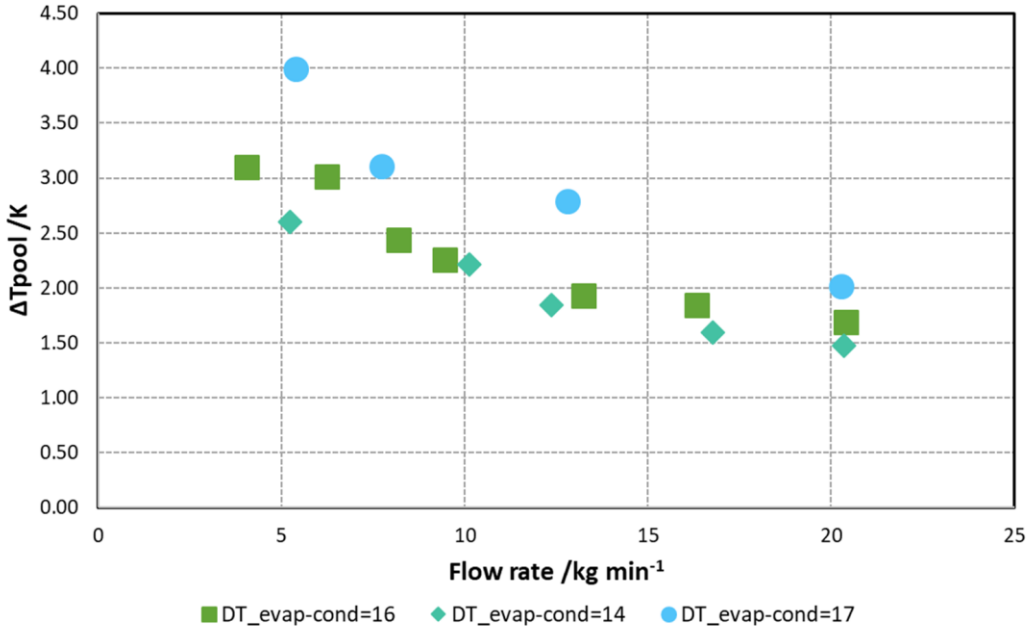

Fig. 2-9: Effect of the flow rate and the condenser-evaporator temperature difference on ΔT_{pool}.

Fig. 2-10 shows the effect of the flow rate on the evaporation power and overall heat transfer coefficient, respectively. The tests are performed using two different ΔTe-c, i.e. 15 K and 19 K. The higher the HTF flow rate the higher is the evaporation power measured. Similarly, it increases with increasing ΔTe-c: for ΔTe-c of 15 K, it ranges from 1.6 to 2.7 kW, whereas for ΔTe-c=19 K, it ranges from 2.2 kW to 2.9 kW. There is a limit value of about 2.8-2.9 kW that might be considered as the limit of the heat exchanger under the conditions tested. The corresponding overall heat transfer coefficients are reported: for ΔTe-c of 15 K, it ranges from 190 to 427 W/(m^{2}K), whereas for ΔTe-c=19 K, it ranges from 289 W/(m^{2}K) to 607 W/(m^{2}K).

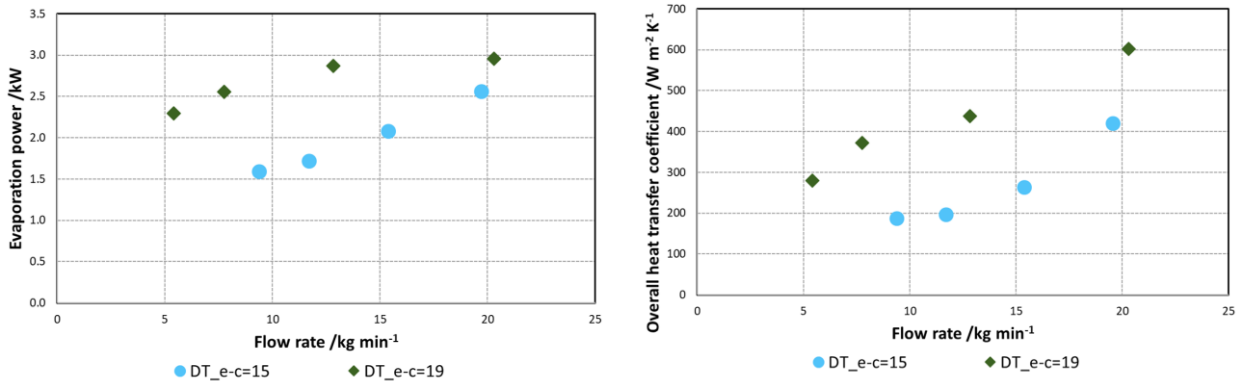

Fig. 2-10: Combined effect of the flow rate and the ΔTc-e on the evaporation power (left-hand side) and on the overall heat transfer coefficient (right-hand side).

The preliminary results reported demonstrate that there is still a strong limitation on the evaporation side, mainly due to the low pressure at which the evaporator works. Nevertheless, even a simple finned flat-tube HEX without any special and expensive surface treatment can reach up to 600 W/(m^{2}K). Future development will be on this way, to optimize the HEX configuration but keeping the cost as low as possible to make it competitive for market applications.

2.2 New developments on adsorption materials and material database

2.2.1 MOFs

One of the key component within an adsorption heat pump or chiller is the sorption material. Whereas silica gels, zeolites, activated carbons or silica-aluminophosphates are well known and have been evaluated for the use in these processes, first evaluations of Metal-organic frameworks (MOFs) for the use with water as adsorptive started in 2009 [46].

Since then, metal-organic frameworks received continuous attention due to their unsurpassed porosity and chemical variability, which both originate from the inherent, molecular cluster linker concept [47]. Based on this “molecular lego” concept, from a thermodynamic point of view, MOFs offer a new dimension for the cycle of choice, as adsorption characteristics can be tuned in a broad range. Eg. the

pore volume and the pore size might be designed by the choice of the organic linker length as already shown by the iso-reticular approach of Yaghi [48]. In addition, due to the narrow pore distribution resulting from the crystalline nature of these materials, the adsorption isotherms are typically s-shaped and the relative pressure, at which pore filling occurs, depends on the pore geometry and the nature of the linker.

Thus, significant improvements in terms of energy efficiency and density has been seen and a wide investigation started. Out of the various possible structures the most common structures for the use with water are depicted in Fig. 2-11 included on top the organic linker, the underlying metal-node and the resulting pore structure [49]. It is common practice to name metal-organic frameworks according to their origin facility, e.g. MIL = Material of Institute Lavoisier, CAU = Christian Albrechts University Kiel, HKUST – HongKong University of Science and Technology. For further details, the reader is referred to the exhausting review articles in scientific literature.

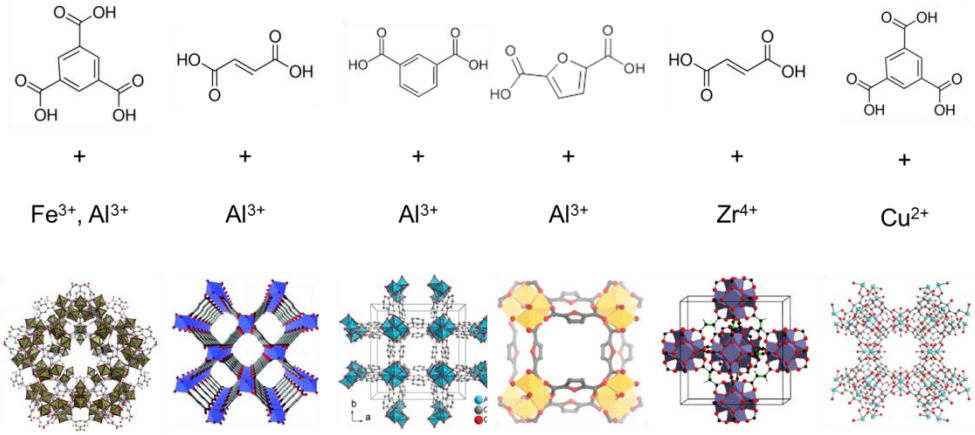

Fig. 2-11. Selected organic linkers (top) and possible metal-clusters (middle) to form the final 3-D framework (bottom). Depicted from left to right organic linkers: benzene-1,3,5-tricarboxylic acid (BTC), fumaric acid (FUM), benzene-1,3-dicarboxylic acid (BDC), 2,5-furandicarboxylic acid (FDC), FUM and again BTC. Combined with the most common metal nodes like iron, aluminium, zircon and copper the following structures from left to right are build: MIL-100, Al-Fumarate, CAU-10-H, MIL-160, Zr-Fumarate, CU-BTC (HKUST-1).

To evaluate the performance of the materials the adsorption equilibrium isotherms or isobars are usually considered. An initial overview of the adsorption capacity and shape of isotherms is given in Fig. 2-12.

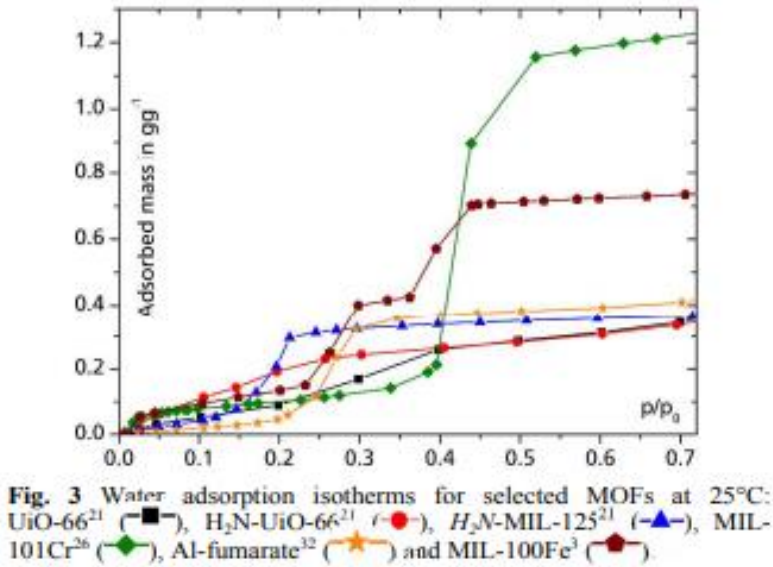

Fig. 3 Water adsorption isotherms for selected MOFs at 25°C: UiO-66[21] (■), H_2N-UiO-66[21] (●), H_2N-MIL-125[21] (▲), MIL-101Cr[26] (◆), Al-fumarate[32] (★) and MIL-100Fe[3] (⬟)

Fig. 2-12. Overview of water adsorption isotherms, taken from [50].

Based on the equilibrium data an first estimation of an achievable COP in a thermally driven heat pump system has been reported by de Lange et al. [51] (s. Fig. 2-13).

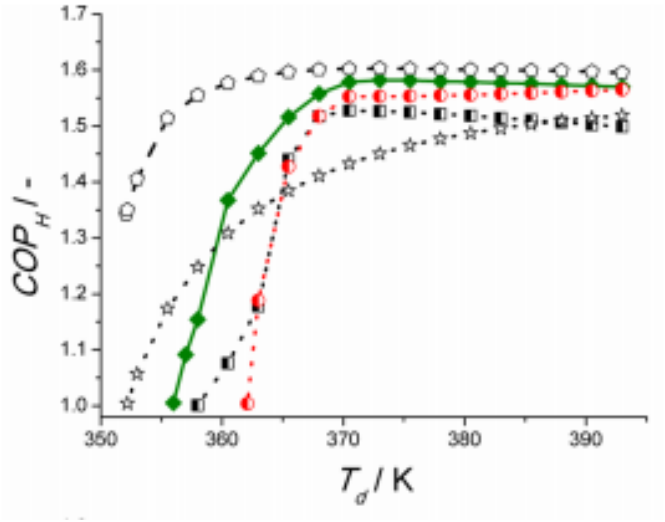

Fig. 2-13: Coefficient of performance based an water adsorption equilibrium data of pure MOF materials taken from ref.[6] for an evaporator temperature of 288K and adsorption temperature of 318K for MOF-801(Zr) (green), MIL-53(Cr) (black), Zn(BDC) (DABCO) (red), compared to activated carbon (star, black dotted line) and AQSOA-Z02 (open symbol, black dotted line).

It is noticeable throughout the state of the art that amongst the most promising metal-organic frameworks for water adsorption applications are mainly materials based on Al, Zr, Fe or Cr as Zn based MOFs tends to be instable under water vapor atmosphere.

Finely powdered, as MOFs normally occur after synthesis, they are not applicable in most industrial processes, nor for heat transformation. Thus different approaches to overcome this issue were developed in recent years, namely binder based coatings and direct crystallization via a thermal gradient method [52].

As final step towards an sorptive device, full scale coated heat exchanger were developed and the performance measured under real application conditions [53, 54].

As an conclusion of the depicted development it can be stated, that improvements for adsorption driven heat pumps by use of metal-organic framework materials are possible but depend strongly on the application conditions.

First of all, the high porosity of the materials come alongside with a low density. Second, the materials show typically a lower hydrophilicity compared to zeolites and thus high temperature spread result in lower coefficient of performance.

2.2.2 Salthydrates, Salt with ammonia

A large number of hygroscopic salts has been suggested as an active component of an sorption system namely CaCl2, Al2(SO4)3, MgSO4, MgCl2, LiCl, LiBr and CaNO3. Due to the fact that the salts tends to form agglomerations or aggregation composites like “Salt inside Porous Matrix” (CSPMs) were developed.

Hereby the one component is a host matrix and the other one is an inorganic salt placed inside the matrix pores. The CSPM have been recognized as promising materials for thermally driven heat pump systems due to their enhanced sorption capacity to common working fluids (water,methanol/ethanol, ammonia). These sorbents are characterized by s-shaped sorption isotherms and tunable adsorption behavior that provides a promising avenue for their application for adsorption heat transformation and storage. The salt S being the main sorbing component of CSPMs reacts with a sorbate vapor V (water, methanol/ethanol, ammonia) that results in the formation of a complex S,nV (hydrate, methanolate etc.).

The role of the porous matrix is also of high importance. It promotes dispersing the salt crystallites on the pore surface, prevents their aggregation and provides heat and mass transport to the salt particles located inside the matrix.

2.2.3 Material database/SorpPropLib

The equilibrium vapor pressure for the sorption materials is critical to the performance of the sorption heat pump systems. An enormous amount of studies have been carried out to identify the correlations of the refrigerant equilibrium vapor pressure with the the sorbent temperature and composition. The vapor pressure properties of working fluids are reported in the literature in a variety of ways, which impedes wide-ranging cross comparisons or screening studies for novel applications.

Therefore, a database for equilibrium vapor pressure properties of both adsorption and absorption materials has been compiled, and the database program SorpSim [55] with the library SorpPropLib [56,

57] has been developed based on the compiled database to provide fast isotherm inquires and support computer simulation of sorption systems.

2.2.3.1 Isotherm database of sorption materials

In this work readily usable vapor pressure sorption properties for 446 working pair correlations for 251 working pairs and 38 refrigerants are compiled. The refrigerants can be broadly categorized into inorganics, hydrocarbons (non-fluorinated), alcohols, and fluorocarbons, and the working pairs included are listed in the Table 2-2 below.

Table 2-2: Summary of sorption working pairs included in the isotherm database

Category	Refrigerant (sorbate)	# of sorbents included
Inorganic	Water	38
	Ammonia	45
	CO_2	12
Hydrocarbon	Propane	6
	Methane	8
	Propylene	5
	Butane	4
	Hexane	1
	Benzene	5
	Toluene	1
	Cyclohexane	4
	Cyclohexene	1
	Acetone	4
	TFE	3
	THF	2
Alcohol	Ethanol	18
	Methanol	11
	Propanol	3

Category	Refrigerant (sorbate)	# of sorbents included
Fluorocarbons	R12	3
	R13B1	1
	R22	4
	R23	1
	R32	13
	R123	1
	R124	1
	R125	11
	R134a	21
	R143a	8
	R152a	6
	R407C	1
	R404A	1
	R410A	2
	R507A	1
	R1234ze(E)	2
	R134a/R227ca	1
	R125/R143a	1
	R22/R142b	1

Numerous functional forms have been found useful for expressing the vapor equilibrium properties of sorption working pairs (s. Table 6-1 in the appendix 6.3). Some of these are derived from first principles, and others are almost purely empirical in origin. In general, solid adsorption working pairs use one of a handful of functional forms with a strong basis in physical first principles: Dubinin-Astakhov, Toth, Dual Site Sips, or Langmuir. In contrast, liquid absorption working pairs have a greater diversity of commonly

used functional forms and also use several that defy classification (referred to herein as “custom” correlations). Some expressions for absorption working pairs are traceable to a first principles analysis (Antoine, Heil). Most use a hybrid approach, where a fundamental expression for the refrigerant vapor pressure is modified by an empirical term.

However, there is a challenge to assemble a database from diverse sources in the literature due to the variations in equation form. For example, a particular functional form (such as Toth) may have originally had a single form. However, over time various researchers have made their own tweaks to the form, resulting in a Toth family of forms. Each member of the family has a similar mathematical form, but the exact number and location of fitting constants vary. In this work, we have genericized each family so that all results in the literature reviewed can be expressed in one master family equation. The master family equations for both adsorption and absorption are summarized in the two tables below.

The adsorption isotherm equations often express the equilibrium uptake (Y) as the function of the the sorbent temperate and vapor pressure. The only exception is the van’t Hoff equation for chemical adsorption working pairs, where the equilibrium vapor pressure is the function of only the sorbent temperature. The coefficients in these equations for each working pair are collected and compiled in the database tables in the appendix 6.4.

For absorption working pairs (s. also summary of the master equation forms of equilibrium correlations in Table 6-2 in the appendix 6.3), the correlations often express the equilibrium vapor pressure as the function of the temperature and concentration of the sorbate in the mixture solution in Antoine and Dühring equations. For the mixing rules based on Peng-Robinson (PR) or Soave-Redlich-Kwong (SRK) equation of state (EOS), the equilibrium vapor pressure is written as:

$$P = \frac{R \cdot T}{V_m - b} - \frac{\alpha(T)}{V_m^2 + m \cdot b \cdot V_m + n \cdot b^2}$$

$$b = b_c \cdot \frac{R \cdot T_c}{P_c}$$

$$\alpha(T_r, \omega) = [1 + \kappa_0(1 - T_r^{0.5})]^2$$

$$\kappa_0 = \sum_{i=0}^{3} c_i * \omega^i$$

The the mixing rules calculate the $\alpha(T)$ and b for the working pair and plug them into the EOS to determine the equilibrium vapor pressure. For the activitity coefficient equations, the equilibrium vapor pressure of the sorbate is calculated by adding an activity coefficient to Raoult's law to reflect the effect of different components as below:

$$P_R = y_R * P_{tot} = P_s * x_R * \gamma_R$$

Thus with the molar fraction (x_R) and calculated activity coefficient (γ_R) of the sorbate in the working pair mixture, the equilibrium vapor pressure can be evaluated.

The compiled database tables of the coefficient constants can be found in the appendix 6.4.

2.2.3.2 SorpPropLib

To facilitate the utilization of the compiled isotherm database in computer simulation of sorption heat pumps, a database program named SorpPropLib has been developed to provide property inquiry support for simulation in various simulation software. The SorpPropLib program contains both the master equation forms of isotherm correlations as well as the coefficient constants for all the compiled working pairs. By providing the name of the working pair and the temperature and composition of the desired state, users can conveniently acquire the equilibrium vapor pressure as well as the original literature of the coefficient constants used in the calculation from SorpPropLib. The data flow in SorpPropLib is shown in Fig. 2-14.

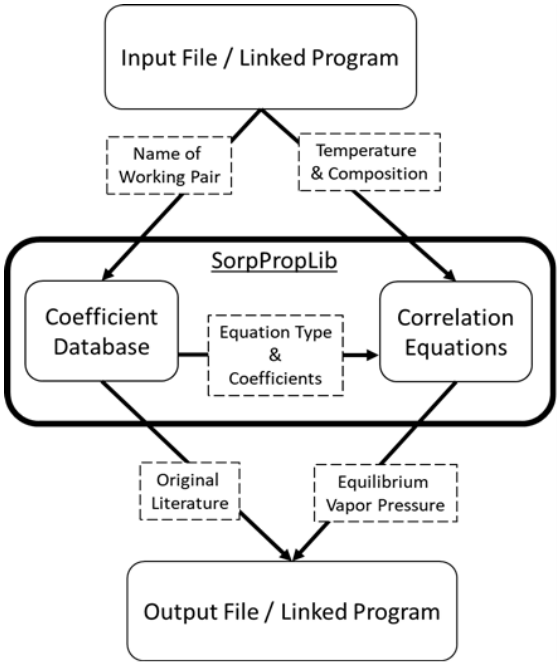

Fig. 2-14: Data flow in SorpPropLib

The coefficient database in the SorpPropLib is stored in JSON file form and can be conveniently expanded and updated with new data for future working pairs. The master equations and calculation control takes the form of a dynamic linked library (.dll) and can be linked to simulation programs such as Sorption system Simulation program (SorpSim), MATLAB, and Engineering Equation Solver (EES). A standalone program is also provided to allow direct inquiry with input from console or text files.

2.3 New developments in absorption technology

2.3.1 Polimi (Politecnico di Milano)

At Politecnico di Milano research is carried out with the objective of developing an air source gas-fired heat pump for space heating and DHW production for domestic applications. To assure a large potential for market penetration, the target of reducing specific costs and size compared to existing products is addressed. As an additional measure to ease the industrialization of the GHP, it has been decided to rely mainly on components derived from large series production, whose manufacturers actively collaborate

to the project. In particular, all heat exchangers, except the desorber, are fusion-bonded plate heat exchangers.

The outcome of the development is a 7.5 kW GAHP prototype, whose diaphragm pump and desorber have been designed to reduce the appliance size to the dimensions of a standard domestic condensing boiler. The effectiveness of different configurations of the refrigerant circuit has been investigated, together with the potential benefits of controlling the flow rate of refrigerant and solution. The achieved performances, measured according to the European Standard EN 12309, are in line with the expectation: a sGUE based on the net calorific value (sGUENCV) of 1.5 has been reached for the average climate (design temperature of -10 °C) and for the high temperature application (supply temperature of 55 °C). However, a detailed analysis shows room for improvements on some of the component, which are expected to boost the sGUENCV up to about 1.6.

2.3.2 Ariston

Ariston Thermo SpA is an Italian corporation that produces heating systems and related products. Ariston has started the development work of a residential absorption GHP.

2.3.3 SMTI

Stone Mountain (SMTI, USA) are developing a range of water-ammonia absorption heat pumps (3 kW for DHW up to 30 kW) for the US market under DoE contracts [58]. They have a track record in the technology, which is broadly similar to Robur's. However unlike Robur they are not a manufacturer but an R&D company. The US perspective emphasises minimum capital cost, similar to the approach needed in the UK.

3. Performance evaluation

3.1 Introduction

Within Task C, the Annex worked on the methodologies and the test procedures used for the performance evaluation of fossil fuel sorption heat pumps both on field (i.e. in real installations) and at test laboratories.

It aims at verifying the adequacy of the available tools for assessing this kind of appliances, both as single units and as integral parts of more complex systems, in terms of applicability, unambiguousness, comprehensiveness and coherency of achieved results.

With this purpose, within this Task, two studies have been carried out in parallel: one focused on real installations, for which a monitoring procedure based on the experience acquired through previous projects, such as "SEPEMO" and "RELAB monitoring", has been developed and applied on different real installations with the dual objective to validate the developed procedure for different system configurations and, at the same time, to increase the experience with integrated fuel driven heating systems in order to increase their acceptance in specific market segments.

The other one focused on the standardized test procedures usually used for the determining the performances of fossil fuel heat pumps for ECO-design and ECO-labelling purposes. For this study, first all the relevant existing standards and guidelines have been collected and analysed; then a round robin test on a prototype put at disposal by a partner of the consortium has been carried out among the project partners by applying two of the analysed procedures: EN 12309 and VDI4650.

This part of the final report contains the main results obtained in the Task C. It can be subdivided in three subchapters: The first part deals with standards and definitions. The second part is related to the monitoring activities where the developed monitoring procedure is fully reported including some examples of the fault detection. Furthermore, in this part, papers concerning monitoring of real installation carried out by applying the developed procedure are attached. The third subchapter, instead, is related to the test activities where the round robin test with the main achieved results is explained.

3.2 Standards and definitions

There are two main CEN standards for testing and performance evaluation of fuel driven sorption heat pumps:

- EN 12309 standard series (parts 1 to 7) [59] for space heating and
- EN13203-6 [60] for domestic hot water preparation.

Besides, there is a number of other national standards and guidelines which, in some cases, play an important role regarding subsidy granting as e.g. VDI 4650-2 [61] in Germany.

Besides, both national and international quality labels are available for fuel driven sorption heat pumps and the technology is also explicitly covered be the EU Ecodesign Regulation and as such part of the Eco Labelling scheme:

3.2.1 EN 12309 standard series: Gas-fired sorption appliances for heating and/or cooling with a net heat input not exceeding 70 kW

The Ecodesign Directive and the corresponding Implementing Regulations for different groups of energy-related products have highlighted the need for unbiased and transparent testing and performance evaluation methods for all technologies. Specifically, the efficiency requirements for gas-fired sorption appliances are defined in Commission Delegated Regulation 811/2013 and Commission Regulation 813/2013 for space and combination heaters and in Commission Delegated Regulation 812/2013 and Commission Regulation 814/2013 for water heaters. In the Communication of the European Commission 2014/C 207/02 [62], a list of harmonised standards for testing and performance evaluation of different heating appliances is provided. For gas fired sorption heat pumps EN 12309 is referred to as the reference document for space heating application. The current version of EN 12309, Parts 1 and 3 to 7 have been published in December 2014. Part 2 “Safety” was published a year later in April 2016. The standard has been developed to be compatible with the corresponding methodologies used for electrically driven heat pumps in EN 14511 and EN 14825 and, thus, uses the same basic methodology

for the testing and calculation of the seasonal performance figures. A basic description of the methodology can be found e.g. in [63].

Within the scope of the standard are gas-fired sorption heat pumps and chillers with a net heat input up to 70 kW. The EN 12309 comprises of the following parts:

- Part 1: Terms and definitions;
- Part 2: Safety;
- Part 3: Test conditions;
- Part 4: Test methods;
- Part 5: Requirements;
- Part 6: Calculation of seasonal performances;
- Part 7: Specific provisions for hybrid appliances.

In Parts 3, 4, 5, 6 and 7 testing methods and conditions for rating as well as testing, conditions and calculation methods for evaluation of seasonal performance according to the requirements of Ecodesign and Eco Labelling Regulations.

The standard rating conditions are provided for indoor and outdoor air, water and brine as heat source and for four different temperature applications, Table 3-1.

Table 3-1: Standard rating conditions of EN 12309-3

Heat source / temperature application	**Outdoor heat exchanger**		**Intdoor heat exchanger**	
	Inlet air dry bulb temperature [°C]	Inlet air wet bulb temperature [°C]	Inlet water temperature [°C]	Outlet water temperature [°C]
Outdoor air				
Low temperature	7	6	a)	35
Medium temperature	7	6	a)	45
High temperature	7	6	a)	55
Very high temperature	7	6	a)	65
Indoor air				
Low temperature	20	12	a)	35
Medium temperature	20	12	a)	45
High temperature	20	12	a)	55
Very high temperature	20	12	a)	65
	Inlet water Temperature [°C]	Inlet wet bulb Temperature [°C]	Inlet water temperature [°C]	Outlet water temperature [°C]
Ground water				
Low temperature	10	7	a)	35
Medium temperature	10	7	a)	45
High temperature	10	7	a)	55
Very high temperature	10	7	a)	65
Borehole (brine)				
Low temperature	0	-3	a)	35
Medium temperature	0	-3	a)	45
High temperature	0	-3	a)	55
Very high temperature	0	-3	a)	65
a) tests should be carried out with nominal flow rates given in the instructions, provided that the difference between the inlet and outlet temperatures at indoor heat exchanger is lower than a defined maximum temperature difference				

During the measurement, the gas input, the heat output and the electricity consumption are measured. In the hydraulic loops, the pressure drop over the unit is also measured at all necessary operating conditions. For rating, the outlet temperature methodology is used – the outlet temperature is fixed, the inlet temperature is a function of the mass flow rate. For the evaluation of the seasonal efficiency, three different test methods are available:

- the outlet temperature method, which is the reference method for monovalent appliances, where the outlet temperature matches the target value from Table 3-1;
- the inlet temperature method, which is the reference method for hybrid appliances and monovalent appliances which operate in on/off cycling, where the inlet temperature matches the target value;
- the mean temperature method where the mean of outlet and inlet temperatures matches the target value.

The operating conditions remain constant throughout the measurement. If applicable, the defrost cycles have to be accounted for in the calculation of the heating capacity and energy consumption. Besides, both the electrical energy consumption and the heating capacity are corrected for the influence of the hydraulic circuit of the test rig – taking into account only the part of the energy that can be attributed to the internal pressure losses of the appliance, both on the heat source and the heat sink side.

For each steady-state testing condition, two performance figures are calculated, the Gas Utilisation Efficiency (GUE) and the Auxiliary Energy Factor (AEF), equations 3-1 and 3-2, respectively:

$$GUEh = \frac{Q_{Eh}}{Q_{gmh}} \tag{3-1}$$

where

GUE_h is the heating gas utilization efficiency, in kilowatts per kilowatt;

Q_{Eh} is the effective heating capacity, in kilowatts;

Q_{gmh} is the measured heating heat input, in kilowatts.

$$AEFh = \frac{Q_{Eh}}{P_{Eh}} \tag{3-2}$$

where

AEF_h is the heating auxiliary energy factor, in kilowatts per kilowatt;

Q_{Eh} is the effective heating capacity, in kilowatts;

P_{Eh} is the effective heating electrical power input, in kilowatts.

Seasonal efficiencies can be calculated for three reference climatic conditions, in accordance with the Ecodesign regulation: Average with the design temperature of -10 °C, Warmer with the design temperature of 2 °C and colder with the design temperature of -22 °C. For that purpose, a serious of measurmenets under part load conditions have to be carried out in order to determine the GUEs and AEFs. For appliances in heating mode, the performance under the following part load conditions have to be measured, Table 3-2. The part load ratios for hybrid units, defined in EN 12309-7, differ from these.

Table 3-2: Part load ratios for the determination of seasonal performance factors for average, warmer and colder climates, according to EN 12309-6

		Part Load Ratio (PLR) in %		
	Outdoor air temperature [°C]	Average (A)	Warmer (W)	Colder (C)
O	-15	-	-	82 (-)
A	-7	88	-	61
B	2	54	100	37
C	7	35	64	24
D	12	15	29	11
E	Operation limit	a (100)	- (100)	a (100)
F	Bivalent	b	b	b
	a, b – calculated from the declared bivalent and operation limit temperatures ( ) – values in brackets apply for water(brine)-to-water appliances			

Part load conditions O to F can be tested with fixed or variable outlet temperature on the indoor heat exchanger and with fixed or variable water mass flow rate. For hybrid units, the inlet temperatures in the indoor heat exchanger are fixed, as described in EN 12309-7.

For each of the climate conditions, a seasonal hourly outdoor air temperature occurrance per temperature bin (1 K) is provided. For the temperature bins given in Table 3-2, the useful heat and the consumed electricity are calculated form the respective measured capacities and then multiplied by the number of hours in which these outdoor temperatures occur in the respective climate to obtain the useful energy and electrical energy consumption. All values inbetween are being interpolated or extrapolated. Finally, the seasonal performance is obtained by summing up the energies and building a ratio, equations 3-3 and 3-4.

$$SGUEh = \frac{\sum_{j=1}^{n} hj \times Ph(Tj)}{\sum_{j=1}^{n} hj \times \left(\frac{Ph(Tj)}{GUEh(Tj)} \right)} \quad (3\text{-}3)$$

where

Tj is the bin temperature;

j is the bin number;

n is the number of bins;

Ph(Tj) is the heating load of the building for the corresponding temperature Tj, expressed in kW;

hj is the number of bin hours occurring at the corresponding temperature Tj;

GUEh(Tj) is the GUEh values of the appliance for the corresponding temperature Tj.

$$SAEFh = \frac{Q_{refh}}{\frac{Q_{refh}}{SAEFh_{on}} + H_{TO} \times P_{TO} + H_{SB} \times P_{SB} + H_{OFF} \times P_{OFF}} \quad (3\text{-}4)$$

where

Q_{refh} is the reference annual heating demand, expressed in kWh;

$SAEFh_{on}$ is the Seasonal Auxiliary Energy Factor in heating mode and active mode;

HT_O, H_{SB}, H_{OFF} are the number of hours the appliance is considered to work in respectively thermostat off mode, standby mode and off mode.

P_{TO}, P_{SB}, P_{OFF} are the electricity consumption during respectively thermostat off mode, standby mode and off mode, expressed in kW.

For the calculation of SAEFh, additional measurements in non-active operation modes are necessary.

As fuel driven heat pumps are consuming both gas and electricity which have in general different primary energy coefficients, the primary energy ratio (roughly corresponding to the $\eta_{s,h}$ from the Ecodesign Regulation) can be calculated according to equation 3-5:

$$SPERh = \frac{1}{\frac{\mathrm{Pr}\,im_{\mathrm{gas}}}{SGUEh} + \frac{\mathrm{Pr}\,im_{\mathrm{elec}}}{SAEFh}} \qquad (3\text{-}5)$$

where

$Prim_{gas}$ is the primary energy factor for gas, value based on ErP Directive (2009/125/EC) or by default equal to 1 on GCV;

$Prim_{elec}$ is the primary energy factor for electricity, value based on ErP Directive (2009/125/EC) or by default equal to 2,5;

3.2.2 EN 13203-6

This European Standard is applicable to gas-fired sorption heat pumps connected to or including a domestic hot water storage tank producing domestic hot water. It applies to a package marketed as single unit or fully specified that have a heat input not exceeding 400 kW and a hot water storage tank capacity not exceeding 2000 l. In the case of combination boilers, with or without storage tank, domestic hot water production is integrated or coupled, the whole being marketed as a single unit.

The standard is part of the EN 13203 family of standards which cover gas appliances, including also hybrid heat pumps (EN 13203-5).

The described tests are to be carried out in several subsequent steps:

- Initial adjustment of the outlet water temperature;
- Measurement of energy consumption in standby mode;
- Measurement of energy consumption during a 24 h tapping cycle and calculation of the energy content of the supplied water;
- Mixed water at 40°C (V_{40} test).

The initial adjustment of the outlet water or water tank temperature is to ensure that the draw-off hot water temperature will be between 55 °C and 65 °C. However, for appliances with an integrated water tank it is not described how this temperature in the tank has to be reached. Further, no provisions for the initial state of the water tank is given.

Generally, the energy (both gas and electricity) consumption in the standby mode should be measured for a period of 24 hours and no hot water draw-offs should occur during this period. However, for the appliances without a control cycle, the gas and electricity consumption may be measured fora duration of one hour only. Further, for the appliances with repeated control cycles for a 24 h period, the gas and electricity consumption may be measured for a duration time equal to one or several control cycles, once the appliance is operating in a regular manner.

The load profiles for the estimation of the daily energy consumption for the production of useful hot water are following the load profiles from the Ecodesign Regulations. The beginning time of the test depends on the appliance characteristics:

- for appliances with no energy consumption between draw-offs, the measured programme starts at 7 o'clock with the appliance cold and finishes when the burner is extinguished after the 21:30 tapping;
- for appliances with energy consumption between draw-offs, the tappings start with the tapping at 21:30. The measured cycle starts from the time the burner is extinguished following the 21:30 draw-off. The measured cycle ends when the burner is extinguished following the last tapping at 21:30 on the next day.

In both cases, the profile will differ from the one established for electrically driven heat pumps in EN 16147. Further, both profiles will differ from the one defined in the Ecodesign Regulations, which can be understood in more than one way.

If during a draw-off the minimum required temperature cannot be reached, the energy consumption is corrected by assuming an additional electricity consumption in order to reach this temperature difference. This is only allowed for tappings with a (ΔT_p) of 45 K.

All tests are to be carried out at operating conditions shown in Table 3-3.

Table 3-3: Test conditions of EN 13203-6

Type of heat source	Heat source Temperature, [°C]	Range of ambient temperature for heat pump, [°C]	Ambient temperature of storage tank, [°C]
Outside air (heat pump indoor) with air duct	7 ± 0,2 (6 ± 0,3)	20 ± 3	20 ± 3
Outside air (heat pump outdoor)	7 ± 0,2 (6 ± 0,3)	7 ± 3	20 ± 3
Exhaust air	20 ± 0,2 (12 ± 0,3)	20 ± 3	20 ± 3
Water (inlet)	10 ± 0,15	20 ± 3	20 ± 3
Brine (inlet)	0 ± 0,15	20 ± 3	20 ± 3
Ground heat source (brine, inlet)	7 ± 0,2	20 ± 3	20 ± 3
Solar collector source (brine, inlet)	0,2	20 ± 3	20 ± 3

For the V_{40} test, the outlet water temperature has to be set to the maximum and the water has to continuously be drawn from the tank until its temperature falls under 40 °C. Declaration of this value is required by the Ecodesign Regulation.

The energy consumption in all tests has to be corrected for the influence of the test equipment in the hydraulic circuits and air ducts in order to provide comparable results between different laboratories, in the same way as in EN 12309 and in comparable EN standards for electrically driven heat pumps (EN 14511 and EN 16147).

The water heating energy efficiency is calculated according to equation (3-6):

$$\eta_{wh} = \frac{Q_{ref}}{(Q_{fuel} + CC \cdot E_{elecco}) \cdot (1 - SCF \cdot smart) + Q_{cor}} \cdot 100 \quad (3\text{-}6)$$

where

Q_{ref} is the total energy delivered by the load profile used, value from Tables 2 to 9, in kWh;
CC is the primary energy conversion coefficient for electricity;
E_{elecco} is the consumption of electricity for water heating over 24 consecutive hours under the declared load profile, expressed in kWh;
Q_{fuel} is the daily fuel consumption for domestic hot water over 24 consecutive hours under the declared load profile, expressed in kWh;
$Q_{gas,S}$ is the daily gas energy consumption in summer mode (kWh) calculated using Net Calorific Value (NCV);
SCF smart control factor (SCF) means the water heating energy efficiency gain due to smart control (no further provisions on how to perform a test with smart control are given in the standard);
smart is the smart control coefficient, is equal to 0 without smart control or 1 with smart control;
Q_{cor} is the ambient correction term equal to 0 for load profiles XXL to 4XL, and for load profiles XS to XL calculated according to a formula.

Besides η_{wh}, formulae for the annual fuel consumption (AFC), annual electricity consumption (AEC) and V_{40} are provided thus covering all necessary parameters from the Ecodesign Regulations.

3.2.3 Other standards and guidelines

Within the project, the following standards and regulations for fuel driven sorption heat pumps were found besides above EN standards, Table 3-4:

Table 3-4: Standards for testing and performance evaluation of fuel-driven sorption heat pumps

Abbreviation	Title	Status	Document type
DIN 33830	Wärmepumpen; Anschlussfertige Heiz-Absorptionswärmepumpen	superseded	standard
DIN V 18599:2011	Energetische Bewertung von Gebäuden	current	standard
ISO 13612-2:2014	Heating and cooling systems in buildings — Method for calculation of the system performance and system design for heat pump systems — Part 2: Energy calculation	current	standard
ANSI/AHRI 560	Standard for Absorption Water Chilling and Water Heating Packages	current	standard
ANSI/ASHRAE 182-2008	Method of Testing Absorption Water-Chilling and Water-Heating Packages	current	standard

EN 15316-4-2	Heating systems in buildings – Method for calculation of system energy requirements and system efficiencies – Part 4.2: Space heating generations systems, heat pump systems	current	standard
DVGW VP 120	Gasbetriebene Sorptionsheizgeräte (Sorptions-Wärmepumpen)	superseded	guideline
DVGW G 5120	Gasbetriebene Sorptionsheizgeräte (Sorptions-Wärmepumpen)	current	guideline
VDI 4650-2	Kurzverfahren zur Berechnung der Jahresheizzahl und des Jahresnutzungsgrads von Sorptionswärmepumpen-anlagen – Gas-Wärmepumpen zur Raumheizung und Warmwasserbereitung	current	guideline

In the following, VDI 4650-2 will be described since it plays an important role in the German federal subsidy scheme for heat pumps.

3.2.3.1 VDI 4650-2: Simplified method for the calculation of the annual coefficient of performance and the annual utilisation ratio of sorption heat pumps - Gas heat pumps for space heating and domestic hot water

The scope of VDI 4650-2 is to define a method to estimate seasonal performance figures of a gas fired thermally driven heat pump based on measurements under part load laboratory conditions. Current version of the guideline was published in January 2013. It is defined for monovalent gas fired sorption heat pumps up to a heating power of 70 kW. As ambient heat sources ground water, boreholes, air and solar radiation gained by a solar collector are considered. The heat is used for domestic hot water preparation and space heating.

Due to a lack of suitable EN standards at the time of the first publication, this VDI guideline for calculation of the seasonal efficiency of gas driven heat pumps was developed mainly for the purpose of granting subsidies for the appliances in Germany and is still used for that.

Basically, two seasonal performance figures are defined. The annual use efficiency η_N is defined as the produced heat per consumed fuel. The annual heating figure ζ, however, is defined as the amount of produced heat per amount of consumed fuel and electricity. Fuel and electricity are weighted equally, thus they are added up as final energies at the mains or the plug not taking into consideration the amount of primary energy needed in the process of energy conversion, transport etc.

More precisely, the guideline defines a calculation procedure for several performance factors and use efficiencies:

- annual use efficiency for space heating with/without solar assistance;
- annual use efficiency for domestic hot water with/without solar assistance;
- annual performance factor for space heating with/without solar assistance;
- annual performance factor for domestic hot water with/without solar assistance;
- total annual use efficiency;
- total annual performance factor.

The calculations of the seasonal use efficiency and the annual heating figure are based on the temperature bin method. This means that the use efficiencies and heating figures are calculated form the measured performance in laboratory for several part load conditions. The average of these values is taken as a seasonal value. Based on DIN 4702-8, the part loads are 13 %, 30 %, 39 %, 48 % and 63 % of full load heating power.

The assumption is that in part loads the volume flows are kept constant, thus part load is defined as a reduction of the heating loop inlet and outlet temperature. A table is given within the document which defines the inlet and outlet temperatures for each part load condition, Table 3-5.

Table 3-5: VDI 4650-2 operation conditions for testing

Relative capacity	Heating temperature 35/28		Heating temperature 355/45		Heating temperature 70/55	
	Tsupply [°C]	Tretum [°C]	Tsupply [°C]	Tretum [°C]	Tsupply [°C]	Tretum [°C]
0,13	22,2	21,3	26,0	24,8	29,7	27,8
0,30	24,9	22,8	32,6	29,6	39,2	34,7
0,39	26,2	23,5	35,6	31,7	43,4	37,6
0,48	27,5	24,2	38,5	33,8	47,6	40,4
0,63	29,7	25,3	43,4	37,2	54,3	44,9

Both gas and electricity consumption should be measured during the tests. The liquid pump for the heating distribution system is considered proportionally to the pressure loss through the heat pump unit.

The annual heating figure ζ_h is calculated according to equations (3-7) and (3-8):

$$\varsigma_h = \frac{5}{\sum_{i=1}^{5} \frac{1}{\varsigma_{h,i}}} \tag{3-7}$$

$$\varsigma_{h,i} = \frac{P_{i,th}}{Q_i + P_{i,el}} \tag{3-8}$$

where

$\zeta_{h,i}$ is the heating figure for each relative capacity;
$P_{i,th}$ is the heating capacity;
Q_i is the fuel consumption per time;
$P_{i,el}$ is the electricity consumption of the heat pump unit per time.

The annual use efficiency is calculated analogously, the partial use efficiencies $\eta_{h,i}$, however, do not contain electricity consumption.

The heat source temperatures are provided for different heat source types, Table 3-6. The guideline also assumes that the temperature of the ambient source is reduced with increasing heating power. Therefore, the guideline also defines standard temperatures for the temperatures within this loop. This is true for bore holes, ground water, air and solar collectors. For solar collectors, an increase in source temperature is assumed due to the solar radiation on the collector. A temperature increase as a function of the aperture area is given (2,1 to 5,6°C) and should be added to the temperatures of the respective primary source.

Table 3-6: VDI 4650-2 heat source temperatures and correction factors for different heat sources

Relative capacity	Ground	Water*		Ambient air			
		7°C	10°C	-10°C	-12°C	-14°C	-16°C
0,13	9	0,98	1,01	16,2	15,9	15,6	15,4
0,30	8	0,99	1,02	10,9	10,3	9,7	9,1
0,39	7	1	1,03	8,4	7,6	6,8	6,0
0,48	6	1,03	1,05	5,7	4,8	3,8	2,9
0,63	5	1,05	1,07	1,2	0,0	-1,3	-2,5
		* correction factors to be used in connection with the test results for ground-source heat pumps					

For systems with direct solar heating or DHW support, a calculation method for both performance figures is provided. It takes into account the solar fraction (provided by the planer) and the additional electricity consumption for the heat transfer fluid.

3.2.4 Quality labels

3.2.4.1 Heat Pump Keymark

The Heat Pump Keymark is a voluntary certification scheme established in 2016 as part of the Keymark certification scheme introduced in 1992 by CEN/CENELEC and is currently the most wide-spread certification for heat pumps in the EU. Electrically driven, gas-fired and hybrid (combination of an electrically driven heat pump with a gas boiler) heat pumps can be certified. The requirements for each of the product groups is different but aiming at guarantee the declaration of the manufacturer for compliance with ErP regulations. The proof of the energy efficiency is based on one of the applicable EN standards.

For gas and hybrid heat pumps, the certification can be granted using one-off admission testing approach without the need of subsequent testing or factory inspections. However, the technical documentation needs to be inspected periodically.

To obtain a HP Keymark, the following requirements have to be met:

Space heating tests for low temperature heat pumps (supply temperature 35 °C or 55 °C)

a) Depending on the heat source: A7/W35(55); A20/W35(55); B0/W35(%%); W10/W35(55) according to EN 12309-4.

b) Bivalent temperature condition for average climate according according to EN 12309-4 and EN 12309-6.

c) One other testing condition for average climate to be chosen by the certification body according to EN 12309-4 and EN 12309-6.

d) For any other climate, bivalent temperature condition shall be tested according to EN 12309-4 and EN 12309-6.

$SPER_h$ (and $SPER_c$) should be calculated according to EN12309-6.

Sound power level tests

In the absence of a dedicated standard for fuel driven heat pumps, tests shall be performed according to EN 12102-1 for average climate at the certified highest temperature application.

For heat pumps certified for brine and water as heat sources, the sound power level test should be performed using brine.

Optionally, space cooling can be certified, both for 7-12 °C and for 18-22 °C applications and the cooling function can only be certified with the space heating function.

Finally, NO_x emissions shall also be measured according the appropriate standard.

3.2.4.2 NF

In France, the NF label is very well established for a number of technologies, including gas-driven sorption heat pumps. It is issued by Eurovent Certita Certification under AFNOR's mandate and it certifies compliance with European and French standards. It is available for 11 product families, in the areas of Indoor climate and Ventilation. The requirements for gas and electrically driven heat pumps are described in the certification reference regulation NF 414 in its current version issued in December 2018.

The certified performance levels are:

- Gas utilisation efficiency GUE_h [kW/kW]. The thresholds of GUE_h at certain operating conditions are given in the tables below.

	T outdoor air [°C]	
T water, outlet	-7	7
30	1,20	1,40
35	1,10	1,35
45	1,00	1,30
50	0,90	1,20
60	0,70	0,90

	T water [°C]	T brine [°C]
T water, outlet	-2,5	7,5
30	1,50	1,52
35	1,50	1,50
45	1,40	1,40
50	1,35	1,35
60	1,25	1,25

- Rated heating capacity Q_{Nh} [kW]
- The effective power input P_E [kW]
- The sound power level L_w [dB(A)]. Sound power levels must be determined under the highest temperature application that the certification was requested for. Outside the building, they must comply with the thresholds in the table below:

Heating capacity P [kW]	Thresholds (identical to Rules 813/2013) Sound power level at the rated heating capacity Pdesignh Lw_A [dB(A)]	
	Indoor	Outdoor
$0 < P \leq 6$	60	65
$6 < P \leq 10$	65	70
$10 < P \leq 12$		
$12 < P \leq 20$	70	78
$20 < P \leq 30$		
$30 < P \leq 50$	80	88
$50 < P \leq 70$		
$70 < P \leq 100$	No threshold defined	

Optionally, the following performance can be certified:

- The particular characteristics of variable capacity regulation HPs:
  - The minimum continuous operation Load Ratio, LRcontmin [%]
  - The GUE at LRcontmin [kW/kW]
  - The performance correction coefficient at LRcontmin, CcpLRcontmin [-]
- The electrical power of the auxiliaries at zero load Paux0 [W]
- Seasonal performance in heating mode at least for an average climate, chosen by the applicant/holder for cooling modes and for the other climates:
  - The reference seasonal gas utilisation efficiency in heating mode SGUEh [kWh/kWh]
  - The reference seasonal efficiency in cooling mode SGUEc [kWh/kWh]
  - The reference seasonal primary energy efficiency in heating mode SPERh [kWh/kWh]
  - The reference seasonal primary energy efficiency in cooling mode SPERc [kWh/kWh]
  - Seasonal energy efficiency η_s = SPER x 100 - |F(1)| - |F(2)| [%]

Additionally, for the cooling function, the following characteristics can also be certified:

- Gas utilisation efficiency GUEc [kW/kW]
- Rated cooling capacity QNc [kW]

The cooling function can only be certified with the space heating function.

Eurovent Certita Certification monitors the certified products from the time when the right to use the NF mark is granted. This process includes in-plant verifications and retests.

3.2.4.3 RAL-UZ118

RAL – Deutsches Institut für Gütesicherung und Kennzeichnung and the federal Ministry for Environment, Nature Protection and Reactor Safety have together set up a framework for granting a quality label for energy saving heat pumps. The basis document is the granting regulation RAL-UZ 118 "Energiesparende Wärmepumpen" in its current issue from April 2012 (RAL 2012). The regulation can be applied to gas driven sorption heat pumps according to EN 12309, DIN 33830 and DVGW VP 120.

In order to obtain the quality label, a heat pump has to fulfil the following requirements:

- Compliance with all relevant guidelines and CE-mark;
- TEWI lower than 218 g CO2eq/kWh for supply temperatures of 55°C and lower than 178 g CO_2eq/kWh for supply temperatures of 35°C. Calculation procedure for TEWI is provided in an annex to the document;
- Noise emissions according to EN 12102;
- Gas emissions levels lower than 20 mg/kWh for CO and 40 mg/kWh for NOx according to DIN 4702-8. Starting from 2015, methane emissions will also have to be estimated according to VDI 2466;
- Liquid pumps have to have an energy efficiency index lower than 0,27 according to the EU guideline 2009/641/EG;
- Adjustment instructions for the installer and the user manual have to comply with a number of requirements stated in the document;
- The design of the product has to follow the state of the art regarding recyclability and material usage, as well as to minimise leakages.

Granting RAL-UZ 118 has been discontinued

3.2.4.4 DVGW Label

DVGW - Deutscher Verein des Gas- und Wasserfaches e.V. - Technisch-wissenschaftlicher Verein (German Technical and Scientific Association for Gas and Water) provides a certification program for a variety of appliances, some of which are not covered by other national or international testing or certification schemes. Gas driven sorption heat pumps can be awarded the DVGW quality mark on the basis of requirements described in the guideline DVGW G 5120 "Gasbetriebene Sorptionsheizgeräte" (gas-fired sorption appliances).

The guideline gives requirements regarding the construction, installation, operation and labeling for appliances up to 70 kW of burner power and maximum supply temperature of 105 °C at maximum 3 bar in the heating and 10 bar in the DHW circuit. The requirements regarding energy efficiency are based on the methodology endorsed by the EN 12309 for the calculation of seasonal energy performance.

3.3 Field test protocol and performance evaluation

In order to evaluate on field the performances of fuel driven heat pumps and to achieve comparable results regardless of the energy system in which they are installed, the use of a common monitoring methodology is mandatory.

Based mainly on the experience acquired during RELAB monitoring projects by Politecnico di Milano [64, 65] and the European project SEPEMO [66, 67], a procedure for monitoring heat pump plants for heating and domestic hot water production, using different heat pumps technologies (included the electrical ones), heat sources (air, water, ground), backup systems and having different sizes and scopes, has been developed.

Following, the approach used, the performance indicators, the monitoring equipment, the methodology for the detection of common faults in design and regulation of these plants as well as of other typical problems of heat pump systems are introduced and described.

3.3.1 Methodology

The first step was the individuation of a set of indicators useful to compare seasonal performances among plants with several configurations, sizes and scopes and using different energy carriers (i.e. electricity, gas, methane).

According to the SEPEMO Project [64] and the current European directives and Commision Decision (ECOLABEL and ECO-design), the following performance indicators have been identified:

- **Seasonal Performance Factor (SPF),** defined as the ratio of the total useful energy to the total energy inputs (electricity, gas, etc.).
- **Seasonal Primary Energy Ratio (SPER),** defined as the ratio of the total useful energy to the total primary energy inputs (electricity, gas, etc.). This indicator is adequate to compare the performances of systems using different energy carriers (i.e. electricity, gas, methane).
- **Seasonal CO_2 emissions Factor (CO_2_F),** defined as the ratio of the total CO_2 emission due to the energy inputs to the total useful energy. It is an index of specific CO_2 emissions per kWh produced (TEWI).
- **Seasonal NO_x emissions Factor (NO_x_F),** defined as the ratio of the total NOx emission due to the energy inputs to the total useful energy. It is an index of specific NO_x emissions per kWh produced.

For the calculation of primary energy, CO2 emissions and NOx emissions, the conversion factors indicated in the ECO-Label directive are used by default.

System boundaries, over which the performance indicators shall be calculated, have been specified. They have been chosen with the aim to analyze the behavior of each meaningful subsystem of the monitored plants, i.e. from the only heat pump to the whole system including pumps, auxiliaries, etc.…. Then, for each defined boundary, the energy flows through it, necessary for calculating the indicators, have been individuated.

On the basis of the quantities to be monitored (energy flows, energy carriers, etc.….) at each system boundary, the typology and the position of measurement equipment have been defined. Specifically, for each sensor (i.e. temperature sensor, flow meter...), the accuracy, sample time and rules for the correct installation, have been specified. This allows having measurement data comparable.

3.3.2 System boundaries

In the present procedure, 5 main system boundaries have been selected for the assessment of fuel heat pump plants. They are following defined:

- **Boundary 1:** contains only the heat pump unit. It allows evaluating the performance of the refrigeration cycle.
- **Boundary 2a:** contains the heat pump unit and the primary loops at source and sink side. In this way the electric power absorbed by the circulation pumps in the primary loops for the heat exchange with the source and the sink, is included; while electrical consumption and heat losses of the secondary loops (distribution circuit, heat extraction circuit at the source, etc..), that shouldn't be ascribed to the heat pump efficiency, are here excluded. This aspect is useful especially for big buildings where the distribution causes big thermal losses.
- **Boundary 2b:** contains the heat pump unit and the primary loop at the sink side and the primary and secondary loops at the source side. This boundary has been introduced because for ground/water heat pumps and air/water heat pumps the distinction between primary and secondary loops at the source side is not possible.
- **Boundary 3:** contains the heat pump unit, the primary and secondary loops at the source side, the primary loop at the sink side and the backup heater. At this level the comparison with the conventional heating systems is possible.
- **Boundary 4:** contains the heat pump unit, the equipment on primary and secondary loops of source and sink (i.e. the heat distribution is included) and the backup heater. At this level the performance of the whole system, from the heat production to the distribution, is assessed.

In the following figures, the defined system boundaries and their application on real water-to-water and air-to-water heat pump plants are shown.

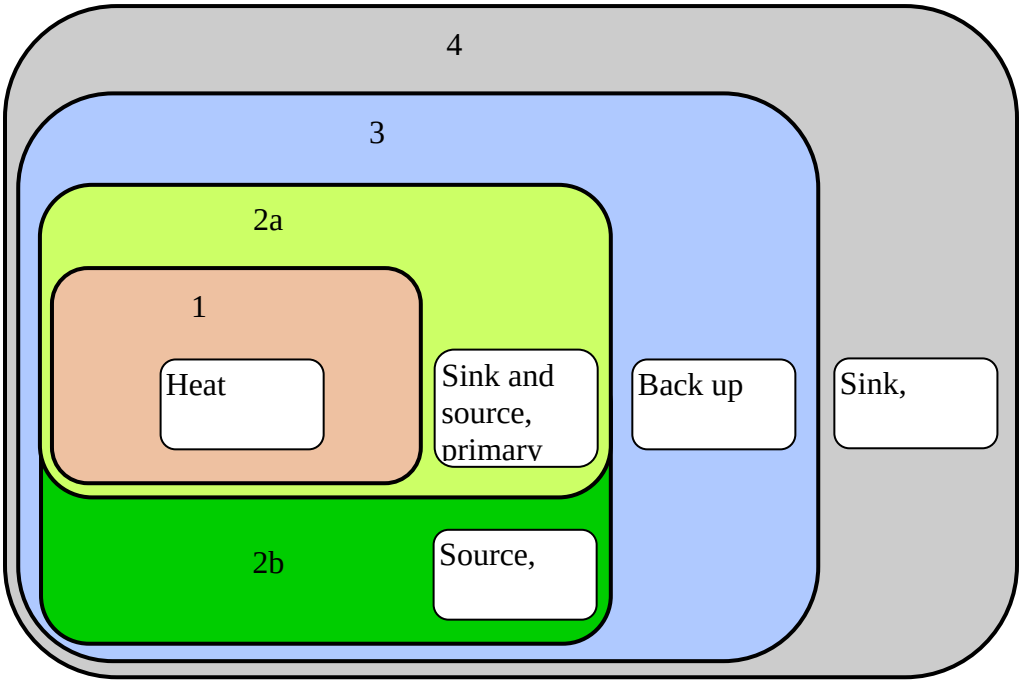

Fig. 3-1: System boundaries

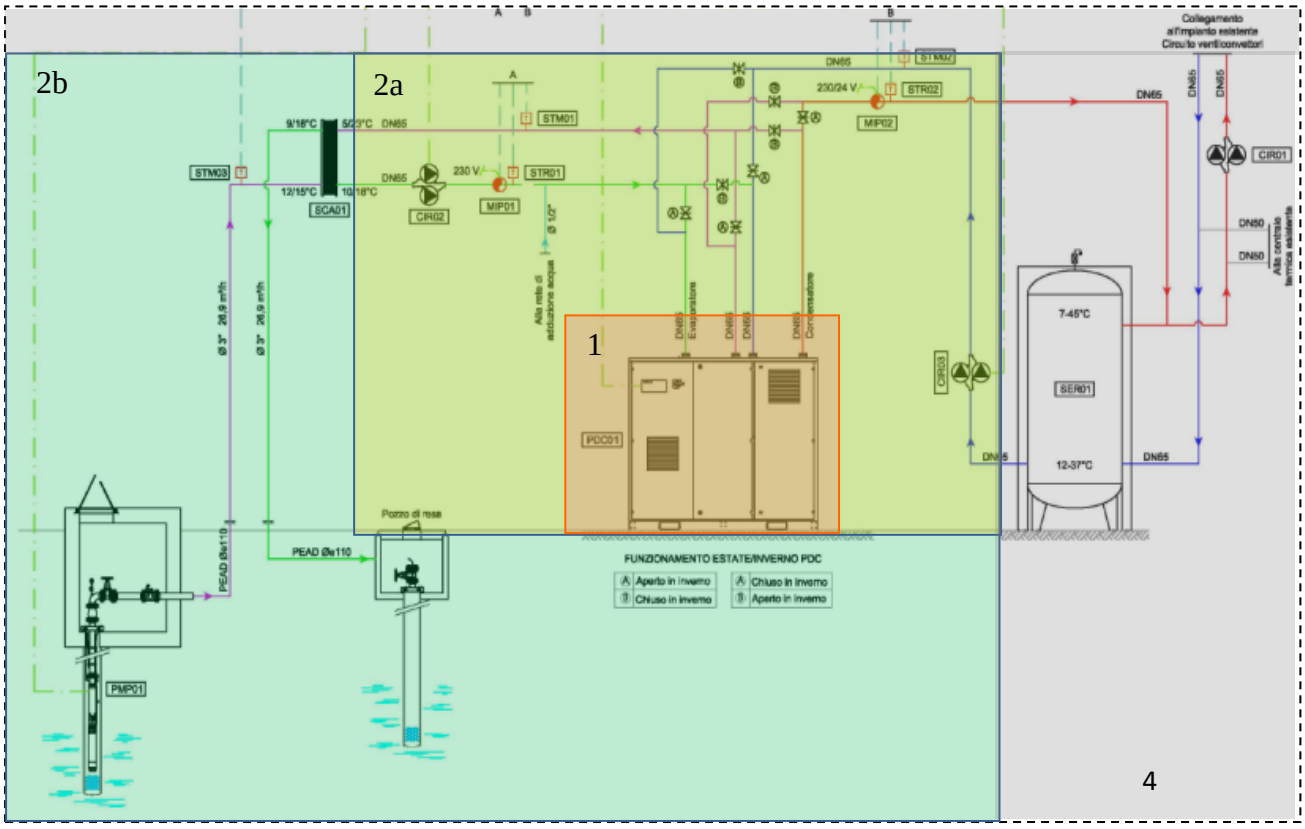

Fig. 3-2: Example of system boundaries on water-to-water Heat Pump plant

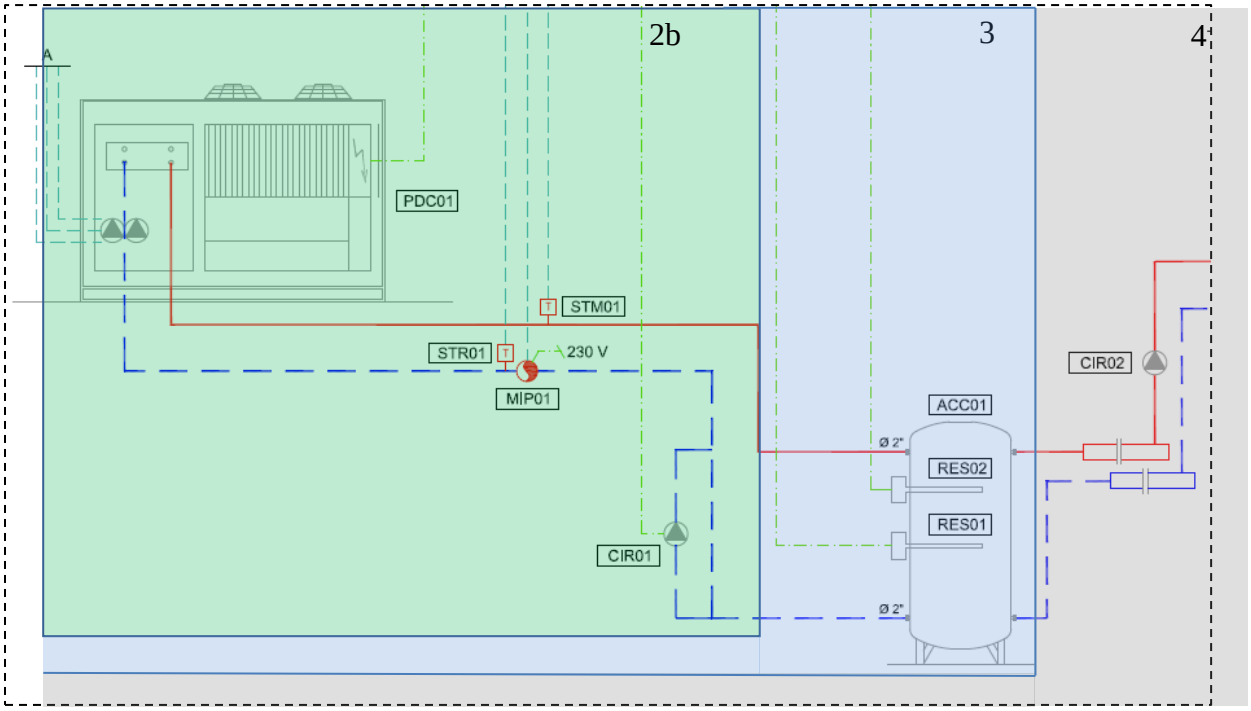

Fig. 3-3: Example of system boundaries on air-to-water Heat Pump plant

3.3.3 Performance Indicators

Below the formulas for calculating the performance indicators are shown in details for each system boundary.

3.3.3.1 Boundary 1 – Only heat pump

Fig. 3-4 shows the system boundary around the heat pump (*Boundary 1*) and the energy flows through it.

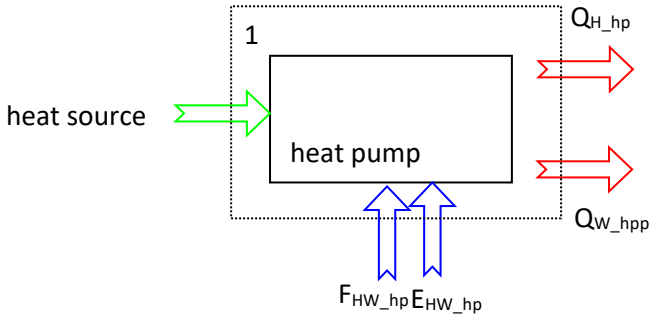

Fig. 3-4: System Boundary 1 and energy flows through it

Starting from the general definitions given in chapter 3.3.1, the performance figures can be calculating as follows:

$$SPF_1 = \frac{Q_{H\_hp}+Q_{W\_hp}}{E_{HW\_hp}+F_{HW\_hp}} \quad (3\text{-}9)$$

$$SPER_1 = \frac{Q_{H\_hp}+Q_{W\_hp}}{E_{HW\_hp}\cdot f_{p.el}+F_{HW\_hp}\cdot f_{p.fuel}} \quad (3\text{-}10)$$

$$CO_{2\_}F_1 = \frac{CO_{2\_E_{HW\_hp}}+CO_{2\_F_{HW\_hp}}}{Q_{H\_hp}+Q_{W\_hp}} \quad (3\text{-}11)$$

$$NO_{x\_}F_1 = \frac{NO_{x\_E_{HW\_hp}} + NO_{x\_F_{HW\_hp}}}{Q_{H\_hp} + Q_{W\_hp}} \quad (3\text{-}12)$$

According to standard EN12309, at this level, i.e. Boundary1, and at levels related to the boundaries 2a and 2b, the SPF shall be calculated also for each energy carrier separately. Specifically, by using the nomenclature adopted in this standard, the SPF becomes:

For the only thermal *input*

- **Seasonal Fuel Utilization Efficiency** defined as the ratio of the total useful energy to the thermal input energy from fuel (i.e. gas, oil, methane) calculated as the product of gross calorific value and fuel volume flow.

$$SFUE_1 = \frac{Q_{H\_hp} + Q_{W\_hp}}{F_{HW\_hp}} \quad (3\text{-}13)$$

In case of gas as fuel, the volume flow shall be converted into standard metric conditions, i.e. at the atmospheric pressure, 101.325 kPa, and at temperature of 15°C according to the following formula:

$$V_{Cj} = V_{mj} \cdot \frac{p_{aj}+p_j-p_{wj}}{1013.25} \cdot \frac{288.15}{273.15+t_{gj}} \quad (3\text{-}14)$$

Where:

V_{mj} is the measured gas flow rate at the considered scan, in cubic meter per hour

p_{aj} is the atmospheric pressure at the considered scan, in millibar

p_j is the gas supply pressure at the gas meter at the considered scan, in millibar

p_{wj} is the partial vapour pressure in the gas used at the considered scan, in millibar

t_{gj} is the gas temperature at the gas meter at the considered scan, in degrees Celsius

In this case SFUE1 is also called as SGUE.

For the only electrical input

- **Seasonal Auxiliary Energy Factor** defined as the ratio of the total useful energy to the electrical energy input from the auxiliaries.

$$SAEF_1 = \frac{Q_{H\_hp}+Q_{W\_hp}}{E_{HW\_hp}} \quad (3\text{-}15)$$

3.3.3.2 Boundary 2a – heat pump and primary circuits at sink and source side

Fig. 3-5 shows the system boundary around the heat pump (Boundary 2a) and the primary circuits at source and sink side. The energy flows through it are also shown.

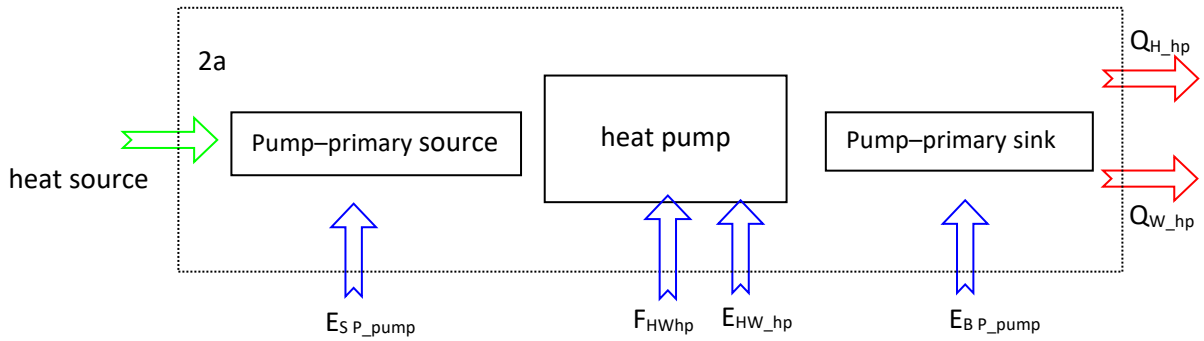

Fig. 3-5: System Boundary 2a and energy flows through it

At this level the performance figures can be calculating as follows:

$$SPF_{2A} = \frac{Q_{H\_hp} + Q_{W\_hp}}{E_{S\ P\_pump} + E_{HW\_hp} + F_{HW\_hp} + E_{B\ P\_pump}} \quad (3\text{-}16)$$

$$SPER_{2A} = \frac{Q_{H\_hp} + Q_{W\_hp}}{(E_{S\ P_{pump}} + E_{HW_{hp}} + E_{B\ P_{pump}}) \cdot f_{p.el} + F_{HW\_hp} \cdot f_{p.fuel}} \quad (3\text{-}17)$$

$$CO_2\ \ F_{\ 2A} = \frac{CO_{2\_E_{S\ P_{pump}}} + CO_{2\_E_{HW_{hp}}} + CO_{2\_E_{B\ P_{pump}}} + CO_{2\_F_{HW\_hp}}}{Q_{H\_hp} + Q_{W\_hp}} \quad (3\text{-}18)$$

$$NO_x\ \ F_{\ 2A} = \frac{NO_{x\_E_{S\ P_{pump}}} + NO_{x\_E_{HW_{hp}}} + NO_{x\_E_{B\ P_{pump}}} + NO_{x\_F_{HW\_hp}}}{Q_{H\_hp} + Q_{W\_hp}} \quad (3\text{-}19)$$

3.3.3.3 Boundary 2b – heat pump, primary circuit at sink side and primary and secondary circuits at source side

Fig. 3-6 shows the system boundary around the heat pump (Boundary 2b) and the primary circuit at sink side and primary and secondary circuits at source side. The energy flows through it are also shown.

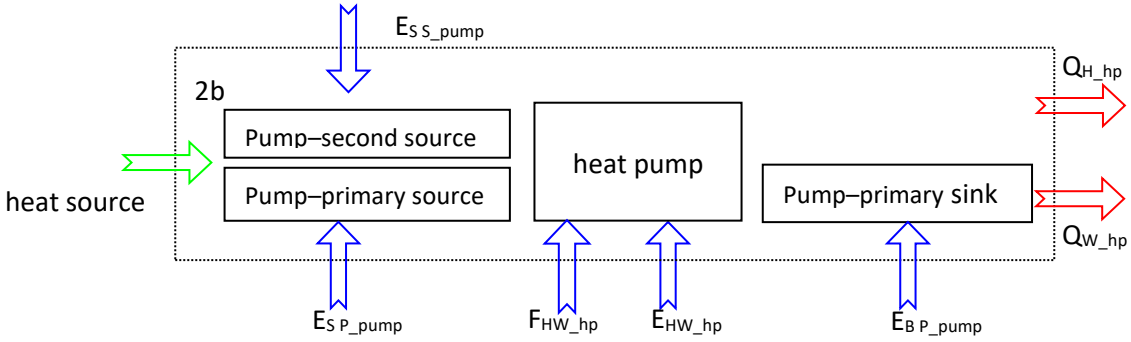

Fig. 3-6: System Boundary 2b and energy flows through it

At this level the performance figures can be calculating as follows:

$$SPF_{2B} = \frac{Q_{H\_hp} + Q_{W\_hp}}{E_{S\ S\_pump} + E_{S\ P\_pump} + E_{HW\_hp} + F_{HW\_hp} + E_{B\ P\_pump}} \quad (3\text{-}20)$$

$$SPER_{2B} = \frac{Q_{H\_hp} + Q_{W\_hp}}{(E_{S\ S\_pump} + E_{S\ P_{pump}} + E_{HW_{hp}} + E_{B\ P_{pump}}) \cdot f_{p.el} + F_{HW\_hp} \cdot f_{p.fuel}} \quad (3\text{-}21)$$

$$CO_2\ F_{2A} = \frac{CO_{2\_E_{S\ P_{pump}}} + CO_{2\_E_{S\ S_{pump}}} + CO_{2\_E_{HW_{hp}}} + CO_{2\_E_{B\ P_{pump}}} + CO_{2\_F_{HW\_hp}}}{Q_{H\_hp} + Q_{W\_hp}} \quad (3\text{-}22)$$

$$NO_x\ F_{2A} = \frac{NO_{x\_E_{S\ P_{pump}}} + NO_{x\_E_{S\ S_{pump}}} + NO_{x\_E_{HW_{hp}}} + NO_{x\_E_{B\ P_{pump}}} + NO_{x\_F_{HW\_hp}}}{Q_{H\_hp} + Q_{W\_hp}} \quad (3\text{-}23)$$

3.3.3.4 Boundary 3 – heat pump, primary circuit on sink, primary and secondary circuits on source, and back-up system

Fig. 3-7 shows the system boundary (Boundary 3) around the heat pump, primary circuit at sink side, primary and secondary circuits at source side and the back-up system. The energy flows through it are also shown.

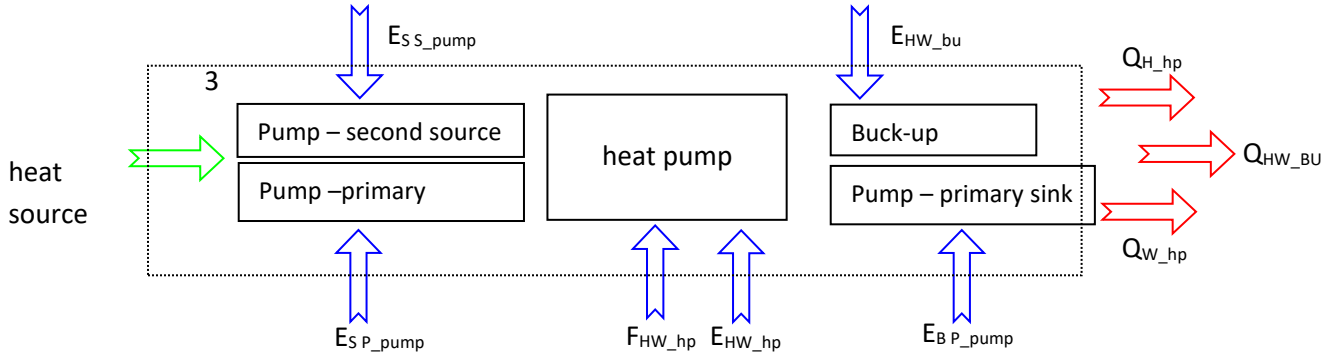

Fig. 3-7: System Boundary 3 and energy flows through it

At this level the performance figures can be calculating as follows:

$$SPF_3 = \frac{Q_{H\_hp} + Q_{W\_hp} + Q_{HW\_bu}}{E_{S\ S\_pump} + E_{S\ P\_pump} + E_{HW\_hp} + F_{HW\_hp} + E_{B\ P\_pump} + E_{HW\_bu}} \quad (3\text{-}24)$$

$$SPER_3 = \frac{Q_{H\_hp} + Q_{W\_hp} + Q_{HW\_bu}}{\left(E_{S\ S_{pump}} + E_{S\ P_{pump}} + E_{HW_{hp}} + E_{B\ P_{pump}}\right) \cdot f_{p.el} + F_{HW_{hp}} \cdot f_{p.fuel} + E_{HW\_bu} \cdot f_p} \quad (3\text{-}25)$$

$$CO_{2\_}F_{-2A} = \frac{CO_{2\_E_{S\ P_{pump}}} + CO_{2\_E_{S\ S_{pump}}} + CO_{2\_E_{HW_{hp}}} + CO_{2\_E_{HW\_bu}} + CO_{2\_E_{B\ P_{pump}}} + CO_{2\_F_{HW\_hp}}}{Q_{H\_hp} + Q_{W\_hp}} \quad (3\text{-}26)$$

$$NO_x\ F_{\ 2A} = \frac{NO_{x\_E_{S\ P_{pump}}} + NO_{x\_E_{S\ S_{pump}}} + NO_{x\_E_{HW_{hp}}} + NO_{x\_E_{HW\_bu}} + NO_{x\_E_{B\ P_{pump}}} + NO_{x\_F_{HW}}}{Q_{H\_hp} + Q_{W\_hp}} \quad (3\text{-}27)$$

3.3.3.5 Boundary 4 – heat pump, primary and secondary circuits on sink, primary and secondary circuits on source, and back-up system

Fig. 3-8 shows the system boundary (Boundary 4) around the heat pump, the primary and secondary circuits at sink and source side and back-up system. The energy flows through it are also shown.

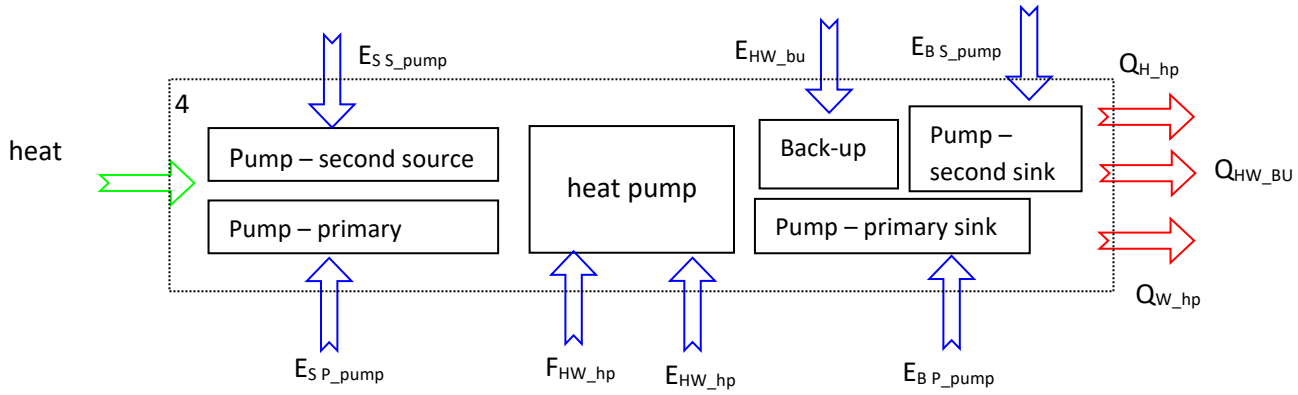

Fig. 3-8: System Boundary 4 and energy flows through it

At this level the performance figures can be calculating as follows:

$$SPF_4 = \frac{Q_{H\_hp} + Q_{W\_hp} + Q_{HW\_bu}}{E_{S\ S\_pump} + E_{S\ P\_pump} + E_{HW\_hp} + F_{HW\_hp} + E_{B\ P\_pump} + E_{HW\_bu} + E_{B\ S\_pump}} \quad (3\text{-}28)$$

$$SPER_4 = \frac{Q_{H\_hp} + Q_{W\_hp} + Q_{HW\_bu}}{\left(E_{S\ S_{pump}} + E_{S\ P_{pump}} + E_{HW_{hp}} + E_{B\ P_{pump}} + E_{B\ S\_pump}\right) \cdot f_{p.el} + F_{HW_{hp}} \cdot f_{p.fuel} + E_H} \quad (3\text{-}29)$$

$$CO_{2\_F\_2A} = \frac{CO_{2\_E_{S\ P_{pump}}} + CO_{2\_E_{S\ S_{pump}}} + CO_{2\_E_{HW_{hp}}} + CO_{2\_E_{HW\_bu}} + CO_{2\_E_{B\ P_{pump}}} + CO_{2\_E_{B\ S}}}{Q_{H\_hp} + Q_{W\_hp}} \quad (3\text{-}30)$$

$$NO_{x\_F\_2A} = \frac{NO_{x\_E_{S\ P_{pump}}} + NO_{x\_E_{S\ S_{pump}}} + NO_{x\_E_{HW_{hp}}} + NO_{x\_E_{HW\_bu}} + NO_{x\_E_{B\ P_{pump}}} + NO_{x\_E}}{Q_{H\_hp} + Q_{W\_hp}} \quad (3\text{-}31)$$

Legend:

$E_{S\ P\_pump}$	electrical energy use of the HP pumps on primary source circuit
$E_{S\ S\_pump}$	electrical energy use of the HP pumps on secondary source circuit
$E_{B\ P\_pump}$	electrical energy use of the primary heat sink (building) pumps
$E_{B\ S\_pump}$	electrical energy use of the secondary heat sink (building) pumps

E_{HW_hp} electrical energy use of the HP for SH and DHW

F_{HW_hp} fuel energy (i.e. gas, oil, methane) use of the HP for SH and DHW

E_{HW_bu} electrical energy use of the back-up heater for SH and DHW

Q_{H_hp} quantity of heat of the HP for SH

Q_{W_hp} quantity of heat of the HP for DHW

Q_{HW_bu} quantity of heat of the back-up for SH and DHW operations

CO_2 quantity of CO_2 emitted by the components of the specific boundary (heat pump, circulation pump, back-up heater, etc.)

NO_x quantity of NO_x emitted by the components of the specific boundary (heat pump, circulation pump, back-up heater, etc.)

fp primary energy conversion factor

For a deeper analysis, it is possible to calculate the performance indicators for different operation mode of the heat pump, i.e.:

- Heating
- DHW
- Defrosting

And for different working conditions:

- stationary condition
- stationary + transient condition
- full condition (it includes periods during which the HP is on and periods during which is in standby)

To characterize the behavior of the only FSHP, it's more significant to analyze the performance indicators calculated on stationary cycles.

Including the transient conditions instead, it's possible to see how the heat pump works also during the first part of the cycles and the influence on performances of the system's design and regulation.

The performance indicator calculated in full conditions (all operation time, including standby heat pump periods) shows the global behavior of the system. For example, it includes also the electrical energy absorbed by the circulation pump even when the heat pump is in standby mode.

3.3.4 Performance evaluations

The Primary Energy Ratio indicator (PER) summarizes the global performance of the heat pump system. To deeper appraise its significance and understand the reasons for good or bad efficiency, it is important to analyse the PER along with further parameters, which characterize the operating conditions of the heat pump and of the other components of the system:

- **External conditions**: external temperature and relative humidity, which determine, on the one hand, the thermal energy requirements of the building and consequently the load factor of the heat pump, and, on the other hand, the performance of the air-source heat pumps.
- **Working conditions of the heat pump**: supply temperature, temperature difference between supply and return to the heat pump, temperature of the renewable energy source; all these parameters, calculated during the running cycle of the heat pump, have a direct influence on the performance of the heat pump itself, thus on PER1/PER1*.
- **Features of the specific operating mode (heat, cool, DHW, defrost)**: supply temperature and percentage of running time for each operating mode. These indicators are useful to evaluate the effect of each operating mode on the performance of the heat pump (PER1/PER1*), for example, the defrosting cycles can considerably affect the efficiency of air/water heat pump systems.
- **Duration and frequency of heat pump cycles**: average duration and daily number of running cycles of the heat pump. These indicators reveal if the heat pump is working in steady state conditions, which allow the machine to develop its useful effect. Otherwise, if the heat pump cycles are short and frequent, PER1/PER1* could be compromised.
- **Management of circulation pumps**: comparison between the running time of the heat pump and that of the circulation pumps, and between the energy consumption of the system during the working cycle of the heat pump and the consumption during the whole period. These indicators represent the relative importance of the electrical consumption of circulation pumps. This becomes a significant percentage of the global consumption, in particular in systems where the circulation pumps are always running, with an impact on PER2b
- **Operation time of the system**: comparison between the working period of the heat pump and the schedule of the occupants of the building. This might reveal an incorrect management of the heat pump system (e.g. in operation while occupants are absent and the heat distribution is turned off), with an impact on the resulting PER1/PER1*.

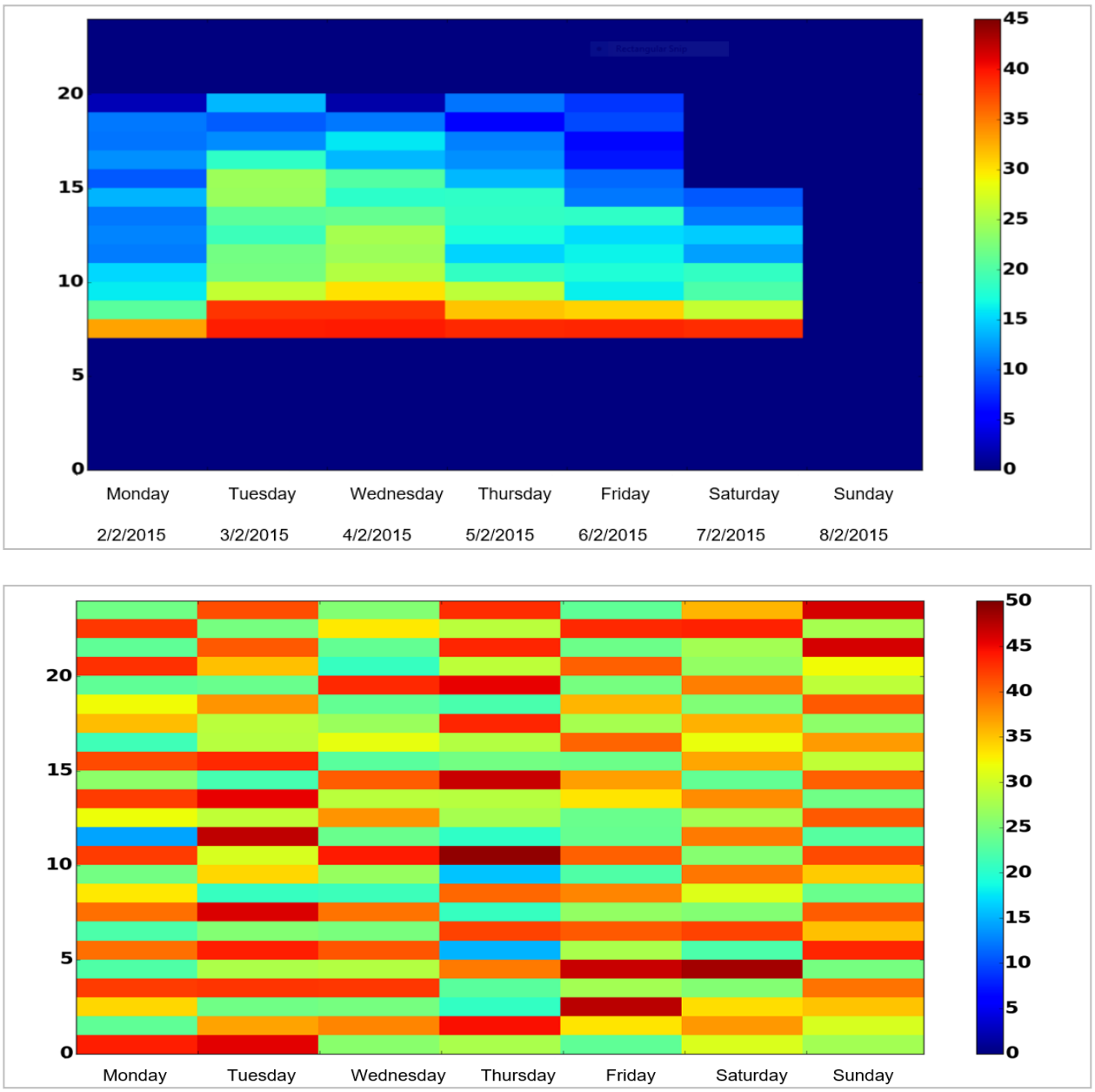

Fig. 3-9: Carpet plot of the hourly trend of the heat pump thermal power during a typical week of a system installed in: above: a city-hall, with a operation time of the system adequate for the building use; below: a school, without any regulation of the operation time (running system h24).

The definition of measuring equipment for the performance evaluation can be found in the appendix 6.5.

3.3.5 Architecture of the data collection, transmission and elaboration system

All the monitoring sensors shall be connected to an acquisition system for the data collection, transmission and elaboration. The system should provide the following requirements:

- automatic recording of monitoring data with a fixed sampling time (a time-step of 1 minutes is recommended);
- safe and reliable connection between the acquisition system and a central data server;
- automatic data saving system with periodic backup (better daily);
  automatic calculation procedures for the data validation, the evaluation of the performance indicators and the fault detection.

The data collection, transmission and elaboration system is represented in Fig. 3-10 a data logger collects each minute the signals from the all sensors (see Appendix 6.5 for details) and sends them to the server once a day; the connection can be provided by a GSM or ADSL system, the last one is more advisable because of its higher stability.

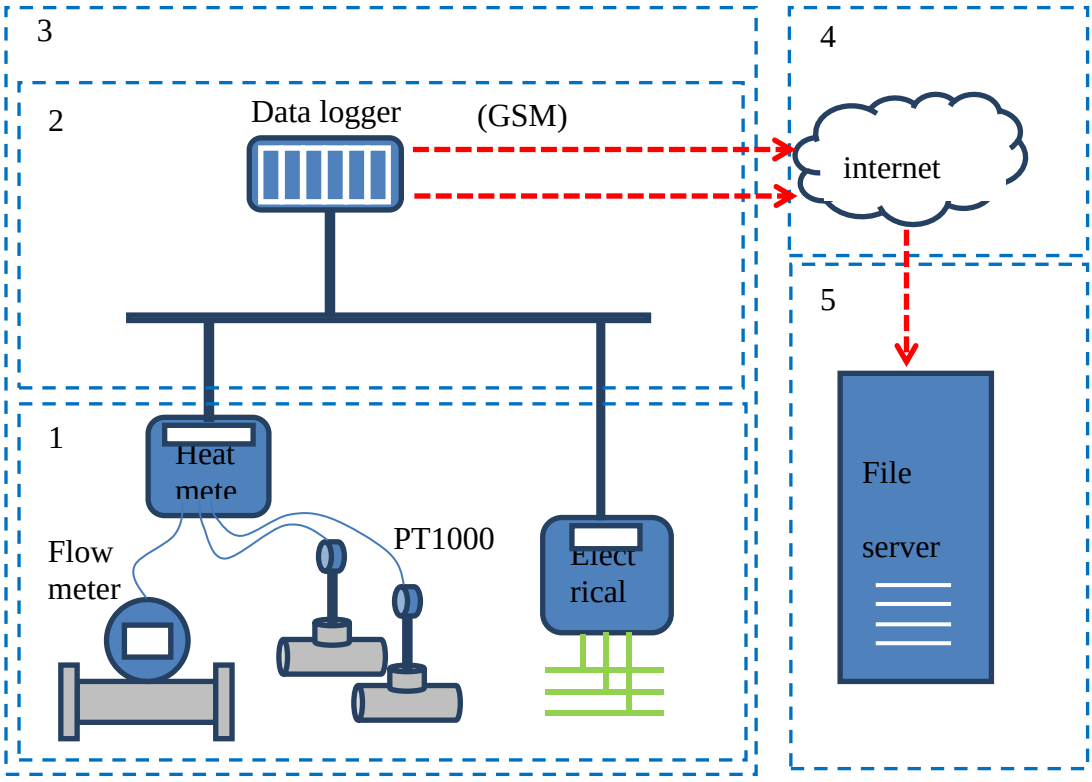

Fig. 3-10: Scheme of the data collection, transmission and elaboration process

3.3.6 Validation procedure

Before doing any evaluation, it is necessary to verify the reliability of the collected data.

A first check shall be done just after having installed the monitoring system in order to assure that each sensor is measuring the wanted physical quantity. This control consists of verifying if the collected data

are coherent or not, for example to check if the flow and return temperature sensors are twisted, or if the flow meter is installed in the same direction of flow, or if the correspondence between input and output energies of the heat pump occurs.

After this check, a continuous validation procedure shall be set and applied on all monitored quantity. For example it shall be checked if there are missing data, if the measured value are inside the validity range previously fixed for each specific quantity, if there is electric consumption of the circulation pump when there is flow, if the energy balance among output and input energies is verified, etc..

Once the data have been validated, they can be elaborated in order to calculate the performance indicators and detect the possible faults due to design and regulation or due to damages of the system components.

3.3.7 Fault detection and diagnosis of design, regulation and control errors

Through monitoring data it's possible to detect different types of errors from the design to the control of the system that can strongly influence its performances. Once they have been identified, corrective measures can be taken to improve the behavior of the system.

Some examples of these errors are shown below, from the easiest to the hardest to be solved:

- control errors (user level): wrong operation time (e.g. in a school FSHP works during night and weekend);
- regulation errors (operator level): flow temperature too high, pumps always running even when compressor is off;
- design errors (designer level): no buffer or small storage tank; oversize heat pump.

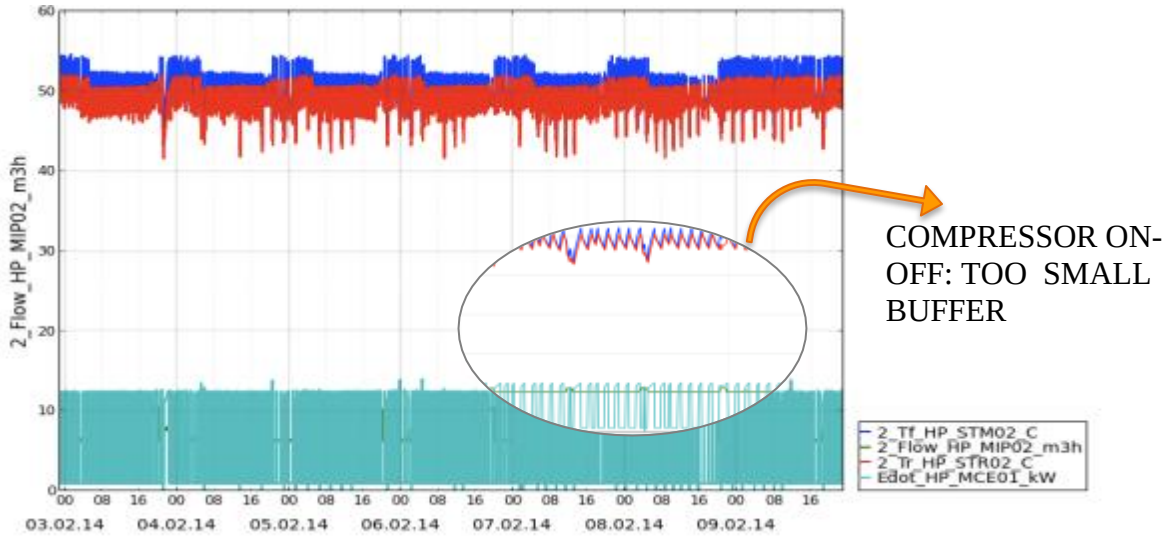

Fig. 3-11: Example of chart showing the heat pump input energy, the supply and the return temperatures; in this system because of the undersized buffer the compressor has very frequent on-off cycling

3.3.8 Detection of system damages

The fault detection aims also at finding wrong behavior or damages of the heat pump and of the system components, such as:

- heat exchanger fouling;
- filter fouling;
- antifreeze electrical resistance that starts when it's not necessary;
- damages of the connection between the compressor and the circulation pump, that continues running even if the compressor is off, causing an overheating of the water;
- flow interrupted because of valves closed erroneously by operators.

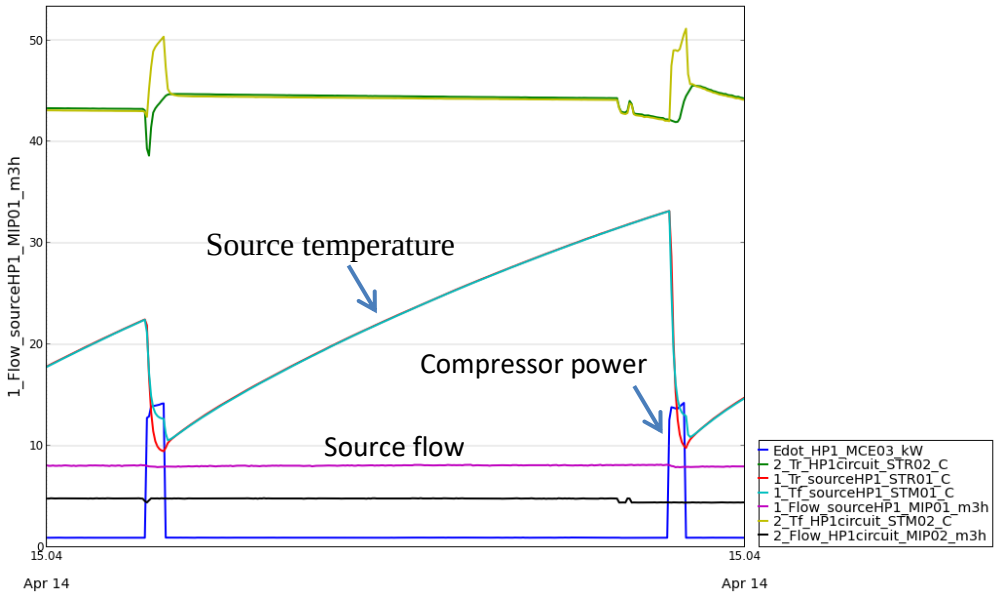

Fig. 3-12: Example of the overheating of the water temperature on the source circuit caused by damaging of the source circulation pump, installed inside the heat pump, which is always running even when the compressor is off.

3.4 Round Robin test on adsorption heat pump

In Task C, the applicability, unambiguousness and comprehensiveness of the existing relevant standards used for assessing fuel heat pumps were investigated. For the purpose, a round robin test on a hybrid fuel heat pump was carried out according to the European standards EN12309:2014 and VDI 4650. The main goals were: collecting comments upon the practical application of the above-mentioned standards to be forwarded to the relevant TC's; to suggest improvements of the test procedures; and to verify the consistency of the results achieved by applying the different methods.

The Round Robin Test (RRT) was performed on a geothermal hybrid heat pump (i.e. VITOSORP 200-F) supplied by a partner of the consortium (VIESSMANN). It consisted of a condensing boiler for the peak

load and of a zeolite heat pump module for the base load. The whole appliance was able to modulate the heating capacity from 1.6 kW to 10 kW.

The choice to test this kind of appliance was dictated mainly by its operational complexity. Indeed, in hybrid heat pumps, the combination of two technologies in one appliance and, in this specific case, the presence of an adsorption heat pump module, generates a discontinuous and cyclical machine's operation.

The tests were carried out at two different temperature applications: low temperature application (28 °C - 35 °C) and medium temperature application (35°C- 45°C C); and at "AVERAGE" climatic conditions. The method used was "Inlet temperature method" while, for results' reproducibility reasons, water was employed as heat transfer medium at outdoor heat exchanger.

Four laboratories were involved in the RRT: AIT, POLITECNICO DI MILANO, ISE and VIESSMANN.

Fig. 3-13 and Fig. 3-14 show respectively the drawing of the main internal components of the hybrid heat pump and main technical characteristics and some pictures of the test installation at POLIMI laboratory.

Fig. 3-15 instead shows the trends of the main quantities of interests during the tests. Specifically, an operation cycle illustrating the machine's behaviour has been extrapolated.

Analysing the operation cycle shown in Fig. 3-15, it's possible to distinguish four different phases: **adsorption phase**, during which only the sorption module is working; **adsorption plus boiler phase**, where both the condensing boiler and the sorption module are working; **boiler phase**, where only the condensing boiler is working; and **desorption phase**, where only the sorption module is working and any heating is produced.

Name manufacturer	Viessmann Werke GmbH & Co. KG
Product name	Vitosorp 200-F
Name national distributor	Viessmann Werke GmbH & Co. KG
Type	Combined gas fired condensing boiler and adsorption heat pump
Working pair: Refrigerant & sorbent	Water/Zeolite
Application	Heating and DHW
Configuration(s)	Heat source: boreholes (~50 m) or ground collectors.
Source of driving energy	Natural gas E, LL and LNG P
Output heating [kW] (VDI 4650-2)	1,8 – 11,0 (35/28°C) 1,8 – 10,3 (55/45°C)
Output DHW [kW]	max. 15,1
Output cooling [kW]	-
Output HP module [kW]	1,8 – 4,5
Nominal annual performance for heating [%] (VDI 4650-2)	124 (H_s, 35/28°C) 115 (H_s, 55/45°C)
Nominal annual performance for DHW [%] (VDI 4650-2)	109
Water temperatures [°C]	?
Electricity consumption [W]	average: 130
Control	Adsorption HP covers the base heating load, condensing boiler covers the peak heating loads as well as DHW demand
Status of product	Commercial product

Fig. 3-13: Hybrid heat pump: drawing and main characteristic

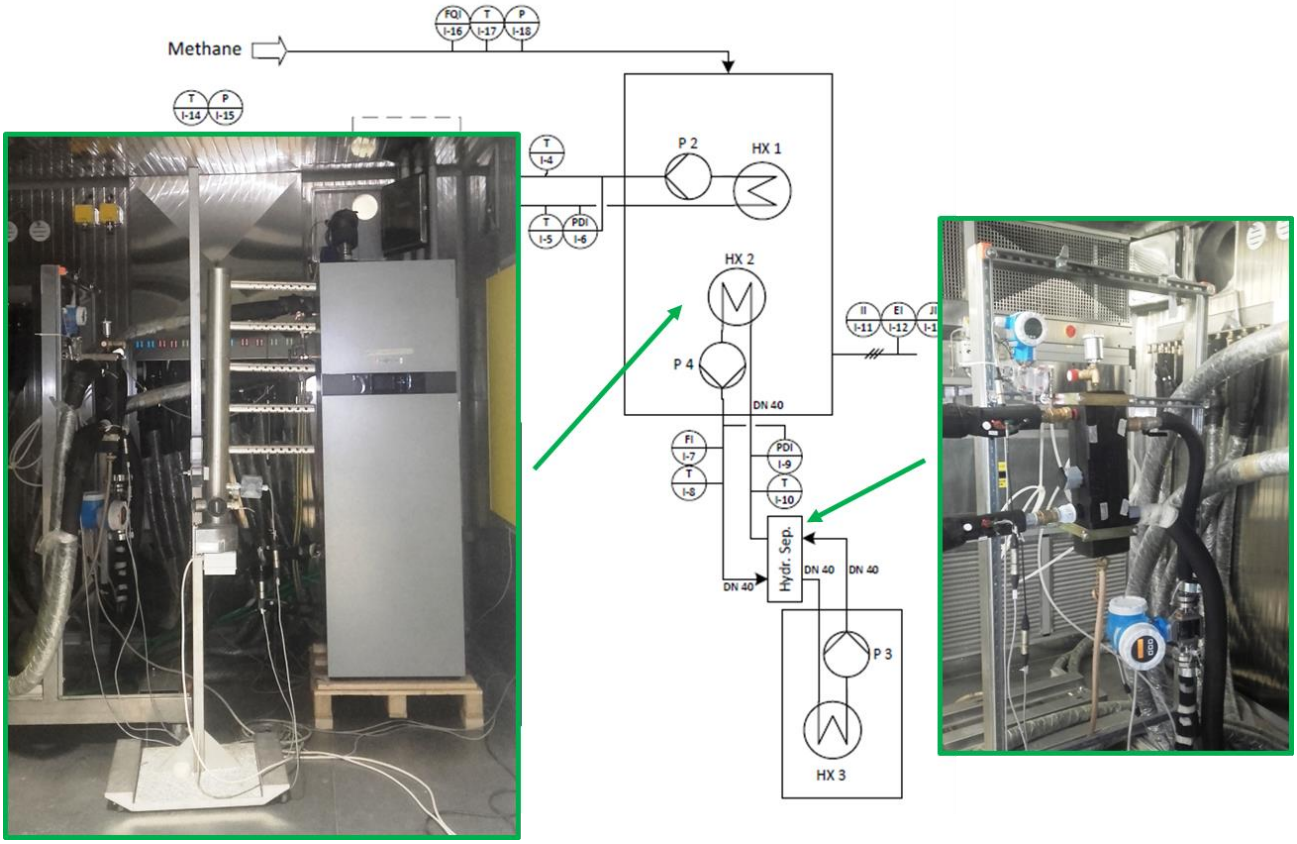

Fig. 3-14: Figure 1 Hybrid heat pump installation at POLIMI Laboratory

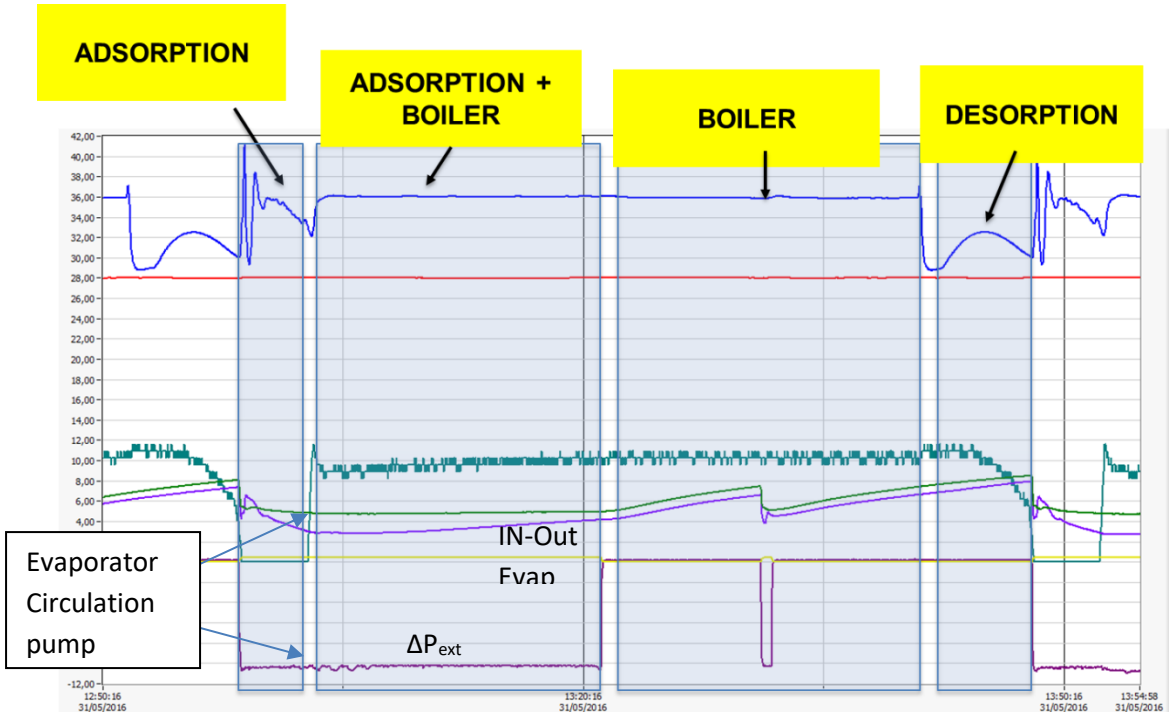

Fig. 3-15: Operation cycle of the hybrid heat pump under test

These four phases and their alternation affect the applicability of several requirements of the analysed test procedure such as the limits on the permissible deviations of the quantities of interest. For example, the evaporator (i.e. the “outdoor” heat exchanger) and the internal circulation liquid pump, responsible for the circulation of the heat transfer medium between the machine and the geothermal probes, work only when the sorption module is adsorbing. This means that the monitored quantities at this component such as the inlet and outlet temperatures, flow rate and the differential external static pressure will have an unsteady behaviour (Fig. 3-16). It’s easy to understand that it’s not possible to respect the limits on permissible deviations prescribed in Table 4 of the standard EN 12309:2014, Part4 (Fig. 3-17).

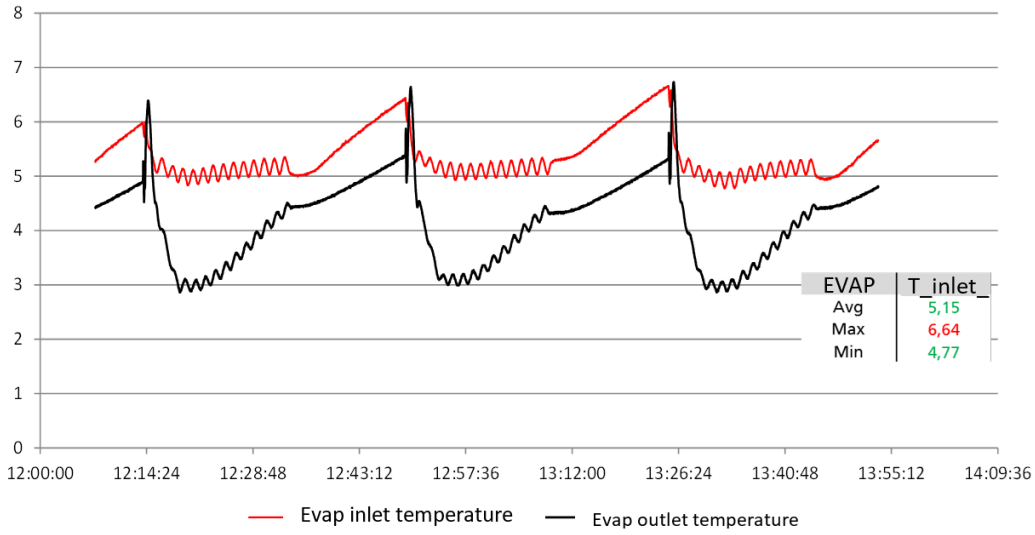

Fig. 3-16: Detail of inlet and outlet temperatures at the evaporator

Table 4 — Permissible deviations on the set values during steady-state operation tests for inlet temperature method

Measured quantity	Permissible deviations of the time average measured values from set values		Permissible deviations of individual measured values from time average measured values	
Outdoor water or brine				
- inlet temperature	maximum > load ≥ 70 % 70 % > load ≥ 40 % load < 40 %	± 0,2 K ± 0,2 K ±0,3 K	maximum > load ≥ 70 % 70 % > load ≥ 40 % load < 40 %	± 0,5 K ± 0,7 K ± 0,9 K
- outlet temperature	maximum > load ≥ 70 % 70 % > load ≥ 40 % load < 40 %	± 0,3 K ± 0,3 K ± 0,4 K	/	/
- flow rate	rated capacities others capacities	± 2 % /	rated capacities others capacities	± 5 % /
Indoor water or brine				
- inlet temperature	maximum > load ≥ 70 % 70 % > load ≥ 40 % load < 40 %	± 0,2 K ± 0,2 K ± 0,3 K	maximum > load ≥ 70 % 70 % > load ≥ 40 % load < 40 %	± 0,5 K ± 0,7 K ± 0,9 K
- outlet temperature	/	/	/	/
- flow rate	rated capacities others capacities	± 2 % /	rated capacities others capacities	± 5 % /
Electrical input				
- voltage	± 4 %		± 4 %	
NOTE Permissible deviation includes the regulating capability of the test apparatus.				

Inlet temperature Tolerance that cannot be respected

Flow rate Tolerance that cannot be respected

Fig. 3-17: Table 4 of EN 12309-4:2014: Permissible deviations for inlet temperature method

The same can be said for the condenser (i.e. indoor heat exchanger), where the only two parameters that have to respect the limits of permissible deviations are the inlet temperature (red line in Fig. 3-18) and the flow rate since, after a certain time, their behaviour depend only by the control of the test rig. The only parameter that, in this case, is influenced by the hybrid heat pump's operation and that therefore has an unsteady behaviour, is the outlet temperature (see Fig. 3-18, dark blue line). Nevertheless, no requirements are foreseen on this parameter even if it is crucial for the distribution system. With this regard, it could be useful to have a requirement (a permissible deviation) on that.

Concerning the permissible deviations of the inlet temperatures instead, they vary (the amplitude) based on machine's load: i.e. as the load decreases, the deviation increases. This is not necessary since the fluctuation of the inlet temperatures depend only on the test rig control and not on the machine. The restrictive one can be used.

Another aspect that was pointed put concerns the test duration, i.e. equilibrium phase plus data collection phase. From the executed tests, it emerged that some "special" cycles occur (see Fig. 3-18). This means that the choice of the test duration shall be done in order to consider all operational peculiarities of the hybrid heat pump under test. According to the prescription given in the paragraph 4.5.2.1 of EN 12309-4:2014, the equilibrium period and the data collection period shall be at least of 40 minutes and 30 minutes respectively.

It’s clear that, for this kind of machines, the definition of these periods in terms of minutes is not representative but it shall be done in terms of complete operational cycle instead. From the tests carried out, it was concluded that minimum appropriate number of operational cycles that can also allowed to collect a significant number of samples could be eight. This number is also high enough to include all possible strange or peculiar cycles.

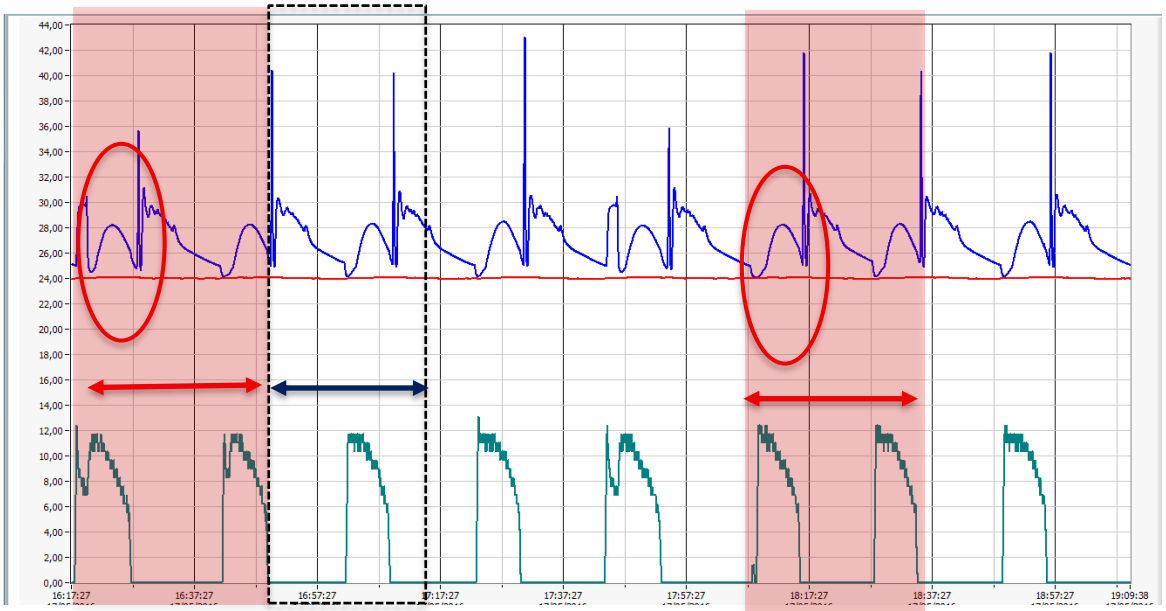

Fig. 3-18: Operational cycles: definition of test duration

Another remark concerns the additional test at 30% part load. See Table 10 of EN 12309-7:2014.

It’s not clear the reason of this request since the heat pumps, in general, follow the climate curve and it is already foreseen a test at around 30% part load and it is the “E” test conditions. Then, always for this additional test there are two “peculiarities”: first, the test conditions are given in terms of inlet temperatures and not ibn terms of outlet temperatures like in the other tables listing the rating conditions and it’s not clear the reason; second, in the note “a” of Table 10 of EN 12309-7:2014 the restriction related to the ΔT is fixed (depending on the temperature application) and not expressed in terms of maximum allowed ΔT. All these aspects could generate confusion for the test labs.

A final remark concerning the reduced capacity tests. According to the standard, when the minimum heating capacity provided by the machine is higher than the required part load (“target”), ON-OFF tests shall be performed, i.e. tests where periods when the machine is ON and works at the minimum allowed capacity alternate with periods when the machine is OFF. The duration of these periods are calculated through a formula. Form the round robin test it emerged that these tests besides to be not representative of the reality, they are also time consuming.

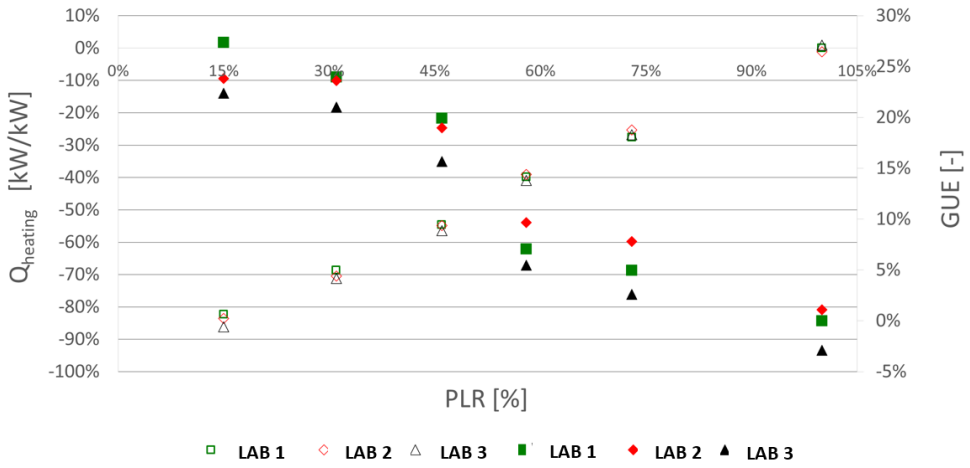

Fig. 3-19: Dimensionless test results: measured heating capacities (left axis) and GUE for each laboratory (right axis)

Fig. 3-19 shows the (dimensionless) results obtained during the round robin test. As it is possible to observe, even if there is the necessity to revise some parts of the test procedure, the achieved results showed a high grade of consistency among them especially in terms of GUE.

While concerning the heating capacity, due to a wrong flow rate at source side used by the laboratory 3, the difference between the highest and the lowest value on the average vary from 3 % to 7 %.

4. Best Case Studies

4.1 Simulation studies GHP (Polimi, Warwick, ISE)

4.1.1 UK Simulation Studies

Introduction

The UK is likely to be a major market for gas heat pumps due to its large winter heating demand in comparison to electrical grid capacity. In order for a complete move to electric heat pumps to occur, the electrical grid and distribution system would require significant upgrade. Peak building heat demand is nearly 250 GW, so assuming electric heat pumps at the coldest period of the winter to have a COP of 2.5 around 100 GW of extra electricity capacity would be needed. The present peak electricity load is less than 50 GW. The required infrastructure upgrades would be vast entailing meeting peak electricity loads up to 3 times present capacity. Whilst some of this could be mitigated by heat storage, the extra load presented by Electric Vehicle (EV) charging and the variability in supply of renewable electricity could make the problem worse. Many scenarios recognise that the gas grid is likely to have a role to play up to

2050, and fuel driven heat pumps could have a role to play in reducing carbon emissions during this period. The gas grid may be partially or wholly replaced with bio-methane or renewably produced hydrogen, and gas heat pumps would have a role in reducing the amount of sustainably produced gas required.

It was therefore decided that a separate UK simulation study would be worthwhile at the request of the UK's Department for Business Energy and Industrial Strategy (BEIS).

Methodology

Housing Types and Climate

Table 4-1 gives a breakdown of the UK housing stock by type [68] rescaled to the complete UK housing stock given in the United Kingdom Housing Energy Fact File [69]. More than half are terraced and semi-detached. The third most common is detached (unless bungalows are treated as a separate housing type in which case it is flats). It was therefore decided that these three housing types would be simulated. Although flats represent a significant number of dwellings, many may not have a gas supply and installation of an air-source unit would be more difficult. They may be better suited to a single communal heating system, which could be catered for by existing larger capacity units.

Table 4-1: UK Housing Stock by Type (Cambrdige Housing Model)

Type	Bungalows not Separated	Bungalows Separated
Terraced	8,076,418 (29%)	7,740,000 (28%)
Semi Detached	7,844,435 (29%)	7,130,000 (26%)
Detached	5,949,144 (22%)	4,560,000 (17%)
Flats	5,550,000 (20%)	5,580,000 (20%)
Bungalow	NA	2,400,000 (9%)
Total	27,420,000	27,420,000

Fig. 4-1 shows a breakdown of the UK housing stock by wall construction type for the three chosen housing types. It can be seen that the most common construction type for terraced houses is uninsulated solid (brick) wall (41%). This was therefore chosen as the construction type for terraced houses. For semi-detached houses the most common is insulated cavity wall and for detached uninsulated cavity. Since many of the insulated cavity walls are post-construction filled and the post-filling process is relatively inexpensive and straightforward, it was decided that the semi-detached and detached types would be modelled as post construction filled cavities. The U-value was taken as 0.65 W $m^{-2}K^{-1}$, in light of studies which found that post-construction filled cavities do not perform as well as previously predicted [70].

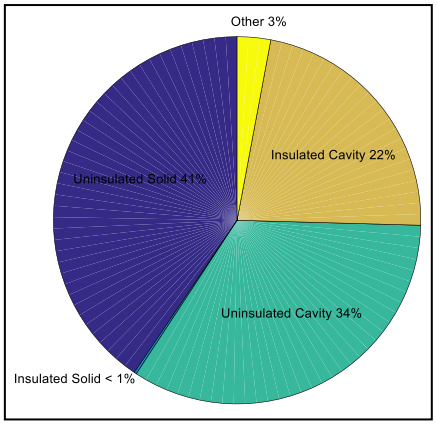

(a) Terraced

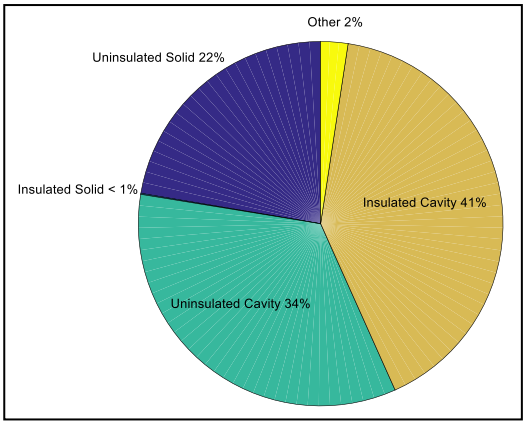

(b) Semi-Detached

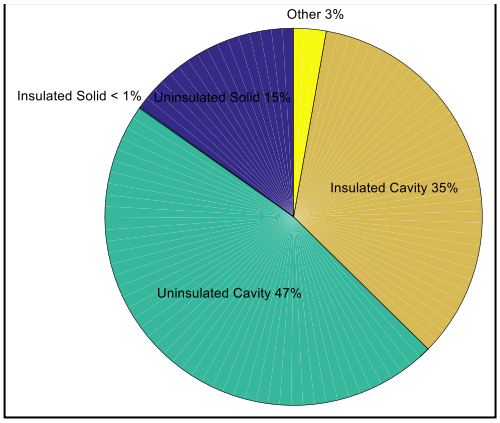

(c) Detached

Fig. 4-1: Housing Wall Construction

Since three quarters of the terraced, semi-detached and detached housing stock is fully double-glazed, with a further 20% having a mixture of double and single glazing, all three types were modelled with double-glazing.

Table 4-2 gives the specifications of the three house types, which were chosen by calculating average values from the Cambridge Housing Model [68]. The terraced and semi-detached houses were oriented with the front and back walls facing East-West and the external side wall of the semi-detached faced North. Windows were distributed evenly over the external walls for all house types. The roofs were considered to be pitched tiled roofs. These were modelled by considering the air within the roof space to be at the ambient external air temperature with no air movement and the convective heat transfer coefficient above the loft insulation taken to be 7.7 W $m^{-2}K^{-1}$.

Table 4-2: Specifications of the three house types

Parameter	Terraced	Semi-Detached	Detached
Wall type	Solid brick	Post construction filled cavity	Post construction filled cavity
External Wall Area (exc. windows)	51 m^2	84 m^2	147 m^2
Window Area	15 m^2	22 m^2	36 m^2
Plan area	6 m × 7 m, 41 m^2	6 m × 8 m, 48 m^2	8.8 m × 8.8 m, 77.4 m^2
Loft Insulation	0.15 m, 0.035 W $m^{-1}K^{-1}$	0.15 m, 0.035 W $m^{-1}K^{-1}$	0.15 m, 0.035 W $m^{-1}K^{-1}$
Party Wall Area	2 × 7.5 m × 5.5 m = 82.5 m^2	1 × 8.0 m × 5.3 m = 42.4 m^2	0 m^2

Climate and Heating Control Strategy

The chosen location was Birmingham, and the model was built in TRNSYS which includes Meteonorm weather data. Two heating control strategies were modelled: Twice per day and All day. For the twice per day heating control the internal set temperature was maintained between 6am-8am and 5pm-10pm. For the all day heating control, the internal set temperature was maintained from 8am to 10pm. The internal set temperature was 20°C.

The EU standard tapping profile No. 2 (100 litres per day) was taken for the Domestic Hot Water (DHW) consumption.

Heating Systems

Five heating systems were modelled for comparison and are detailed in the table below.

Table 4-3: Modelled Heating Systems

No.	Heating System	Capacity
1	Condensing Boiler (CB)	12 kW
2	Gas Fueled Heat Pump (GFHP)	18 kW
3	GFHP with Condensing Boiler backup	9+12 kW
4	15 kW Electric HP + Auxiliary Electric Heater	15 kW
5	9 kW Electric HP + Auxiliary Electric Heater	9 kW

The GFHP capacity was 18 kW as per the Robur K18 and with a turndown ratio of 5:1. In anticipation that 18 kW may be slightly oversized, a half capacity 9 kW machine with condensing boiler backup was also modelled for comparison. It was assumed that this machine would have the same Gas Utilisation Efficiency (GUE, the ratio of heat output to gas input) and half the parasitic electrical power requirement of the 18 kW machine. The GUE of the GFHP is shown in the figure below at 100% and 33% capacity.

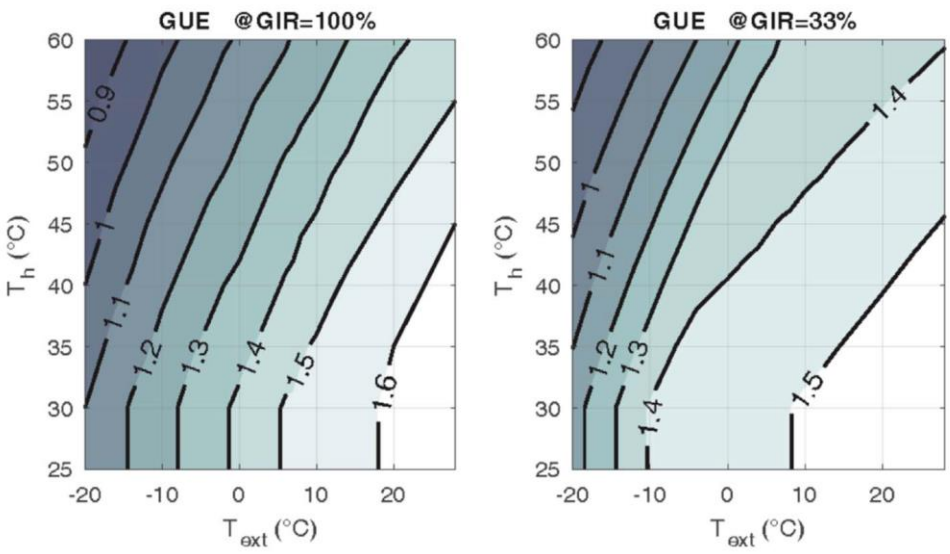

Fig. 4-2: GFHP GUE at 100% and 33% capacity [71]

Two electric heat pumps: 15 kW and 9 kW were also modelled for comparison on the basis of running costs and CO_2 emissions. The COP (Coefficient of Performance, the ratio of heat output to electricity input) of the electric heat pump is shown in the figure below at 100% and 33% capacity.

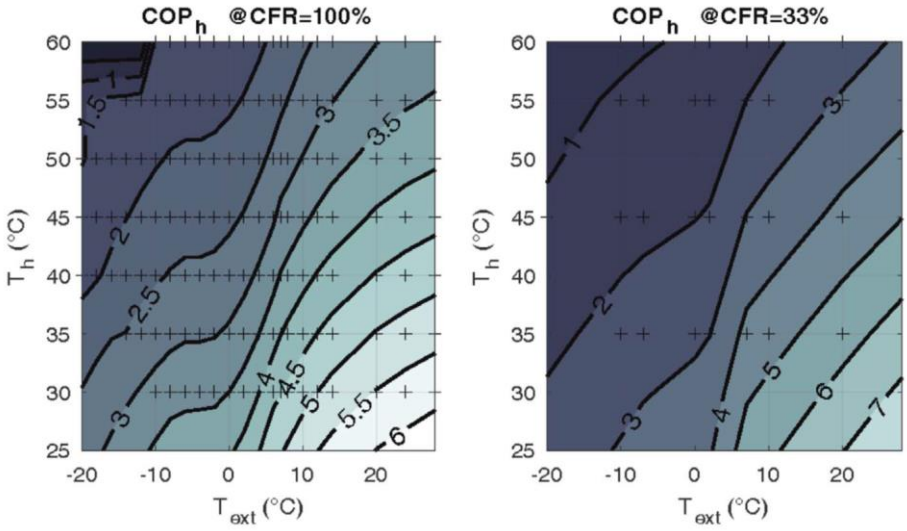

Fig. 4-3: Electric Heat Pump COP at 100% and 33% capacity [71]

The heat emitters were considered to operate at the EU standard 'high' temperature with 55°C supply temperature. This is generally sufficient for standard radiators fitted to UK houses, as a heat pump would operate at a lower output over a longer period of time than a boiler which would tend to cycle on and off frequently. For houses where the radiators are undersized this can often be remedied by replacing type 11 and 21 radiators with types 22 and 33.

Model

The modelling was carried out by Politecnico di Milano (POLIMI) using TRNSYS and is described in [71]. It includes modelling of the thermal mass of the building structure and contents.

Results

The tables below show the results for the twice per day and all day heating control. The gas price was taken as 2.8 p kWh^{-1} and the electricity price 12.4 p kWh^{-1}. The latest BEIS conversion factors (July 2018) were used for the gas and electricity CO_2 emissions at 0.18396 kg CO_2e/kWh and 0.28307 kg CO_2e/kWh, respectively.

Table 4-4: Model Results: Twice per Day Heating Control

Building	Plant		Heating Control : Twice per day. 6am-8am and 5pm-10pm								
	Type	Size	Sim Code	GUE/COP	Heat Delivered [kWh]	Gas Used [kWh]	Electricity Used [kWh]	CO2 [kg]	Fuel Cost [£]	% Heat Delivered by HP	Heat Pump GUE/COP
	CB	12 kW	1.1	0.892	31640	35466	243	6593	£ 1,023	0	-
Detached	GHP	18 kW	2.1	1.37	31619	23059	827	4476	£ 748	100	1.37
	GHP+CB	9+12 kW	4.1	1.26	31663	25163	1135	4950	£ 845	78	1.45
	CB	12 kW	6.1	0.9	18120	20124	181	3753	£ 586	0	-
Semi-Detached	GHP	18 kW	7.1	1.37	18141	13214	541	2584	£ 437	100	1.37
	GHP+CB	9+12 kW	9.1	1.31	18131	13867	785	2773	£ 486	88	1.43
	CB	12 kW	11.1	0.904	22050	24390	220	4549	£ 710	0	-
	GHP	18 kW	12.1	1.37	22076	16113	676	3156	£ 535	100	1.37
Terraced	GHP+CB	9+12 kW	14.1	1.33	22061	16531	917	3301	£ 577	89	1.43
	EHP+AEH	15 kW	15.1	2.4	22046	0	9187	2601	£ 1,139	94	2.66
	EHP+AEH	9 kW	16.1	2.09	21999	0	10517	2977	£ 1,304	80	2.85

Table 4-5: Model Results: All Day Heating Control

Building	Plant		Heating Control: Once per day. 8am-10pm								
	Type	Size	Sim Code	GUE/COP	Heat Delivered [kWh]	Gas Used [kWh]	Electricity Used [kWh]	CO2 [kg]	Fuel Cost [£]	% Heat Delivered by HP	Heat Pump GUE/COP
	CB	12 kW	1.2	0.898	33983	37858	268	7040	£ 1,093	0	-
Detached	GHP	18 kW	2.2	1.38	34034	24708	901	4800	£ 804	100	1.38
	GHP+CB	9+12 kW	4.2	1.3	34006	26166	1234	5163	£ 886	84	1.45
	CB	12 kW	6.2	0.908	19247	21201	203	3958	£ 619	0	-
Semi-Detached	GHP	18 kW	7.2	1.37	19257	14017	584	2744	£ 465	100	1.37
	GHP+CB	9+12 kW	9.2	1.34	19256	14407	831	2886	£ 506	92	1.43
	CB	12 kW	11.2	0.907	23556	25965	239	4844	£ 757	0	-
	GHP	18 kW	12.2	1.38	23571	17149	710	3356	£ 568	100	1.38
Terraced	GHP+CB	9+12 kW	14.2	1.38	23564	17349	977	3468	£ 607	91	1.43
	EHP+AEH	15 kW	15.2	2.56	23556	0	9206	2606	£ 1,142	96	2.76
	EHP+AEH	9 kW	16.2	2.3	23505	0	10211	2890	£ 1,266	85	3.01

The electric heat pump was only modelled for the terraced house, so the charts below show the CO_2 emissions (s. Fig. 4-4) and running cost comparison (s. Fig. 4-5) for the terraced house with twice per day heating control. The results are not significantly different for the all day heating control.

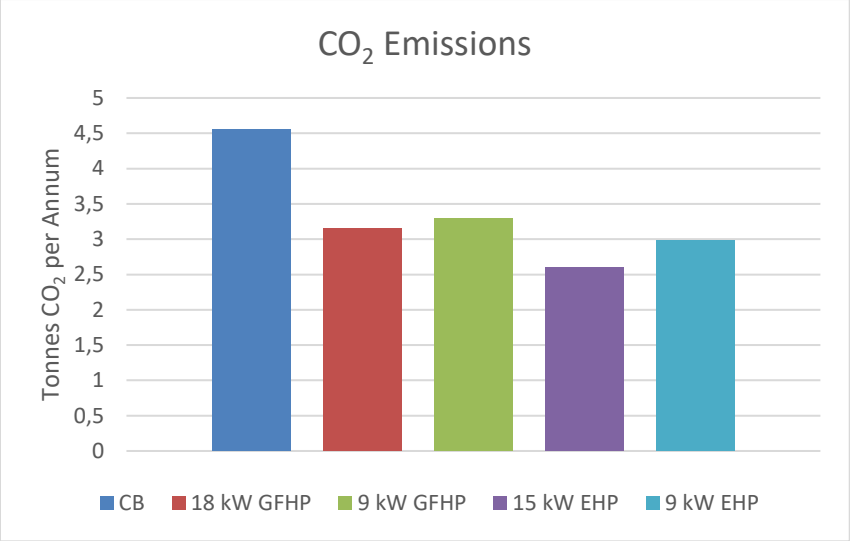

Fig. 4-4: Annual CO_2 Emissions for Terraced House with Twice per Day Heating Control

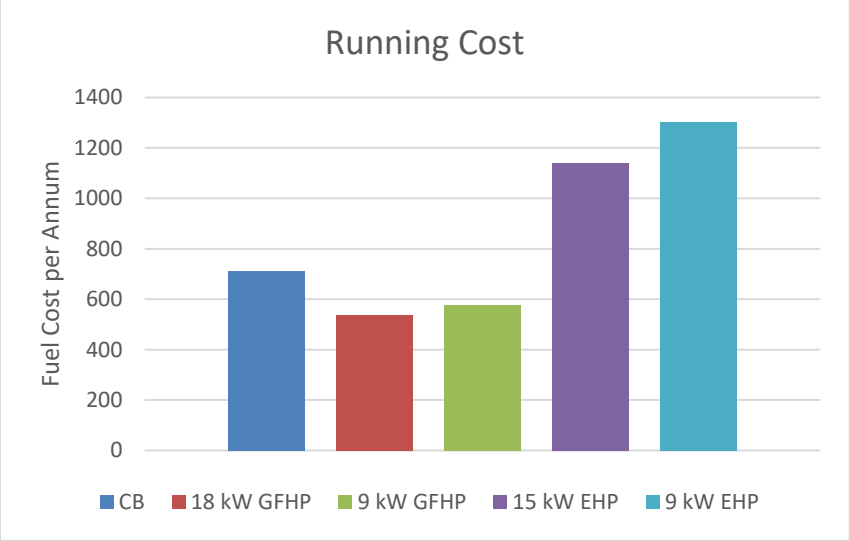

Fig. 4-5: Annual Fuel Cost for Terraced House with Twice per Day Heating Control

Analysis

The results show that an 18 kW GFHP with 5:1 turndown ratio performs well in all 3 house types, giving a seasonal GUE of 1.37-1.38 and a fuel cost saving of between 25 and 27% compared to a condensing boiler. However, a 9 kW machine with condensing boiler backup could provide more than 80% of the demand via the heat pump and still save 18-20%. If a 9 kW machine were introduced at significantly lower capital cost than an 18 kW machine, then its payback time would be shorter. The conclusion is therefore that a machine in the region of 10 kW would be ideal for the UK market.

The running cost of the GFHP is around half that of the electric heat pump at current electricity prices. Electricity grid CO_2 emissions are extremely low at the present time which means that the electric heat

pump has 18% lower CO_2 emission than the GFHP. This is a grid average however and it remains to be seen if this can be maintained in winter as more electric heat pumps are installed, as well as once demand from electric vehicles increases. GFHP CO_2 emissions are 31-32% lower than a condensing boiler, a figure which will change very little.

Potential Effect on UK CO_2 Emissions

Two scenarios for GFHPs are considered and compared in Fig. 4-6: The first assumes that the market will saturate at a 70% share of gas heating appliances annual sales after approximately 12 years (the rest of the market remaining as condensing boilers). The second assumes that after 7 years on the market, the cost of GFHPs reaches the point where legislation requiring their use is introduced, in much the same way as was carried out for condensing boilers replacing non-condensing boilers.

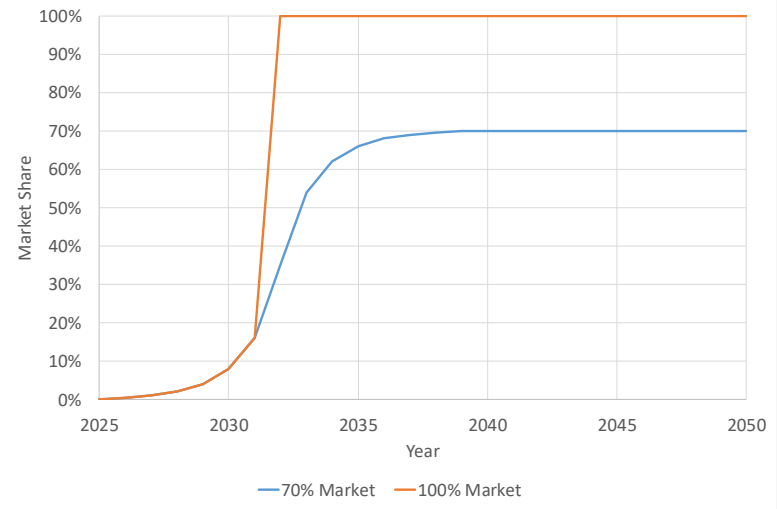

Fig. 4-6: Scenarios for GFHP Market Share

Current CO_2 emissions from domestic gas fired heating systems are around 55 Mt per annum, compared to around 80 Mt in 1990. Fig. 4-7 shows firstly what happens if the status quo is maintained (blue line) of replacing boilers with condensing boilers (current mean UK boiler efficiency obtained from the Cambridge House Model and an assumed boiler lifetime of 15 years). Emissions would reach around 49 Mt by 2040 if all boilers were by then condensing.

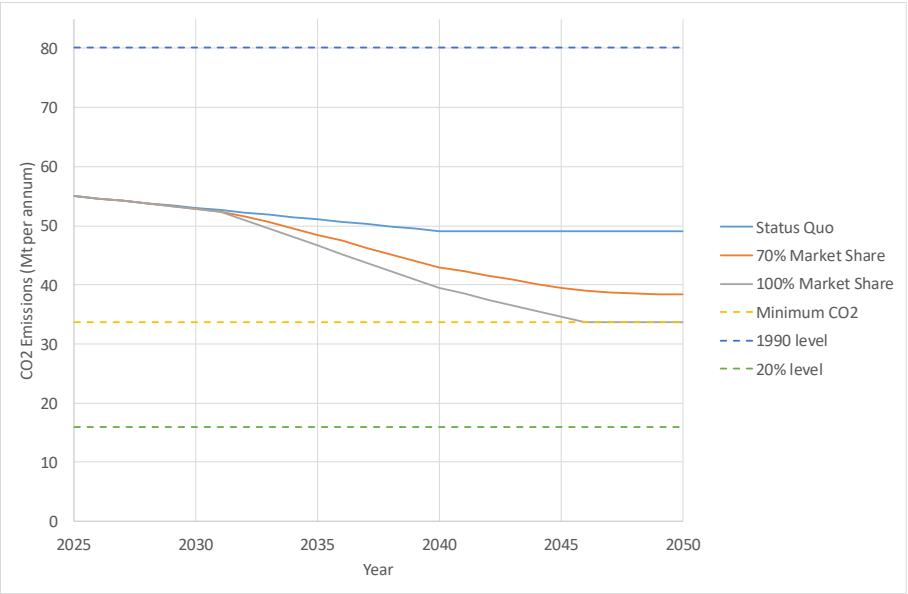

Fig. 4-7: Potential Domestic Gas Heating Appliance CO_2 reductions

By replacing boilers with GFHPs, the figure shows that CO_2 emissions could reach a minimum of 34 Mt by around 2045, representing a 6% reduction in overall UK CO_2 emissions compared to today and a 4% reduction compared to the status quo scenario. This is a major impact for just a single technology.

Conclusions

Modelling has shown that a GFHP could achieve an annual Gas Utilisation Efficiency of around 1.38 in UK homes and save between 25 and 27% in fuel costs compared to a condensing boiler. The ideal machine capacity for minimum payback time is likely to be in the region of 10 kW.

4.1.2 Polimi Simulation Studies

Introduction

Several studies about the development, optimization and integration of efficient heating devices are available in the literature, although most of these works deal with electric heat pumps and buildings characterized by very low heating demands. Advanced system configurations are also investigated, with heat pumps coupled with other technologies, as internal combustion engines, solar thermal or photovoltaic-thermal systems. To provide a wideer and in-depth view of the performance of different heating systems in Europe, including fuel driven sorption heat pumps and buildings with different energy demands, a simulation study is carried out. The analysis focuses on the residential market and on single-family houses, which represent 66% of the residential buildings in EU28 by floor area [72]. To provide results of general applicability, the comparison is performed for several cases, changing the variables that mostly affect the performances, i.e. the climatic condition and the quality of the building envelope. Care is given to simulate the part load behaviour of the appliances. As for the selection of the heating systems the criteria of low cost, simple installation, low maintenance and large potential market have been followed. The six resulting heating system layouts are the following:

- Condensing boiler (CB);
- Condensing boiler with solar system for DHW production (CB+SS);
- Electric heat pump with electric back-up (EHP+AEH);
- Hybrid system with electric heat pump and gas back-up (EHP+CB);
- Gas absorption heat pump monovalent (GHP);
- Gas absorption heat pump with gas fired back-up (GHP+CB).

With the purpose of providing relevant and exhaustive results, the comparison has been carried out based on three indicators: primary energy, CO2 emissions and economics.

Methodology

The comparison among the different heating system has been performed for nine cases defined as the combination of three climatic conditions, identified by the main European standards on this topic [73, 74] (average, cold and warm), and three building standards, namely "old", "refurbished" and "new" buildings representative for each climate. The nine resulting buildings have been modelled in TRNSYS 16, using Type 56. The heat demand for space heating has been calculated through six minutes time-step simulations and coupled with the DHW demand to generate the heating demand for the system model. Separating simulations for building and system is considered the most suitable approach, thanks to simplicity and stability of the simulation results. System has been sized by means of the "Maximum heat load calculation" method, which sets the ambient temperature at the minimum of the given location and switches off the internal and solar gains.

Building modelling

The selection of the building features has been done considering two antithetic needs, namely representativeness of the typical buildings in each climatic condition and minimization of the number of cases to analyze. Consequently, the nine cases share common building geometry, occupancy and internal loads, while they differ on U-values and envelope permeability.

Climate data

Three different climate zones were selected, corresponding with the three different climates defined by the European ERP Directive. For the weather data, the following Meteonorm weather files have been used:

- Helsinki (cold climate): FI-Helsinki-Kaisani-29980
- Strasbourg (average climate): FR-Strasbourg-71900
- Athens (warm climate): GR-Athinai-167140

Buildings description

The heating load profiles were defined for a single-family house (further referred to as SFH), based on the outcome of Task 44 “Solar and Heat Pump Systems” of the IEA Solar Heating and Cooling program [75]. The building consists of two levels, with a floor area of 70 m² each. The simulation is carried out considering the buildings as a single thermal zone. The features of the envelope have been selected coherently with the building location. For each climate, the envelope of the old, refurbished and new buildings have been defined based on the results of the European projects TABULA and EPISCOPE [76]. The selected buildings are reported in Table 4-4, identified according to the nomenclature used in the TABULA database. In

Table 4-5, the resulting U-values for the different surfaces and for each building are summarized. Additionally, it is reported the U-value variation due to the thermal bridges and the infiltration rate. The required ventilation rate is obtained by the difference between the air change for hygienic purposes, set to 0.4 h-1 for all the building, and the infiltration rate. When the air change is provided by a mechanical ventilation system, a heat recovery system with an effectiveness of 60% is considered. The reference buildings have been selected according to the following criteria:

1) The year of construction of the old building is antecedent the implementation of energy efficiency regulation and the period of construction is the most representative one. For the warm climate, the database contains a single typology for all buildings before 1980, which has been selected as representative of the old building.
2) The refurbished building corresponds to the same building typology of the old building, but refurbished according to the "usual refurbishment" approach reported in the TABULA datatabase.
3) For the new building, the "improved standard" has been considered for the average and the cold climate, whereas the "ambitious standard" has been chosen for the warm climate to better differentiate from the refurbished building.

Table 4-4: Building selected from the TABULA database as reference for the modelled buildings.

Climate	building condition	building ID
average	existing state	DE.N.SFH.05.Gen – 1958-68
	usual refurbishment	DE.N.SFH.05.Gen – 1958-68
	improved standard	DE.N.SFH.12.Gen – after 2016
Warm	existing state	GR.ZoneB.SFH.02.Gen – before 1980
	usual refurbishment	GR.ZoneB.SFH.02.Gen – before 1980
	ambitious standard	GR.ZoneB.SFH.04.Gen – after 2011
Cold	existing state	NO.N.SFH.02.Gen – 1956-1970
	usual refurbishment	NO.N.SFH.02.Gen – 1956-1970
	improved standard	NO.N.SFH.07.Gen – after 2011

Table 4-5: Main building features for the nine cases.

		Average climate			Cold climate			Warm climate		
		Old	Refurb.	New	Old	Refurb.	New	Old	Refurb.	New
U_{wall}	W/(m^2 K)	1.10	0.23	0.15	0.41	0.29	0.10	2.20	0.41	0.35
U_{roof}		0.80	0.41	0.13	0.36	0.21	0.08	3.70	0.40	0.30
U_{floor}		1.00	0.31	0.15	0.90	0.90	0.15	0.95	0.95	0.75
$U_{windows}$		2.80	1.30	1.10	2.80	1.90	0.80	4.70	3.00	1.82
U_{door}		3.00	1.30	1.30	3.00	1.30	1.30	3.00	1.30	1.30
$\Delta U_{t.\ brid.}$		0.10	0.10	0.05	0.10	0.05	0.02	0.15	0.10	0.05
Infiltr.	h^{-1}	0.40	0.20	0.10	0.40	0.20	0.05	0.40	0.10	0.05
Vent. System	-	No	Yes	Yes	No	Yes	Yes	No	No	No

Internal gains

Internal gains due to the presence of occupants and to the use of equipment and lighting are considered in the calculations. One person is associated with 20 W of convective and 40 W of radiative gains. The latent heat, usually about 40 W, is not considered in the simulation, as humidity is not controlled by the system. Both the profiles for the occupation and equipment and lighting are described by an hourly schedule, as reported in [75] and assumed identical for each day. The corresponding yearly energy amounts to 3.0 kWh/m2/y of convective and 6.0 kWh/m2/y of radiative gains for occupation and 13.4 kWh/m2/y for equipment.

Heating set points

The heating set point is 20 °C between 6:00 and 22:00 while it is lowered at 16°C for the remaining hours. For each building, the heating season has been defined according to the building location (see Table 4-6).

Table 4-6: Heating season limits for the different climates.

	Helsinki	Athens	Strasbourg
From	01-sep	01-nov	01-oct
To	31-may	30-apr	30-apr

Domestic hot water demand

The tapping profiles defined in the Commission Delegated Regulation (EU) No 812/2013 [77], concerning water heaters, have been considered. The cycles define a DHW demand over a period of 24 hours, specifying for each tapping the typology, the beginning time and the amount of energy in the hot water, according to the typology. In the present work, coherently with the building size, the tapping cycle “L” has been used, corresponding to a household with four occupants. According to the Standard, the inlet water temperature has been set a 10 °C for all the buildings. Over the 24 hours of the cycle, an amount of water equivalent to 200 litres at 60 °C is drawn, corresponding to 11.7 kWh per day. Concerning DHW

system layout, a storage tank of 80 litres has been used, heated up by means of an internal coil. The set point temperature in the tank is 60 °C, with dead band equal to 5 °C.

Plant modelling

System layout and sizing criteria

A general layout of the hydraulic schemes is reported in Fig. 4-8. The back-up, when present, is installed in series with the main heating device. The hydraulic separator (HS) has a volume of 50 litres and the mass flow rate on the primary and secondary circuit are constant and set according to the maximum space heating demand of each building.

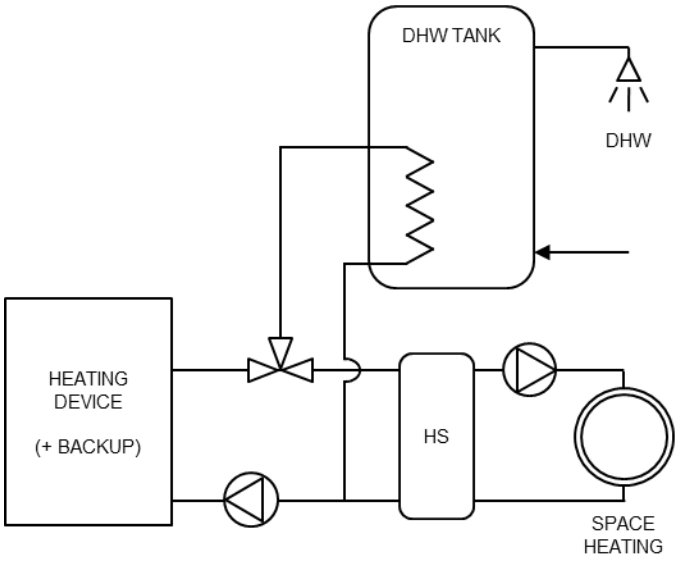

Fig. 4-8: Generic scheme of the systems layout.

At the design temperature the main heating device and the back-up provide the heating capacity corresponding to the maximum steady-state heat load of the building. When a back-up system is installed, the main heating device is able to meet the demand only above a certain external temperature, called bivalent temperature. Above the bivalent temperature, the heating device modulates its heating capacity. For the different system configurations, the following dimensioning criteria have been followed:

1) CB, CB+SOL and GHP: the size of the monovalent appliances is chosen to provide the maximum building load at the design air and water outlet temperatures. As the solar system is used for DHW only, the CB operates as a monovalent appliance for space heating.
2) GHP+CB: lacking more detailed studies about the proper set of the bivalent temperature of a GHP with a CB as back-up, a preliminary investigation on the optimal sizing has shown that, as a rule of thumb, the GHP design conditions shall cover about 50% of the maximum building load.
3) EHP+AEH: as the EHP is always more efficient than an electric resistance, the EHP should run whenever possible. Thus, a bivalent temperature equal to the minimum operating temperature has

been chosen. Below the minimum operating temperature, the load is fully covered by the electric heater.

4) EHP+CB: the heat pump capacity is lower than the maximum building demand. The bivalent temperatures for the warm and cold climate are set according to the limits proposed by the Standard UNI EN 14825, i.e. 7 °C for warm climate and -7 °C for cold climate. Since in both cases the ambient temperature is lower than the bivalent temperature for about 9% of the heating season, the same criterion has been used to decide the value of the bivalent temperature for the average climate, set to -2 °C.

The resulting heating capacity for each system is reported in Table 4-7. When two numbers are displayed, the first refers to the main heating device, the second to the back-up. The reported capacities are related to the rating conditions defined by the Standards [73, 78], i.e. the external air temperature of 7 °C and water temperature 40/45 °C and 41.3/55 °C for the EHP and GHP respectively.

Table 4-7: Capacity of main and back-up heating devices.

		Old		ren.		new	
		Q_{main_nom}	Q_{backup}	Q_{main_nom}	Q_{backup}	Q_{main_nom}	Q_{backup}
cold climate	CB	13.0	-	10.0	-	6.0	-
	CB+SOL	13.0	-	10.0	-	6.0	-
	EHP+E	19.3	12.2	17.8	9.9	9.5	6.0
	EHP+CB	10.2	13.0	7.9	10.0	3.9	6.0
	GHP	17.2	-	13.5	-	6.6	-
	GHP+CB	8.7	7.0	6.7	5.0	3.3	3.0
average climate	CB	14.3	-	6.3	-	4.5	-
	CB+SOL	14.3	-	6.3	-	4.5	-
	EHP+E	15.4	4.2	9.4	0.0	6.3	0.0
	EHP+CB	14.1	5.0	5.8	3.0	3.7	2.0
	GHP	18.6	-	7.7	-	4.9	-
	GHP+CB	9.4	8.0	4.0	4.0	2.5	3.0
warm climate	CB	20.0	-	6.0	-	5.0	-
	CB+SOL	20.0	-	6.0	-	5.0	-
	EHP+E	23.2	6.0	7.9	0.0	5.3	0.0
	EHP+CB	12.3	11.0	3.8	4.0	2.7	3.0
	GHP	22.3	-	6.6	-	4.5	-
	GHP+CB	11.2	10.0	3.3	3.0	2.2	3.0

Emission system and set point temperature

The emission system of the old building is based on radiators, thus, the water supply temperature at the design conditions is 65 °C. For what concerns the refurbished building, it is assumed that the emission system is not changed with the renovation. However, the supply temperature is set at 55 °C, under the hypothesis that the refurbishment of the envelope, reducing the heating demand, allows lower radiators temperature. For the new building, it is assumed that an underfloor heating system is used, with a supply

temperature of 35 °C. A climatic curve is used to modulate the supply temperature according to the external air temperature. In particular, the climatic curves have been shaped based on the test conditions of the Standards for heat pumps seasonal performance assessment [73, 74], dependent on the climate and on the nominal supply temperature. The supply temperature is set at the highest value at the design conditions and reduced linearly as the outdoor air temperature increases.

Condensing boiler model

The gas condensing boiler model is based on the European Standard CEN EN 15316-4-1 and, specifically, the "boiler cycling method" and the "high efficiency modulating gas condensing boiler" suggested by the standard. The resulting efficiency is mainly influenced by the return water temperature and the load factor (LF). Fig. 4-9 shows the resulting thermal efficiency (ηGCV) against the return water temperature, calculated for three different load factors.

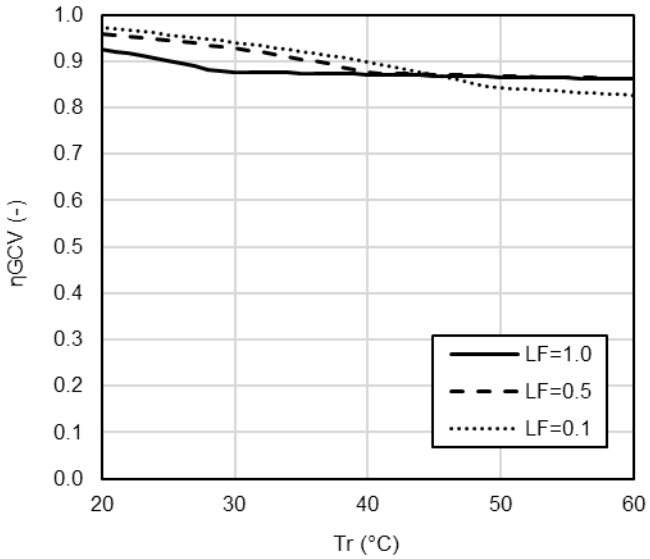

Fig. 4-9: Boiler thermal efficiency on the GCV against the return water temperature for three LF.

Electric heat pump model

The electric heat pump model is based on the data included in a performance map provided by a manufacturer [79], reporting the appliance capacity and COP with air temperature ranging from -20 °C to 40 °C and compressor frequency ratio (CFR) of 33%, 66% and 100%. More details can be found in [71]. The selected appliance is an air-to-water heat pump for residential application, with an inverter driven compressor and with a nominal heating capacity of 15 kW at air 7 °C and water 40/45 °C. It has been verified that the appliance is representative of the units available on the market by comparing its efficiency with the efficiency of appliances from the Eurovent database [80].

Gas absorption heat pump model

The GHP model, which details can be found in [81], is based on experimental data carried out on an ammonia/water gas driven heat pump prototype designed for residential applications. The data have been collected according to the test procedure defined in the EN 12309-4 and cover a range of more than 50 working conditions, obtained by the combination of various air temperature, outlet temperature and capacity ratio (CR). The model consists of a set of algebraic equations that allow calculating the Gas Utilization Efficiency (GUE) and the Auxiliary Energy Factor (AEF), defined as in Eq. (4-1) and Eq. (4-2), based on the external air temperature, the return water temperature and the CR.

$$GUE = \dot{Q}_h / \dot{Q}_{gas} \quad (4\text{-}1)$$

$$AEF = \dot{Q}_h / \dot{W} \quad (4\text{-}2)$$

Once the GUE and AEF are known, the gas ($\dot{Q}_{gas}$) and electrical ($\dot{W}$) inputs can be calculated from the required heating capacity ($\dot{Q}_h$). More details can be found in [71].

Solar system model

The solar system is composed by a field of flat plate solar thermal panels, a circulation pump and a heat exchanger immersed in the DHW tank (Fig. 4-10). The flat plate solar thermal panels thermal performance has been assessed using the Trnsys Type 1. The used efficiency equation parameters are: 0.8 for the intercept value, 3.6 W/m2/K for the slope and 0.014 W/m2/K2 for the curvature. Lastly, about the effects of off-normal solar incidence there are 5 possibilities for considering it using the Trnsys Type 1. In this instance, a linear function has been used to compute the incidence angle modifier (IAM). The coefficient of the function used is 0.2 for the 1st order IAM.

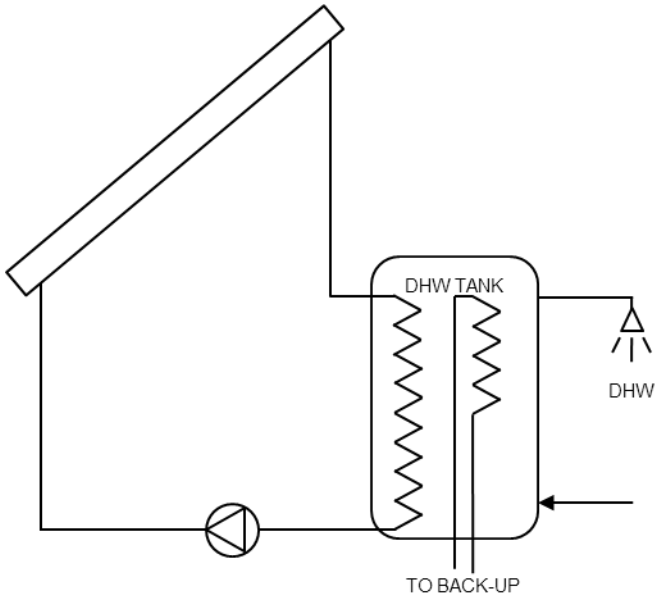

Fig. 4-10: Scheme of the solar system

Results

Heating need

The yearly SH demand for the nine buildings are reported in Table 4-8. The DHW demand, equal for the nine cases, is 30.5 kWh/m2/y. The monthly details can be found in Fig. 4-11, Fig. 4-12 and Fig. 4-13, for the warm, average and cold climate respectively. The vertical bars display the monthly SH and DHW demand profiles for the old (O), refurbished (R) and new (N) buildings, while the lines show the trend of the maximum, average and minimum monthly mean air temperatures.

Table 4-8: Building heating needs for the various cases.

climate	building	SH needs kWh/m^2/y
warm	old	208.1
	refurbished	58.5
	new	42.5
average	old	230.6
	refurbished	65.6
	new	25.0
cold	old	202.8
	refurbished	146.1
	new	29.0

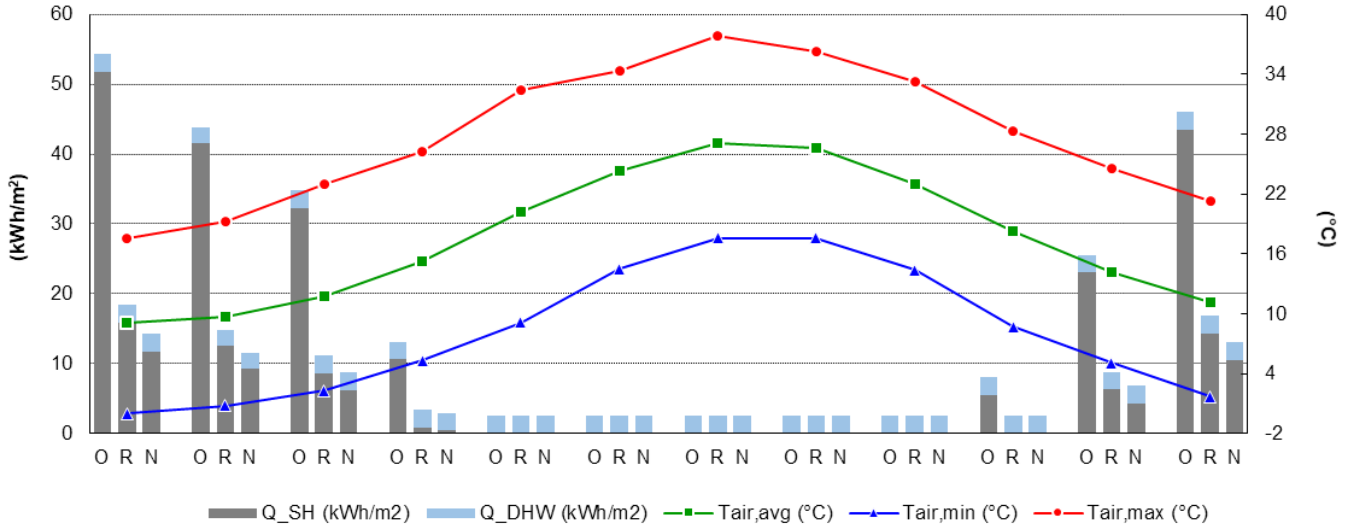

Fig. 4-11: Monthly SH and DHW demand and external mean air temperatures for the warm climate.

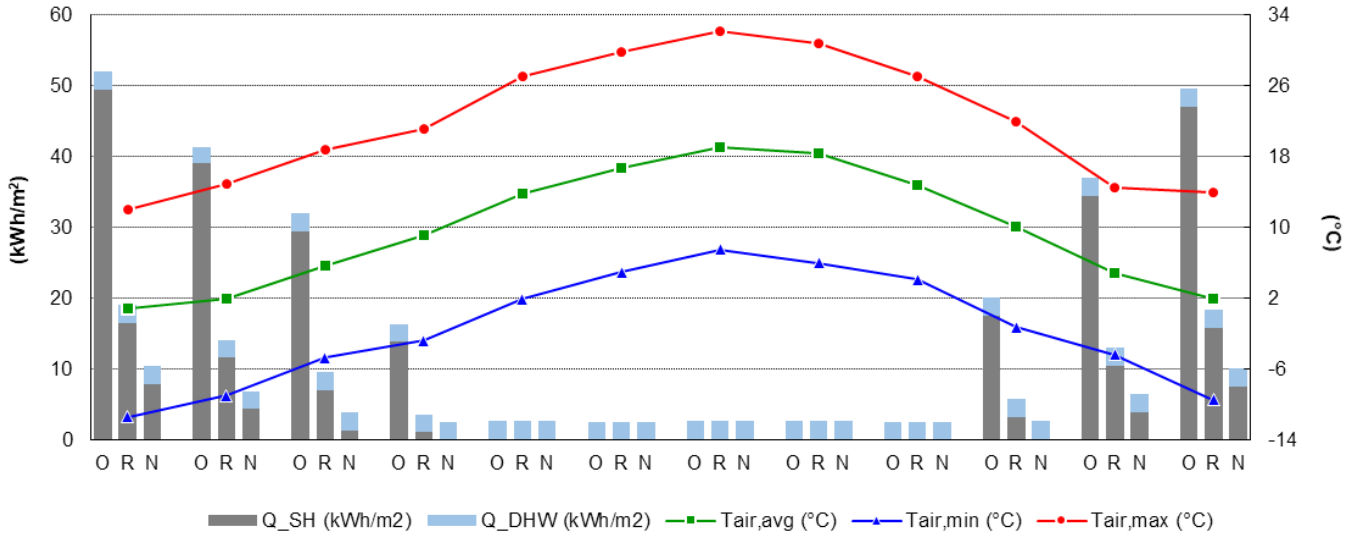

Fig. 4-12: Monthly SH and DHW demand and external mean air temperatures for the average climate.

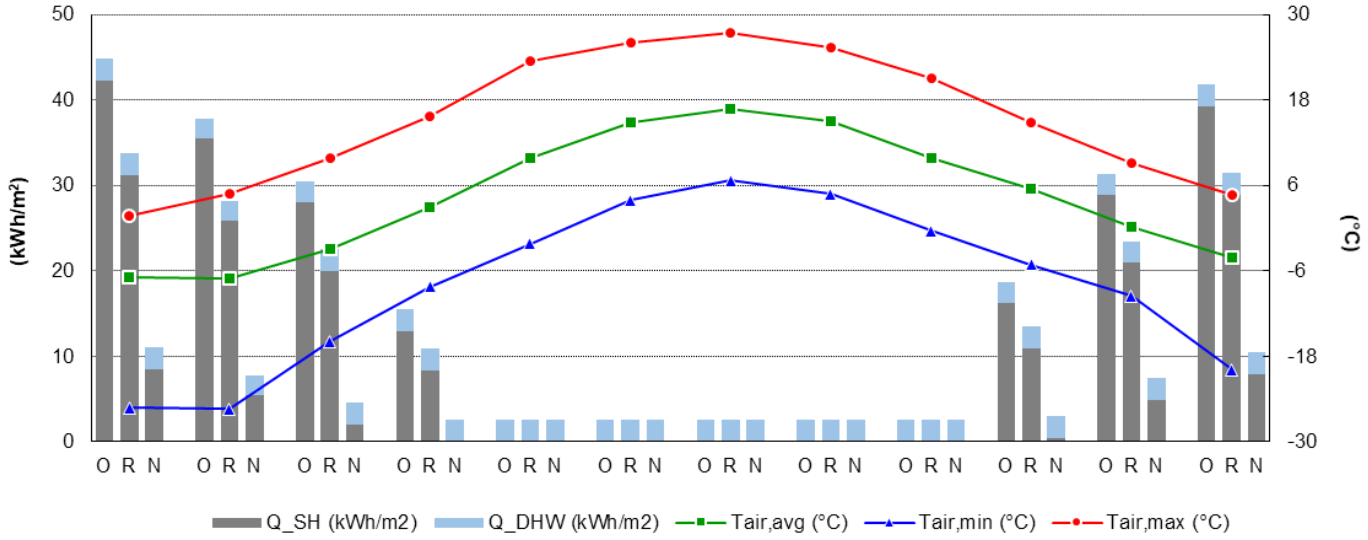

Fig. 4-13: Monthly SH and DHW demand and external mean air temperatures for the cold climate.

Primary energy consumption

The performances of the different systems are summarized in Fig. 4-14, Fig. 4-15 and Fig. 4-16 for the old, refurbished and new buildings respectively. In the charts, the light grey bars represent the gas yearly input and the dark grey bars are the required electrical input. The considered electrical input is limited to the auxiliaries of the heating device, while the consumption of circulation pumps or system controls has not been accounted in the comparison. In fact, since these contributions depend on the building and not on the heating device, they just represent a constant offset on the analysis. Thus, for condensing boiler the amount of electrical energy consumption is barely visible, due to the negligible auxiliaries, and for gas driven heat pumps it is rather small, being associated to the fan and solution pump operation only. The electric heat pump with electrical back-up does not require any gas input, while for the system with electrical heat pump and back-up boiler, inputs of both gas and electricity are required. The dots represent the Primary Energy Ratio (PER), calculated according to Eq. (4-3) with different values of the Primary Energy Factor (PEF). In fact, the calculation of the primary energy consumption for each case depend on the PEF used for the conversion of electrical energy into primary energy.

$$PER = \frac{Q_h}{Q_{gas} + W_{in}\, PEF} \qquad (4\text{-}3)$$

For this work, the calculations have been performed for PEF values of 2.5, 2.0 and 1.8, i.e. the actual, the newly proposed and an even lower value, which may become the reference in a future scenario with higher renewable energy penetration. As expected, the variation of the PER with the PEF is almost negligible for the systems with condensing boiler or GHP, while it becomes significant when an electrical heat pump is used. Comparing the different systems, in the cold climate, the results suggest that the monovalent GHP is the system with the higher PER for all the buildings, regardless of the PEF. This result

can be explained with the capability of GHP to maintain a high GUE even at high thermal lifts, both given by low ambient temperature and high water temperature. The gap between GHP and EHP increases in the new building, even if the underfloor heating system allows relatively low thermal lift for space heating, because the average lift along the year is increased by the high share of heating energy delivered for the DHW production. With a PEF for electrical energy of 2.0 or below the systems based on an EHP have a PER higher than the condensing boiler, except for the system with electrical back-up in the cold climate. Considering the average climate, the monovalent GHP remains the solution with the highest PER in both the old and refurbished building, while both the systems with EHP perform better in the new building. This is explained considering that EHP have a steeper relation between thermal lift and performances. Thus, even if their efficiency is lower at high lift, it becomes higher when climatic conditions or supply temperature allow low lifts. Therefore, the PER of EHP-based systems results higher also for the warm climate, except for the new building in the warm climate, where the fraction of heating power at high temperature required for the DHW production is high. In this case the PER of the monovalent GHP and the EHP+CB are very similar, with the value of PEF for electricity above 2.0. A dependence of the performance by the fraction of delivered energy dedicated to the DHW production is found also on the impact of the solar system on the system performances. In old buildings, where the demand for the DHW is about 10% of the overall heating demand, the increase of the PER is small. In new buildings, where the DHW can reach 50% of the heating demand, the improvement of the PER much more evident. Besides the building typology, the climatic conditions affect the performance of the solar system, with a higher contribution in the warm climate than in the average and cold. Summarizing, the calculations show that systems alternative to the condensing boiler can provide higher efficiency in terms of primary energy. Additionally, the results suggest that climate and building typology drive the selection of the system configuration. In particular, fuel driven heat pumps result the most suitable technology for retrofitting the heating system of existing buildings when the original high-temperature emission system is maintained. Additionally, they can also be preferred to EHP for new buildings in the cold climate. Electric heat pumps best fit the warm climate and the new buildings in the average climate.

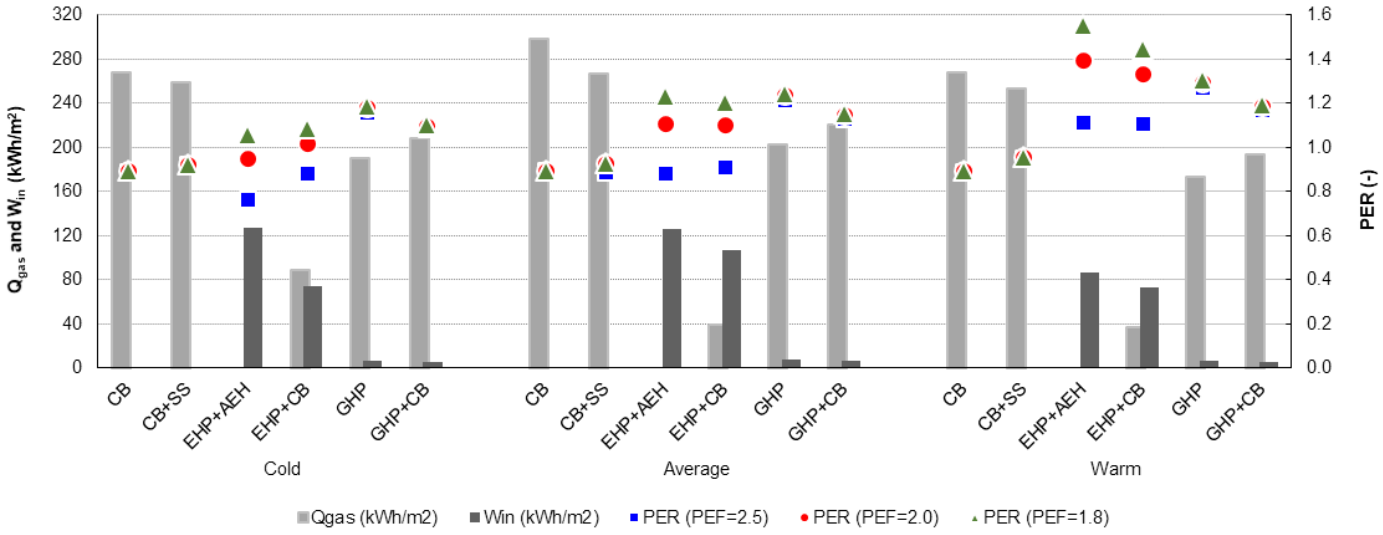

Fig. 4-14: Yearly gas and electricity demand and PER for the old building in the three climates.

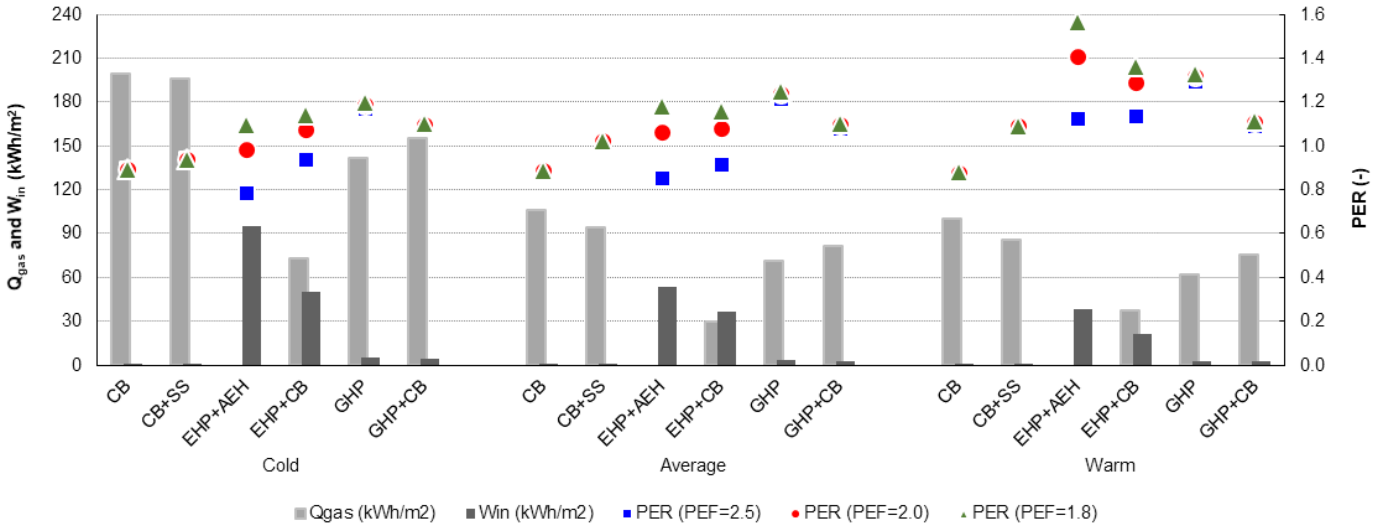

Fig. 4-15: Yearly gas and electricity demand and PER for the refurbished building in the three climates.

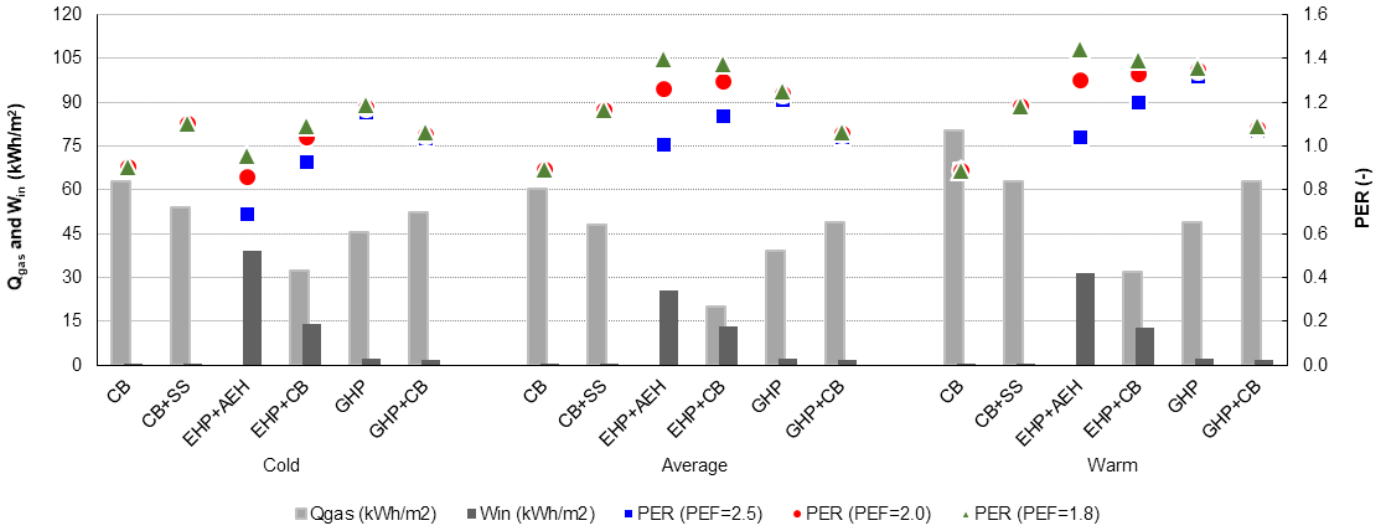

Fig. 4-16: Yearly gas and electricity demand and PER for the new building in the three climates.

CO_2 emissions

Besides primary energy, CO_2 emissions represent another useful indicator for policy makers when comparing different heating technologies. The calculations have been performed at UE level, using a CO_2 emission intensity for electricity generation of 275.9 g_{CO2}/kWh, as reported by the European Environmental Agency [82]. For what concerns the natural gas, a value of 205 g_{CO2}/kWh has been used. The results reported in

Table 4-9 for the different climatic conditions and building typology, show that all the alternative systems guarantee CO_2 savings compared to the condensing boiler. The savings given by the solar system depend only on the climate, as solar energy is used only for DHW production, which is independent on the building typology. On the contrary, EHP and GHP guarantee savings that are dependent on the heating demand, higher in the old buildings and lower in the new ones. Comparing the alternative configurations investigated for the EHP and the GHP, in both cases the solution with a condensing boiler as back-up system gives the least CO_2 savings. In the case of the EHP, this can be explained with the different sizing criteria applied, which reduce significantly the operation of the electric back-up compared to the condensing boiler back-up. For what concerns the cases with the GHP, the CO_2 savings depend only on the seasonal efficiency of the system that is always lower for the monovalent appliance.

Table 4-9: Yearly CO_2 emission savings and relative variation compared to condensing boiler.

		CO_2 savings (kg_{CO2}/y)					
		Cold		average		Warm	
Old	CB+SS	263	(-3%)	327	(-4%)	501	(-7%)
	EHP+AEH	2 844	(-37%)	3 914	(-46%)	4 391	(-57%)
	EHP+CB	2 335	(-30%)	3 550	(-41%)	3 892	(-50%)
	GHP	2 010	(-26%)	2 511	(-29%)	2 525	(-33%)
	GHP+CB	1 549	(-20%)	2 011	(-23%)	2 003	(-26%)
Renovated	CB+SS	271	(-5%)	397	(-13%)	564	(-19%)
	EHP+AEH	2 234	(-39%)	1 337	(-44%)	1 678	(-58%)
	EHP+CB	1 868	(-32%)	1 120	(-37%)	1 264	(-44%)
	GHP	1 517	(-26%)	917	(-30%)	1 016	(-35%)
	GHP+CB	1 142	(-20%)	717	(-23%)	635	(-22%)
New	CB+SS	334	(-18%)	408	(-23%)	571	(-25%)
	EHP+AEH	530	(-29%)	907	(-52%)	1 244	(-54%)
	EHP+CB	475	(-26%)	763	(-44%)	990	(-43%)
	GHP	460	(-25%)	518	(-30%)	822	(-36%)
	GHP+CB	290	(-16%)	294	(-17%)	443	(-19%)

Cost targets

Prime cost is usually the main factor hindering the diffusion of more efficient heating technologies. Thus, an economic analysis is required to complete the picture provided by this comparison. However, a direct comparison based on actual market prices would not provide meaningful results, because of the differences levels of maturity among the technologies. Using the condensing boiler as reference technology, the acceptable cost difference has been calculated as an economic indicator, i.e. the additional cost that can be accepted for a given technology compared to a condensing boiler. The calculation has been performed for some representative European Countries, using the natural gas and electricity prices provided by Eurostat [83, 84], which include taxes and levies, and reported in Table 4-10. Unlike for primary energy and CO_2 emissions, for what costs are concerned, it makes less sense to carry out an analysis at European level, since the economic and boundary conditions of the space heating and DHW markets vary significantly from country to country. The results of the economic analysis can be found in Table 4-11, where the considered climatic condition is reported within brackets for each country. To improve readability, the results have been rounded to the nearest hundredth. The acceptable additional cost is strongly dependent on the heating demand of the building, thus it is usually higher in the old buildings and lower in the new ones. Additionally, it depends on the gas and electricity prices and on the ratio between the two prices. Looking at two extreme situations, in Sweden, with high gas price and low ratio between electricity and gas prices the acceptable additional cost is high for all the technologies, especially for EHP. On the contrary, in Germany the price of electricity is high, while the ratio between electricity and the gas prices are rather low. Thus, EHP are not economically convenient and also the technologies using gas as main energy source have a lower acceptable additional cost than in other countries.

Table 4-10: Electricity and natural gas prices in € and ration between the two prices.

	Sweden	France	Germany	Italy	Netherlands	UK	Greece
electricity price	0.19	0.17	0.30	0.24	0.18	0.19	0.18
gas price	0.12	0.07	0.07	0.08	0.08	0.06	0.07
ratio	1.7	2.3	4.4	2.8	2.3	3.1	2.4

Table 4-11: Additional acceptable cost compared to condensing boiler for a simple pay-back time of 5 years for different European countries (in €).

		Sweden (cold)	France (average)	Germany (average)	Italy (average)	Netherlands (average)	UK (average)	Greece (warm)
old	CB+SS	700	600	500	700	600	500	900
	EHP+AEH	5 000	1 000	-10 700	-2 500	1 300	-3 300	3 300
	EHP+CB	4 800	1 200	-8 700	-1 600	1 600	-2 400	3 100
	GHP	5 500	4 000	3 200	4 600	4 500	3 200	4 200
	GHP+CB	4 300	3 200	2 500	3 600	3 600	2 600	3 300
refurbished	CB+SS	800	700	700	800	800	600	1 000
	EHP+AEH	4 100	200	-4 100	-1 100	300	-1 400	1 300
	EHP+CB	4 100	400	-2 600	-400	600	-700	1 300
	GHP	4 200	1 500	1 100	1 700	1 600	1 200	1 700
	GHP+CB	3 100	1 000	700	1 100	1 100	800	1 000
new	CB+SS	900	700	700	800	800	600	1 000
	EHP+AEH	700	500	-1 500	0	700	-300	800
	EHP+CB	1 000	800	-400	600	900	300	1 100
	GHP	1 300	800	600	900	900	600	1 400
	GHP+CB	800	400	300	500	500	300	700

Conclusions

The seasonal energy efficiency of six different heating systems for space heating and DHW production in a single-family house has been compared numerically in terms of primary energy. To include the main variables affecting the results, the analysis has been carried out for three different representative European climates and for three different building standards for each climate.

- The benefit given by the solar systems are higher in warm climates and in new buildings, where the energy need for DHW is comparable with the need for space heating.
- The thermal lift impacts on the performances of the heat pumps, but more significantly on vapour compression than on absorption appliances. Consequently, the GHP would result a promising option for high-lift applications, i.e. in the cold climate and for existing buildings, with radiator-based emission system
- The distinction of the most suitable heating device for each building becomes less obvious if the comparison is made in terms of CO_2 emissions or costs.

- From a comparison at EU level based on CO_2 savings, all the considered technologies provide an emission reduction compared to the condensing boiler. In particular, systems with an EHP result the less impacting, especially if an auxiliary electric heater is used.
- The economic comparison evaluated the maximum acceptable additional cost compared to the cost of a condensing boiler. The prices of natural gas and electricity influenced significantly the results. In particular, in old buildings, in countries with high electricity prices as Germany, Italy or UK, the EHP have to be less expensive than condensing boilers to be economically convenient. In Germany this is the case for refurbished and new buildings too. On the contrary, in countries with higher gas prices or lower electricity prices, the additional prices for EHP and GHP are comparable.

4.1.3 ISE Simulation Studies

A simulation study has been performed to provide performance numbers of gas fired sorption heat pumps in the residential sector in order to assess the impact of such systems with respect to environmental effects, compared to conventional heating systems.

Scope

A comparative approach is applied in this study: two different fuel driven sorption heat pump technologies based on currently developed technologies are compared with conventional heating technology, representing the exclusive use of a condensing gas boiler (reference system). The phrase 'current technology' in this context means one market available technology (ammonia-water absorption technology) as well as present laboratory test status of a water-zeolite adsorption technology. For these technologies, reliable data to execute the comparative calculations are available. Other technologies (e.g. ammonia-active carbon adsorption, ammonia – salt absorption, other ammonia-water absorption cycles) are still under development and may achieve promising performance results in the near future, see sections above.

To assess the potential of the heat pump systems, building loads from typical residential buildings are applied. The loads are generated through building simulation, but on base of well-defined building standards. The applied building models range from non-retrofitted multi-family houses (MFH) to new single family houses (SFH, present building standard). All calculations are executed for meteorological conditions of five European sites.

Economical aspects and life-cycle aspects are not topic of this study. An energetic and economic comparison of absorption and electrically driven compression heat pumps is e.g. shown in [71].

Thus, the performance figures and environmental savings presented in this study reflect the running system operation. The results are presented as annual values of performance (i.e., gas utilization efficiency) and environmental savings in comparison to the reference system (i.e., CO2 and primary energy savings and primary energy ratio).

Sites and thermal building loads

Climate data of five European sites (London, Potsdam, Paris, Strasbourg, Milano) were applied in the study, to determine the building heat loads. From a meteorological point of view, the sites correspond to

the climate classification [85] of Cfb (warm temperate climate, fully humid, warm summer) with the exception of Milano, corresponding to Cfa (warm temperate, fully humid, hot summer) respectively.

Despite of identical or similar climate classification, the site dependent temperature conditions reveal large differences in heating demand for the buildings in the survey. For the calculation of the heat demand, hourly data of ambient temperature and humidity were generated for each site by use of the meteorological engineering software Meteonorm [86].

For four sites, the minimum ambient temperatures are still above -10°C and thus conform with the ‘average climate‘, as classified in the European Standard EN12309, part 7 [86], whereas the Potsdam site normally fits to the ‘cold climate‘ classification. Nevertheless, in the light of the very few hours of falling below -10°C at Potsdam site and for reasons of a better comparison of the results, the heating system temperature curve of the ‘average climate‘ was applied in the calculations to all sites.

The meteorological data set of Strasbourg is additionally used for the performance calculation of a representative European site (EU), applying European conversion numbers for primary energy use and greenhouse gas emission instead of individual national conversion numbers.

In the building sector, multi-family houses (MFH) play an important role in greenhouse gas avoidance strategies, as their share on building stock and on living space area is high. e.g., in Germany, 31% of the living space accounts to small and medium size MFH with 3 to 12 apartments [87]. Another reason for the interest in MFH in the context with this study is that the market available gas fired sorption heat pump from the manufacturer Robur with its capacity of 18 kWth or above yet does not fit to small residential buildings.

For the assessment in this study in the context with a larger gas driven heat pump, an MFH model was applied, which was defined within the activities in the Low-Ex project group [88]. The building model images an MFH with 3 floors and 3 apartments on each floor. The building standard corresponds to the construction period of 1959-1978, as compiled by the Tabula/Episcope Projects (see: http://episcope.eu); the total number of occupants is 13. The building model setup and calculation of thermal loads was performed in the simulation environment of TRNSYS, version 17 [89].

Two versions of the building are applied:

1. MFH as representative for an average German non-retrofitted building (building stock);
2. MFH+ retrofitted in a conventional way according to Tabula/Episcope specifications for Germany, which resemble the requirements of the German EnEV 2014/2016 [90].

The load data are transferred to hourly data of each hour of a representative year of meteorological data for the sites previously specified. Additionally, thermal loads for preparing domestic hot water (DHW) for the buildings are included. The annual share of heat demand for DHW preparation on the total heat demand is shown in Fig. 4-17, revealing the distinctly higher significance of hot water preparation in buildings with higher energy saving standards.

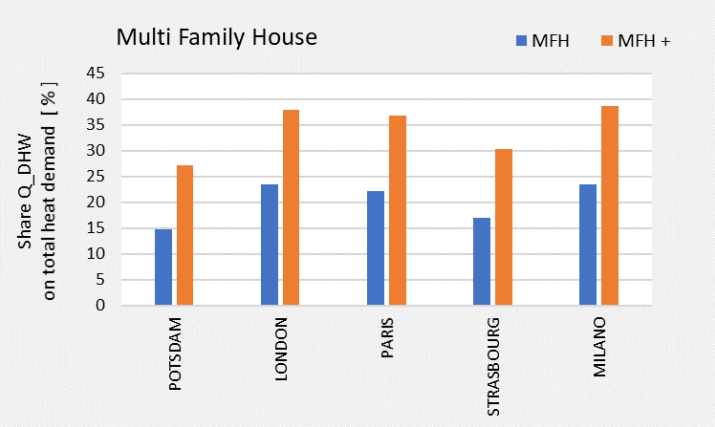

Fig. 4-17: MFH: Share of heat demand for DHW preparation on the total heat demand.

For small capacity gas fired adsorption heat pumps, the market of single family houses (SFH) is of especial interest. Within this comparative study, two single family houses were modelled and heat loads for the sites given in Figure 2.1 have been determined:

1. SFH+ as representative for a retrofitted building with 120 m² living area;
2. SFH_{NEW} as representative of a new building with 150 m² living area.

The load calculations were carried out with a one-node building model according to DIN EN ISO 13790 [91]. The adopted U-values of the key building components are the averages of the published values of the respective countries.

The load data are determined as hourly data of each hour of a representative year of meteorological data for the sites previously specified. An overview on site dependent heating loads is given in Annex A1 of this study. The number of occupants in both buildings is 4; the DHW loads are calculated accordingly on base of the approaches, used for the MFH.

The annual share of heat demand for DHW preparation on the total heat demand is shown in Fig. 4-18. In general, the set value of supply temperature in heating systems is expressed as a function of the ambient temperature. This heating system temperature is essential in the calculations, since the performance of sorption heat pumps as with all heat pumps is very sensitive to the supply temperature level.

In this study, the heating system temperature relations are derived from EN12309, part 7 [86]. The High Temperature curve (max. 55°C) requires moderate effort in exchange of e.g. appropriate radiators and is applied in the calculations of the multi-family buildings (stock and retrofit) in combination with the gas driven ammonia-water heat pump.

The Medium Temperature curve (max. 45°C) requires more ambition in the heating distribution system and is applied in the MFH+ and additionally in the calculations of the single family houses, where adsorption heat pumps are considered.

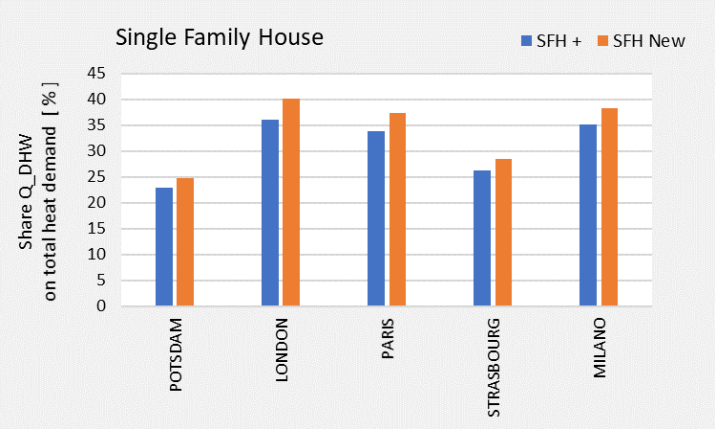

Fig. 4-18: SFH: Share of heat demand for DHW preparation on the total heat demand.

Thermally driven heat pump models

Ammonia-Water absorption heat pump

The model is based on the gas fired absorption heat pump from Robur, model K18. The machine uses the fluid pair ammonia and water and requires ambient air as low-temperature source. Since the evaporator is integrated into the machine, the heat pump is designed for external installation. The K18 model provides a heating capacity of 18 kWth (some basic data are given in [92]). Due to the ability to deliver hot water of up to 60°C, DHW can be prepared beside space heating. The simulation model of the Robur K18 heat pump was developed by POLIMI [92] and has been applied in other comparative studies as well, such as [71, 81].

The simulation of the K18 heat pump system reflects a system setup where either the DHW buffer storage is heated or the space heating is served. In the latter case, a backup gas boiler is implemented to cover peak loads on demand. This is especially required in applications with a high exploitation of the heat pump and at colder sites (e.g., Potsdam, Strasbourg).

Water-zeolite adsorption heat pump

The adsorption heat pump model is based on experimental laboratory tests at Fahrenheit GmbH and modelling based on these results by Fraunhofer ISE; the machine is not market available yet. In the experimental setup, the working pair water with the zeo-type material SAPO-34 as adsorbent is applied. The adsorption module consists of two similar heat exchangers, one acting as combined evaporator/condenser (EC) and the other as adsorption heat exchanger (AdHX). The AdHX is coated with SAPO-34 with the partial support transformation technique as by Bauer et al. [40]. The experimental results and the component data were published by Wittstadt et al. [43].

A detailed numerical model of the adsorption module was developed at Fraunhofer ISE and validated with the experimental data. The model allows the variation of geometric key parameters of the components in order to optimize the adsorption module for a given application [93]. The data presented here are obtained with geometrically optimized components for the heating application. One important difference between the experimentally tested module and the optimized module is the size of the EC. The size of the EC was reduced significantly in order to improve the efficiency without worsening the overall dynamics of the module. The model takes into account important loss mechanisms such as condensation of the working fluid on the housing and heat flux from AdHX to EC.

The heat pump for this study is considered to be connected to a ground tube as low temperature source, as low temperatures < 5°C until now cannot efficiently be used with water as working fluid due to freezing in the evaporator.

The following operation boundaries were included in the model:

Low temperature source temperature: 5°C - 9°C;

Medium temperature (inlet into AdHP): 25°C – 43°C;

Desorption temperature (driving heat from gas boiler): 80 °C – 120 °C

The source temperature is determined as a function of the ambient temperature in accordance with VDI 4650, which provides corresponding values for heating operation [94]. The maximum heating capacity of the AdHP research unit is approx. 7 kWth. However, in the comparative study, the capacity is site dependently adjusted to the building load with the target to maximize the annual overall sGUE (heating and DHW, including gas boiler performance). Thus, the maximum capacity in calculations ranges from 7 to 11 kWth.

To emphasize a special advantage of adsorption modules, the cycling period of the sorption process can be controlled in a variable way. In the model, this period is varied between 75 s (high power output, but moderate to low GUE values) to 500 s, resulting in low power output in part-load situations, but performing at distinctively higher GUE values.

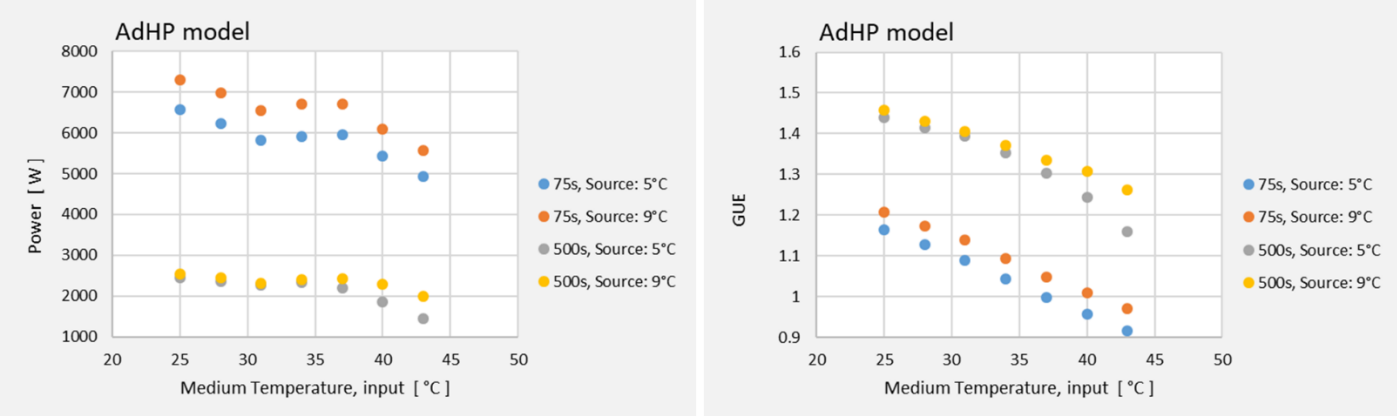

Fig. 4-19: Performance of the AdHP versus the medium temperature input. Displayed for the minimum and maximum cycling period (75s and 500s resp.) and for the low temperature bounderies 5°C and 9°C. The lowest GUE values occur at medium temperatures close the upper limit and at lowest source temperature (5°C) and at short cycling period. In this operation mode, the efficiency is comparative to the gas boiler efficiency.

For the determination of the actual GUE in the simulation, the gas boiler runs in desorption with fixed efficiency of 85%, but additional heat recovery in the flue gas heat exchanger increases the heating capacity and thus the GUE. This is considered through an increase in overall boiler efficiency, using the relation between hot water temperature (Medium temperature) and efficiency as described.

To illustrate the scope of the AdHP performance, Fig. 4-19 shows examples on modelled performance for the minimum and maximum low temperature source and for the minimum cycling period (high capacity) and maximum cycling period (low capacity, high GUE).

In the comparative study, a gas boiler, foreseen to be integrated into the AdHP and actually turning it into a hybrid heat pump being able to run in direct or heat pump mode, serves as high temperature source for desorption. Moreover, the boiler is used as peak-load and backup boiler (e.g., heating to the set point, in case the output temperature of the sorption unit is not matching the set value, given by the heating temperature curve). The boiler additionally covers all of the DHW heat demand, since the inlet temperature range into the heating circuit of the sorption unit is below the temperature levels of the DHW buffer: the lowest temperature level in the DHW buffer in the simulation is 45°C; this corresponds well with field monitoring results, gained in the German 'WP Monitor' project [95].

The system integration, applied in the comparative study for the AdHP development, is shown in Fig. 4-20.

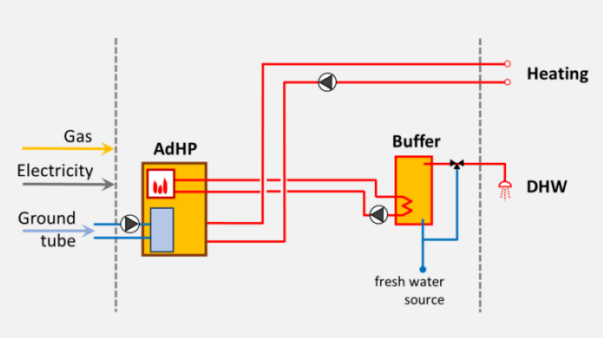

Fig. 4-20: Sketch of the heating system with the Adsorption heat pump (AdHP).

Condensing gas boiler

The GAHP model returns the GUE for each time step; the model is based on test data. Thus, the internal boiler efficiency for heating and DHW preparation with the sorption module is indirectly included. For the external peak load boiler in the GAHP and for the gas boiler in the AdHP system (Fig. 4-20), the efficiency (base: gross calorific value GCV) is simply calculated as function of the hot water input temperature into the boiler. The function is shown in Fig. 4-21 and is derived from Haller et al. [96].

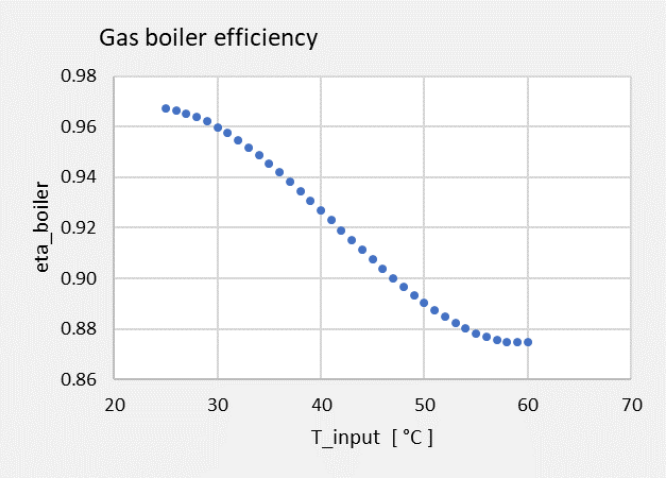

Fig. 4-21: Efficiency model of the gas boiler (peak load use and DHW heating in the AdWP system).

Results

In the following, annual results from the simulations are depicted for the sites, buildings and heat pump systems as described. For the five sites, national conversion factors for primary energy use and CO_2 emissions were used to determine the environmental performance figures.

For each site and building, a reference calculation is carried out, considering a system without heat pump but with a gas condensing boiler as only heat source for heating and domestic hot water (DHW) preparation. Focus is on the performance (seasonal Gas Utilization Efficiency, sGUE) and on environmental benefits such as CO_2 and primary energy savings (relative to the expenditures in the reference system) and on the primary energy ratio PER. The total annual $sGUE_{total}$ is calculated by including all gas input into the heat pump and peak load boiler for both heating and DHW preparation.

The calculation of environmental benefits includes beside natural gas consumption the electricity consumption in the low temperature sources (fan of air source unit, pump of ground tube circuit respectively) and auxiliary electricity demands, e.g. for the gas boiler fan. Electricity demand for heat distribution in the building is not considered, as no substantial deviations from the reference system for this purpose are expected.

Table 4-12 summarizes the results by order of the building types. The range of the results expresses site dependent differences.

The results are interpreted in the following way:

Absorption heat pump system (ammonia-water):

Highest performance is achieved at applications with a high degree of utilization (high workloads), as the heat pump performs more favorable in this operation mode. This is especially the case in the non-retrofitted MFH;

The performance in combination with MFH+ is comparatively low due to unfavorable part-load operation of the heat pump, since the machine is oversized for this building loads (since the market available Robur 18 kW_{th} is modelled, the capacity is not varied in the simulations). Thus, in an additional calculation two buildings are served by one heat pump in order to achieve more appropriate workloads (case: MFH+, 2 units). This leads to increased performance, comparative to the results obtained in the MFH;

If in the retrofitted MFH+ the heat distribution systems are additionally replaced by low-temperature distribution systems, allowing the Medium Temperature heating system curve. In this combination, the highest system performance and environmental benefits are achieved (MFH+, 2 units; Medium heating temperature);

In the most favorable applications, the sGUE (GCV) exceeds 1.35 and annual CO_2 savings up to 30 % are obtained;

The high performance in nearly all applications is supported by the ability of the ammonia-water heat pump to cover the DHW demand as well. This is especially important in retrofitted buildings, which show a high share of DHW on the overall heat demand.

Table 4-12: Summary of the results for the two different heat pump systems, sorted by building types. The range of the results is due to site dependent differences. The most favorable applications are highlighted in blue. The capacity factor indicates the adjustment of the heat pump capacity, in order to achieve an adequate heat pump operation. The factor is applied to the nominal capacity of the adsorption unit (7 kWth). The absorption heat pump model was not adjusted, as this unit is market available.

	Heating Curve	$sGUE_{total}$	Relative CO2 savings	Relative PE savings	PER / PER_{Ref}	Capacity factor
		-	%	%	%	-
Absorption: Ammonia-Water						
MFH	High	**1.30 – 1.36**	**22.9 – 28.8**	**21.5 – 26.0**	**27.4 – 35.1**	**1**
MFH$^+$	High	1.22 – 1.30	19.2 – 26.3	19.5 – 24.0	21.3 – 31.5	1
MFH$^+$, 2 units	High	1.29 – 1.35	23.0 – 29.2	21.6 – 26.5	27.6 – 36.0	1
MFH$^+$, 2 units	Medium	**1.32 – 1.37**	**24.7 – 30.0**	**23.1 – 27.2**	**30.1 – 37.3**	**1**
Adsorption: Water-Zeolite						
SFH$^+$	High	1.13 – 1.16	16.5 – 18.7	16.4 – 18.0	19.7 – 22.0	1
SFH^{NEW}	High	1.12 – 1.13	15.9 – 17.5	15.7 – 16.7	18.6 – 20.0	1
SFH$^+$	Medium	**1.17 – 1.21**	**18.6 – 21.3**	**18.5 – 20.4**	**22.7 – 25.6**	**1**
SFH^{NEW}	Medium	**1.15 – 1.20**	**17.5 – 20.5**	**17.4 – 19.8**	**21.1 – 24.7**	**1**
MFH	High	1.07 – 1.12	9.8 – 14.6	9.8 – 14.5	10.9 – 16.9	1.5
MFH$^+$	High	1.06 – 1.13	11.0 – 15.8	11.0 – 15.7	12.4 – 18.6	1.5
MFH$^+$	Medium	1.12 – 1.15	14.9 – 17.7	14.9 – 17.1	17.3 – 20.6	1.5

Adsorption heat pump system (water-zeolite):

The performance is lower than in the ammonia-water systems in some operation modes. However, in part-load operation modes, the adsorption system benefits from the possibility to increase the performance switching to higher cycle periods and thus showing in such operation modes an inverse behaviour than the ammonia-water heat pump. An appropriate layout and control of the adsorption system is therefore essential;

The performance is affected due to the fact, that DHW demand is not supported by the heat pump, but completely served through the gas boiler. The latter fact is important, since in retrofitted or new buildings the DHW share on the total heat demand increases;

The heating system temperature curve is more important in the application of this heat pump than in case of the ammonia-water heat pump. Thus, the highest performance is achieved in buildings, allowing the medium heating temperature curve;

In the most favorable applications, the sGUE is in the range of 1.2 and annual CO_2 savings up to 21% are obtained.

It needs to be kept in mind that a very simple configuration of an adsorption GHP has been modelled, which does not allow for any kind of heat recovery. Also, the limitations of the zeolite-water working pair reflect in the fact that the device cannot be run in heat pump mode for LT source temperatures below 0°C due to freezing in the evaporator. Both issues might be overcome by recent technological developments e.g. with Active Carbon – Ammonia as working pair or by making use of an LT heat source >0°C, see above.

Table 4-13 presents the results by order of the sites. The range thus reflects the influence of building types and applied heating temperature curves.

Table 4-13: Summary of the results for the two heat pump systems and different buildings and heating system curves, ordered by sites. EU denotes the representative European site, using climate data of Strasbourg and default European conversion factors (primary energy use and CO_2 emissions in electricity consumption).

	Building, Heating Curve	$sGUE_{total}$	Relative CO2 savings	Relative PE savings	PER / PER_{Ref}	Capacity factor
		-	%	%	%	-
Absorption: Ammonia-Water						
Potsdam	all	1.22 – 1.32	19.2 – 24.7	19.5 – 24.9	24.4 – 33.3	1
London	all	1.30 – 1.37	24.3 – 27.6	24.0 – 27.2	31.5 – 37.3	1
Paris	all	1.28 – 1.36	26.3 – 30.0	20.7 – 24.8	26.1 – 33.0	1
Strasbourg	all	1.23 – 1.33	23.4 – 28.1	17.6 – 23.1	21.3 – 30.1	1
Milano	all	1.27 – 1.36	22.4 – 27.1	22.6 – 27.0	29.2 – 37.0	1
EU	all	1.23 – 1.33	20.7 – 25.8	20.4 – 25.6	25.6 – 34.3	1
Adsorption: Water-Zeolite						
Potsdam	all	1.06 – 1.21	9.8 – 20.3	9.8 – 20.4	10.9 – 25.6	1 – 1.5
London	all	1.12 -1.18	14.6 – 18.9	14.5 – 18.8	16.9 – 23.1	1 – 1.5
Paris	all	1.11 -1.18	14.1 – 20.2	12.6 – 18.5	14.4 – 22.7	1 – 1.5
Strasbourg	all	1.07 – 1.20	11.6 – 21.3	10.1 – 19.4	11.2 – 24.1	1 – 1.5
Milano	all	1.08 – 1.17	11.8 – 18.6	11.7 – 18.6	13.3 – 22.8	1 – 1.5
EU	all	1.07 – 1.20	10.9 – 20.4	10.8 – 20.3	12.1 – 25.5	1 – 1.5

Considering the two heat pump systems (absorption and adsorption), a difference occurs at the 'colder' sites Potsdam and Strasbourg: In the ammonia-water heat pump system, the performance at Potsdam and Strasbourg is below the performance at the other sites. This is due to the fact that higher heating supply temperatures in general affect the performance. In principle, this is true as well in the water-zeolite system, but the effect can be superposed by the DHW preparation: due to the high heating loads at these sites, the share of heat demand for DHW is smaller than at other sites. For this reason, the influence of the low-performance DHW preparation done by the gas boiler is smaller as well. Consequently, the overall performance achieves comparatively high values in some applications. In the ammonia-water system this effect is not appearing, since hot water is prepared by the sorption heat pump as well.

4.2 Best case example

Residential Space-Water Heating Field Test – Lacrosse, Wisconsin (USA)

In February 2018, SMTI installed a 23 kW GAHP prototype (single-effect NH3-H2O, 4:1 modulating) on a 250 m^2 single-family home in Lacrosse, Wisconsin. The GAHP is connected to a hydronic air-hander (modulating) and a 300 liter indirect DHW storage tank. Controls are designed to always deliver supply air temperatures of 38 to 50°C. The GAHP system replaced a 93% (HCV) 2-stage gas furnace and 227 liter gas-fired storage water heater. In February 2019, the GAHP saw ambient temperatures drop to -34°C on concecutive nights where it maintained a 19.5°C indoor temperature and the DHW storage tank at 52°C without a backup heating source. Initial results demonstrat 32-46% reduction in natural gas use for space heating and a 50% reduction for water heating. The field test is still active. Gas Technologies Institute (GTI) designed and installaed the M&V system.

5. Conclusional remarks

Over the last 4 years, the IEA HPT Annex 43 has worked on Fuel Driven Sorption Heat Pumps (GHP). GHP have been identified as an efficient solution for space heating and sanitary hot water preparation. There was advance on several ongoing developments both for ad- and absorption technology. A water-ammonia absorption GHP based on plate heat exchangers (PHE) is under development and shows promising results both in terms of compactness and efficiency. An absorption GHP for the residential market is being developed. Another participant is working on the development of an adsorption gas heat pump with active carbon and ammonia as working fluid, using a promising new adsorber design. The development of a zeolite-water based GHP is pursued with a consortium of industry and research partners. The open source SorpPropLib materials database allows evaluation of materials for sorption heat pumps in SorpSim or other platforms. A common view on market requirements and potential was found for different markets.

Although the performance figures of the sorption heat pump technologies, analyzed in the context of residential building heating, are promising, many steps towards a higher share of market penetration have still to be done. With respect to the adsorption technology (zeolite-water), a challenge remains in enabling domestic hot water preparation, i.e., to increase the supply temperature level, and further to allow the use of a more widely available low temperature source, in the best case ambient air or building exhaust air. Identifying proper materials and heat pump design allowing for this, will make the technology complementary to present absorption (i.e., ammonia-water) technologies in the residential sector.

Other obstacles in market penetration are connected with cost, awareness of building planners and building service companies and system integration. However, gas fired sorption heat pump systems are still a new technology and demonstrate great potential to decrease the gas consumption considerably on the one hand without stressing the public electricity grids on the other hand. Thus, the technology can assist European and national efforts towards a low-carbon energy supply system transformation.

Gas (natural gas, biogas, hydrogen etc.) heat pumps for domestic use are potentially a huge market if they can become the successor technology to condensing boilers whose worldwide production exceeds 13 million/year. Sorption technology can reduce gas consumption for domestic heating by almost 40% (existing products) and might increase the saving to 60% with corresponding benefits in GHG emissions.

6. Appendix

6.1 National projects and contributions

Germany

Adoso: From 2013-2016, Fraunhofer ISE, SorTech AG (now Fahrenheit AG) and Stiebel Eltron worked together in a national collaborative project (FKZ 03ET1127) on the development of a gas adsorption heat pump based on zeolite directly crystalized onto novel aluminium fibre structure heat exchangers). A very compact adsorption module has been developed and first steps for integration into a GHP have been done within this project.

AdoSan: Since 2018, Fraunhofer ISE, Fahrenheit AG, Herrmann Burners, Haugg GmbH and other research partners work together to develop an adsorption GHP for multi-family homes based on zeolite-water as working pair, making use of the technologies developed in the project Adoso.

Between 2016 and 2019 Bosch Thermotechnik, Robert Bosch GmbH and Fraunhofer ISE cooperated on the development of a gas absorption heat pump suitable for the high supply temperatures required by existing buildings. The activities focussed on increasing efficiency and compactness by new absober concepts and extending the modulation range. Additional objectives were the revision of methods for experimental characterization and optimizing system control strategies. All activities stopped when Bosch Thermotechnik dropped out of the GHP development in spring 2019.

Italy

CNR ITAE from 2013 to 2015 worked on the PON “Ricerca e Competitività 2007-13” n°02_00153_2939517, in the frame of the project T.E.S.E.O. (Efficient Technologies for Energy Sustainability and Environmental On Board) – P.O.N. (Research and Competition 2007/2013), focusing on the development of novel adsorption heat pumps for heating and cooling for naval applications.

CNR ITAE from 2013 to 2016 worked on the “AdP MSE-CNR per la Ricerca di Sistema elettrico” funded by the Italian Ministry for the Economic Development, on the development of coated adsobers and innovative evaporator configurations for adsorption heat pumps.

Sweden

The company SaltX has worked on the development of a gas-driven heat pumps based on salts-ammonia as working pair in the course of the Annex.

USA

Several projects conducted in the US contributed to the Annex. This includes the following partial list of projects funded by the US Department of Energy, Building Technologies Office:

- Pre-commercial scale up of a gas absorption heat pump [97]
- Residential gas-fired triple state sorption heat pump [98]
- Combined water heater dehumidifier and cooler [99]
- Commercial absorption heat pump water heater [100]

Additional projects are described in more detail below:

Residential Space-Water Heating Field Test – Erwin, Tennessee (USA)
In March 2016, SMTI installed an early 23 kW GAHP prototype (single-effect NH3-H2O, 4:1 modulating) on a 200 m^2 single-family home in Erwin, Tennessee. The GAHP is connected to a hydronic air-hander with a 3-speed fan and a 300 liter indirect DHW storage tank. The GAHP system replaced a Carrier 92% (HCV) gas furnace and 190 liter electric resistance water heater. The field test, originally scheduled to last 12-18 months, is still active because the home-owners love the system and requested it to remain. Gas Technologies Institute (GTI) designed and installaed the M&V system.

Residential Space-Water Heating Field Test – Lacrosse, Wisconsin (USA)
In February 2018, SMTI installed a 23 kW GAHP prototype (single-effect NH3-H2O, 4:1 modulating) on a 250 m^2 single-family home in Lacrosse, Wisconsin. The GAHP is connected to a hydronic air-hander (modulating) and a 300 liter indirect DHW storage tank. Controls are designed to always deliver supply air temperatures of 38 to 50^oC. The GAHP system replaced a 93% (HCV) 2-stage gas furnace and 227 liter gas-fired storage water heater. In February 2019, the GAHP saw ambient temperatures drop to -34^oC on concecutive nights where it maintained a 19.5^oC indoor temperature and the DHW storage tank at 52^oC without a backup heating source. The field test is still active. Gas Technologies Institute (GTI) designed and installaed the M&V system.

In December 2018, SMTI installed 23 kW GAHP prototytypes on two additional homes in Lacrosse, Wisconsin. One home is configured for space and water heating, the other is space heating only. The field tests remain active. Gas Technologies Institute (GTI) designed and installaed the M&V system.

Multi-Family Space-Water Heating Field Test – Chicago, Illinois (USA)
In June 2019, SMTI installed an early-stage 40 kW GAHP prototype on a 6-unit multi-family building in northern Chicago. The GAHP is connected to an 800 liter indirect storage tank which is connected to both the space heating (hydronic baseboard) and domestic hot water (60^oC) systems. Two non-condensing gas boilers cover the peak load when the GAHP cannot keep up. The space heating system

supply temperature is a function of the ambient temperature, ranging from 50 to 70°C. Gas Technologies Institute (GTI) designed and installaed the M&V system.

Residential Space-Water Heating Field Test – Chicago, Illinois (USA) and Toronto, Canada
In December 2019, SMTI installed three late-stage 23 kW GAHP prototypes on three different homes in the Chicago, Illinois area. All three homes are configured for space and water heating, without a backup energy source. A fourth home will be commissioned in January 2020 on a single family home in Toronto, Canada where the 23 kW GAHP will provide all of the space and water heating. Gas Technologies Institute (GTI) designed and installed the M&V systems.

Full-Service Restaurant Water Heating-Space Cooling Field Test – Los Angelos, California (USA)
In March 2019, SMTI installed a 23 kW GAHP prototype on two different full-service restaurants in the Los Angelos, California area. Each GAHP is connected to a 435 liter indirect storage tank for domestic hot water. The GAHP prototypes are configured to automatically direct the cooling load from the evaporator either to the indoor space of the restaurant (if the thermostat is calling for cooling) or to the outdoor ambient air. Gas Technologies Institute (GTI) designed and installed the M&V systems. The project is funded by the California Energy Commission (CEC), GTI prime contractor.

Small GAHP for Space-Water Heating in Low-Load Homes (R&D)
In 2018, SMTI designed and tested an initial 6 kW GAHP (single-effect NH3-H2O, 2:1 modulating) prototype for space and water heating in low-load homes or multi-family units with individual heating systems. Additional development is on-going. GRDF/Engie provided the initial R&D funding.

Hybrid GAHP-Chiller for Year-Round Space-Water Heating and Cooling (R&D)
In September 2019, SMTI began development of a gas-fired 11 kW GAHP (single-effect NH3-H2O, 2:1 modulating) with an integrated 5.5 kW electric vapor compression chiller. This “Hybrid“ design will be capable of provding year-round space and water heating plus cooling. Intial lab testing is anticipated before the end of 2020. The Canadian Gas Association (NGIF) is providing the initial R&D funding.

Liquid-Fuel GAHP Development (R&D)
SMTI has begun development of a liquid-fuel (fuel-oil, bio-diesel, etc) fired 23 kW GAHP prototype with 3:1 modulation. An initial field test is scheduled for the winter of 2020-2021. The National Oil-Heat Research Alliance (NORA) is providing the initial funding.

France

The company Boostheat has developed a gas-driven heat pump in the course of the Annex. Although this is not a sorption heat pump, the development is mentioned here since the technology has been introduced to the market and sets a further benchmark with respect to cost and efficiency.

Austria

NexGen: Gas absorption heat pump of the next generation (AIT, TU Graz): The cooperative research project, conducted by AIT, the IWT, and the Austrian SME E-Sorp GmbH, aimed at evaluating different GAX implementations for small-scale absorption heat pumps with respect to their efficiency. Additionally control strategies for such an appliance were developed.

ThermoPump: Thermally driven solution Pump (TU Graz): The goal of this project, which is a cooperation of the IWT and the two Austrian companies Pink GmbH and Heliotherm GmbH, was the development of a thermally driven solution pump as an alternative to the nowadays common electrical solution pump in absorption heat pumps.

DoublePump: New concept of a thermally driven solution pump suitable for small-capacity ammonia/water-absorption heat pumping systems (TU Graz): This project was a follow-up project of ThermoPump and is carried out by the project partners Pink GmbH, E-Sorp GmbH, and IWT. A new dual-flow concept of a thermally driven solution pump was developed.

IEA HPP Annex 34: Thermal decomposition and corrosion in NH3/H2O heat pumps (TU Graz): This project was executed within the framework of IEA HPP Annex 34. The scope was an experimental examination of the formation of inert gases in ammonia-water absorption heat pumps by both corrosion and decomposition of ammonia.

SOptA: Optimization of NH3/H2O heat pumps by means of simulation (TU Graz): This project was a cooperation between the German company Bosch Thermotechnology GmbH and the IWT. Scope of the project was the analysis and optimization of a small-scale (18 kW heating capacity) gas absorption heat pump prototype.

UK

The UK's Department of Energy and Climate Change (now Department for Business, Energy and Industrial Strategy, BEIS) awarded the University of Warwick grant TRN:478/09/2012 to participate in the Annex and report the results to DECC/BEIS. Five publications were submitted to BEIS, available here: https://www.gov.uk/government/publications/fuel-driven-heat-pumps

During the course of the Annex, BEIS awarded the University of Warwick a Low Carbon Heating Technology Innovation Fund grant number LCHTIF1021 to develop their adsorption gas heat pump into a marketable product:
https://assets.publishing.service.gov.uk/government/uploads/system/uploads/attachment_data/file/825616/BEIS_Low_Carbon_Heating_Technology_Innovation_Fund___summary_project_details.pdf

6.2 Meetings and publications

Table 6-1: List of meetings

22.-23.11.2011	End Annex 34, Annex 43 Definition Meeting
9.-10.10.2013	Kick-off Fraunhofer ISE, Freiburg, Germany
4.-5.6.2014	Expert Meeting GdF-Suez, Paris, France
6.-7.11.2014	Expert Meeting Fraunhofer ISE, Freiburg, Germany
9.-10.6.2015	Expert Meeting, AIT, Vienna, Austria
14.-16.09.2015	Workshop „Friends of Sorption“
20.-21.10.2015	Heat Pump Summit Nürnberg, own Session on gas heat pumps (Workshop)
9.-10.12.2015	Expert Meeting, Bosch, Wernau, Germany
15.-16.6.2016	Expert Meeting, Polimi, Milano, Italy
26.-27.1.2017	Expert Meeting, ORNL, Las Vegas, USA
Jan. 2017	ASHRAE Winter Meeting, Session on Annex 43 (Workshop)
6.-7.12.2017	Expert Meeting, EHPA, Brussels, Belgium
16.-17.05.2018	Expert Meeting, SaltX, Stockholm,Sweden
16.-18.07.2018	Sorption Friends 2, Workshop, Pisa, Italy
26.-28.11.2018	Final Meeting, Freiburg, Germany

Table 6-2: List of publications

Bendix, P., Füldner, G., Möllers M., Kummer, H., Schnabel, L., Henninger, S.K., Henning, H.-M.: Optimization of power density and metal-to-adsorbent weight ratio in coated adsorbers for adsorptive heat transformation applications, Applied Thermal Engineering, 124, pp.83-90, 2017.
Rivero-Pacho, A.M., Critoph, R.E., Metcalf, S.J.: Alternative monolithic/composite carbons for adsorption generators and simulation for optimal performance, Applied Thermal Engineering, 126, pp. 350-357, 2017.
Scoccia, R., Toppi, T., Aprile, M., Motta, M.: Absorption and compression heat pump systems for space heating and DHW in European buildings: Energy, environmental and economic analysis, Journal of Building Engineering, 16, pp. 94-105, 2018.
Zhu, C., Gluesenkamp, K.R., Yang, Z., Blackman, C.: Unified thermodynamic model to calculate COP of diverse sorption heat pump cycles: Adsorption, absorption, resorption, and multistep crystalline reactions [Modèle thermodynamique unifié pour calculer le COP de divers cycles de pompe à chaleur à sorption: adsorption, absorption, résorption, et réactions cristallines en plusieurs étapes] International Journal of Refrigeration, 99, pp. 382-392, 2019.
Gluesenkamp, Kyle R.; Andrea Frazzica, Andreas Velte, Steven Metcalf, Zhiyao Yang, Mina Rouhani, Corey Blackman, Ming Qu, Eric Laurenz, Angeles Rivero-Pacho, Sam Hinmers, Robert Critoph, Majid Bahrami, Gerrit Füldner, and Ingemar Hallin (2020). “Experimentally Measured Thermal Masses of Adsorption Heat Exchangers,” ***Energies***, 2020 v.13, 1150.
Malenković, I.: Existing and Emerging International Standards for Evaluation of Fuel-Fired Sorption Heat Pumps. Oral contribution for the 2017 ASHRAE Winter Conference, Las Vegas, USA.

Malenković, I., Schossig, P.: Gaswärmepumpen, Stand der Technik und Energieeffizienz (IEA HPP Annex 34 und Annex 43). Oral contribution at the 21. Wärmepumpentagung on June 17th, 2015, Burgdorf, Switzerland.
Malenković, I., Wittstadt, U., Bongs, C., Schossig, P.: FUEL DRIVEN SORPTION HEAT PUMPS: OVERVIEW OF THE TECH-NOLOGY, MARKET AND SYSTEM PERFORMANCE. Oral contribution at the Gustav Lorentzen Natural Working Fluids Conference 2016, Edinburgh, UK.
Malenković, I., Schossig, P.: IEA HPP Annex 43: Fuel Driven Heat Pumps. Oral contribution at the European Heat Pump Summit 2013 in Nuremberg, Germany
Malenković, I.: Gas heat pump development and performance evaluation - IEA HPT Annex 43. Oral contribution at the European Heat Pump Summit 2015 in Nuremberg, Germany
Schossig, P., Nienborg, B., Füldner, G., Heilck, J., Critoph, B., Aprile, M.: Seasonal Performance Evaluation of Gas Heat Pumps with Different Working Pairs under Varying Boundary Conditions. Oral contribution at the 2017 International Sorption Heat Pump Conference in Tokyo, Japan.
Melograno, P.N., Malenković, I., Schossig, P.: Assessment of Standardised Test and Performance Evaluation Methods for Fuel Driven Sorption Heat Pumps. Oral contribution for the 13th IEA Heat Pump Conference 2020 in Jeju, Korea. (Postponed for April 2021)

6.3 Additional tables

Table 6-1: Summary of the master equation forms of the equilibrium correlation for adsorption working pairs

Equilibrium Correlation Type	Equation Form	Coefficient Constants
Langmuir	$Y = Y_0 * K * P * \left(1 - \frac{Y}{Y_0}\right)^a$ $K = K^0 * \exp\left(-\frac{\Delta H}{RT}\right)$	$a, Y_0, K^0, \Delta H$
Dubinin-Astakov (D-A) & Dubinin-Radushkevich (D-R)	$Y = Y_0 * \exp\left[-\left(\frac{A}{E}\right)^n\right]$ $A = R * T * ln\left(\frac{P_s}{P}\right)$	Y_0, E, n
Toth	$Y = Y_0 * \frac{b^m * P}{(1 + b^k * P^n)^{1/n}}$ $b = b_0 * \exp\left(-\frac{q^*}{RT}\right)$ $n = n_0 + \frac{c}{T}$	$Y_0, b_0, q^*, n_0, c, m, k$
Freundlich	$Y = \left(\sum A_i T^i\right) * \left(\frac{P}{P_{eq}(T)}\right)^{\sum B_i T^i}$	A_i, B_i

Dual Site Sips (DSS)	$Y = Y_A * \frac{(b_A P)^{\frac{1}{\eta_A}}}{1 + (b_A P)^{\frac{1}{\eta_A}}} + Y_B * \frac{(b_B P)^{\frac{1}{\eta_B}}}{1 + (b_B P)^{\frac{1}{\eta_B}}}$ $b = b_0 * \exp\left[\frac{\Delta H}{RT} * \left(1 - \frac{T}{T_0}\right)\right]$	$Y_A, b_{A,0}, q_A^*, n_A, Y_B, b_{B,0}, q_B^*, n_B$
Van't Hoff	$\log P_{eq} = -\frac{\Delta H}{RT} + \frac{\Delta S}{R}$	$\Delta H, \Delta S$

Table 6-2: Summary of the master equation forms of equilibrium correlations for absorption working pairs

Equilibrium Correlation Type		Equation Form	Coefficient Constants
Antoine		$\log_{10} P = \sum_{i=0}^{k} \left[A_i + \left\{\frac{1000 * B_i}{T - 43.15}\right\}\right] * (100 * X)^i$	$A_0 \sim A_3, B_0 \sim B_3$
Dühring		$P = r * \exp\left(C + \frac{D}{T_{ref,sat,abs}} + \frac{E}{T_{ref,sat,abs}^2}\right)$ $T_{sol} = \frac{\frac{n * T_{ref,sat} + m - B}{A}}{n} - m$ $A = a_0 + a_1 X_S + a_2 X_S^2 + a_3 X_S^3$ $B = b_0 + b_1 X_S + b_2 X_S^2 + b_3 X_S^3$	$a_0 \sim a_3, b_0 \sim b_3, n, m, r, q, C, D, E$
Mixing rules	One parameter van der Waals (1PVDW)	$a(T) = \sum_{i,j=1}^{N} x_i x_j \sqrt{a_i a_j}\,(1 - k_{ij})$ $b = \sum_i x_i b_i$	k_{ij}, T_c, P_c, ω
	Van der Waals-Berthelot	$a(T) = \sum_{i,j=1}^{N} x_i x_j \sqrt{a_i a_j}\, f(T)(1 - k_{ij})$ $f(T) = 1 + {}^{t_{ij}}/_{T}$ $k_{ij} = \frac{l_{ij} l_{ji} (x_i + x_j)}{l_{ji} x_i + l_{ij} x_j}$ $b = \frac{1}{2} \sum_{i,j=1}^{N} (b_i + b_j)(1 - m_{ij}) x_i x_j$	$l_{ij}, l_{ji}, m_{ij}, t_{ij}$
	Two-parameter conventional mixing rule (2PCMR)	$a(T) = \sum_{i,j=1}^{N} x_i x_j \sqrt{a_i a_j}\,(1 - k_{ij})$ $b = \sum_i \sum_j x_i x_j \frac{b_i + b_j}{2}(1 - l_{ij})$	k_{ij}, l_{ij}
Activity coefficient	Wilson	$\ln \gamma_1 = -\ln(x_1 + \Lambda_{12} x_2) + x_2 \left[\frac{\Lambda_{12}}{x_1 + \Lambda_{12} x_2} - \frac{\Lambda_{21}}{x_2 + \Lambda_{21} x_1}\right]$ $\Lambda_{12} = \frac{V_{m,2}}{V_{m,1}} \exp\left(-\frac{\lambda_{12} - \lambda_{22}}{RT}\right)$ $\Lambda_{21} = \frac{V_{m,1}}{V_{m,2}} \exp\left(-\frac{\lambda_{21} - \lambda_{11}}{RT}\right)$	$\lambda_{12}, \lambda_{21}$

	Tsuboka and Katayama	$\ln\gamma_1 = -\ln(x_1 + x_2\,\Lambda_{21}) + x_2\left[\frac{\Lambda_{21}}{x_1 + x_2\Lambda_{21}} - \frac{\Lambda_{12}}{x_1\Lambda_{12} + x_2}\right] + \ln(x_1 + x_2\rho_{21}) - x_2\left[\frac{\rho_{21}}{x_1 + x_2\rho_{21}} - \frac{\rho_{12}}{x_1\rho_{12} + x_2}\right]$ $\rho_{ij} = {V_{m,j}}/{V_{m,i}}$	$\lambda_{12}, \lambda_{21}$
	Wang and Chao	$\ln\gamma_1 = -\ln(x_1 + x_2\,\Lambda_{21}) + x_2\left[\frac{\Lambda_{21}}{x_1 + x_2\Lambda_{21}} - \frac{\Lambda_{12}}{x_1\Lambda_{12} + x_2}\right] + \frac{1}{RT}\left(\frac{z}{2}\right)\left[x_{21}^2(\lambda_{21} - \lambda_{11}) + x_2 x_{22}\frac{x_{12}}{x_1}(\lambda_{12} - \lambda_{22})\right]$ $x_{ji} = \frac{x_j e^{-{\lambda_{ji}}/{RT}}}{\sum_k (x_k\, e^{-{\lambda_{ki}}/{RT}})}$	$\lambda_{12}, \lambda_{21}$
	Non-random two liquid (NRTL)	$\ln\gamma_1 = (1 - x_1)^2\left(\tau_{21}\left(\frac{\exp(-2\alpha_{12}\tau_{21})}{x_1 + (1 - x_1)\exp(-\alpha_{12}\tau_{21})}\right)^2 + \tau_{12}\frac{\exp(-2\alpha_{12}\tau_{12})}{[(1 - x_1) + x_1\exp(-\alpha_{12}\tau_{12})]^2}\right)$ $\tau_{ij} = \frac{\Delta g_{ij}}{RT}\ (i, j = 1,2)$	$\Delta g_{ij}, \Delta g_{ji}, \alpha_{12}$
	Universal Quasi-chemical (UNIQUAC)	$\ln\gamma_1 = \ln\frac{\phi_1}{x_1} + (\frac{z}{2})q_1\ln\frac{\theta_1}{\phi_1} + l_1 - \frac{\phi_1}{x_1}\sum_j x_j l_j - q_1\ln\left(\sum_j \theta_j\,\tau_{ji}\right) + q_1 - q_1\sum_j \frac{\theta_j\tau_{ij}}{\sum_k \theta_k\tau_{kj}}$ $\tau_{ij} = \exp\left(-\frac{\Delta u_{ij}}{RT}\right)$ $l_j = \left(\frac{z}{2}\right)(r_j - q_j) - (r_j - 1)$	$\Delta u_{ij}, \Delta u_{ji}, r_i, r_j, q_i, q_j$
	Heil	$\ln\gamma_1 = -\ln(x_1 + x_2\,\Lambda_{21}) + x_2\left[\frac{\Lambda_{21}}{x_1 + x_2\Lambda_{21}} - \frac{\Lambda_{12}}{x_1\Lambda_{12} + x_2}\right] + x_2^2\left[\tau_{12}\left(\frac{\Lambda_{21}}{x_1 + x_2\Lambda_{21}}\right)^2 + \frac{\tau_{12}\Lambda_{12}}{(x_2 + x_1\Lambda_{12})^2}\right]$ $\Lambda_{ij} = \frac{V_{m,j}}{V_{m,i}} * \exp\left(-\frac{\Delta\lambda_{ij}}{RT}\right)$ $\tau_{ij} = \frac{\Delta\lambda_{ij}}{RT}$	$\lambda ij, \lambda_{ji}$
	Flory-Huggins	$\ln\gamma_1 = \ln\left(1 - \left(1 - \frac{1}{r}\right)\phi_2^*\right) + \left(1 - \frac{1}{r}\right) * \phi_2^* + \chi * \phi_2^{*2}$ $\phi_2^* = \frac{r x_2}{x_1 + r x_2}$ $\chi = \frac{w^0}{RT}\left(1 + \frac{w^1}{T}\right)$	w^0, w^1, r

6.4 Coefficient constants in sorption isotherm database

6.4.1 Toth

Table 6-3: Coefficients for Toth equation

Refrigerant	Adsorbent		Y_0 [g/kg]	b_0 *10^6 [1/kPa]	$\frac{q^*}{R}$ [K]	n_0 [-]	C [K]	m [-]	k [-]	Literature	Valid range
CO_2	Zeolite	5A	642.4	6.761e-2	5.625e3	2.7e-1	-2.002e1	1	n	[101]	-45~175°C
		13X	585.2	4.884e2	2.991e3	7.487e-2	3.805e1	1	n	[101]	-45~175°C
	SG	-	655.6[b]	5.164e-1	2.330e3	-3.053e-1	2.386e2	1	n	[101]	10~55°C
	Activated carbon fiber (ACF)	A-20	1.56e3	2.55e-1	2.313e3	0.696	0	1	n	[102]	-10~70°C
	Activated carbon	Maxsorb III	3.06e3	1.17e-1	2.45e3	0.664	0	1	n	[102]	-10~70°C
H_2O	Zeolite	5A	423	4.714e-4	9.955e3	3.548e-1	-5.114e1	1	n	[101]	0~100°C
		13X	271.8	2.408e-1	6.852e3	3.974e-1	-4.199	1	n	[101]	0~100°C
	SG	-	1.14e8	2.787e-5	1.093e3	-1.190e-3	2.213e1	1	n	[101]	0~75°C
		Fuji Davison Type RD	450	7.3e-4	3.239e5	12	0	1	n	[103]	[a]
Propylene	Zeolite	13X	112.56	3.5e-1	5.1e3	0.608	0	1	n	[104]	30~200°C
		13X	108.78	2.5e-1	5.1e3	0.658	0	1	n	[105]	60~120°C
		4A	85.26	7.4	3.6e3	0.666	0	1	n	[104]	30~200°C
		5A crystal	168.84	1.33e4	1.684e3	0.40	0	2.5	1	[106]	70~200°C
		5A pellets	123.06	2.02e4	1.612e3	0.36	0	2.78	1	[106]	70~200°C
	Carbon molecular sieve	-	80.934	1.32e4	1.726e3	0.325	0	3.08	1	[107]	70~150°C
Propane	Zeolite	13X	117.92	3.5e-1	4.3e3	0.58	0	1	n	[104]	30~200°C
		13X	96.8	2.5e-1	4.438e3	0.892	0	1.12	1	[105]	60~120°C
		4A	89.32	6e2	0	1	0	1	n	[104]	30~200°C
		5A crystal	160.16	4.3e3	1.828e3	0.46	0	2.17	1	[106]	70~200°C
		5A pellets	114.84	4.94e2	2.393e3	0.58	0	1.72	1	[106]	70~200°C
	CMS	-	77.308	1.81e4	1.378e3	0.356	0	2.81	1	[107]	70~150°C
1-Butene	Zeolite	13X	121.8	2.5e-1	6.543e3	0.452	0	2.21	1	[105]	60~120°C
HFO-1234ze(E)	Activated carbon	Maxsorb III	3.74e3	1.3	3.685e3	0.295	0	1	n	[108]	[a]
R-134a	Activated carbon	Maxsorb III	4.32e3	3.51	3027e3	0.321	0	1	n	[108]	[a]

[a] not provided in original literature
[b] note from original literature: silica is not fully saturated

6.4.2 Dubini-Astakhov (D-A) and Dubinin-Radushkevich (D-R)

Refrigerant	Adsorbent		W_0 [m3/kg]	E [J/mol]	n [-]	Literature	Valid range of adsorption potential A [J/g]
Ammonia	Zeolite	NaX	0.000221	18994	2	[109]	[a]
Water	Silica gel	A5BW	0.000455	3585	1.25	[110]	[a]
	Silica gel	RD2560	0.000327	4384	1.35	[110]	[a]
	Silica gel	A++	0.000489	3804	1.35	[110]	[a]
	Zeolite	-	0.000269	19596	2	[111]	[a]
Ethanol	Composite silica gel	LiBr	0.00068	6900	1.8	[112]	Approximate range: from 20 to 410 [b]
	AC	SRD 1352/3	0.00082	8780	1.5	[112]	Approximate range: from 20 to 410 [b]
		AP4-60	0.00045	10600	2	[112]	Approximate range: from 20 to 410 [b]
		ATO	0.00061	11200	1.7	[112]	Approximate range: from 20 to 410 [b]
		COC-L1200	0.00044	13300	2	[112]	Approximate range: from 20 to 410 [b]
	ACF	FR20	0.00075	13500	2	[112]	Approximate range: from 20 to 410 [b]
Methanol	AC	G32-H	0.000482	19220	2.59	[113]	Approximate range: from 10 to 540 [b]

		Norit R 1 Extra	0.000519	17380	2.27	[113]	Approximate range: from 10 to 540 [b]
		RUTGERS CG1-3	0.000535	14260	1.8	[113]	Approximate range: from 10 to 540 [b]
		Norit RX 3 Extra	0.000551	16890	2.06	[113]	Approximate range: from 10 to 540 [b]
		Carbotech C40/1	0.000633	12460	1.85	[113]	Approximate range: from 10 to 540 [b]
		Carbotech A35/1	0.000786	11720	1.76	[113]	Approximate range: from 10 to 540 [b]
		AC35	0.000425	6906	2.15	[114]	-10~120°C
		207E4	0.000365	5947	1.34	[115]	[a]
		Chinese LSZ30	0.000405	4941	1.26	[115]	[a]
		Thai MD6070	0.000988	4402	1.12	[115]	[a]
		LH	0.000860	4356	1.321	[116]	20~110°C
		DEG	0.000534	5625	1.31	[116]	54~88°C
		PKST	0.000258	8500	2	[116]	91°C
		AC-35	0.000427	7100	2.15	[116]	-10-120°C
		BPL	0.000414	6700	1.45	[116]	38-107°C
		RORIT RB	0.000415	7800	2	[116]	20°C
		AC-5060	0.000363	7072	1.599	[117]	[a]
R-507A	Charcoal	Maxsorb III	0.001175	5740	1.47	[118]	Approximate range: from 10 to 100 [b]
R-32	AC	Maxsorb III	0.00405	3939	1.15	[119]	Approximate range: from 5 to 100 [b]
	ACF	A-20	0.00458	4098	1.09	[119]	Approximate range: from 5 to 100 [b]
R-134a	Charcoal	Chemviron	0.000279	14870	1.60	[120]	Approximate range: from 5 to 140 [b]
		Fluka	0.000449	8897	0.95	[120]	Approximate range: from 5 to 140 [b]
		Maxsorb	0.001548	8269	1.50	[120]	Approximate range: from 5 to 140 [b]
		Maxsorb III	0.001649	8460	1.3	[121]	Approximate range: from 10 to 140 [b]
	AC	SRD 1352/3	0.000767	10916.6	1.7	[122]	Approximate range: from 10 to 100 [b]
	ACF	A-20	0.00101	8611.7	1.5	[122]	Approximate range: from 10 to 100 [b]
R-410A [c]	AC	Maxsorb III	0.00596	4327	1.17	[123]	Approximate range: from 15 to 150 [b]
	ACF	ACF A-20	0.00325	5263.5	1.43	[123]	Approximate range: from 15 to 150 [b]
R -407C	AC	AquaSorb 2000	0.001139	6885.8	1.36	[124]	Approximate range: from 10 to 170 [b]
R-404A	AC	AquaSorb 2000	0.001035	9579.4	1.03	[125]	Approximate range: from 5 to 120 [b]
Difluoroethane	AC	Maxsorb III	0.003438	5947.8	1.3	[125]	Approximate range: from 15 to 190 [b]
Methane	AC	Maxsorb III	0.002193	4757.3	1.05	[126]	[a]
		AX21	0.00108	5464.1	1.26	[126]	[a]
		BPL	0.00036	7040	1.54	[126]	[a]
		Norit R1 Extra	0.00043	7500	1.73	[126]	[a]
		F30/470	0.000389	7742.9	1.81	[126]	[a]
		Chemviron	0.000407	8684.1	1.86	[126]	[a]
		Calgon AC	0.000309	8955.1	2.41	[126]	[a]
	ACF	ACF (A-20)	0.000717	6198.4	1.51	[126]	[a]

[a] Not provided in the original literature
[b] adsorption potential [J/g]
[c] Phase volume calculated according to the reported equation $v_a = [A - BT - \frac{1}{v_g}]^{-1}$. V_g is the sat. vapor pressure, A and B are pair specific from Srinivasan phys. Chem. Chem. Phys. 2011.

Table 6-4: Coefficients for D-A and D-R equation (volume-based)

Table 6-5: Coefficients for D-A and D-R equation (mass-based)

Refrigerant	Adsorbent		Y_0 [g/kg]	E [J/mol]	n [-]	Literature	Valid range
Water	Zeotype	AQSOA-Z01	210	4000	5	[127]	Approximate range: <160 [a]
			210	4000	5	[128]	Fitting accuracy not extremely high @ A>200 [a]
		AQSOA-Z02	285	7600	2.9	[127]	Approximate range: from 30 to 500 [a]
			310	7000	3	[128]	Fitting accuracy not extremely high @ A>200 [a]
		AQSOA-Z05	220	2700	6	[127]	Approximate range: <100 [a]
		ETS-10	129	13986.3	1.98	[129]	Approximate range: from 10 to

							700 [a]
	Silica gel	Siogel	380	3960	1.1	[130]	Approximate range: from 80 to 1100 [a]
	MOF	COP-27(Ni)	462	10014.1	4	[131]	Approximate range: from 15 to 630 [a]
	Polymer adsorbent	PS-I	1200	852.6	0.5	[132]	Approximate range: from 40 to 450 [a]
		PS-2	1760	753.1	0.5	[132]	Approximate range: from 40 to 450 [a]
R-134a	AC	Maxsorb III	222	7332.69	1.29	[133]	Approximate range: from 5 to 100 [a]
	AC	Granular	1680	9575	1.83	[134]	20-90C
	ACF	A-20	129	7136.01	1.49	[133]	Approximate range: from 5 to 100 [a]
R-410A	AC	Maxsorb III	207	5254.38	1.36	[133]	Approximate range: from 5 to 100 [a]
R507a	AC	Maxsorb III	2050	7547.2	1.34	[133]	Approximate range: from 5 to 120 [a]
	ACF	A-20	1190	8100.78	1.45	[133]	Approximate range: from 5 to 120 [a]
Ethanol	AC	Maxsorb III	1240	5265	1.9	[135]	Approximate range: from 10 to 150 [a]
			1200	5538	1.75	[136]	Approximate range: from 10 to 300 [a]
		KOH-H2 treated Maxsorb III	1090	5331	1.6	[135]	Approximate range: from 10 to 150 [a]
		H2 treated Maxsorb III	1250	4780	1.9	[135]	Approximate range: from 10 to 150 [a]
	ACF	A-20	797	6347.1	2	[136]	Approximate range: from 20 to 290 [a]
		A-20	797	6347.1	2	[137]	Approximate range: from 20 to 290 [a]
		A-15	570	8049.2	2	[136]	Approximate range: from 20 to 290 [a]
	MOF	MIL-101Cr	1100	6527.4	2.6033	[138]	Approximate range: from 10 to 140 [a]
	Composite	50% Maxsorb III, 40% EG, 10% binder	610	5.758	2	[124]	Approximate range: from 15 to 215 [a]
		70% Maxsorb III, 20% EG, 10% binder	890	5.482	1.8	[124]	Approximate range: from 15 to 215 [a]
	Phenol resin	KOH4-PR	1430	5.897	2	[139]	Approximate range: from 10 to 170 [a]
		KOH6-PR	1980	4.146	1.5	[139]	Approximate range: from 10 to 170 [a]
Propane	Carbon molecular sieve	-	60.148	18.23	2	[107]	Approximate range: from 150 to 500 [a]

[a] adsorption potential [J/g]

Table 6-6: Coefficients for D-A and D-R equation (mass-based) (continued)

Refrigerant	Adsorbent		Y_0 [g/kg]	E [J/mol]	n [-]	Literature	Valid range of adsorption potential A [J/g]
	Zeolite	5A crystal	148.28	19.4	2.24	[106]	Approximate range: from 150 to 500 [a]
		5A pellets	112.64	18.2	2.47	[106]	Approximate range: from 150 to 500 [a]
	AC	Maxsorb III	900	8577.9	1.22	[133]	Approximate range: from 10 to 290 [a]
n-butane	AC	Maxsorb III	800	5172	1.05	[140]	25~55°C
Propylene	Carbon molecular sieve	-	70.098	21.23	2	[107]	Approximate range: from 200 to 550 [a]
	Zeolite	5A crystal	157.5	23.4	2.28	[106]	Approximate range: from 200 to 550 [a]
		5A pellets	113.82	23.4	2.13	[106]	Approximate range: from 200 to 550 [a]
Methanol	AC	207C Calgon carbon	150	6843.6	1.72	[141]	Approximate range: from 80 to 260 [a]
		207EA Calgon carbon	280	6912.2	2.08	[141]	Approximate range: from 80 to 260 [a]
			330	6571.2	1.655	[142]	Approximate range: from 5 to 200) [a]
		WS-480 Calgon carbon	270	5654.2	1.78	[141]	Approximate range: from 80 to 260 [a]
			490	4776.8	1.65	[142]	Approximate range: from 5 to 200 [a]
		Tsurumi coal HC-20C	705	4790.8	2	[143]	Approximate range: from 20 to 250 [a]
	ACF	A-20	1190	8100.78	1.45	[133]	Approximate range: from 5 to 120 [a]

[a] adsorption potential [J/g]

Table 6-7: Coefficients for D-A and D-R equation (mass-based)

Refrigerant	Adsorbent		Y_0 [g/kg]	k [-]	n [-]	T_s [K]	Literature	Valid range
Ammonia	Monolithic AC	LM001	270.0	4.3772	1.1965		[144]	[a]
		LM127	362.9	3.6571	0.94		[144]	[a]
		LM128	333.3	3.6962	0.99		[144]	[a]
		LM279	383.7	4.2434	1		[144]	[a]
		SDS	245.0	5.6069	2.1389		[144]	[a]
		KOH-AC	624.5	4.6130	1.0554		[144]	[a]
	Granular AC	208C	307.7	4.4390	1.187		[144]	[a]
		607C	347.5	3.5943	1.05		[144]	[a]
		C119	285.2	3.8615	1		[144]	[a]
		SRD 1352/2	839.2	5.0775	0.8529		[144]	[a]
		SRD 1352/3	569.1	6.6738	1.1489		[144]	[a]
		SRD 06038	446.4	6.7116	1.1295		[144]	[a]
		SRD 06039	452.7	5.3630	1.053		[144]	[a]
		SRD 06040	348.3	5.5936	1.1714		[144]	[a]
		SRD 06041	230.3	5.5622	1.5252		[144]	[a]
	ACF	ACF CC200	304.0	4.6110	1.468		[144]	[a]
		ACF CC250	315.0	5.5690	1.602		[144]	[a]
		FM 10/700	448.9	5.9276	1.148		[144]	[a]
		ACF-20	781.7	4.4783	0.7573		[144]	[a]
	Powder AC	C-2132	925.8	4.1005	0.85		[144]	[a]
		AX-21	549.0	9.0780	2		[144]	[a]
		MSC-30	1059.5	5.6621	0.8115		[144]	[a]
	AC	208C	290	3.1853	1.0957		[145]	25-200C
		Monolithic	270	4.3772	1.1965		[145]	25-200C
		PVDC based	232	4.6342	1.8065		[145]	25-200C
		YKAC	290	3.57	1.38		[146]	20-130C

[a] Not provided in the original literature

Table 6-8: Coefficients for D-A and D-R equation (mass-based)

Refrigerant	Adsorbent		Y_0 [g/kg]	k [-]	n [-]	T_s [K]	Literature	Valid range of adsorption potential A [J/g]
		Granular	465.5	4.282	0.81	-	[147]	25-140C
		ENG-TSA	470.3	5.551	0.89	-	[147]	25-140C
	Charcoal	208C1	249	10.758	2		[148]	[a]
		208C2	234	5.985	2		[148]	[a]
		208C3	216	6.398	2		[148]	[a]
		BPL	204	10.062	2		[148]	[a]
		SC11	254	9.495	2		[148]	[a]
		AS12	317	10.06	2		[148]	[a]
		AX21	555	8.866	2		[148]	[a]
		AX31	451	12.294	2		[148]	[a]
		CC200	282	7.984	2		[148]	[a]
		CC250	295	8.395	2		[148]	[a]
		CC700	261	7.677	2		[148]	[a]
Water	Zeolite	13X	123.3	4.268	1.3	-	[149]	60-150C
	Zeolite	13X	270	5.63	1.73	-	[150]	[a]
	Zeolite	-	269	4.33	2	-	[151]	[a]
	Zeolite	-	261	5.36	1.73	-	[152]	20-250C
	Silica gel	-	346	5.6	1.6	-	[153]	[a]
	LiCl	Silica gel	489	0.342	1.604	-	[154]	[a]
R32	AC	208C	476	2.4634	1.3880		[145]	25-40C
	AC	monolithic	461	2.6729	1.3326		[145]	25-40C
butane	AC	208C	259	1.2895	1.1428		[145]	25-200C
	AC	monolithic	237	1.3693	1.3921		[145]	25-200C
Methanol	AC	YKAC	450	13.38	1.5		[146]	20-100C
	AC	Shanghai YK	284	10.21	1.39	288.3	[155]	[a]
	AC	Shanghai 18#	238	13.3	1.33	298.1	[155]	[a]
	AC	Italy Eshland	266	11.57	1.41	295.5	[155]	[a]
	AC	Pellet	356	32.65	2	-	[156]	[a]
	AC	Cloth	602	1.272	8.8135	-	[156]	[a]
	ACF	ACF0	400	17.19	1.66	290.9	[155]	[a]
	ACF	ACF1	682	10.84	1.21	297.2	[155]	[a]
	ACF	ACF2	662	10.94	1.31	295.5	[155]	[a]
	ACF	ACF3	516	15.13	1.49	287.2	[155]	[a]
	Zeolite	CBV901	218	28.48	1.7		[157]	[a]

[a] Not provided in the original literature

6.4.3 Freundlich

Table 6-9: Coefficients for Freundlich

Refrigerant	Adsorbent		A0	A1	A2	A3	B0	B1	B2	B3	Literature	Valid range
water	Silica gel	Fuji RD Type	-6.5314	0.072452	-0.23951e-3	0.25493e-6	-15.587	0.15915	-0.50612e-3	0.5329e-6	[158]	[a]
		Fuji RD Type	522	0	0	0	0.625	0	0	0	[159]	[a]
		Fuji A Type	346	0	0	0	0.625	0	0	0	[160]	[a]
			31.198	-0.2665	0.769e-3	-0.73898e-6	41.581	-0.35435	0.10199e-2	-0.97034e-6	[161]	[a]

[a] Not provided in the original literature

6.4.4 Dual Site Sips (DSS)

Table 6-10: Coefficients for Dual Site Sips (DSS) equation

Refrigerant	Adsorbent		Y_A [g/kg]	$b_{A,0}$ [1/kPa]	$q^*_{,A}$ [kJ/mol]	η_A [-]	Y_B [g/kg]	$b_{B,0}$ [1/kPa]	$q^*_{,B}$ [kJ/mol]	η_B [-]	Literature	Valid range
Propane	MOF	CuBTC	273.24	0.07	28.7	0.82	50.16	0.16	34.1	0.32	[162]	50-150°C
Propylene	MOF	CuBTC	297.78	0.42	41.9	1.00	51.24	0.06	47.0	0.80	[162]	50-150°C
Isobutane	MOF	CuBTC	296.96	0.82	37.9	0.55	63.8	0.06	40.8	1.00	[162]	50-150°C

6.4.5 Langmuir

Table 6-11: Coefficients for Langmuir equation

Refrigerant	Adsorbent		Y_0 [g/kg]	a [-]	K^0 [1/kPa]	$-\Delta H$ [kJ/mol]	Literature	Valid range
Propylene	Zeolite	4A	109.2	2.612	8.44e-6	28.2	[163]	[a]
Propane	Zeolite	4A	136.53	2.189	2.81e-5	15.6	[163]	[a]

[a] Not provided in the original literature

6.4.6 Van't Hoff

Table 6-12: Coefficients for van't Hoff equation

Working pair	ΔH/ mol NH3	ΔS/mol NH3	Working pair	ΔH/ mol NH3	ΔS/mol NH3
NH4Cl-3/0	29433	207.9	NiCl2-1/0	89810	233.01
LiCl-4/3	36828	224.6	CuCl2-10/6	31387	227.72
LiCl-3/2	44780	229.8	CuCl2-5/3.3	50241	230.75
LiCl-2/1	48128	230.6	CuCl2-3.3/2	56497	237.22
CoCl2-6/2	53987	228.1	ZnCl2-10/6	29588	219.23
CoCl2-2/1	78134	232.17	ZnCl2-6/4	44779	230.24
CoCl2-1/0	88303	232.8	ZnCl2-4/2	49467	230.24
MgCl2-6/2	55661	230.63	ZnCl2-2/1	80352	229.72
MgCl2-2/1	74911	230.3	ZnCl2-1/0	104625	227.79
MgCl2-1/0	87048	230.88	NaBr-5.25/0	35363	225.2
CaCl2-8/4	41013	230.3	SrCl2-8/1	41432	228.8
CaCl2-4/2	42269	229.92	MgBr2-6/2	63612	230.2
CaCl2-2/1	63193	237.34	CaBr2-6/2	48965	230.4
CaCl2-1/0	69052	234.14	SnCl2-9/4	31806	224.86
FeCl2-6/2	51266	227.99	SnCl2-4/2.5	38920	229.82
FeCl2-2/1	76167	231.91	FeBr2-6/2	55828	228.1
FeCl2-1/0	86880	233.01	BaCl2-8/0	38250	227.25
MnCl2-6/2	47416	228.07	NaI-4.5/0	39339	224.5
MnCl2-2/1	71019	232.35	KI-4/1	32015	219.8
MnCl2-1/0	84202	233.18	SrBr2-8/2	45617	229.3
LiBr-5/4	33689	225.9	FeI2-6/2	60683	227.5
NiCl2-6/2	59218	227.75	CaI2-8/6	35991	229.3
NiCl2-2/1	79515	232.17	CaI2-6/2	58590	231
BaI2-6/4	46454	231.6	BaBr2-8/4	41850	229.8
BaI2-4/2	47291	230.3	BaBr2-4/2	42687	230.7
BaI2-2/0	56079	235	PbCl2-8/3.25	34317	223.76
PbI2-5/2	40595	229.1	PbCl2-3.25/2	39339	230.27

Table 6-13: Coefficients for van't Hoff equation (continued)

Working pair	ΔH/ mol NH3	ΔS/mol NH3	Working pair	ΔH/ mol NH3	ΔS/mol NH3
MnBr2-6/2	53066	228.3	PbCl2-2/1.5	46035	230.89
CoBr2-6/2	58590	227.5	PbCl2-1.5/1	47290	232.5
MnI2-6/2	59301	227.4	PbCl2-1/0	55660	231.04
NiBr2-6/2	64240	227.2	PbBr2-5.5/3	37665	229.4
NiI2-6/2	65453	224.1	PbBr2-3/2	39758	229.4
SrI2-6/2	52731	230.5			

6.4.7 Antoine

Table 6-14: Constants for working pairs using the Antoine equation

Refrigerant	Absorbent	i	Ai	Bi	Reference	Valid range
H2O	LiBr/CH3COOK 2:1	0	6.95	-1.64	[164]	20-60°C
		1	-1.33e-2	1.83e-3		
		2	-9.02e-6	-2.52e-6		
	LiBr/CH3CH(OH)COONa 2:1	0	6.77	-1.64	[164]	25-60°C
		1	5.11e-3	5.26e-4		
		2	-2.2e-4	-5.79e-7		
	LiBr/H2N(CH2)2OH 3.5:1	0	1.2279e2	-3.83335e1	[165]	45-145°C
		1	-7.18812	2.25982		
		2	1.65853e-1	-5.16583e-2		
		3	-1.6883e-3	5.19714e-4		
		4	6.41261e-6	-1.95693e-6		
	LiBr/HO(CH2)3OH 3.5:1	0	-2.42919e2	8.21856e1	[166]	52-122°C
		1	1.66295e1	-5.58505		
		2	-4.09338e-1	1.37650e-1		
		3	4.42060e-3	-1.48924e-3		
		4	-1.76792e-5	5.95856e-6		
	LiBr/LiNO3-LiI-LiCl 5:1:1:2 by mol, 435:69:134:84 by mass	0	-1.276429e3	4.37412e2	[167]	57-137°C
		1	8.764646e1	-3.008232e1		
		2	-2.233375	7.690697e-1		
		3	2.517102e-2	-8.697553e-3		
		4	-1.058556e-4	3.669313e-5		
	LiBr/LiI-OH(CH2)3OH 174:57:15	0	9.537943	-2.181261	[168]	66-171°C
		1	-1.303482e-1	2.793675e-2		
		2	1.919265e-3	-3.596105e-4		
		3	-7.926247e-6	2.400981e-8		
	LiBr/LiNO3 348:69	0	3.55978	-6.69528e-1	[169]	47-169°C
		1	6.30491e-1	-1.02025e-1		
		2	-2.17120e-2	3.55250e-3		
		3	3.14477e-4	-5.12741e-5		
		4	-1.62820e-6	2.43695e-7		
TFE [CF_3CH_2OH]	NMP [C_5H_9NO]	0	6.8199e0	-2.07689e0	[170]	[a]
		1	5.75253e-3	1.53768e-3		
		2	1.10093e-4	2.58101e-5		
		3	-1.84889e-6	7.32551e-7		
		4	7.87523e-9	-7.19646e-6		

[a] Not provided in the original literature

6.4.8 Dühring

Table 6-15: Coefficients for Dühring equation

Ref.	Abs	i	a_i	b_i	n	m	r	q	C	D	E	Reference	Valid range
H2O	LiBr	0	-2.00755	321.128	1.8	32	0.145	459.72	6.21147	-2886.373	-337269.46	[171]	4-177°C
		1	0.16976	-19.322									
		2	-3.133362e-3	0.37438									
		3	1.97668e-5	-2.0637e-3									
	NaOH-KOH-CsOH	0	6.164233723	-5.380343163e1	1	0	1	273.15	6.427154896	-1208.919437	-166159.9630	[172]	9-170 °C
		1	-2.746665026e-1	5.004848451									
		2	4.916023734e-3	-1.228273028e-1									
		3	-2.859098259e-5	1.096142341e-3									

6.4.9 Equation of state (EOS)

6.4.9.1 Mixing rules

van der Waals one-fluid mixing rules (1PVDW)

Table 6-16: Coefficients for 1PVDW mixing rules using PR and SRK EOS

Refrigerant	Absorbent		k_{ij_PR}	k_{ij_SRK}	T_crit,s	P_crit,s	W_s	Literature	Valid range
CO2	IL	[C4mim][NTf2]	0.0493	0.0512	1077.0	2.765	0.3004	[173]	40-50°C
		[C10mim][NTf2]	0.0056	0.0625	800.0	1.867	0.5741		
		[Pyrr4,1][NTf2]	0.00526	0.0568	1093.1	2.425	0.3467		
		[N4,1,1,1][NTf2]	-0.0006	-0.0018	1079.6	2.588	0.3334		
		[N1,8,8,8][NTf2]	-0.0008	0.0147	750.6	1.064	0.9962		
		[P6,6,6,14][NTf2]	-0.0032	0.0488	805.5	0.795	0.7947		
		[P6,6,6,14][Cl]	0.0912	0.1111	803.9	0.851	0.8915		
Isobutane	Lubricant	POE ISO7	0.01749	-	743.1	1.127	0.7915	[174]	[a]

[a] Not provided in the original literature

Table 6-17: Coefficients for 1PVDW mixing rules using PRSV EOS

Refrigerant	Absorbent		k_1_PRSV_s	K_1_PRSV_r	K_{ij_PRSV}	T_crit,s	P_crit_s	W_s	Literature	Valid range
HCFC125	Lubricant	BAB 15	-0.1331	-0.0502	0.1645	763.35	1.199	0.716075	[175]	40-80°C
		BAB32	-0.0986	-0.0502	0.1837	772.89	1.138	0.694728		
HFC134a	Lubricant	BAB 15	-0.1331	-0.0077	0.1496	763.35	1.199	0.716075		
		BAB32	-0.0986	-0.0077	0.1598	772.89	1.138	0.694728		
HFC143a	Lubricant	BAB 15	-0.1331	-0.0399	0.1293	763.35	1.199	0.716075		
		BAB32	-0.0986	-0.0399	0.1380	772.89	1.138	0.694728		
HFC32	Lubricant	BAB 15	-0.1331	-0.0499	0.1339	763.35	1.199	0.716075		
		BAB32	-0.0986	-0.0499	0.1457	772.89	1.138	0.694728		

Two-parameter conventional mixing rule (2PCMR) (for high-pressure phase behavior)

Table 6-18: Coefficients for 2PCMR mixing rules using PR and SRK EOS

Refrigerant	Absorbent		k_{ij_PR}	l_{ij_PR}	k_{ij_SRK}	l_{ij_SKR}	Literature	Valid range
R23	AB	phenyltetradecane	0.168	-0.006	0.1695	-0.0062	[176]	-20-95°C

Modified van der Waals-Berthelot (VDWB) (from [177])

Table 6-19: Coefficients for modified vdW-Berthelot mixing rules by Yokozeki

Refrigerant	Adsorbent		L-12	L-21	m	t	Np	Literature	Valid range
HFC32	Lubricant	POE-32	0.0646	0.0266	0	0	23	[177]	[a]
		POE-68	0.0871	0.0138	0.0128	0	30		
		PEB-8	20.058	0.0698	0.0121	-78.2	28		
		HAB-32	0.1276	0.1422	-0.1536	0	16		
HFC125	Lubricant	POE-32	0.0179	0.0029	0.0296	0	60		
		POE-68	0.0245	0.0047	0.0246	0	57		
		PEB-8	0.0005	0.0005	0.0119	0	24		
		HC-16	0.1556	0.1556	-0.2174	5.42	64		
		HAB-32	0.1276	0.1422	-0.1536	0	16		
		HAB-15	0.0915	0.1297	-0.157	12.2	22		
HFC134a	Lubricant	POE-32	0.0561	0.0254	-0.0106	0	40		
		POE-68	0.0678	0.0351	-0.0109	0	46		
		PEB-8	0.0504	0.0359	-0.0193	0	23		
		HC-16	0.0928	0.1074	-0.163	4.19	115		
		HC-13	0.0859	0.1068	-0.1734	0	25		
		HC-20	0.0782	0.1029	-0.1536	0	16		
		HAB-32	0.1146	0.1332	-0.1661	0	12		
HFC143a	Lubricant	PEB-8	-0.0845	-0.0934	0.0959	-41.9	24		
		HC-16	0.1167	0.1167	-0.1544	0	56		
		HAB-15	0.058	0.0904	-0.09	-3.68	25		
HFC152a	Lubricant	PEB-8	-0.0656	-0.082	0.094	-14.5	24		
		HC-16	0.0788	0.09	-0.1254	3.49	56		
HCFC12	Lubricant	AB-32	0.0339	0.0385	0	0	54		
HCFC22	Lubricant	AB-32	0.0569	0.0694	-0.0395	3.29	54		
HCFC13-B1	Lubricant	AB-32	0.0598	0.1994	-0.0299	6.09	36		
HCFC123	Lubricant	MO-56	0.0384	0.0384	-0.048	7.58	61		

[a] Not provided in the original literature

6.4.9.2 Flory-Huggins

Table 6-20: Coefficients for Flory-Huggins equation

Refrigerant	Absorbent	w0/k [K]	w1 [K]	r	Literature	Valid range
R32	PEC9	839	-158	14.93	[178]	30-90°C
	PEB6	680	-209	7.77		50-90°C
	PEB8	775	-177	11.58		30-90°C
	Pentaerythritol tetrapentanoate ester	806	-197	9.78	[179]	30-90°C
R125	PEC9	997	-208	6.91	[178]	30-90°C
	PEB6	993	-271	3.94		50-90°C
	PEB8	998	-238	5.81		30-90°C
	Pentaerythritol tetrapentanoate ester	967	-262	3.47	[179]	30-90°C
R134a	PEC9	938	-176	10.41	[178]	30-90°C
	PEB6	973	-233	7.03		50-90°C
	PEB8	808	-203	6.94		30-90°C
	Pentaerythritol tetrapentanoate ester	878	-221	6.17	[179]	30-90°C
R143a	PEC9	817	-152	7.79	[178]	30-90°C
	PEB6	772	-199	4.31		50-90°C
	PEB8	703	-162	5.76		30-90°C
	Pentaerythritol tetrapentanoate ester	849	-183	5.28	[179]	30-90°C
R152a	PEC9	654	-152	10.03	[178]	30-90°C
	PEB6	491	-205	5.19		50-90°C
	PEB8	707	-169	9.76		30-90°C
	Pentaerythritol tetrapentanoate ester	482	-204	4.62	[179]	30-90°C

6.4.9.3 Wilson

Table 6-21: Coefficients for Wilson equation with fixed A

Refrigerant	Adsorbent		A_{12} [J/mol]	A_{21} [J/mol]	Literature	Valid range
Water	IL	[EMIM][(CF3SO2)2N]	7363.8	16736	[180]	80°C
		[BMIM][(CF3SO2)2N]	7985.2	16736	[180]	80°C
Acetone	IL	[EMIM][(CF3SO2)2N]	-286.4	-2185.1	[180]	80°C
		[BMIM][(CF3SO2)2N]	-200.0	-2410.4	[180]	80°C
2-propanol	IL	[EMIM][(CF3SO2)2N]	1189.3	16736	[180]	80°C
		[BMIM][(CF3SO2)2N]	1276.8	9689.7	[180]	80°C
R32	POE		2650.4	20000	[181]	[a]
	R125		190.7	0.4	[181]	[a]
R125	POE		1441	20000	[181]	[a]
R1234ze(E)	POE (RL68H)		20000	1908	[182]	0-80°C
R12	Naphthenic		1986	263.9	[183]	-45-121°C
	Paraffinic		2634	7415	[183]	-18-121°C
R22	POE		-403	20000	[184]	-20-60°C
R134a	PAG		3441	-8128	[184]	-10-70°C
	POE		2003	17569	[183]	-18-121°C
			2510	18449	[184]	-10-70°C

[a] Not provided in the original literature

$$A_{ij}/K = \Delta\lambda^{C}_{ij}/K + \Delta\lambda^{T}_{ij}(T/K - 273.15)$$

Table 6-22: Coefficients for Wilson equation with temperature-dependent A

Refrigerant	Adsorbent	$\Delta\lambda^{C}_{12}$/K	$\Delta\lambda^{C}_{21}$/K	$\Delta\lambda^{T}_{12}$ [J/mol]	$\Delta\lambda^{T}_{21}$ [J/mol]	Literature	Valid range
R134a	TriEGDME	-149.128	368.189	0.959291	0.929126	[185]	10-50°C

6.4.9.4 Tsuboka and Katayama (modified Wilson)

Table 6-23: Coefficients for Tsuboka and Katayama equation

Refrigerant	Adsorbent	$\Delta\lambda_{12}$ [J/mol]	$\Delta\lambda_{21}$ [J/mol]	Literature	Valid range
R12	Naphthenic	517	2029	[183]	-45-121°C
	Paraffinic	1847	-4437	[183]	-18-121°C
R22	POE	-889	-11472	[184]	-20-60°C
R134a	PAG	-247	-15259	[184]	-10-70°C
	POE	1721	-5389	[183]	-18-121°C
		2366	-12013	[184]	-10-70°C
R125	POE	918	-4941	[181, 184]	-30-60°C
R32	POE	1143.9	-15057.2	[181]	[a]
	R125	-69.4	-10.1	[181]	[a]

[a] Not provided in the original literature

6.4.9.5 Wang and Chao (modified Wilson)

Table 6-24: Coefficients for Wang and Chao equation

Refrigerant	Adsorbent	$\Delta\lambda_{12}$ [J/mol]	$\Delta\lambda_{21}$ [J/mol]	Literature	Valid range
R12	Naphthenic	-189	2199	[183]	-45-121°C
	Paraffinic	-43	4115	[183]	-18-121°C
R22	POE	-1070	5716	[184]	-20-60°C
R134a	PAG	2715	-1609	[184]	-10-70°C
	POE	-136	4212	[183]	-18-121°C
		1886	20000	[184]	-10-70°C
R125	POE	-381	4579	[181, 184]	-30-60°C
R32	POE	2084.5	157744.1	[181]	[a]
	R125	78.7	0	[181]	[a]

[a] Not provided in the original literature

6.4.9.6 NRTL

Binary mixtures are covered by Table 6-25 and Table 6-26 and ternary mixtures by Table 6-27 and Table 6-28.

Table 6-25: Coefficients for binary mixture NRTL equation with fixed Δg

Refrigerant	Adsorbent		Δg_{12} [J/mol]	Δg_{21} [J/mol]	α_{12}	Literature	Valid range
water	Ionic Liquid	[EMIM][OAc]	28938	-25691	0.10243	[186]	30-80°C
		[DEMA][OMs]	-1051.4	-5039.9	0.70862	[186]	30-80°C

		[EMIM][(CF3SO2)2N]	12900.7	-1457	0.28	[180]	80°C
		[BMIM][(CF3SO2)2N]	19416.9	-348.6	0.3	[180]	80°C
Acetone	Ionic Liquid	[EMIM][(CF3SO2)2N]	4608	-4917.4	0.47	[180]	80°C
		[BMIM][(CF3SO2)2N]	7788.2	-1002.9	0.6	[180]	80°C
2-propanol	Ionic Liquid	[EMIM][(CF3SO2)2N]	4090	-5084.6	0.47	[180]	80°C
		[BMIM][(CF3SO2)2N]	7013.6	-854	0.8	[180]	80°C
R1234ze(E)	POE	RL68H	-3082.7	7567.5	0.5	[182]	0-80°C
R12	naphthenic		-1105	4571	0.5	[183]	-45-121°C
	paraffinic		-2059	6981	0.5	[183]	-18-121°C
R22	POE	RL68H	-4709	-967	0.5	[184]	-20-60°C
		Castrol SW 46	2818	-4620	0.5	[187]	-20-70°C
R134a	PAG		-4788	-359	0.5	[184]	-10-70°C
	POE		-2528	7421	0.5	[183]	-18-121°C
		RL68H	-2784	9498	0.5	[184]	-10-70°C
		Castrol SW 46	3936	-1240	0.5	[187]	-20-70°C
R125	POE	RL68H	-3363	8481	0.5	[181, 184]	-30-60°C
R32	POE		-2852.1	20000	0.5	[181]	[a]
	R125		237.5	-398.1	0.5	[181]	[a]

[a] Not provided in the original literature

$$\Delta g_{ij} = a_{ij} + b_{ij} * T$$

Table 6-26: Coefficients for binary mixture NRTL equation with temperature-dependent Δg

Refrigerant	Adsorbent		a12 [J/mol]	a21 [J/mol]	b12 [J/mol-K]	b21 [J/mol-k]	α	Literature	Valid range
Benzene	IL	[MMIM][(CH3SO2)2N]	-60994.4	-5319.1	340.92	15.10	0.2	[188]	80°C
		[EMIM][(CF3SO2)2N]	45120.3	842.2	45.37	-3.32	0.2		
		[BMIM][(CF3SO2)2N]	156912.6	741.6	251.86	-3.96	0.2		
		[EMIM][C2H5OSO3]	28115.2	-1595.1	-52.92	-1.42	0.2		
		[C2H5NH][C2H5OC2H4OSO3]	10539.5	-1719.5	-	-	0.2		
Cyclohexane	IL	[MMIM][(CH3SO2)2N]	3748.1	7324.9	25.34	-13.32	0.2		
		[EMIM][(CF3SO2)2N]	36714.6	9986.4	-6.00	-17.36	0.2		
		[BMIM][(CF3SO2)2N]	6391.1	4691.5	19.29	-12.83	0.2		
		[EMIM][C2H5OSO3]	-2612.9	13608.9	57.74	-25.19	0.2		
Hexane	IL	[EMIM][(CF3SO2)2N]	15003.4	610.7	-28.03	12.85	0.2		
Cyclohexene	IL	[EMIM][(CF3SO2)2N]	49643.2	11324.4	-68.86	-29.60	0.2		
Toluene	IL	[C2H5NH][C2H5OC2H4OSO3]	8690.6	129.1	-	-	0.2		

Table 6-27: Coefficients for ternary mixture NRTL equation

Ref	Absorbate	Coef.	$\alpha_{j,i}$	$C_{j,i}$ [J/mol]	Reference	Valid range
TFE [CF_3CH_2OH] (1)	H2O (2) + E181 [$CH_3O(CH_2CH_2O)_4CH_3$] (3)	1,1	0	0	[189]	60-200°C
		1,2	0.2885	-267.6310		
		1,3	0.7298	-115.2119		
		2,1	0.2885	1713.0375		
		2,2	0	0		
		2,3	0.0330	11742.636		
		3,1	0.7298	-1333.6693		
		3,2	0.0330	-7783.061		
		3,3	0	0		
R134a (1) and R227ea (2)	Castrol SW 46 POE (3)	1,1	0	0	[187]	[a]
		1,2	0.5	165.73		
		1,3	0.5	3936		
		2,1	0.5	192.62		
		2,2	0	0		
		2,3	0.5	4436		
		3,1	0.5	-1240		
		3,2	0.5	-1062		
		3,3	0	0		
R22 (1) and R142b (2)	Castrol SW 46 POE (3)	1,1	0	0	[187]	[a]
		1,2	0.5	289.6		
		1,3	0.5	2818		
		2,1	0.5	327.9		
		2,2	0	0		
		2,3	0.5	8074		
		3,1	0.5	-4620		
		3,2	0.5	-2215		
		3,3	0	0		
R125 (1) and R143a (2)	Castrol SW 46 POE (3)	1,1	0	0	[187]	[a]
		1,2	0.5	-35.58		
		1,3	0.5	5643		
		2,1	0.5	-48.93		
		2,2	0	0		
		2,3	0.5	8649		
		3,1	0.5	-1806		
		3,2	0.5	-2402		
		3,3	0	0		
NH3 (1)	H2O(2) + LiBr(3) + NH3-H2O(4) + H2O-LiBr(5) +NH3-LiBr(6)	1,1	0	0	[190]	30-153°C
		1,2	0.126	30516		
		1,3	0.819	79785		
		1,4	5.626	1750		
		1,5	0.041	33274		
		1,6	0	-26826		
		2,1	0.126	-5029		
		2,2	0	0		
		2,3	0.651	-13728		
		2,4	0.006	-17358		
		2,5	0.170	-6206		
		2,6	0.001	-22979		
		3,1	0.819	51081		
		3,2	0.651	-6878		
		3,3	0	0		
		3,4	0.003	-49		
		3,5	0	0		
		3,6	0	0		
		4,1	5.626	-142		
		4,2	0.006	16295		

[a] Not provided in the original literature

Table 6-28: Coefficients for ternary mixture NRTL equation (continued)

Ref	absorbate	Coef.	$\alpha_{j,i}$	$C_{j,i}$ [J/mol]	reference	Valid range
NH3 (1)	H2O(2) + LiBr(3) + NH3-H2O(4) + H2O-LiBr(5) +NH3-LiBr(6)	4,3	0.003	26754	[190]	30-153°C
		4,4	0	0		
		4,5	0.036	73252		
		4,6	1.883	37119		
		5,1	0.041	4579		
		5,2	0.170	644		
		5,3	0	0		
		5,4	0.036	46450		
		5,5	0	0		
		5,6	0	0		
		6,1	0	-55521		
		6,2	0.001	-16128		
		6,3	0	0		
		6,4	1.883	10317		
		6,5	0	0		
		6,6	0	0		

6.4.9.7 UNIQUAC

Table 6-29: Coefficients for UNIQUAC equation with fixed Δu

Refrigerant (1)	Adsorbent (2)		Δu_{12} [J/mol]	Δu_{21} [J/mol]	r_1	r_2	q_1	q_2	Literature	Valid range
Water	IL	[EMIM][(CF3SO2)2N]	67.2	2906.5	0.92	9.89	1.4	8.78	[180]	80°C
		[BMIM][(CF3SO2)2N]	345.3	3057.1	0.92	11.16	1.4	10.2		80°C
		[MMIM][(CH3)2PO4]	-2949.3	-3130.1	0.92	7.162	1.4	5.844	[188]	80°C
Acetone	IL	[EMIM][(CF3SO2)2N]	-1393.9	1393.9	2.5735	9.89	2.336	8.78	[188]	80°C
		[BMIM][(CF3SO2)2N]	-1368.8	1368.8	2.5735	11.16	2.336	10.2		80°C
		[MMIM][(CH3)2PO4]	51731	-2380.6	2.573	7.162	2.336	5.844	[188]	80°C
2-Propanol	IL	[EMIM][(CF3SO2)2N]	1536.4	-292.4	2.7791	9.89	2.508	8.78	[188]	80°C
		[BMIM][(CF3SO2)2N]	1200.8	156.2	2.7791	11.16	2.508	10.2		80°C
THF	IL	[EMIM][(CF3SO2)2N]	2353.4	-1298.8	2.941	9.89	2.720	8.78	[188]	80°C
		[MMIM][(CH3)2PO4]	6594	-1331.8	2.941	7.162	2.720	5.844	[188]	80°C
Methanol	IL	[MMIM][(CH3)2PO4]	-2409.9	-2864.5	1.431	7.162	1.432	5.844	[188]	80°C
Ethanol	IL	[MMIM][(CH3)2PO4]	-586.6	-2027.5	2.105	7.162	1.972	5.844	[188]	80°C
R1234ze(E)	POE RL68H		1662.8	1981.2	2.74	29.4	2.49	24.4	[182]	0-80°C
R12	paraffinic		5897	277	2.6243[c]	24.50	2.376[c]	20.28	[183]	-18-121°C
R22	POE		-1366	4115	1.59	29.4	1.39	24.36	[184]	-20-60°C
R134a	POE		971	1334	2.46	24.01	2.36	20.18	[183]	-18-121°C
			1144	79.8	2.46	29.40	2.36	24.36	[184]	-10-70°C
	hexadecane		-212.8	2810.1	2.46	23.14 [b]	2.36	17.06 [b]	[191]	20-90°C
R32	POE		-200	20000	1.43	29.40	1.42	24.36	[181]	[a]
	R125		125.6	0.9	1.43	2.61	1.42	2.49		[a]
R125	POE		1715	-570	2.61	29.40	2.49	24.36	[181, 184]	-30-60°C
	hexadecane		-167.9	2618.9	2.61	23.14 [b]	2.49	17.06 [b]	[191]	20-90°C

[a] Not provided in the original literature

[b] From Romain Richard, Nicolas Ferrando, Marc Jacquin. Liquid-liquid equilibria for ternary systems aceticacid + n-butyl acetate + hydrocarbons at 293.15 K. Fluid Phase Equilibria, Elsevier, 2013, vol. 356, pp. 264-270. ff10.1016/j.fluid.2013.07.032. hal-01065438

[c] From Naidoo, R. D. (2003). The Thermodynamics of Liquids in Solution at 298 K and 1 Atm (Doctoral dissertation, University of Natal, Durban).

$$\Delta u_{ij} = a_{ij} + b_{ij} * T$$

Table 6-30: Coefficients for UNIQUAC equation with temperature-dependent Δu

Refrigerant	Adsorbent		a12 [J/mol]	a21 [J/mol]	b12 [J/mol-K]	b21 [J/mol-k]	r_1	r_2	q_1	q_2	Literature	Valid range
Benzene	IL	[MMIM][(CH3SO2)2N]	5347.2	1942.3	-6.75	2.30	3.188 [a]	9.26	2.4 [a]	8.08	[192]	80°C
		[EMIM][(CF3SO2)2N]	751.8	-816.7	7.03	-1.49	3.188 [a]	9.89	2.4 [a]	8.78		80°C
		[BMIM][(CF3SO2)2N]	0.0	-749.0	12.94	-3.50	3.188 [a]	11.16	2.4 [a]	10.2		80°C
		[EMIM][C2H5OSO3]	8890.2	-3943.0	-21.45	11.83	3.188 [a]	7.94	2.4 [a]	7.21		30°C
		[C2H5NH][C2H5OC2H4OSO3]	696.5	1149.3	0	0	3.188 [a]	8.78	2.4 [a]	6.96		60°C
Cyclohexane	IL	[MMIM][(CH3SO2)2N]	1126.4	1216.9	-3.30	4.15	4.064 [a]	9.26	3.240 [a]	8.08		80°C
		[EMIM][(CF3SO2)2N]	190886.6	1268.5	-517.44	-4.97	4.064 [a]	9.89	3.240 [a]	8.78		80°C
		[BMIM][(CF3SO2)2N]	-1202.8	2743.6	3.41	-2.35	4.064 [a]	11.16	3.240 [a]	10.2		80°C
		[EMIM][C2H5OSO3]	-34328.1	4016.4	293.26	-10.75	4.064 [a]	7.94	3.240 [a]	7.21		30°C
Hexane	IL	[EMIM][(CF3SO2)2N]	-2451.7	5699.7	3.23	-4.78	4.5 [a]	9.89	3.856 [a]	8.78		80°C
Toluene	IL	[C2H5NH][C2H5OC2H4OSO3]	209.5	1627.7	0	0	3.923 [a]	8.78	2.968 [a]	6.96		60°C

[a] from S.I. Sandler, Chemical and Engineering Thermodynamics, third ed., Jon Wiley and Sons, New York, 1999

6.4.9.8 Heil

Table 6-31: Coefficients for Heil equation

Refrigerant	Adsorbent	$\Delta\lambda_{12}$ [J/mol]	$\Delta\lambda_{21}$ [J/mol]	Literature	Valid range
R12	naphthenic	1024	804	[183]	-45-121°C
	paraffinic	1307	1615	[183]	-18-121°C
R22	POE	-224	6371	[184]	-20-60°C
R134a	PAG	1667	-4626	[184]	-10-70°C
	POE	948	3993	[183]	-18-121°C
		1122	4417	[184]	-10-70°C
R125	POE	642	5493	[184]	-30-60°C

6.5 Definition of Measuring Equipment for the performance evaluation

6.5.1 Sensors for the measuring of the physical quantities

In Table 6-32 the sensors required for measuring the quantities used in the performance indicators' calculation and that shall be monitored are listed.

Table 6-32: Sensor required for measuring the quantities used in the performance indicators calculation

MONITORED QUANTITY	TEMPERATURE SENSOR	RH% SENSOR	FLOW METER	PRESSURE SENSOR	ELECTRICITY METER
$E_{S\ P\_pump}$					x
$E_{S\ S\_pump}$					x
$E_{B\ P\_pump}$					x
$E_{B\ S\_pump}$					x
E_{HW_hp}					x
F_{HW_hp}	X		X	x	
E_{HW_bu}					x
Q_{H_hp}	X		X		
Q_{W_hp}	X		X		
Q_{HW_bu}	X		X		
External temperature	X				
External Relative Humidity		X			
Source Temp. for W/W HP	X				

6.5.2 Requirements of the measuring system

For the choice of the measuring equipment, it is important to define the requirements of sensors according to the goal of monitoring. For example, to evaluate the performance of the system and analyze its dynamic behavior accurately, high accuracy and high resolution of the measured data will be required.

Table 6-33 shows an example of the measuring equipment and its requirements for monitoring of FSHP systems.

The sensors' accuracy has been specified according to the MID (Measuring Instruments Directive) 2004/22/CE of 31/03/2004.

6.5.3 Sampling time

In order to detect all the FSHP operating conditions, especially those related to transient operation such as the defrost or the shift between the adsorbent beds, which usually last few minutes, it's important to choose an appropriate sampling time and sensors able to measure all meaningful data according to it.

The suggested value for sampling the quantities of interest is one minute.

Table 6-33 Example of measuring equipment for the indicated measured quantity

MEASURED QUANTITY	UNIT	ACCURACY	SENSOR TYPE	RESOLUTION	NOTES
WATER OR BRINE					
Temperature	°C	± 0,15 °C	PT 100, 4-wires	0,01°C	To be calibrated in couple and connected to the energy meter
Temperature Difference	°C	± 0,21 °C	PT 100, 4-wires	0,01°C	
Flow Meter	m^3/h	± 1%	Electromagnetic or ultrasonic flow meters.	0,001 m^3/h	
AIR					
Temperature	°C	± 0,4 °C	PT 100 (3-wires) or Thermocouple	0,1°C	
Humidity	°C	± 2%	Capacitive sensor	0,°C	
HEAT INPUT					
Fuel Flow rate	m^3/h or Kg/h	+/- 1%	Volumetric or Mass meter	0,001 m^3/h or Kg/h	
Calorific Value	kWh/Nm^3	+/- 3%	Data taken from the Fuel Distribution company or from EUROSTAT or Country database		Sampled weekly at the closets dispatching site
THERMAL OUTPUT					
Thermal Output	kWh	Class 2	Calorimeter	1Wh	Accuracy according to the EN 1434-1
ELECTRIC INPUT					
Electricity Consumption	kWh	± 2%	Electric Meter	1imp/Wh	

6.5.4 Guidelines for a correct installation of the sensors

To guarantee reliable measuring it is very important to respect some rules for the good installation of the sensors.

General indications:

Before and after the installation of the sensors, it's important to clean up the system to remove dirt and residuals from the pipes.

- Clean the filters after the installations.
- Check the presence of leakages from the valves.

Flow meters:

In order to limit the pressure drops due to the flow meter installation on the pipe, it is recommended to use ultrasonic or electromagnetic flow meters.

Concerning electromagnetic flow meters, it is important to keep in mind that they can attract the iron particles present in the fluid (e.g. water) which lay down on the electrodes and reduce the measuring sensitivity of the instrument. For this reason, it is better to avoid them in old systems with iron pipes. Furthermore, when electromagnetic flow meters are used, it is also recommended to:

- use a flow meter with a diameter smaller than that one of the pipe on which it is installed in order to increase the velocity of the flow and gain an higher sensor's accuracy;
- install the instrument on a straight pipe, according to the specific installation requirement of the sensor, without other devices installed upstream and downstream of it (this to not disturb the flow and improve the accuracy of measurement);

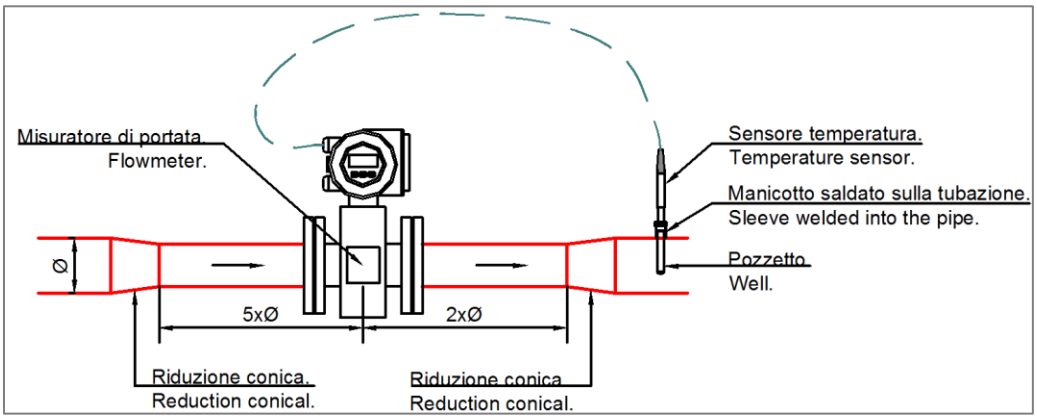

- install the flow meter on the return circuit to avoid high temperature stress;
- install air vent valves in the circuit in order to avoid measurement errors due to entrained air or gas bubble formation in the measuring tube;
- not install the flow meter at the highest point of a pipeline in order to avoid the risk to accumulate air in the instrument;
- not install the flow meter on a vertical pipe with flow going down.

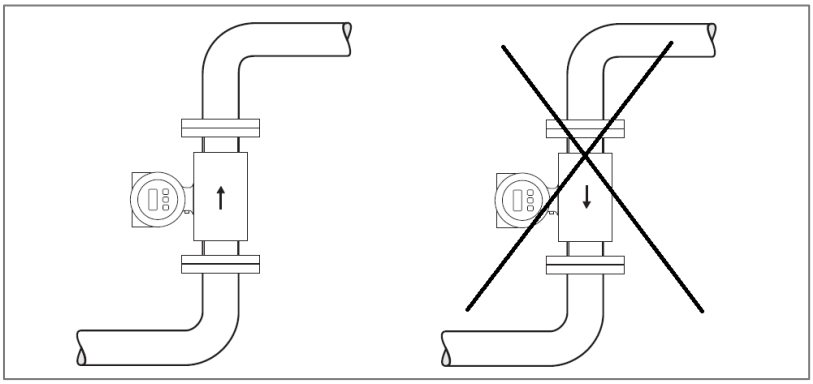

Temperature sensors:

- The sensors shall be installed in the same way (same depth in the pipe, etc.), in order to have comparable measurements, and far away from intersections between pipes.
- The sensor shall be immersed in the flow in the middle of the pipe. The best position is in curve and in counter flow or tilted of 45°.

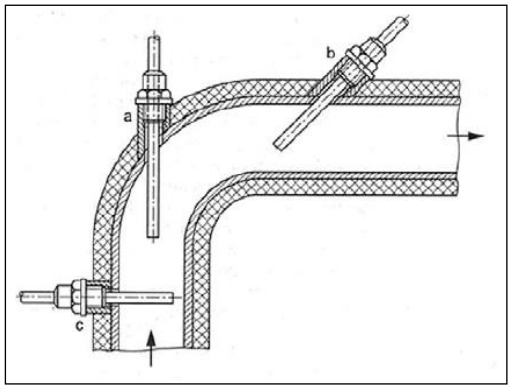

- The sensors that measure a temperature difference shall be calibrated in pairs in order to increase the accuracy of the measurement.

Electrical devices:

- The cables that transmit the measures have to be installed farer then 50mm from power cables.
- Cables between sensors and data collector need to be continuous without junctions.

External temperature and relative humidity sensors:

- The external temperature sensor shall be installed up to the north to avoid direct radiation.
- The sensor has to be installed far from heat source (i.e. exhaust pipes, etc.)

7. References

[1] K. E. Herold, R. Rademacher, and S. Klein, *Absorption Chillers and Heat Pumps*. New York: CRC press, 1996.

[2] G. Alefeld and R. Radermacher, *Heat conversion systems*. Boca Raton: CRC press, 1994.

[3] IEA HPP, Ed., "Annex 34. Thermally Driven Heat Pumps for Heating and Cooling: Final Report," Borås, Schweden, 2014.

[4] R. E. Critoph and Y. Zhong, "Review of trends in solid sorption refrigeration and heat pumping technology," *P I Mech Eng E-J Pro*, vol. 219, E3, pp. 285–300, 2005, doi: 10.1243/095440805x6982.

[5] K. Gluesenkamp and R. Rademacher, *Heat-activated cooling technologies for small and micro combined heat and power (CHP) applications,* V. D. I. Verein Deutscher Ingenieure, Ed.: Woodhead Publishing Limited, 2011.

[6] F. Ziegler, "State of the art in sorption heat pumping and cooling technologies (Reprinted from Proceedings International Energy Agency Heat Pump Conference (IEAHPC 99), Berlin, 31, May-2 June, 1999)," *Int J Refrig*, vol. 25, no. 4, pp. 450–459, 2002, doi: 10.1016/S0140-7007(01)00036-6.

[7] K. Gluesenkamp, Y. Hwang, and R. Radermacher, "High efficiency micro trigeneration systems," *Appl Therm Eng*, vol. 50, no. 2, pp. 1480–1486, 2013, doi: 10.1016/j.applthermaleng.2011.11.062.

[8] Y. H. Hwang, R. Radermacher, A. Al Alili, and I. Kubo, "Review of solar cooling technologies," *Hvac&R Res*, vol. 14, no. 3, pp. 507–528, 2008, doi: 10.1080/10789669.2008.10391022.

[9] R. E. Critoph and S. J. Metcalf, "PROGRESS IN THE DEVELOPMENT OF A CARBON-AMMONIA ADSORPTION GAS-FIRED DOMESTIC HEAT PUMP," in *International Sorption Heat Pump Conference, May 2011; Padua, Italy*, 2011.

[10] S. K. Henninger, F. P. Schmidt, and H. M. Henning, "Water adsorption characteristics of novel materials for heat transformation applications," *Appl Therm Eng*, vol. 30, no. 13, pp. 1692–1702, 2010, doi: 10.1016/j.applthermaleng.2010.03.028.

[11] M. Schicktanz, P. Hugenell, and S. K. Henninger, "Evaluation of methanol/activated carbons for thermally driven chillers, part II: The energy balance model," *Int J Refrig*, vol. 35, no. 3, pp. 554–561, 2012, doi: 10.1016/j.ijrefrig.2011.03.014.

[12] S. Plura, M. Radspieler, and C. Schweigler, "INNOVATIVE DOUBLE-EFFECT/SINGLE-EFFECT TRI-GENERATION SYSTEM - EXPERIENCE FROM THE FIRST YEAR OF OPERATION," in *International sorption heat pump conference, 23-26 September 2008; Seoul, Korea*, 2008.

[13] "boostHEAT, A global Player for energy," presented 9th Annex meeting, Stockholm, 2018.

[14] BOOSTHEAT.20. [Online]. Available: https://fr.boostheat.com/## (accessed: Jan. 30 2020).

[15] J. Demierre, S. Henchoz, and D. Favrat, “Prototype of a thermally driven heat pump based on integrated Organic Rankine Cycles (ORC),” *Energy*, vol. 41, no. 1, pp. 10–17, 2012, doi: 10.1016/j.energy.2011.08.049.

[16] J. Demierre and D. Favrat, “LOW POWER ORC-ORC SYSTEMS FOR HEAT PUMP APPLICATIONS,” in *9th International IEA Heat Pump Conference, 20 - 22 May 2008; Zürich, Switzerland*, 2008.

[17] J. Demierre and D. Favrat, “THEORETICAL STUDY OF THERMALLY DRIVEN HEAT PUMPS BASED ON DOUBLE ORGANIC RANKINE CYCLE: WORKING FLUID COMPARISON AND OFF-DESIGN SIMULATION.,” in *10th IEA Heat Pump Conference, 16 - 19 May 2011; Tokyo, Japan.*, 2011.

[18] Zion Market Research, *Global Heat Pumps Market Worth Reach USD 98.39 Billion By 2025.* [Online]. Available: https://www.zionmarketresearch.com/news/heat-pumps-market## (accessed: Feb. 4 2020).

[19] International Energy Agency IEA, *Heat pumps – Tracking Buildings – Analysis - IEA.* [Online]. Available: https://www.iea.org/reports/tracking-buildings/heat-pumps## (accessed: Feb. 4 2020).

[20] D. Ürge-Vorsatz, L. F. Cabeza, S. Serrano, C. Barreneche, and K. Petrichenko, “Heating and cooling energy trends and drivers in buildings,” *Renewable and Sustainable Energy Reviews*, vol. 41, pp. 85–98, 2015, doi: 10.1016/j.rser.2014.08.039.

[21] “Dieryckx, M. (2011). New Refrigerants in heat pumps – Perspective of a leading equipment manufacturer. 4th EHPA European Heat Pump Conference. London-Paddington.,”

[22] Simon Pezzutto, Agne Toleikyte, Matteo De Felice, “Assessment of the Space Heating and Cooling Market in the EU28: A Comparison between EU15 and EU13 Member States,” 2015. [Online]. Available: https://www.researchgate.net/publication/299740303_Assessment_of_the_Space_Heating_and_Cooling_Market_in_the_EU28_A_Comparison_between_EU15_and_EU13_Member_States

[23] *Climate change: Mitigation of climate change Working Group III contribution to the Fifth Assessment Report of the Intergovernmental Panel on Climate Change*. New York NY: Cambridge University Press, 2014. [Online]. Available: https://www.ipcc.ch/report/ar5/wg3/

[24] Michael Taylor, “Technology Roadmap Energy-efficient Buildings: Heating and Cooling Equipment,” page 26, 2011.

[25] Henning, H.-M., Palzer, “Studie: What will the energy transformation cost?,” Fraunhofer ISE, Freiburg im Breisgau, 2015.

[26] Thomas Nowak, “European Heat Pump Market and Statistics Report 2014,” 2014.

[27] Thomas Nowak, “European Heat pump Market and statistics, Report 2019,” 2019.

[28] “Cooper-China-HPC meeting-V2_0516,” [Online]. Available: https://www.google.com/url?sa=t&rct=j&q=&esrc=s&source=web&cd=3&cad=rja&uact=8&ved=

2ahUKEwidk4b_3JTnAhW2QUEAHdFnCYsQFjACegQIBBAB&url=
https%3A%2F%2Fhpc2017.org%2Fwp-content%2Fuploads%2F2017%2F06%2Fo211.pdf&usg=
AOvVaw2YOdMmYnpjGVgHGOkY0Y0G

[29] Brilliance Consulting, China, “Coal to Electricity Study,” 2017.

[30] *Gas heating ban for new homes from 2025.* [Online]. Available: https://www.bbc.com/news/
science-environment-47559920## (accessed: Feb. 4 2020).

[31] “CCC, 2013d. Fourth Carbon Budget Review – Technical Report Sectoral Analysis of the cost-
effective path to the 2050 target.,”

[32] T. Lefevre, “Low Carbon Heat: Heat pumps in London,” 2018. [Online]. Available: https://
www.google.com/url?sa=t&rct=j&q=&esrc=s&source=web&cd=26&cad=rja&uact=8&ved=
2ahUKEwiEqJzTgLjnAhU_UhUIHZaQCVcQFjAZegQICBAB&url=
https%3A%2F%2Fwww.london.gov.uk%2Fsites%2Fdefault%2Ffiles%2Flow_carbon_heat_-
_heat_pumps_in_london_.pdf&usg=AOvVaw3bKNSRoWrHDOEPIiZkcHIe

[33] U.S. Energy Information Administration, *Energy Information Administration (EIA)- About the
Residential Energy Consumption Survey (RECS)Table HC1.1 Fuels used and end uses in U.S. homes by
housing unit type, 2015.* [Online]. Available: https://www.eia.gov/consumption/residential/data/
2015/hc/php/hc6.1.php## (accessed: Feb. 4 2020).

[34] Melissa Lapsa, Gannate Khowailed, Karen Sikes, Van Baxter, “Heat Pumps in North America – 2017
Regional Report,” 2017. [Online]. Available: https://www.google.com/url?sa=t&rct=j&q=&esrc=s&
source=web&cd=1&cad=rja&uact=8&ved=
2ahUKEwiFj7uy6bfnAhUSUBUIHTDwACUQFjAAegQIARAB&url=
http%3A%2F%2Fhpc2017.org%2Fwp-content%2Fuploads%2F2017%2F05%2FP.2.1.3-Heat-Pumps-
in-North-America-%25E2%2580%2593-2017-Regional-Report.pdf&usg=
AOvVaw0ubCn25wf3oQovIOMQND6e

[35] BSRIA Inc., *World Heat Pump Market Study 2019.* [Online]. Available: https://www.bsria.com/us/
news/article/world-heat-pump-market-study-2019/## (accessed: Feb. 4 2020).

[36] R. Sterrer, “Bedeutung der Wärmepumpe für eine erfolgreiche Energiewende: FH Salzburg,” 2018.
[Online]. Available: https://www.google.com/url?sa=t&rct=j&q=&esrc=s&source=web&cd=1&cad=
rja&uact=8&ved=2ahUKEwjkz7-16rfnAhV6SxUIHU4PAHkQFjAAegQIBBAB&url=
https%3A%2F%2Fwww.energieaktiv.at%2Fdownload%2Findex%2Fmediafile%2F699%2Ftalk_for_ex
perts_sterrer_fhs.pdf&usg=AOvVaw0pIx6hWjRNzzdup__sLBeW

[37] Van Baxter, Karen Sikes, Ronald Domitrovic, Karim Amrane, “IEA HPP Annex 42: Heat Pumps in
Smart Grids,” 2014. [Online]. Available: https://www.google.com/url?sa=t&rct=j&q=&esrc=s&
source=web&cd=1&cad=rja&uact=8&ved=2ahUKEwjyzJjF67fnAhVYQhUIHSDLAD4QFjAAegQIBRAB&
url=https%3A%2F%2Finfo.ornl.gov%2Fsites%2Fpublications%2Ffiles%2FPub37730.pdf&usg=
AOvVaw3ORWwPzfSJuZ-aPyl3Ba2p

[38] Umweltbundesamt, *Umsatz und Marktanteil von Wärmepumpen.* [Online]. Available: https://www.umweltbundesamt.de/bild/umsatz-marktanteil-von-waermepumpen## (accessed: Feb. 4 2020).

[39] M. Fink, O. Andersen, T. Seidel, and A. Schlott, "Strongly Orthotropic Open Cell Porous Metal Structures for Heat Transfer Applications," *Metals*, vol. 8, no. 7, p. 554, 2018, doi: 10.3390/met8070554.

[40] J. Bauer, R. Herrmann, W. Mittelbach, and W. Schwieger, "Zeolite/aluminum composite adsorbents for application in adsorption refrigeration," *Int. J. Energy Res.*, vol. 33, no. 13, pp. 1233–1249, 2009, doi: 10.1002/er.1611.

[41] G. Füldner, L. Schnabel, U. Wittstadt, H.-M. Henning, and F. P. Schmidt, "Numerical layer optimization of aluminum fibre/sapo-34 composites for the application in adsorptive heat exchangers," in Padua, Italy, 2011.

[42] U. Wittstadt, G. Füldner, O. Andersen, R. Herrmann, and F. Schmidt, "A New Adsorbent Composite Material Based on Metal Fiber Technology and Its Application in Adsorption Heat Exchangers," *Energies*, vol. 8, no. 8, pp. 8431–8446, 2015, doi: 10.3390/en8088431.

[43] U. Wittstadt *et al.,* "A novel adsorption module with fiber heat exchangers: Performance analysis based on driving temperature differences," *Renewable Energy*, vol. 110, pp. 154–161, 2017, doi: 10.1016/j.renene.2016.08.061.

[44] U. Wittstadt *et al.,* "Entwicklung einer Gasadsorptionswärmepumpe mit einem aufkristallisiertem Adsorptionswärmeübertrager und einem neuartigen Verdampfer/Kondensator-Apparat (ADOSO) : Abschlussbericht : Laufzeit des Vorhabens: 01.05.2013-30.09.2018 : 03ET1127B: Teilvorhaben B - Entwicklung einer optimierten 3D-Wärmeübertragerstruktur für optimierte Wärme- und Stofftransportprozesse (Fraunhofer)," 2018.

[45] U. Wittstadt, A. Velte, M. Kleinstück, R. Volmer, C. Kostmann, and O. Andersen, "Entwicklung einer Gasadsorptionswärmepumpe mit einem aufkristallisierten Adsorptionswärmeübertrager und einem neuartigen Verdampfer/Kondensator-Apparat (ADOSO) : Teilvorhaben A: Entwicklung des Gesamtsystems der Adsorptionswärmepumpe : Teilvorhaben C: Aufkristallisation und Weiterentwicklung Zeolith auf Metallfaserstrukturen : gemeinsamer Abschlussbericht : Laufzeit des Vorhabens: 01.05.2013-31.10.2016," 2016.

[46] S. K. Henninger, H. A. Habib, and C. Janiak, "MOFs as adsorbents for low temperature heating and cooling applications," *Journal of the American Chemical Society*, vol. 131, no. 8, pp. 2776–2777, 2009, doi: 10.1021/Ja808444z.

[47] G. Férey, "Hybrid porous solids: past, present, future," *Chemical Society reviews*, vol. 37, no. 1, pp. 191–214, 2008, doi: 10.1039/b618320b.

[48] M. Eddaoudi *et al.,* "Systematic design of pore size and functionality in isoreticular MOFs and their application in methane storage," *Science*, vol. 295, no. 5554, pp. 469–472, 2002, doi: 10.1126/science.1067208.

[49] S. K. Henninger *et al.,* "New materials for adsorption heat transformation and storage," *Renew Energ*, vol. 110, pp. 59–68, 2017, doi: 10.1016/j.renene.2016.08.041.

[50] F. Jeremias, D. Fröhlich, C. Janiak, and S. K. Henninger, "Water and methanol adsorption on MOFs for cycling heat transformation processes," *New J. Chem.*, vol. 38, no. 5, pp. 1846–1852, 2014, doi: 10.1039/c3nj01556d.

[51] M. F. de Lange, K. J. F. M. Verouden, T. J. H. Vlugt, J. Gascon, and F. Kapteijn, "Adsorption-Driven Heat Pumps: The Potential of Metal-Organic Frameworks," *Chemical reviews*, vol. 115, no. 22, pp. 12205–12250, 2015, doi: 10.1021/acs.chemrev.5b00059.

[52] F. Jeremias, S. K. Henninger, and C. Janiak, "High performance metal-organic-framework coatings obtained via thermal gradient synthesis," *Chemical communications (Cambridge, England)*, vol. 48, no. 78, pp. 9708–9710, 2012, doi: 10.1039/c2cc34782b.

[53] D. Lenzen *et al.,* "Scalable Green Synthesis and Full-Scale Test of the Metal-Organic Framework CAU-10-H for Use in Adsorption-Driven Chillers," *Advanced materials (Deerfield Beach, Fla.)*, vol. 30, no. 6, 2018, doi: 10.1002/adma.201705869.

[54] H. Kummer *et al.,* "A Functional Full-Scale Heat Exchanger Coated with Aluminum Fumarate Metal–Organic Framework for Adsorption Heat Transformation," *Ind. Eng. Chem. Res.*, vol. 56, no. 29, pp. 8393–8398, 2017, doi: 10.1021/acs.iecr.7b00106.

[55] I. GitHub, *SorpSim.* [Online]. Available: https://www.github.com/oabdelaziz/sorpsim## (accessed: 19.12.19).

[56] I. GitHub, *SorpPropLib.* [Online]. Available: https://github.com/zhiyaoyang/sorpproplib

[57] I. GitHub, *sorpproplib_JSON.* [Online]. Available: https://github.com/zhiyaoYang/sorpproplib_JSON

[58] M. Garrabrant, "Presentation at 7th Annex meeting Las Vegas 2017," 2017.

[59] "CEN, EN12309, Parts 1 to 7, Air conditioners, liquid chilling packages and heat pumps for space heating and cooling and process chillers, with electricylly driven compressors. CEN, 2014/2016," X1.

[60] "CEN, EN 13203-6, Gas-fired domestic appliances producing hot water – Part 6: Assessment of energy consump-tion of adsorption and absorption heat pumps. CEN, 2019," X2.

[61] "VDI, VDI 4650-2, Simplified method for the calculation of the annual heating energy ratio and the annual gas utilisation efficiency of sorption heat pumps – gas heat pumps for space heating and domestic hot water. VDI, 2013," X3.

[62] “CEN, Commission communication in the framework of the implementation of Commission Regulation (EU) No 813/2013 implementing Directive 2009/125/EC of the European Parliament and of the Council with regard to ecodesign requirements for space heaters and combination heaters and of Commission Delegated Regulation (EU) No 811/2013 supplementing Directive 2010/30/EU of the European Parliament and of the Council with regard to the energy labelling of space heaters, combination heaters, packages of space heater, temperature control and solar device and packages of combination heater, temperature control and solar device. CEN, 2014,” X4.

[63] “Wemhöner, C., Afjei, T., IEA HPP Annex 28 – A uniform energy-related characterisation of heat pump systems. Article from the 5th IEA Heat Pump Conference 2005 in Las Vegas, USA. Accessed on 03.11.2019 from https://heatpumpingtechnologies.org/publications/iea-hpp-annex-28-a-uniform-energy-relatedcharacterisation-of-heat-pump-systems/,”

[64] M. Fumagalli, A. Sivieri, M. Aprile, M. Motta, and M. Zanchi, “Monitoring of gas driven absorption heat pumps and comparing energy efficiency on primary energy,” *Renew Energ*, vol. 110, pp. 115–125, 2017, doi: 10.1016/j.renene.2016.12.058.

[65] M. Fumagalli, T. Toppi, M. Aprile, and M. Motta, “Monitoring experience of three fuel driven absorption HP systems,” in *12th IEA HEAT PUMP CONFERENCE*, 2017.

[66] A. Zottl and R. Nordman, “D4.1. / D2.3. Guideline for heat pump field measurements for hydronic heating systems, Project SEPEMO - SEasonal PErformance factor and MOnitoring for heat pump systems in the building sector SEPEMO-Build, 20 September 2011,” 2011.

[67] A. Zottl and R. Nordman, “D4.2. /D 2.4. Concept for evaluation of SPF - Heat pumps with hydronic heating systems, Project SEPEMO - SEasonal PErformance factor and MOnitoring for heat pump systems in the building sector SEPEMO-Build, 31 May 2012,” 2012.

[68] Cambridge Architectural Research, *Cambridge Housing Model Cambridge Housing Model.* [Online]. Available: www.gov.uk/government/publications/cambridge-housing-model-and-user-guide

[69] UK Department of Energy and Climate Change, *United Kingdom Housing Energy Fact File.* [Online]. Available: https://www.gov.uk/government/uploads/system/uploads/attachment_data/file/345141/uk_housing_fact_file_2013.pdf

[70] J. Russill, “Thermal transmittance of walls of dwellings before and after application of cavity wall insulation: UK Energy Saving Trust Report number 222077,” 2008.

[71] R. Scoccia, T. Toppi, M. Aprile, and M. Motta, “Absorption and compression heat pump systems for space heating and DHW in European buildings: Energy, environmental and economic analysis,” *Journal of Building Engineering*, vol. 16, pp. 94–105, 2018, doi: 10.1016/j.jobe.2017.12.006.

[72] K. Pollier, L. Gynther, and Lapillonne. B., “Energy Efficiency Trends and Policies in the Household and Tertiary Sectors,” 2015.

[73] *Gas-fired sorption appliances for heating and/or cooling with a net heat input not exceeding 70 kW*, EN 12309, 2015.

[74] *Air conditioners, liquid chilling packages and heat pumps, with electrically driven compressors, for space heating and cooling - Testing and rating at part load conditions and calculation of seasonal performance*, UNI EN 14825:2013.

[75] R. Dott, M. Y. Haller, J. Ruschenburg, F. Ochs, and J. Bony, "The Reference Framework for System Simulations of the IEA SHC Task 44 / HPP Annex 38: Part B: Buildings and Space Heat Load, IEA SHC Task 44/HPP Annex 38, Report C1 Part B,"

[76] TABULA & EPISCOPE, *Joint website of the TABULA and EPISCOPE projects.* [Online]. Available: www.episcope.eu## (accessed: Jan. 10 2020).

[77] "COMMISSION DELEGATED REGULATION (EU) No 812/2013 of 18 February 2013: Supplementing Directive 2010/30/EU of the European Parliament and of the Council with regard to the energy labelling of water heaters, hot water storage tanks and packages of water heater and solar device," 2013.

[78] *Air conditioners, liquid chilling packages and heat pumps with electrically driven compressors for space heating and cooling - Part 2: Test conditions.*, UNI EN 14511-2: 2011.

[79] *Aermec model ANLI 071: performance data.* [Online]. Available: http://global.aermec.com/

[80] *Certified product for the Eurovent certified performance website.* [Online]. Available: http:// www.eurovent-certification.com/index.php?lg=en

[81] T. Toppi, M. Aprile, M. Motta, and C. Bongs, "Seasonal performance calculation and transient simulation of a newly developed 18 kW air-source water-ammonia gas heat pump for residential applications: IEA Heat Pump Conference 2014, Montreal, Paper O.3.6.2,"

[82] *European Environmental Agency, CO2 emission intensity.* [Online]. Available: https:// www.eea.europa.eu/ds_resolveuid/828de623d905428ba1816addcab3ac00## (accessed: Jan. 10 2020).

[83] *Eurostat, Electricity prices for domestic consumers - bi-annual data.* [Online]. Available: http:// appsso.eurostat.ec.europa.eu/nui/show.do?dataset=nrg_pc_204&lang=en## (accessed: Jan. 10 2020).

[84] *Eurostat, Gas prices for domestic consumers - bi-annual data.* [Online]. Available: http:// appsso.eurostat.ec.europa.eu/nui/show.do?dataset=nrg_pc_202&lang=en## (accessed: Jan. 10 2020).

[85] M. Kotteck, *World Map of Köppen-Geiger Climate Classification updated.* [Online]. Available: http:// koeppen-geiger.vu-wien.ac.at/pdf/Paper_2006.pdf

[86] CEN, *EN12309-2: 2000 Gas-fired absorption and adsorption air-conditioning and/or heat pump appliances with a net heat input not exceeding 70 kW – Part 2: Rational use of energy*. Brussles.

[87] V. Bürger, *Klimaneutraler Gebäudebestand 2050 in: Climate Change 06/2016. Published by Umweltbundesamt, Dessau-Roßlau (Germany).* [Online]. Available: https://www.umweltbundesamt.de/sites/default/files/medien/378/publikationen/climate_change_06_2016_klimaneutraler_gebaeudebestand_2050.pdf

[88] B. Ebert, "Systematische Analyse von Mehrfamilien-Bestandsgebäuden - LowEx-Bestand Analyse Abschlussbericht zu AP 1.1 ; Karlsruhe Institute of Technology, Germany," 2018.

[89] University of Wisconsin, Ed., "TRNSYS – transient simulation tool, developed by .: Version 17," USA. [Online]. Available: https://sel.me.wisc.edu/trnsys/

[90] "Energieeinsparverordnung; national framework for requirements on energy saving in residential and non-residential buildings: Regularly updated; requirements not higher than in issue 2016 were applied," Accessed: Jan. 16 2020. [Online]. Available: http://www.enev-online.com/enev_2014_volltext/00_titelseite.htm

[91] *Energy performance of buildings - Calculation of energy use for space heating and cooling*, DIN EN ISO 13790:2008.

[92] Robur Advanced Heating and Cooling Technologies, *Product catalogue of the Robur K18 gas absorption heat pump, providing base data.* [Online]. Available: https://www.robur.com/downloads/2957/499/ROBUR_K18-5-2017_UK_b.pdf## (accessed: Jan. 17 2020).

[93] A. Velte, "Experimentelle Arbeiten und Entwicklung von numerischen Modellen zur Analyse und Optimierung von erweiterten Adsorptionskreisläufen für die Wärmeversorgung von Gebäuden," PhD Theses (submitted), Universität Freiburg, Freiburg, 2019.

[94] *Simplified method for the calculation of the annual heating energy ratio and the annual gas utilisation efficiency of sorption heat pumps - Gas heat pumps for space heating and domestic hot water*, VDI 4650 Blatt 2:2013-01.

[95] *Final report of the WP Monitor project.* [Online]. Available: https://wp-monitoring.ise.fraunhofer.de/wp-monitor-plus/german/index/ergebnisse.html

[96] M. Y. Haller† *et al.,* "A unified model for the simulation of oil, gas and biomass space heating boilers for energy estimating purposes. Part I: Model development," *Journal of Building Performance Simulation*, vol. 4, no. 1, pp. 1–18, 2011, doi: 10.1080/19401491003671944.

[97] M. Garrabrant, "Pre-commercial scale up of a gas absorption heat pump: DOE Building Technologies Office 7th Annual Peer Review, April 15–10, 2019, Crystal City, Virginia," 2019. [Online]. Available: https://www.energy.gov/sites/prod/files/2019/05/f62/bto-peer-2019-stone-mountain-pre-comm-scale-up.pdf

[98] K. R. Gluesenkamp, “Residential Gas-Fired Cost-Effective Triple-State Sorption Heat Pump: DOE Building Technologies Office 7th Annual Peer Review, April 15–10, 2019, Crystal City, Virginia,” 2019. [Online]. Available: https://www.energy.gov/sites/prod/files/2019/05/f62/bto-peer-2019-ornl-res-gas-fired-heatpump.pdf

[99] S. Moghaddam, “A Combined Water Heater Dehumidifier and Cooler (WHDC): DOE Building Technologies Office 5th Annual Peer Review, March 13-16, 2017, Arlington, Virginia,” 2017. [Online]. Available: https://www.energy.gov/sites/prod/files/2017/04/f34/9_312100_Moghaddam_031517-1600.pdf

[100] P. Geoghegan, “Commercial absorption heat pump water heater: DOE Building Technologies Office 5th Annual Peer Review, March 13-16, 2017, Arlington, Virginia,” 2017. [Online]. Available: https://www.energy.gov/sites/prod/files/2017/04/f34/4_32226e_Geohagen_031417-1000.pdf

[101] Y. Wang and M. D. LeVan, “Adsorption equilibrium of carbon dioxide and water vapor on zeolites 5A and 13X and silica gel: pure components,” *Journal of Chemical & Engineering Data*, vol. 54, no. 10, pp. 2839–2844, 2009.

[102] B. B. Saha, S. Jribi, S. Koyama, and I. I. El-Sharkawy, “Carbon dioxide adsorption isotherms on activated carbons,” *Journal of Chemical & Engineering Data*, vol. 56, no. 5, pp. 1974–1981, 2011.

[103] H. T. Chua, K. C. Ng, W. Wang, C. Yap, and X. L. Wang, “Transient modeling of a two-bed silica gel–water adsorption chiller,” *International Journal of Heat and Mass Transfer*, vol. 47, no. 4, pp. 659–669, 2004, doi: 10.1016/j.ijheatmasstransfer.2003.08.010.

[104] F. A. Da Silva and A. E. Rodrigues, “Adsorption equilibria and kinetics for propylene and propane over 13X and 4A zeolite pellets,” *Industrial & engineering chemistry research*, vol. 38, no. 5, pp. 2051–2057, 1999.

[105] N. Lamia *et al.,* “Equilibrium and Fixed Bed Adsorption of 1-Butene, Propylene and Propane Over 13X Zeolite Pellets,” *Separation Science and Technology*, vol. 43, no. 5, pp. 1124–1156, 2008.

[106] C. A. Grande, C. Gigola, and A. E. Rodrigues, “Adsorption of propane and propylene in pellets and crystals of 5A zeolite,” *Industrial & engineering chemistry research*, vol. 41, no. 1, pp. 85–92, 2002.

[107] C. A. Grande, V. M. Silva, C. Gigola, and A. E. Rodrigues, “Adsorption of propane and propylene onto carbon molecular sieve,” *Carbon*, vol. 41, no. 13, pp. 2533–2545, 2003.

[108] S. Jribi, B. B. Saha, S. Koyama, A. Chakraborty, and K. C. Ng, “Study on activated carbon/HFO-1234ze (E) based adsorption cooling cycle,” *Applied Thermal Engineering*, vol. 50, no. 2, pp. 1570–1575, 2013.

[109] L. M. Sun, Y. Feng, and M. Pons, “Numerical investigation of adsorptive heat pump systems with thermal wave heat regeneration under uniform-pressure conditions,” *International Journal of Heat and Mass Transfer*, vol. 40, no. 2, pp. 281–293, 1997, doi: 10.1016/0017-9310(96)00113-5.

[110] K. Thu, A. Chakraborty, B. B. Saha, and K. C. Ng, “Thermo-physical properties of silica gel for adsorption desalination cycle,” *Applied Thermal Engineering*, vol. 50, no. 2, pp. 1596–1602, 2013, doi: 10.1016/j.applthermaleng.2011.09.038.

[111] N. Douss and F. Meunier, “Effect of operating temperatures on the coefficient of performance of active carbon-methanol systems,” *Heat Recovery Systems and CHP*, vol. 8, no. 5, pp. 383–392, 1988, doi: 10.1016/0890-4332(88)90042-7.

[112] V. Brancato, A. Frazzica, A. Sapienza, L. Gordeeva, and A. Freni, “Ethanol adsorption onto carbonaceous and composite adsorbents for adsorptive cooling system,” *Energy*, vol. 84, pp. 177–185, 2015.

[113] S. K. Henninger, M. Schicktanz, P. P.C. Hügenell, H. Sievers, and H.-M. Henning, “Evaluation of methanol adsorption on activated carbons for thermally driven chillers part I: Thermophysical characterisation,” *International journal of refrigeration*, vol. 35, no. 3, pp. 543–553, 2012.

[114] M. Pons and P. Grenier, “A phenomenological adsorption equilibrium law extracted from experimental and theoretical considerations applied to the activated carbon + methanol pair,” *Carbon*, vol. 24, no. 5, pp. 615–625, 1986, doi: 10.1016/0008-6223(86)90151-X.

[115] H. Jing and R. H. B. Exell, “Simulation and sensitivity analysis of an intermittent solar-powered charcoal/methanol refrigerator,” *Renewable Energy*, vol. 4, no. 1, pp. 133–149, 1994, doi: 10.1016/0960-1481(94)90076-0.

[116] E. Passos, F. Meunier, and J. C. Gianola, “Thermodynamic performance improvement of an intermittent solar-powered refrigeration cycle using adsorption of methanol on activated carbon,” *Journal of Heat Recovery Systems*, vol. 6, no. 3, pp. 259–264, 1986, doi: 10.1016/0198-7593(86)90010-X.

[117] M. A. Alghoul, M. Y. Sulaiman, K. Sopian, and B. Z. Azmi, “Performance of a dual-purpose solar continuous adsorption system,” *Renewable Energy*, vol. 34, no. 3, pp. 920–927, 2009, doi: 10.1016/j.renene.2008.05.037.

[118] B. B. Saha, I. I. El-Sharkawy, K. Habib, S. Koyama, and K. Srinivasan, “Adsorption of equal mass fraction near an azeotropic mixture of pentafluoroethane and 1, 1, 1-trifluoroethane on activated carbon,” *Journal of Chemical & Engineering Data*, vol. 53, no. 8, pp. 1872–1876, 2008.

[119] A. A. Askalany *et al.,* “Adsorption isotherms and heat of adsorption of difluoromethane on activated carbons,” *Journal of Chemical & Engineering Data*, vol. 58, no. 10, pp. 2828–2834, 2013.

[120] B. S. Akkimaradi, M. Prasad, P. Dutta, and K. Srinivasan, “Adsorption of 1, 1, 1, 2-tetrafluoroethane on activated charcoal,” *Journal of Chemical & Engineering Data*, vol. 46, no. 2, pp. 417–422, 2001.

[121] B. B. Saha, K. Habib, I. I. El-Sharkawy, and S. Koyama, “Adsorption characteristics and heat of adsorption measurements of R-134a on activated carbon,” *International journal of refrigeration*, vol. 32, no. 7, pp. 1563–1569, 2009.

[122] B. B. Saha, I. I. El-Sharkawy, R. Thorpe, and R. E. Critoph, “Accurate adsorption isotherms of R134a onto activated carbons for cooling and freezing applications,” *International journal of refrigeration*, vol. 35, no. 3, pp. 499–505, 2012.

[123] A. A. Askalany, B. B. Saha, and I. M. Ismail, “Adsorption isotherms and kinetics of HFC410A onto activated carbons,” *Applied Thermal Engineering*, vol. 72, no. 2, pp. 237–243, 2014.

[124] M. M. El-Sharkawy, A. A. Askalany, K. Harby, and M. S. Ahmed, “Adsorption isotherms and kinetics of a mixture of Pentafluoroethane, 1, 1, 1, 2-Tetrafluoroethane and Difluoromethane (HFC-407C) onto granular activated carbon,” *Applied Thermal Engineering*, vol. 93, pp. 988–994, 2016.

[125] M. Ghazy, A. A. Askalany, K. Harby, and M. S. Ahmed, “Adsorption isotherms and kinetics of HFC-404A onto bituminous based granular activated carbon for storage and cooling applications,” *Applied Thermal Engineering*, vol. 105, pp. 639–645, 2016.

[126] K. A. Rahman, A. Chakraborty, B. B. Saha, and K. C. Ng, “On thermodynamics of methane+ carbonaceous materials adsorption,” *International Journal of Heat and Mass Transfer*, vol. 55, no. 4, pp. 565–573, 2012.

[127] H. W. B. Teo, A. Chakraborty, and W. Fan, “Improved adsorption characteristics data for AQSOA types zeolites and water systems under static and dynamic conditions,” *Microporous and Mesoporous Materials*, vol. 242, pp. 109–117, 2017.

[128] S. Kayal, S. Baichuan, and B. B. Saha, “Adsorption characteristics of AQSOA zeolites and water for adsorption chillers,” *International Journal of Heat and Mass Transfer*, vol. 92, pp. 1120–1127, 2016.

[129] J. M. Pinheiro, A. A. Valente, S. Salústio, N. Ferreira, J. Rocha, and C. M. Silva, “Application of the novel ETS-10/water pair in cyclic adsorption heating processes: measurement of equilibrium and kinetics properties and simulation studies,” *Applied Thermal Engineering*, vol. 87, pp. 412–423, 2015.

[130] A. Sapienza *et al.,* ““Water-Silica Siogel” working pair for adsorption chillers: Adsorption equilibrium and dynamics,” *Renewable Energy*, vol. 30, no. 1, e7, 2016.

[131] E. Elsayed, A.-D. Raya, S. Mahmoud, A. Elsayed, and P. A. Anderson, “Aluminium fumarate and CPO-27 (Ni) MOFs: characterization and thermodynamic analysis for adsorption heat pump applications,” *Applied Thermal Engineering*, vol. 99, pp. 802–812, 2016.

[132] M. Sultan *et al.,* “Insights of water vapor sorption onto polymer based sorbents,” *Adsorption*, vol. 21, no. 3, pp. 205–215, 2015.

[133] W. S. Loh, A. B. Ismail, B. Xi, K. C. Ng, and W. G. Chun, "Adsorption isotherms and isosteric enthalpy of adsorption for assorted refrigerants on activated carbons," *Journal of Chemical & Engineering Data*, vol. 57, no. 10, pp. 2766–2773, 2012.

[134] A. A. Askalany, M. Salem, I. M. Ismail, A. H. H. Ali, and M. G. Morsy, "Experimental study on adsorption–desorption characteristics of granular activated carbon/R134a pair," *International journal of refrigeration*, vol. 35, no. 3, pp. 494–498, 2012, doi: 10.1016/j.ijrefrig.2011.04.002.

[135] K. Uddin *et al.,* "Adsorption characteristics of ethanol onto functional activated carbons with controlled oxygen content," *Applied Thermal Engineering*, vol. 72, no. 2, pp. 211–218, 2014.

[136] El-Sharkawy, II, B. B. Saha, S. Koyama, J. He, K. C. Ng, and C. Yap, "Experimental investigation on activated carbon–ethanol pair for solar powered adsorption cooling applications," *International journal of refrigeration*, vol. 31, no. 8, pp. 1407–1413, 2008.

[137] B. B. Saha, I. I. El-Sharkawy, A. Chakraborty, S. Koyama, S.-H. Yoon, and K. C. Ng, "Adsorption rate of ethanol on activated carbon fiber," *Journal of Chemical & Engineering Data*, vol. 51, no. 5, pp. 1587–1592, 2006.

[138] A. Rezk, A.-D. Raya, S. Mahmoud, and A. Elsayed, "Investigation of Ethanol/metal organic frameworks for low temperature adsorption cooling applications," *Applied energy*, vol. 112, pp. 1025–1031, 2013.

[139] I. I. El-Sharkawy *et al.,* "Adsorption of ethanol onto phenol resin based adsorbents for developing next generation cooling systems," *International Journal of Heat and Mass Transfer*, vol. 81, pp. 171–178, 2015.

[140] B. B. Saha *et al.,* "Isotherms and thermodynamics for the adsorption of n-butane on pitch based activated carbon," *International Journal of Heat and Mass Transfer*, vol. 51, no. 7, pp. 1582–1589, 2008.

[141] Y. Zhao, E. Hu, and A. Blazewicz, "A comparison of three adsorption equations and sensitivity study of parameter uncertainty effects on adsorption refrigeration thermal performance estimation," *Heat and Mass Transfer*, vol. 48, no. 2, pp. 217–226, 2012.

[142] J. W. Wu, S. H. Madani, M. J. Biggs, P. Phillip, C. Lei, and E. J. Hu, "Characterizations of activated carbon–methanol adsorption pair including the heat of adsorptions," *Journal of Chemical & Engineering Data*, vol. 60, no. 6, pp. 1727–1731, 2015.

[143] El-Sharkawy, II, M. Hassan, B. B. Saha, S. Koyama, and M. M. Nasr, "Study on adsorption of methanol onto carbon based adsorbents," *International journal of refrigeration*, vol. 32, no. 7, pp. 1579–1586, 2009.

[144] Z. Tamainot-Telto, S. J. Metcalf, R. E. Critoph, Y. Zhong, and R. Thorpe, "Carbon–ammonia pairs for adsorption refrigeration applications: ice making, air conditioning and heat pumping," *International journal of refrigeration*, vol. 32, no. 6, pp. 1212–1229, 2009.

[145] R. E. Critoph, “Evaluation of alternative refrigerant—adsorbent pairs for refrigeration cycles,” *Applied Thermal Engineering*, vol. 16, no. 11, pp. 891–900, 1996, doi: 10.1016/1359-4311(96)00008-7.

[146] L. W. Wang, R. Z. Wang, Z. S. Lu, C. J. Chen, K. Wang, and J. Y. Wu, “The performance of two adsorption ice making test units using activated carbon and a carbon composite as adsorbents,” *Carbon*, vol. 44, no. 13, pp. 2671–2680, 2006, doi: 10.1016/j.carbon.2006.04.013.

[147] L. W. Wang, S. J. Metcalf, R. E. Critoph, R. Thorpe, and Z. Tamainot-Telto, “Development of thermal conductive consolidated activated carbon for adsorption refrigeration,” *Carbon*, vol. 50, no. 3, pp. 977–986, 2012, doi: 10.1016/j.carbon.2011.09.061.

[148] L. H. Turner, “Improvement of activated charcoal-ammonia adsorption heat pumping/refrigeration cycles: investigation of porosity and heat/mass transfer chacteristics,” Warwick, University of, 1992.

[149] İ. Solmuş, C. Yamalı, B. Kaftanoğlu, D. Baker, and A. Çağlar, “Adsorption properties of a natural zeolite–water pair for use in adsorption cooling cycles,” *Applied energy*, vol. 87, no. 6, pp. 2062–2067, 2010, doi: 10.1016/j.apenergy.2009.11.027.

[150] X. J. Zhang and R. Z. Wang, “A new combined adsorption–ejector refrigeration and heating hybrid system powered by solar energy,” *Applied Thermal Engineering*, vol. 22, no. 11, pp. 1245–1258, 2002, doi: 10.1016/S1359-4311(02)00043-1.

[151] A. Adell, “Comparison of the performance obtained in a tropical country, of a solid adsorption, solar-driven refrigerator and a photovoltaic refrigerator,” *Journal of Power Sources*, vol. 15, no. 1, pp. 1–12, 1985, doi: 10.1016/0378-7753(85)80056-2.

[152] Y. Z. Lu, R. Z. Wang, M. Zhang, and S. Jiangzhou, “Adsorption cold storage system with zeolite–water working pair used for locomotive air conditioning,” *Energy Conversion and Management*, vol. 44, no. 10, pp. 1733–1743, 2003, doi: 10.1016/S0196-8904(02)00169-3.

[153] İ. Solmuş, D. Andrew S. Rees, C. Yamalı, and D. Baker, “A two-energy equation model for dynamic heat and mass transfer in an adsorbent bed using silica gel/water pair,” *International Journal of Heat and Mass Transfer*, vol. 55, no. 19, pp. 5275–5288, 2012, doi: 10.1016/j.ijheatmasstransfer.2012.05.036.

[154] L. X. Gong, R. Z. Wang, Z. Z. Xia, and C. J. Chen, “Adsorption equilibrium of water on a composite adsorbent employing lithium chloride in silica gel,” *Journal of Chemical & Engineering Data*, vol. 55, no. 8, pp. 2920–2923, 2010.

[155] R. Z. Wang *et al.,* “Study on a New Solid Absorption Refrigeration Pair: Active Carbon Fiber—Methanol,” *Journal of Solar Energy Engineering*, vol. 119, no. 3, p. 214, 1997, doi: 10.1115/1.2888021.

[156] M. J. Tierney, “Feasibility of driving convective thermal wave chillers with low-grade heat,” *Renewable Energy*, vol. 33, no. 9, pp. 2097–2108, 2008, doi: 10.1016/j.renene.2007.12.005.

[157] S. D. Waszkiewicz, M. J. Tierney, and H. S. Scott, “Development of coated, annular fins for adsorption chillers,” *Applied Thermal Engineering*, vol. 29, no. 11, pp. 2222–2227, 2009, doi: 10.1016/j.applthermaleng.2008.11.004.

[158] T. Miyazaki, A. Akisawa, B. B. Saha, I. I. El-Sharkawy, and A. Chakraborty, “A new cycle time allocation for enhancing the performance of two-bed adsorption chillers,” *International journal of refrigeration*, vol. 32, no. 5, pp. 846–853, 2009, doi: 10.1016/j.ijrefrig.2008.12.002.

[159] S.-H. Cho and J.-N. Kim, “Modeling of a silica gel/water adsorption-cooling system,” *Energy*, vol. 17, no. 9, pp. 829–839, 1992, doi: 10.1016/0360-5442(92)90101-5.

[160] A. Sakoda and M. Suzuki, “FUNDAMENTAL STUDY ON SOLAR POWERED ADSORPTION COOLING SYSTEM,” *Journal of Chemical Engineering of Japan*, vol. 17, no. 1, p. 52, 1984, doi: 10.1252/jcej.17.52.

[161] B. B. Saha *et al.,* “Performance evaluation of a low-temperature waste heat driven multi-bed adsorption chiller,” *International Journal of Multiphase Flow*, vol. 29, no. 8, pp. 1249–1263, 2003, doi: 10.1016/S0301-9322(03)00103-4.

[162] N. Lamia, M. Jorge, M. A. Granato, F. A. A. Paz, H. Chevreau, and A. E. Rodrigues, “Adsorption of propane, propylene and isobutane on a metal–organic framework: Molecular simulation and experiment,” *Chemical Engineering Science*, vol. 64, no. 14, pp. 3246–3259, 2009.

[163] C. A. Grande and A. E. Rodrigues, “Adsorption kinetics of propane and propylene in zeolite 4A,” *Chemical Engineering Research and Design*, vol. 82, no. 12, pp. 1604–1612, 2004.

[164] A. de Lucas, M. Donate, and J. F. Rodríguez, “Vapour pressures, densities, and viscosities of the (water+ lithium bromide+ potassium acetate) system and (water+ lithium bromide+ sodium lactate) system,” *The Journal of Chemical Thermodynamics*, vol. 38, no. 2, pp. 123–129, 2006.

[165] J.-S. Kim, Y. Park, and H. Lee, “Solubilities and vapor pressures of the water+ lithium bromide+ ethanolamine system,” *Journal of Chemical & Engineering Data*, vol. 41, no. 2, pp. 279–281, 1996.

[166] Y. Park, J.-S. Kim, and H. Lee, “Physical properties of the lithium bromide+ 1, 3-propanediol+ water system,” *International journal of refrigeration*, vol. 20, no. 5, pp. 319–325, 1997.

[167] K.-K. Koo, H.-R. Lee, S. Jeong, Y.-S. Oh, D.-R. Park, and Y.-S. Baek, “Solubilities, vapor pressures, and heat capacities of the water+ lithium bromide+ lithium nitrate+ lithium iodide+ lithium chloride system,” *International journal of thermophysics*, vol. 20, no. 2, pp. 589–600, 1999.

[168] J.-S. Kim and H. Lee, “Solubilities, vapor pressures, densities, and viscosities of the LiBr+ LiI+ HO (CH2) 3OH+ H2O system,” *Journal of Chemical & Engineering Data*, vol. 46, no. 1, pp. 79–83, 2001.

[169] S. Iyoki, R. Yamanaka, and T. Uemura, “Physical and thermal properties of the water-lithium bromide-lithium nitrate system,” *International journal of refrigeration*, vol. 16, no. 3, pp. 191–200, 1993.

[170] X. Shiming, L. Yanli, and Z. Lisong, “Performance research of self regenerated absorption heat transformer cycle using TFE-NMP as working fluids,” *International journal of refrigeration*, vol. 24, no. 6, pp. 510–518, 2001.

[171] A. F. Handbook, “American society of heating, refrigerating and air-conditioning engineers,” *Inc.: Atlanta, GA, USA*, 2009.

[172] K. E. Herold, R. Radermacher, L. Howe, and D. C. Erickson, “Development of an absorption heat pump water heater using an aqueous ternary hydroxide working fluid,” *International journal of refrigeration*, vol. 14, no. 3, pp. 156–167, 1991.

[173] M. S. Manic, A. J. Queimada, E. A. Macedo, and V. Najdanovic-Visak, “High-pressure solubilities of carbon dioxide in ionic liquids based on bis (trifluoromethylsulfonyl) imide and chloride,” *The Journal of Supercritical Fluids*, vol. 65, pp. 1–10, 2012.

[174] M. A. M. Neto and J. R. Barbosa, “Solubility, density and viscosity of a mixture of R-600a and polyol ester oil,” *International journal of refrigeration*, vol. 31, no. 1, pp. 34–44, 2008.

[175] K. Takigawa, S. I. Sandler, and A. Yokozeki, “Solubility and viscosity of refrigerant/lubricant mixtures: hydrofluorocarbon/alkylbenzene systems,” *International journal of refrigeration*, vol. 25, no. 8, pp. 1014–1024, 2002.

[176] C. Bogatu, D. Geană, R. Vîlcu, A. Duţă, W. Poot, and T. W. de Loos, “Fluid phase equilibria in the binary system trifluoromethane+ 1-phenyloctane,” *Fluid phase equilibria*, vol. 295, no. 2, pp. 186–193, 2010.

[177] A. Yokozeki, “Solubility of refrigerants in various lubricants,” *International journal of thermophysics*, vol. 22, no. 4, pp. 1057–1071, 2001.

[178] Å. Wahlström and L. Vamling, “Solubility of HFCs in pentaerythritol tetraalkyl esters,” *Journal of Chemical & Engineering Data*, vol. 45, no. 1, pp. 97–103, 2000.

[179] Å. Wahlström and L. Vamling, “Solubility of HFC32, HFC125, HFC134a, HFC143a, and HFC152a in a pentaerythritol tetrapentanoate ester,” *Journal of Chemical & Engineering Data*, vol. 44, no. 4, pp. 823–828, 1999.

[180] M. Döker and J. Gmehling, “Measurement and prediction of vapor–liquid equilibria of ternary systems containing ionic liquids,” *Fluid phase equilibria*, vol. 227, no. 2, pp. 255–266, 2005.

[181] C. Burton, Am Jacobi, and S. S. Mehendale, “Vapor-liquid equilibrium for R-32 and R-410A mixed with a polyol ester: non-ideality and local composition modeling,” *International journal of refrigeration*, vol. 22, no. 6, pp. 458–471, 1999.

[182] J. Bock, *Vapor-liquid equilibria of a low GWP refrigerant, R-1234ze (E), mixed with a POE lubricant*: University of Illinois at Urbana-Champaign, 2015.

[183] J. J. Grebner, "The effects of oil on the thermodynamic properties of dichlorodifluoromethane (R-12) and tetrafluoroethane (R-134a)," Air Conditioning and Refrigeration Center. College of Engineering. University of Illinois at Urbana-Champaign., 1992.

[184] W. L. Martz and Am Jacobi, "Refrigerant-oil mixtures and local composition modeling," Air Conditioning and Refrigeration Center. College of Engineering. University of Illinois at Urbana-Champaign., 1994.

[185] P. Marchi, G. Scalabrin, E. C. Ihmels, K. Fischer, and J. Gmehling, "Bubble pressure measurements for the (1, 1, 1, 2-tetrafluoroethane+ triethylene glycol dimethyl ether) system," *The Journal of Chemical Thermodynamics*, vol. 38, no. 11, pp. 1247–1253, 2006.

[186] C. Römich, N. C. Merkel, A. Valbonesi, K. Schaber, S. Sauer, and T. J. S. Schubert, "Thermodynamic properties of binary mixtures of water and room-temperature ionic liquids: Vapor pressures, heat capacities, densities, and viscosities of water+ 1-ethyl-3-methylimidazolium acetate and water+ diethylmethylammonium methane sulfonate," *Journal of Chemical & Engineering Data*, vol. 57, no. 8, pp. 2258–2264, 2012.

[187] J. S. Fleming and Y. Yan, "The prediction of vapour–liquid equilibrium behaviour of HFC blend–oil mixtures from commonly available data," *International journal of refrigeration*, vol. 26, no. 3, pp. 266–274, 2003.

[188] R. Kato and J. Gmehling, "Measurement and correlation of vapor–liquid equilibria of binary systems containing the ionic liquids [EMIM][(CF 3 SO 2) 2 N],[BMIM][(CF 3 SO 2) 2 N],[MMIM][(CH 3) 2 PO 4] and oxygenated organic compounds respectively water," *Fluid phase equilibria*, vol. 231, no. 1, pp. 38–43, 2005.

[189] K. Stephan and R. Hengerer, "Heat transformation with the ternary working fluid TFE-H2O-E181: Transformation de chaleur avec le fluide de travail ternaire TFE-H2O-E181," *International journal of refrigeration*, vol. 16, no. 2, pp. 120–128, 1993.

[190] R. Peters, C. Korinth, and J. U. Keller, "Vapor-liquid equilibria in the system NH3+ H2O+ LiBr. 2. Data correlation," *Journal of Chemical and Engineering Data*, vol. 40, no. 4, pp. 775–783, 1995.

[191] L. Vamling, "The solubility of HFC125, HFC134a, HFC143a and HFC152a in n-eicosane, n-hexadecane, n-tridecane and 2, 6, 10, 14-tetramethylpentadecane," *The Canadian Journal of Chemical Engineering*, vol. 75, no. 3, pp. 544–550, 1997.

[192] R. Kato, M. Krummen, and J. Gmehling, "Measurement and correlation of vapor–liquid equilibria and excess enthalpies of binary systems containing ionic liquids and hydrocarbons," *Fluid phase equilibria*, vol. 224, no. 1, pp. 47–54, 2004.

www.heatpumpingtechnologies.org

Heat Pump Centre
c/o RISE - Research Institutes of Sweden
PO Box 857
SE-501 15 BORÅS
Sweden
Tel: +46 10 516 5512
E-mail: hpc@heatpumpcentre.org

www.heatpumpingtechnologies.org

Report no. HPT-AN43-1